Mathematical Modeling of Chain Shuttling Polymerization

by

Ibrahim M. H. Maafa

A thesis
presented to the University of Waterloo
in fulfillment of the
thesis requirement for the degree of
Doctor of Philosophy
in
Chemical Engineering

Waterloo, Ontario, Canada, 2016

AUTHOR'S DECLARATION

I hereby declare that I am the sole author of this thesis. This is a true copy of the thesis, including any required final revisions, as accepted by my examiners.

I understand that my thesis may be made electronically available to the public.

Abstract

Chain shuttling polymerization with dual catalysts has introduced a new class of polyolefin called olefin block copolymers (OBCs). The Dow Chemical Company developed this new material in 2006 with a chain shuttling agent used to exchange living and dormant chains between two single-site catalysts reversibly. One catalyst may produce a soft/amorphous ethylene/α-olefin block due to its high reactivity ratio towards α-olefin insertion, while the other catalyst makes a hard/semi-crystalline ethylene/α-olefin block due to its low α-olefin reactivity ratio. The soft block provides elastomeric properties, whereas the hard block works as a physical crosslink to connect the elastomeric blocks.

Characterization of these novel materials is challenging because there are no analytical methods that can measure the distribution of blocks in OBCs. A mathematical model that can describe the detailed microstructure of these products is, therefore, an important step towards understanding how different polymerization conditions and kinetic parameters affect their microstructure. The main objective of this thesis is to develop such detailed models for semi-batch and continuous stirred tank reactors (CSTR).

Starting from the polymerization mechanism generally accepted for chain shuttling polymerization, we developed two different mathematical models to predict OBC microstructures made under different conditions. The first and simpler model uses population balances and the method of moments to predict chain length and composition averages for the overall (whole) OBC and for populations with different number of blocks. The second, and more complex model, uses dynamic Monte Carlo techniques to predict complete distributions of chain length and chemical composition.

The simulations described in this thesis show that OBCs have complex, multiblock structures, that depend strongly on several polymerization kinetic parameters, reactor conditions, and reactor modes of operation. As these conditions change, number average chain lengths, chemical compositions, average number of blocks, and block distribution among the OBC populations are also affected, and possibly the application properties of these advanced polyolefins. The models

proposed herein allow us to quantify the trends of this microstructural changes, and hopefully can help researchers design OBCs with better controlled molecular architectures.

Acknowledgements

My greatest gratitude is to Allah, the Almighty, who guided me in every step of this work with his infinite wisdom and grace.

I humbly acknowledge the guidance and support of my adviser, Professor Joao Soares, for his support of and assistance in my efforts to complete this work.

I would also like to express my thanks to my supervisory committee members: Professor Leonardo Simon, Professor Zhu Shiping, Professor Jean Duhamel, Professor Ali Elkamel, and Professor Zhongwei Chen.

Additionally, I thank my sponsors, Saudi Cultural Bureau and Jazan University, for their financial support.

I extend my deepest gratitude to my wife, Nuha Fagihi, and our children, Mohammed, Riyam and Firas, who have borne my preoccupation with my studies and absence with patience and understanding over the years. You have been my inspiration and motivation.

I would further like to extend my deep appreciation to my brothers, Hassan and Yahya; my sisters, Fatimah and Gana; my nephew, Ali, and their families for their love and continuous prayers.

Above all, I wish to express my gratitude to my mother, Aisha Maafa, who has always believed in me and encouraged me.

Dedication

To

My Mother, Aisha Maafa

My Beloved Wife, Nuha Fagihi

My Beloved Children, Mohammed, Riyam and Firas

My Sisters, Fatimah and Gana

My Brothers, Hassan and Yahya

Table of Contents

List of Figures

List of Tables

Nomenclature

$[C]$	catalyst concentration
$[H_2]$	hydrogen concentration
$[M]$	ethylene concentration
$[S_0]$	chain shuttling agent concentration
>=2S,2H	chains with 4 or more blocks (multi-blocks)
1, 2	catalyst type *P* and *Q*
1H	chains with single hard block
1S	chains with single soft block
1S,1H	chains with di-blocks
1S,2H	chains with tri-blocks (1soft and 2 hards)
2S,2H	chains with tri-blocks (2softs and 1 hard)
A, *B*	ethylene and 1-octene
A_p	ethylene consumption by catalysts *P* and *Q*
$A_{p,1}$	ethylene consumption by catalyst *P*
$A_{p,2}$	ethylene consumption by catalyst *Q*
B_p	1-octene consumption by catalysts *P* and *Q*
$B_{p,1}$	1-octene consumption by catalyst *P*
$B_{p,2}$	1-octene consumption by catalyst Q
C	active site
C_1, C_2	active site from catalyst *P* and *Q*
CCD	chemical composition distribution
C_d	deactivated site of catalyst

C_{d1}	deactivated site of catalyst P
C_{d2}	deactivated site of catalyst Q
$C^{in}{}_{tot}$	total catalysts molar flow rate
CLD	chain length distribution
CSA	chain shuttling agent
CSP	chain shuttling polymerization
CSTR	continuous stirred tank reactor
C_{tot}	total catalysts concentration
D_r	dead polymer chain of length r
$D_{r,i}$	dead polymer chain of length r and number of block i made in catalyst type P and Q
H_2	hydrogen
$H_2{}^{in}$	hydrogen molar flow rate
HDPE	high density polyethylene
i, j	number of blocks
$k_{C1}{}^{MC}$	microscopic deactivation of active catalyst P reaction rate constant
$k_{C2}{}^{MC}$	microscopic deactivation of active catalyst Q reaction rate constant
k_{CSA}	chain shuttling rate constant to dormant chain
k_{CSA0}	chain shuttling rate constant to CSA
$k_{CSA01}{}^{MC}$	microscopic chain shuttling reaction rate constant to CSA for catalyst P
$k_{CSA02}{}^{MC}$	microscopic chain shuttling reaction rate constant to CSA for catalyst Q
$k_{CSA0}{}^{MC}$	microscopic chain shuttling reaction rate constant to CSA
$k_{CSA1cross}{}^{MC}$	microscopic cross-chain shuttling reaction rate constant to dormant chain for catalyst P

$k_{CSA1self}^{MC}$	microscopic self-chain shuttling reaction rate constant to dormant chain for catalyst P
$k_{CSA2cross}^{MC}$	microscopic cross-chain shuttling reaction rate constant to dormant chain for catalyst Q
$k_{CSA2self}^{MC}$	microscopic self-chain shuttling reaction rate constant to dormant chain for catalyst Q
k_{CSA}^{MC}	microscopic chain shuttling reaction rate constant to dormant chain
k_d	deactivation rate constant
k_{d1}^{MC}	microscopic deactivation of growing chain reaction rate constant for catalyst P
k_{d2}^{MC}	microscopic deactivation of growing chain reaction rate constant for catalyst Q
k_{dC}^{MC}	microscopic deactivation of active catalyst reaction rate constant
k_{dP}^{MC}	microscopic deactivation of growing chain reaction rate constant
k_{H1}^{MC}	microscopic chain transfer to hydrogen reaction rate constant for catalysts P
k_{H2}^{MC}	microscopic chain transfer to hydrogen reaction rate constant
k_{H2}^{MC}	microscopic chain transfer to hydrogen reaction rate constant for catalysts Q
k_i	initiation rate constant
k_{iA1}^{MC}	microscopic initiation reaction rate constant for ethylene in catalysts P
k_{iA2}^{MC}	microscopic initiation reaction rate constant for ethylene in catalysts Q
k_{iB1}^{MC}	microscopic initiation reaction rate constant for 1-octene in catalysts P
k_{iB2}^{MC}	microscopic initiation reaction rate constant for 1-octene in catalysts Q
k_i^{MC}	microscopic initiation reaction rate constant
k_p	propagation rate constant
k_{pA1}^{MC}	microscopic propagation reaction rate constant for ethylene in catalysts P
k_{pA2}^{MC}	microscopic propagation reaction rate constant for ethylene in catalysts Q
k_{pB1}^{MC}	microscopic propagation reaction rate constant for 1-octene in catalysts P

k_{pB2}^{MC}	microscopic propagation reaction rate constant for 1-octene in catalysts *Q*
k_p^{MC}	microscopic propagation reaction rate constant
k_{tH}	chain transfer to hydrogen rate constant
$k_{t\beta}$	β-hydride elimination chain transfer rate constant
$k_{t\beta 1}^{MC}$	microscopic β-hydride elimination chain transfer reaction rate constant for catalysts *P*
$k_{t\beta 2}^{MC}$	microscopic β-hydride elimination chain transfer reaction rate constant for catalysts *Q*
$k_{t\beta}^{MC}$	microscopic β-hydride elimination chain transfer reaction rate constant
LCB	long chain branches
LDPE	low density polyethylene
LLDPE	linear low density polyethylene
M	ethylene
MC	Monte Carlo
M^{in}	ethylene molar flow rate
M^{in}_{tot}	total monomers molar flow rate
MM	method of moments
M_n	number average molecular weight
M_p	ethylene consumption
M_{tot}	total monomers concentration
M_w	weight average molecular weight
MWD	molecular weight distribution
n	maximum number of blocks
N_A	Avogadro's number

n_A	number of ethylene molecules
n_B	number of 1-octene molecules
n_c	number of catalyst molecules
n_{c1}	number of catalyst *P* molecules
n_{c2}	number of catalyst *Q* molecules
nCDp	number of deactivated chains from catalyst *P*
nCDq	number of deactivated chains from catalyst *Q*
nDP	number of dead chains from catalyst *P*
nDQ	number of dead chains from catalyst *Q*
n_{H2}	number of hydrogen molecules
n_M	number of ethylene molecules
nP	number of living chains from catalyst *P*
nQ	number of living chains from catalyst *Q*
n_{S0}	number of chain shuttling agent molecules
nSP	number of dormant chains from catalyst *P*
nSQ	number of dormant chains from catalyst *Q*
OBC	olefin block copolymer
P_1	living polymer chain of length 1
$P_{1,1}$	living polymer chain of length 1 and number of block 1 made in catalyst type *P*
PDI	polydispersity index
P_r	living polymer chain of length *r*
$P_{r,i}$	living polymer chain of length *r* and number of block *i* made in catalyst type *P*

P_s	living polymer chain of length s
$Q_{1,1}$	living polymer chain of length 1 and number of block 1 made in catalyst type Q
$Q_{r,i}$	living polymer chain of length r and number of block i made in catalyst type Q
r, s	chain length
r_1 and r_2	random number and reactivity ratios
R_{C1}^{MC}	Monte Carlo deactivation of active catalyst P reaction rate
R_{C2}^{MC}	Monte Carlo deactivation of active catalyst Q reaction rate
R_{CSA01}^{MC}	Monte Carlo chain shuttling reaction rate to CSA for catalyst P
R_{CSA02}^{MC}	Monte Carlo chain shuttling reaction rate to CSA for catalyst Q
R_{CSA0}^{MC}	Monte Carlo chain shuttling reaction rate to CSA
$R_{CSA1cross}^{MC}$	Monte Carlo cross-chain shuttling reaction rate to dormant chain for catalyst P
$R_{CSA1self}^{MC}$	Monte Carlo self-chain shuttling reaction rate to dormant chain for catalyst P
$R_{CSA2cross}^{MC}$	Monte Carlo cross-chain shuttling reaction rate to dormant chain for catalyst Q
$R_{CSA2self}^{MC}$	Monte Carlo self-chain shuttling reaction rate to dormant chain for catalyst Q
R_{CSA}^{MC}	Monte Carlo chain shuttling reaction rate to dormant chain
R_{d1}^{MC}	Monte Carlo deactivation of growing chain reaction rate for catalyst P
R_{d2}^{MC}	Monte Carlo deactivation of growing chain reaction rate for catalyst Q
R_{dC}^{MC}	Monte Carlo deactivation of active catalyst reaction rate
R_{dP}^{MC}	Monte Carlo deactivation of growing chain reaction rate
R_{H1}^{MC}	Monte Carlo chain transfer to hydrogen reaction rate for catalysts P
R_{H2}^{MC}	Monte Carlo chain transfer to hydrogen reaction rate
R_{H2}^{MC}	Monte Carlo chain transfer to hydrogen reaction rate for catalysts Q

R_{iA1}^{MC}	Monte Carlo initiation reaction rate for ethylene in catalysts *P*
R_{iA2}^{MC}	Monte Carlo initiation reaction rate for ethylene in catalysts *Q*
R_{iB1}^{MC}	Monte Carlo initiation reaction rate for 1-octene in catalysts *P*
R_{iB2}^{MC}	Monte Carlo initiation reaction rate for 1-octene in catalysts *Q*
R_i^{MC}	Monte Carlo initiation reaction rate
r_n	number average chain length
R_{pA1}^{MC}	Monte Carlo propagation reaction rate for ethylene in catalysts *P*
R_{pA2}^{MC}	Monte Carlo propagation reaction rate for ethylene in catalysts *Q*
R_{pB1}^{MC}	Monte Carlo propagation reaction rate for 1-octene in catalysts *P*
R_{pB2}^{MC}	Monte Carlo propagation reaction rate for 1-octene in catalysts *Q*
R_p^{MC}	Monte Carlo propagation reaction rate
R_T^{MC}	total Monte Carlo reaction rates
$R_{t\beta 1}^{MC}$	Monte Carlo β-hydride elimination chain transfer reaction rate for catalysts *P*
$R_{t\beta 2}^{MC}$	Monte Carlo β-hydride elimination chain transfer reaction rate for catalysts *Q*
$R_{t\beta}^{MC}$	Monte Carlo β-hydride elimination chain transfer reaction rate
r_w	weight average chain length
s	reciprocal of the average residence time in CSTR
S_0	chain shuttling agent
S_0^{in}	chain shuttling agent molar flow rate
SBR	semi-batch reactor
SCB	short chain branches
SP_r	dormant polymer chain of length *r*

$SP_{r,i}$	dormant polymer chain of length r and number of blocks i made in catalyst type P
SP_s	dormant polymer chain of length s
$SQ_{r,i}$	dormant polymer chain of length r and number of blocks i made in catalyst type Q
SX_0	0^{th} moments of dormant chains
SX_1	1^{st} moments of dormant chains
SX_2	2^{nd} moments of dormant chains
$SX_{k,P}$	k^{th} moments of dormant chains for which catalyst P made the last block
$SX_{k,P,i}$	k^{th} moments of dormant chains having i blocks for which catalyst P made the last block
$SX_{k,Q}$	k^{th} moments of dormant chains for which catalyst Q made the last block
$SX_{k,Q,i}$	k^{th} moments of dormant chains having i blocks for which catalyst Q made the last block
t	polymerization time
T_g	glass transition temperature
T_m	melting temperature
V	simulation volume
x	ethylene molar conversion
X_0	0^{th} moments of dead chains
X_1	1^{st} moments of dead chains
X_2	2^{nd} moments of dead chains
x_B	1-octene mole fraction
$X_{k,P}$	k^{th} moments of dead chains for which catalyst P made the last block
$X_{k,P,i}$	k^{th} moments of dead chains having i blocks for which catalyst P made the last block
$X_{k,Q}$	k^{th} moments of dead chains for which catalyst Q made the last block

$X_{k,Q,i}$	k^{th} moments of dead chains having i blocks for which catalyst Q made the last block
x_p	catalyst P mole fraction (make soft block)
Y_0	0^{th} moments of living chains
Y_1	1^{st} moments of living chains
Y_2	2^{nd} moments of living chains
$Y_{k,P}$	k^{th} moments of the living chains growing in catalyst P
$Y_{k,P,i}$	k^{th} moments of living chains growing in catalyst P having i blocks
$Y_{k,Q}$	k^{th} moments of the living chains growing in catalyst Q
$Y_{k,Q,i}$	k^{th} moments of living chains growing in catalyst Q having i blocks
τ	average residence time (chapters 4 and 6)
τ	elapsed time between the consecutive reactions (chapters 3 and 5)

1. Introduction

Polyolefins such as polyethylene and polypropylene are among the most important thermoplastics worldwide due to their low cost, limited impact on the environment, and broad range of applications such as in household goods (grocery bags, food containers and toys), engineering plastics, automotive parts, medical appliances, and prosthetic implants.[1] Development of new polymers, and modifying and enhancing old polymers are goals for many researchers in both industry and academia.

Copolymerization is a way to produce a polymer with properties that are intermediate between the properties of two or more respective homopolymers.[2] Depending on the arrangement of the monomeric units along the backbone, the copolymers can be classified into three types: alternating, random and block copolymers. In alternating copolymers, comonomer molecules alternate in the chain. In random copolymers, the placement of the comonomers in the chain is random. In the block copolymer, long sequences of one comonomer are followed by long sequences of the other comonomer. Block copolymers can be di-blocks, tri-blocks or multi-blocks depending on the number of comonomer types used during polymerization.[3]

Block copolymers can be made with living polymerization by adding monomers of different types sequentially to the polymerization reactor.[4] One type of monomer (or combination of comonomers) is first polymerized to produce one block. In the absence of chain transfer reactions, this chain will continue growing when a different monomer (or combination of comonomers) is added in a subsequent step to make a second block type. In principle, the process can be repeated to make multi-block copolymers. The disadvantages of this strategy is that only one polymer is produced per catalyst molecule. In addition, the molecular weight distribution (PDI) is close to one, making the polymer difficult to process.[5] Controlled free radical polymerization, on the other hand, can be used to make block copolymers in a more efficient way, but these techniques cannot polymerize olefins.[3,6]

Olefin block copolymers (OBCs) can be produced using two catalysts with different reactivity ratios toward α-olefin incorporation in the presence of a chain shuttling agent (CSA) used to transfer growing polymer chains between the two different catalysts. This process is called *chain shuttling polymerization*, and it enables the preparation of a new class of thermoplastic elastomers

consisting of at least two blocks, one *soft* (high α-olefin fraction) and one *hard* (low α-olefin fraction). The soft block provides rubber-like (elastomeric) properties, such as hardness with a low glass transition temperature ($T_g < -40°C$). The hard block works as a physical crosslink to connect the rubbery blocks with high melting temperatures ($T_m \approx 135°C$). The chain shuttling polymerization resolves the problems of having to deal with both low reactivity and low polymerization temperature that are associated with living polymerization through sequential monomers to synthesize block copolymers.[7,8]

Building a mathematical model can help researchers understand the microstructure of polyolefins made by chain shuttling polymerization. The main objective of this thesis is to develop mathematical models to predict the microstructure of OBCs made in different reactor types and under distinct modes of operation. To reach this objective, the method of moments and Monte Carlo simulation were used to simulate OBCs production in semi-batch reactors and in continuous stirred tank reactors (CSTR) operated at steady state or under dynamic conditions. It is important to simulate semi-batch reactors because this is how catalysts are commonly tested in laboratory scales in most olefin polymerization laboratories in academia and industry, but it is even more important to simulate CSTRs because this is the type of reactor used industrially to make polyolefins. Having models that apply to both modes of operation will help scientists to determine how results obtained in their laboratories will translate into the industrial production of OBCs.

Olefin block copolymers are a new class of materials with yet undiscovered potential applications; to some academic and industrial researchers, they constitute a revolution in polyolefin production. Only a few published mathematical models have described the detailed molecular structure of OBCs. In this thesis, we developed comprehensive mathematical models for these interesting novel materials using various techniques, such as the method of moments and the Monte Carlo method.

The main objectives of this thesis are summarized below:

1. Apply the method of moments to model the ethylene chain shuttling polymerization in a semi-batch reactor using a single catalyst.
2. Apply the method of moments to model the ethylene chain shuttling polymerization in a CSTR dynamically and the steady state using a single catalyst.

3. Apply the dynamic Monte Carlo method to model the ethylene chain shuttling polymerization in a semi-batch reactor using a single catalyst.
4. Apply the method of moments to model the chain shuttling copolymerization in a semi-batch reactor using a dual catalyst.
5. Apply the method of moments to model the chain shuttling copolymerization in a CSTR dynamically and the steady state using a dual catalyst.
6. Apply the dynamic Monte Carlo method to model the chain shuttling copolymerization in a semi-batch reactor using a dual catalyst.

This thesis is divided into seven chapters, as summarized below:

Chapter 1 presents the introduction, research objectives, and thesis outline.

Chapter 2 reviews the literature on olefin polymerization and olefin block copolymers, including techniques used to develop the models employed in my research project.

Chapter 3 applies the method of moments and a dynamic Monte Carlo method to simulate the ethylene chain shuttling polymerization in a semi-batch reactor using a single catalyst. Different kinetic rate constants and operation conditions are investigated, and the dynamic Monte Carlo method and method of moments are compared.

Chapter 4 uses the method of moments to simulate the ethylene chain shuttling polymerization in a CSTR operated dynamically and at steady state. Different kinetic rate constants and operation conditions are investigated. Chapter 4 also examines the effect of the reactor type on polymer properties.

Chapter 5 applies the method of moments and a dynamic Monte Carlo simulation to investigate the detailed microstructure of OBCs made by chain shuttling copolymerization in a semi-batch reactor. Different kinetic rate constants and operation conditions are investigated. The discussion also compares the results obtained by dynamic Monte Carlo simulation and the method of moments.

Chapter 6 simulates OBC production in a CSTR operated dynamically or at steady state using the method of moments. Different kinetic rate constants and operation conditions and the effect of the reactor type on the polymer and block properties are investigated.

Chapter 7 summarizes the main conclusions of this thesis and proposes recommendations for future work.

2. Background and Literature Review

2.1 Introduction to Polyethylene

Polyethylene is the most popular and widely used commodity polymer today.[9] It can be conveniently classified into three main types: low density polyethylene (LDPE), linear low density polyethylene (LLDPE), and high density polyethylene (HDPE). Low density polyethylene, produced by free radical polymerization in high temperature and high pressure autoclave or tubular reactors, is the oldest type of polyethylene. It contains short chain branches (SCB) formed by backbiting and long chain branches (LCB) resulting from chain transfer to the polymer. The SCBs lowers its density to values varying from 0.91-0.94 g/cm^3, while the LCBs increase its melt strength and make LDPE easy to process in extruders with high throughput. The other two main types of polyethylenes, LLDPE and HDPE, are made with coordination catalysts, not by free radical polymerization. Linear low density polyethylene is a copolymer of ethylene and α-olefins (1-butene, 1-hexene, 1-octene) with densities in the range of 0.915-0.94 g/cm^3. Copolymerization of ethylene with α-olefins disrupts the order of polyethylene chains due to the introduction of SCBs. High density polyethylene is similar to LLDPE, but has fewer SCBs, with density in the range of 0.941-0.97 g/cm^3. Thus, the density, crystallinity and rigidity of LLDPE is lower than that of HDPE. Figure 2-1 illustrates the structures of these three main polyethylene types.[1]

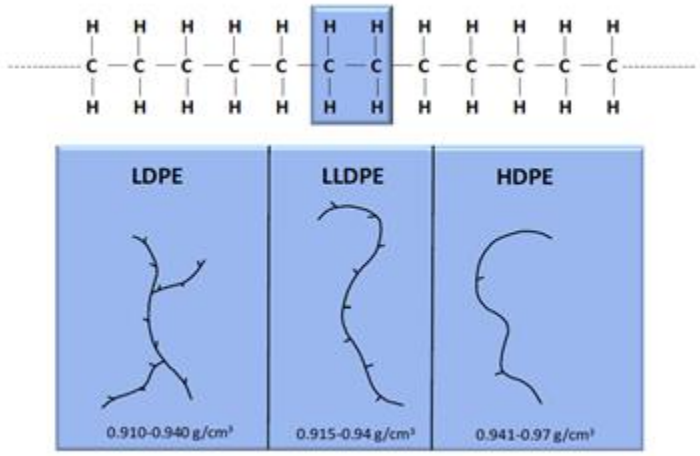

Figure 2-1. Polyethylene types.[1]

Four catalyst types are used to make HDPE and LLDPE resins: Ziegler-Natta, Phillips, metallocene, and post-metallocenes catalysts.

Zeigler-Natta catalysts were discovered by Karl Ziegler and Giulio Natta in the early 1950s. They consist of a transition metal salt from groups IV to VII (pre-catalyst), such as titanium tetrachloride ($TiCl_4$), and organometallic compounds from groups I to III of the periodic table (co-catalysts or activators), such as trimethyl aluminum (TMA), triethyl aluminum (TEA), or diethyl aluminum chloride (DEAC). The majority of Ziegler-Natta catalysts are solid (heterogeneous), although soluble (homogeneous) Ziegler-Natta catalysts, derived from vanadium compounds, are commonly used to make ethylene/propylene/diene (EPDM) rubbers. Heterogeneous Ziegler-Natta catalysts produce HDPE and LLDPE with broad molecular weight distributions (MWD) with a polydispersity index (PDI) in the range of 4-6, and broad and often bimodal chemical composition distributions (CCD) due to the presence of multiple active site types. Hydrogen is commonly used as a chain transfer agent to control polymer molecular weight.[1]

Hogan and Banks discovered the Phillips catalysts in 1951. Phillips catalysts are made by impregnating a chromium compound, such as CrO_3, onto a porous carrier, such as SiO_2, followed by calcination in dry air at high temperatures. Phillips catalysts do not need to be activated by a co-catalyst, but are instead activated by heat treatment at temperatures above 500 °C to fix the Cr species onto the silica surface. Hydrogen is not an effective chain transfer agent for these systems, but the MWD can be controlled by altering the characteristics of the support. Phillips catalysts also produce polymers with broad MWD, generally broader than those made with Ziegler-Natta catalysts, with PDI commonly exceeding 10. Phillips catalysts are mainly used to produce HDPE due to their lower reactivity ratios toward α-olefins. They account for approximately one-third of all HDPE produced globally.[1]

Effective metallocene catalysts for olefin polymerization were discovered in the 1980s. They are organometallic compounds based on early transition metals (typically Zr, Ti, or Hf) bonded by π-bonds between the metal and one or more aromatic rings, such as cyclopentadienyl or its derivatives. Figure 2-2 shows the general structure of a metallocene catalyst. Metallocene catalysts

also require an activator. Alkyl aluminum compounds, such as TMA and TEA, can be used to activate metallocenes, but the resulting system has poor activity. In 1977, Kaminsky and Sinn increased the activity of metallocenes by a factor of about 10,000 by using methylalumoxane (MAO) as an activator.[10] Unlike heterogeneous Ziegler-Natta catalysts, metallocenes are homogeneous molecular catalysts having only one type of active site. Therefore, they produce polyethylenes with narrow MWD, a theoretical PDI of 2, and narrow CCD.[1]

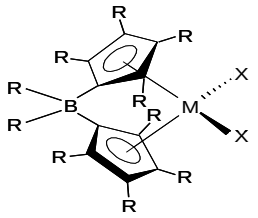

Figure 2-2. Generalized structure for a metallocene catalyst. M: transition metal; X: hydrocarbyl, alkylidene, halogen radicals; R: hydrogen, hydrocarbyl radicals; B: bridging group.

Late-transition metal catalysts (sometimes called post-metallocenes) were discovered by Brookhart and DuPont researchers in the early 1990s. These single-site catalysts are based on late-transition metals, such as palladium (Pd), nickel (Ni), and iron (Fe). They can be used to copolymerize ethylene with polar comonomers. Some late-transition metal catalysts, such as Ni-diimine complexes, can produce SCBs through the chain walking mechanism without the addition of α-olefin comonomers.[1]

Both LLDPE and HDPE are statistical copolymers of ethylene and α-olefins that have been in commercial production since the early 1950s. More recently, Dow Chemical showed that block copolymers[8,7,11,12,13] could be made if ethylene and α-olefins were copolymerized with two different coordination catalysts in the presence of a *chain shuttling agent* (CSA), and called these novel materials olefin block copolymers (OBC). Olefin block copolymers, made by *chain shuttling polymerization* (CSP) are the main subject of this thesis.

2.2 Chain Shuttling Copolymerization and Block Copolymers

Thermoplastic elastomer (TPE) block copolymers consist of at least two types of domains: soft and hard.[14] They may have different numbers of blocks, including linear di-block, tri-block, and multi-block, but they may also have branched structures, as shown in Figure 2-3.[15]

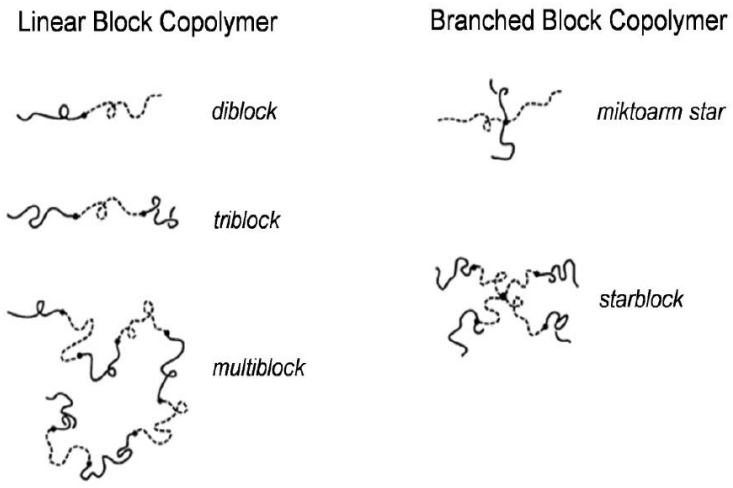

Figure 2-3. Block copolymer types.[15]

Polymers of different types usually do not mix, but tend to separate into different phases. Because the blocks in a block copolymer are linked by covalent bonds, they do not phase separate, but rather form microphase-separated morphologies. The formation of these separate phases depends on four factors: choice of monomers, molecular architecture, composition, and molecular size.[15]

Block copolymers can be made with living polymerization by adding monomers of different types sequentially to the polymerization reactor.[4] One type of monomer (or combination of comonomers) is first polymerized to produce one block. In the absence of chain transfer reactions, this chain will continue growing when a different monomer (or combination of comonomers) is added in a subsequent step to make a second block type. In principle, the process can be repeated to make multi-block copolymers.[5,16] The disadvantage of this strategy is that only one polymer is produced per catalyst molecule. In addition, the MWD is close to 1, making the polymer difficult

to process. Controlled free radical polymerization, on the other hand, can be used to make block copolymers in a more efficient way, but these techniques cannot polymerize olefins.[6,3]

Linear olefin block copolymers (OBCs) can be produced using two catalysts with different reactivity ratios toward α-olefin incorporation in the presence of a chain shuttling agent (CSA) used to transfer growing polymer chains between the two different catalysts. This process is called *chain shuttling polymerization*, and it makes a new class of thermoplastic elastomers consisting of at least two blocks, one *soft* (high α-olefin fraction) and one *hard* (low α-olefin fraction). This process is illustrated in Figure 2-4.

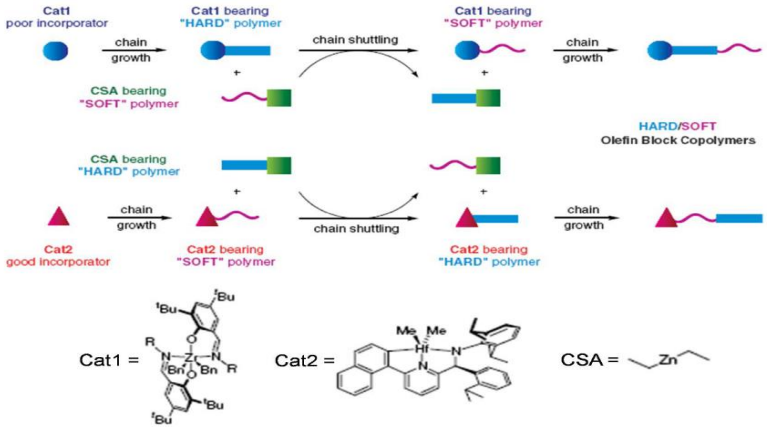

Figure 2-4. Mechanism of chain shuttling polymerization.[7]

The soft block provides rubber-like (elastomeric) properties with a low glass transition temperature (T_g < −40°C). The hard block works as a physical crosslink to connect the rubbery blocks with high melting temperatures (T_m ≈ 135°C). The large range between T_m and T_g makes these new polymers available for new applications, such as higher temperature applications. The potential applications for the OBC are the flexible extruder profile, such as refrigerator gaskets and flexible molded goods, such as soft-touch automotive and appliance parts. Other potential applications for OBC are elastic film and foam applications. The chain shuttling polymerization resolves the problems of having to deal with both low reactivity and low polymerization temperature that are

associated with living polymerization through sequential monomers to synthesis block copolymers.[12]

The mechanism for chain shuttling copolymerization consists of six steps: catalyst activation with cocatalyst, catalyst initiation with monomer, chain propagation, chain transfer, catalyst deactivation, chain shuttling to virgin chain shuttling agent (CSA), and chain shuttling to polymeryl-CSA.

With the exception of the steps involving CSA, these are the same elementary reactions present in all polymerizations with coordination catalysts, as shown in Figure 2-5. The pre-catalyst, Cp_2ZrCl_2, is activated by MAO to generate the monomethyl complex (Cp_2ZrCH_3Cl), and the use of excess MAO leads to $Cp_2Zr(CH_3)_2$ and ion-paired species $[Cp_2ZrCH_3]^+$ along with the counter $[X\text{-}Al(Me)O^-]_n^-$ (X=Cl, Me). The active center $[Cp_2ZrCH_3]^+$ attracts π-electrons in the olefin double bond (ethylene) and initiates the polymerization (n = 1), which is followed by a step-by-step insertion of ethylene achieving the cationic alkyl zirconocene. A β-hydride elimination reaction produces a dead polymer chain with terminal vinyl unsaturation and a metal hydride center (zirconocene cation), which can initiate a new polymer chain.[17]

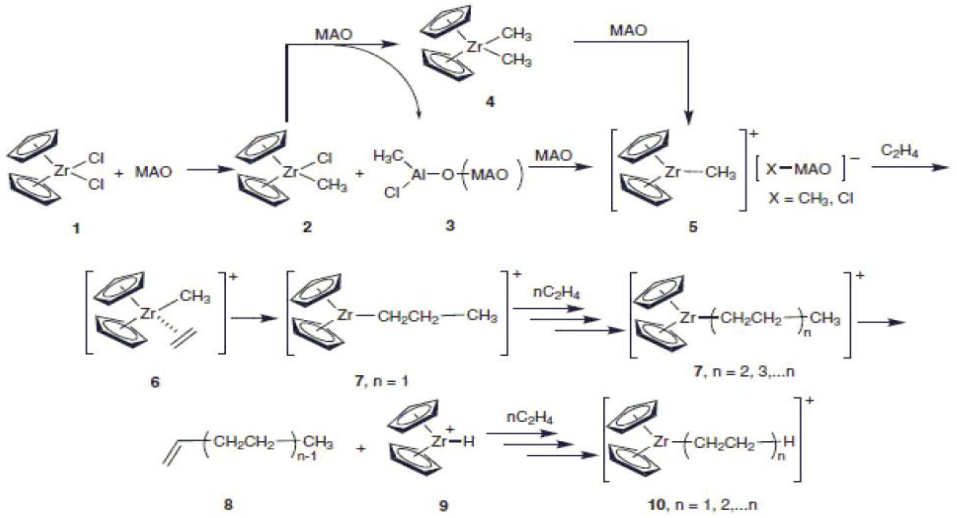

Figure 2-5. Ethylene polymerization mechanism with a zirconium complex.[17]

Adding a CSA to this system will generate other elementary reaction steps. During chain shuttling to a virgin CSA, the growing polymer chain of chain length r (P_r) transfers from an active site to a CSA (S_0) molecule, forming a dormant polymer chain (SP_r) while releasing an active center (C) than can form a new polymer chain, as shown in Equations (2-1),[18]

$$P_r + S_0 \xrightarrow{k_{CSA0}} SP_r + C \tag{2-1}$$

We assume that the active sites resulting from chain shuttling to CSA have the same behavior as those originally produced in the activation step.

Chain shuttling to a dormant chain is a reversible reaction between growing and dormant chains, as shown in Equation (2-2).

$$P_r + SP_s \xrightarrow{k_{CSA}} P_s + SP_r \tag{2-2}$$

where P_r and P_s are growing chains of length r and s, SP_r and SP_s are dormant chains of length r and s, k_{CSA0} is the chain shuttling rate constant to CSA and k_{CSA} is the chain shuttling rate constant to the dormant chain.

If we add two different catalysts P and Q to the system, every catalyst produces growing polymer chains (P_r and Q_r). These growing polymer chains react with CSA as shown in Equations (2-3) and (2-4), forming dormant polymer chains (SP_r and SQ_r) while releasing two active centers that can form two new polymer chains.

$$P_{r,i} + S_0 \xrightarrow{k_{CSA01}} SP_{r,i} + C_1 \tag{2-3}$$

$$Q_{r,i} + S_0 \xrightarrow{k_{CSA02}} SQ_{r,i} + C_2 \tag{2-4}$$

The CSA shuttles the growing polymer chains between the two active sites. When a CSA molecule reacts with a growing polymer chain, the latter becomes a dormant chain. A dormant chain generated by catalyst P attached to a CSA molecule, represented by $SP_{s,j}$, has two possibilities: 1) self-shuttling: it may be shuttled to catalyst P, represented by $P_{s,i}$, followed by a propagation step producing no new block (i.e., it will keep extending the length of the soft block, as shown in Equation (2–5)); or 2) cross-shuttling: it may be shuttled to catalyst Q, followed by a propagation

step, starting a new polymer block (generated by catalyst *Q*) attached to the soft block generated by catalyst *P*, as described in Equation (2–7). This process is repeated several times until chain transfer takes place or the polymerization stops. A similar process occurs for dormant chains made by catalyst *Q*, represented by $SQ_{s,j}$.[18]

$$P_{r,i} + SP_{s,j} \xrightarrow{k_{CSA1self}} P_{s,j} + SP_{r,i} \tag{2-5}$$

$$P_{r,i} + SQ_{s,j} \xrightarrow{k_{CSA1cross}} P_{s,j+1} + SP_{r,i} \tag{2-6}$$

$$Q_{r,i} + SP_{s,j} \xrightarrow{k_{CSA2cross}} Q_{s,j+1} + SQ_{r,i} \tag{2-7}$$

$$Q_{r,i} + SQ_{s,j} \xrightarrow{k_{CSA2self}} Q_{s,j} + SQ_{r,i} \tag{2-8}$$

In Equations (2-5) to (2-8), $k_{CSA1self}$ and $k_{CSA2self}$ are self-chain shuttling rate constants (growing and dormant chains made in the same catalyst) for catalyst *P* and *Q*, $k_{CSA1cross}$ and $k_{CSA2cross}$ are cross-chain shuttling rate constants (growing and dormant chains made in different catalyst) for catalyst *P* and *Q*, and *i* and *j* are number of blocks per chain.

In their landmark paper, Arriolla et al.[7] tested a series of catalysts and CSAs to find a suitable set of conditions for the synthesis of OBCs. They determined that diethylzinc (Et_2Zn) was a good candidate for CSA, combined with a dual catalyst system formed by zirconium bis(phenoxyimine) and hafnium pyridylamide. The cocatalyst used to activate these single-site catalysts was fluorinated phenylborate. The monomer was ethylene and the comonomer was 1-octene.[19] The polymerization temperature was greater than 120 °C to prevent polymer precipitation. Arriolla et al. investigated every catalyst individually and as a mixture, in the absence or presence of CSA. In the absence of Et_2Zn, the copolymers have a high molecular weight and bimodal MWD (PDI = 13.8), but in the presence of Et_2Zn, the molecular weight of the copolymer decreased and the MWD converged to the most probable molecular weight distribution (PDI = 1.97) as shown in Figure 2-6.[8]

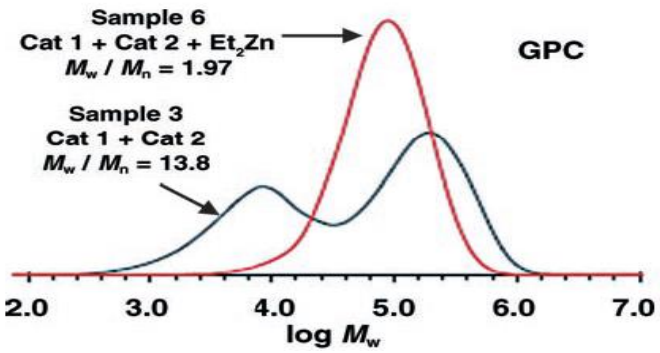

Figure 2-6. Effect of CSA on the MWD of an ethylene/1-octene copolymer made with two catalysts in a semi-batch reactor.[12]

Diethyl zinc (Et_2Zn) had long been used as a chain transfer agent with Ziegler-Natta catalysts, but for many decades it has been replaced by hydrogen.[20] Et_2Zn decreases the polymer molecular weight and reduces catalyst activity due to the formation of strong heterodinuclear adducts of the type $[L_2Zr(\mu\text{-alkyl})\ (\mu\text{-R})ZnR]^+$. It can also be used as an impurity scavenger with Phillips catalysts. Wei[21] reported that adding a suitable amount of Et_2Zn to ethylene polymerization using metallocene/MAO can increase the activity four to five times and double it for ethylene copolymerization compared to polymerization without Et_2Zn; however, the molecular weight decreases as the Zn/Zr ratio increases. Wei claimed that the reduction of the molecular weight is not significant at low concentrations of Et_2Zn. Zirconium bis(phenoxyimine) was independently discovered by Fujita et al.[22] and Coates[23] in 1998. It is highly active for ethylene polymerization, being twice as active as Cp_2ZrCl_2 under the same conditions.[24] In 2004, Dow Chemical discovered hafnium pyridylamide,[25] which is also very active for ethylene polymerization and shows highly isotactic selectivity in the case of polypropylene and good α-olefin incorporation. This catalyst is thermally robust and produces polymers with high molecular weights.

The advantage of chain shuttling polymerization over other methods that may be used to make block copolymers is that it uses two active propagation centers and can be conveniently operated in a CSTR at high production rates. The use of a CSTR also produces OBCs with the most probable distribution for both block length and molecular weight, making these polymers easier to process.[18]

Chain shuttling polymerization may also be used to produce mainly di-block OBCs using a single catalyst and two CSTRs in series operated under different polymerization conditions. Hustad et

al.[11] synthesized a di-block by using the catalyst hafnium pyridylamide following the procedure illustrated in Figure 2-7: 1) ethylene, α-olefin (low concentration), catalyst, and CSA were fed to the first CSTR to produce HDPE blocks; 2) the contents of the first CSTR flowed continuously to the second CSTR to which fresh catalyst, ethylene, and a high amount of α-olefin was added to produce very low density polyethylene (VLDPE) blocks. This procedure makes a di-block polymer with hard (HDPE) and soft (VLDPE) blocks, differently with the multi-block polymers made with two catalysts in a single CSTR.

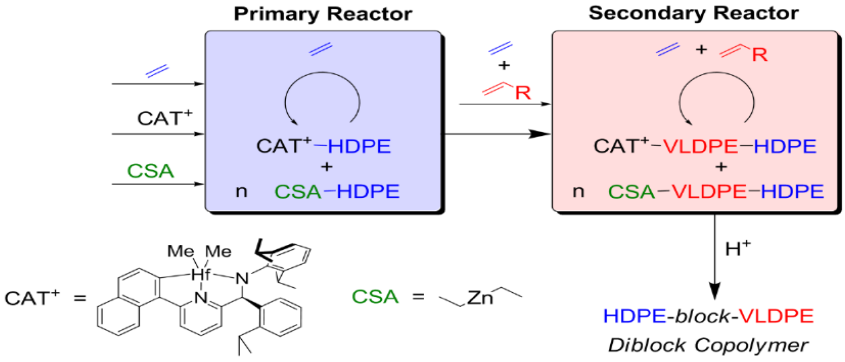

Figure 2-7. Preparation of di-block OBC.[11]

Chain shuttling polymerization may also be combined with chain walking polymerization to synthesize linear-hyperbranched multiblock polyethylene using a mixture of two catalysts where one catalyst (such as a Ni-diimine catalyst) produces branched polyethylene via chain walking polymerization, and the other catalyst (such as a metallocene) makes linear polyethylene in the presence of a CSA to shuttle blocks between the two catalyst types.[26,27] Martins et al. [26] reported the synthesis of such block ethylene copolymers using an α-diimine nickel and rac-ethylene bis(H_4-indenyl)$ZrCl_2$, and Et_2Zn as a CSA at different temperatures. The authors found that polymerizing ethylene with the two catalysts without Et_2Zn produced a less crystalline polyethylene, but when Et_2Zn was introduced in the reactor, the crystallinity increased. The polymer produced by the α-diimine nickel catalyst was amorphous, whereas that made with rac-ethylene bis(H_4-indenyl)$ZrCl_2$ had a high melting temperature. The polymer made by the catalyst mixture without Et_2Zn had a melting temperature lower than or equal to that of the polymer produced by rac-ethylene bis(H_4-indenyl)$ZrCl_2$ alone. However, adding Et_2Zn led to the

production of polymer with a higher melting temperature. No data was provided for the MWD, and since chain shuttling cannot be confirmed from the melting temperature data alone, it is questionable whether the authors indeed made block copolymers in their experiments. Similar work was carried out by Xiao et al.[27], but they used different catalysts: α-diimine nickel (II)bromide and rac-Et(Ind)$_2$ZrCl$_2$. The resulting polymer was a linear-hyperbranched multiblock polyethylene due to the exchange of the growing polymer chain between the two catalysts via CSA. Without CSA, the produced polyethylene was bimodal with a broad MWD with PDI = 3.77, but by introducing CSA the MWD became unimodal with PDI = 1.91. ^{13}C NMR was used to confirm the branching structure, demonstrating that short branches from methyl, ethyl, butyl, and amyl were produced. The authors proposed that their polymer would have better end-use properties, such as a higher melting temperature due to the existence of linear polyethylene and increased toughness due to the existence of hyper-branched polyethylene.

Van Meurs et al.[28] reported different catalysts for ethylene polymerization in the presence of MAO with and without Et$_2$Zn. In the presence of Et$_2$Zn, they found most catalysts produced polymers with MWD between Flory's to Poisson's distribution.

Chain shuttling polymerization can be also used to make isotactic stereoblock polypropylene. Xiao et al.[29] investigated the effect of Et$_2$Zn as a CSA on polypropylene synthesized with two metallocene catalysts: rac-Et(Ind)$_2$ZrCl$_2$ (isotactic polypropylene) and Cp$_2$ZrCl$_2$ (atactic polypropylene). The addition of Et$_2$Zn decreased the activity of the dual catalysts, the melting point, and the crystallinity of polypropylene. It also decreased the average molecular weight due to the chain shuttling reaction, but strangely, the MWD did not change. They found that the value of the [*mmmm*] pentad decreased from 92 to 84 with the presence of Et$_2$Zn and new peaks of [*rmmr*] and [*rmrr+mmrm*] pentads appeared when Et$_2$Zn was used as confirmed by ^{13}C NMR due to the altering of the microstructure of polypropylene by chain shuttling polymerization.

Chien et al.[30] studied the polymerization of propylene using a mixture of two zirconium catalysts: rac-ethylenebis- (1-η^5-indenyl)zirconium dichloride as Cat1 or rac-dimethylsilylenebis(1-η^5-indenyl)zirconium dichloride as Cat2 (Cat1 and Cat2 make isotactic polypropylene, i-PP) and ethylenebis(9-η^5-fluorenyl)zirconium dichloride as Cat3 (make syndiotactic polypropylene, s-PP) with the presence of triisobutylaluminum (TIBA), a cocatalyst. They use Cat1/Cat3 or Cat2/Cat3 as a mixture in the ratio from 8:2 to 1:9 and individually to polymerize the propylene in different

polymerization conditions. The obtained polymer was a blend of isotactic (i-PP) and syndiotactic (s-PP) polypropylene as well as a small stereoblock fraction (i-PP-b-a-PP). The ^{13}C nuclear magnetic resonance (^{13}C- NMR) and the microscopy analysis showed the presence of the stereoblock fraction. The gel permeation chromatography (GPC) showed broad MWD (PDI = 2.82).

Chien et al.[31] studied the polymerization of propylene using a mixture of two zirconium catalysts: diphenylmethylidene (1-η^5-cyclopentadienyl)-(9-η^5-fluorenyl)zirconium dichloride (makes s-PP) and rac-ethylenebis- (1-η^5-indenyl)zirconium dichloride (makes i-PP) with the presence of TIBA, a cocatalyst. A bimodal molecular weight distribution was detected by GPC. Fourier transform infrared spectroscopy (FTIR) showed that GPC fractions contain i-PP and s-PP. The authors proposed the exchange of propagation chains between the two catalyst sites and concluded that this principle can be used to produce i-PP and s-PP segments in the same chain.

Przybyla and Fink[32] used two different catalysts supported on the same silica carrier to produce isotactic, syndiotactic, and stereoblock polypropylene. They studied two systems: 1) rac-$Me_2Si[Ind]_2ZrCl_2$ (makes i-PP) and i-Pr[FluCp]-$ZrCl_2$ (makes s-PP) are supported on a PQ-Silica/MAO and 2) rac-$Me_2Si[IndR_2]_2ZrCl_2$ and i-Pr[FluCp]-$ZrCl_2$ are supported on a Grace Silica/MAO. They were able to produce stereoblock polypropylene using the first system. The existence of stereoblock chains was proven by the fractionating results by using TREF followed by ^{13}C-NMR and GPC analysis. The GPC analysis showed that the first fraction consisted mainly of i-PP and parts of a stereoblock, the fifth fraction was nearly pure s-PP and parts of a stereoblock, and the third fraction was a stereoblock. The NMR showed that the fifth fraction was nearly pure s-PP with traces of a stereoblock. The melting temperature of all polymer fractions varied between the melting temperature of i-PP and s-PP.

Lieber and Brintzinger[33] reported the polymerization of propylene using Me_2Si(2-Me-4-tBu-$C_5H_2)_2ZrCl_2$/MAO (makes i-PP), Me_2Si(2-MeInd)$_2ZrCl_2$/MAO (makes i-PP), $H_4C_2(Flu)_2ZrCl_2$/MAO (makes a-PP), and $Ph_2C(Cp)FluZrCl_2$/MAO (makes s-PP). Different catalysts were studied, both individually and as a mixture, and the authors concluded that the formation of stereoblock polypropylene depended on the exchange between the catalyst centers and the Al centers of the cocatalyst.

Tynys et al.[34] studied the effect of diphenylmethyl(cyclopentadienyl)(9-fluorenyl)zirconium dichloride and *rac*-dimethylsilybis(4-tert-butyle-2-methyle-cyclopentadienyl)zirconium dichloride on the polymerization of propylene. The first catalyst produced high molecular weight syndiotactic polypropylene and the second low molecular weight isotactic polypropylene. To shuttle the polymer chain between the two catalysts, trimethylaluminium (TMA) was used as a CSA. The product was a mixture of isotactic and syndiotactic polypropylene. The GPC analysis showed a bimodal peak, indicating extremely limited reversible transfer. Even the isotactic and syndiotactic polypropylene blocks had a high melting temperature ($T_m \approx 133°C$), but relatively high glass temperatures ($T_g \approx 0°C$).

Pan et al.[35] reported the first example of chain-shuttling copolymerization of styrene, isoprene, and butadiene using binary mixtures of the three catalysts shown in Figure 2-8 and TiBA as a CSA. Catalyst 1 has high activity and high selectivity for syndiotactic polystyrene (s-PS), but low activity and low selectivity for isoprene; Catalyst 2 has high activity and high cis-1,4-selectivity for isoprene polymerization, but low activity and low selectivity for styrene polymerization; Catalyst 3 has high 3,4-selectivity for isoprene polymerization. Using catalyst 1 and catalyst 2 without CSA, the copolymerization of styrene and isoprene gave a polymer mixture of cis-1,4-PIP homopolymer and a styrene–isoprene copolymer containing mainly s-PS blocks with mixed 1,4-/3,4-PIP units. By adding the CSA to the previous mixture, the copolymerization of styrene and isoprene took place. A perfect s-PS and highly regulated cis-1,4-PIP blocks with high molecular weight (M_n=109.4 kg/mol) and narrow MWD (PDI = 1.43) was prepared. Using catalyst 1 and catalyst 3 without CSA, the copolymerization of styrene and isoprene gave PS and PIP sequences. By adding CSA to the previous mixture, the copolymerization of styrene and isoprene had perfect s-PS (>99%) and 3,4-PIP (90%) blocks.

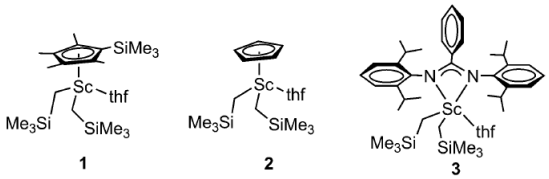

Figure 2-8. Structure of scandium catalysts used by Pan et al.[35]

Valente et al.[36] classified the chain shuttling polymerization of ethylene, propylene and α-olefins into three cases: 1) Single monomer (ethylene) and multiblock linear-branched polyethylene: one catalyst makes linear polyethylene blocks, and the other produces branched blocks via chain-walking polymerization; 2) Two monomers (ethylene/α-olefin) and multiblock linear polyethelene: one catalyst forms HDPE blocks, and the other makes lower density blocks; and 3) Single monomer (propylene) and multiblock stereoblock polypropylene: one catalyst produces isotactic polypropylene blocks, and the other makes syndiotactic or atactic polypropylene.

2.3 Chain Shuttling Polymerization Modeling and Characterization

The characterization of the OBC microstructure is a challenging task because the conventional characterization technique cannot directly probe either the distribution or the average number of blocks per chain. We can fractionate mixtures of substances and characterize the comonomer content, for example, using NMR, but in the case of OBC, it is impossible to separate the hard and soft blocks because they are covalently connected.[37]

In olefin copolymers, Flory's equilibrium melting theory showed that the relationship between melting temperature and mole fraction of crystallizable unit is linear by plotting Ln (X) vs 1/T as shown in Figure 2-9. In OBCs, the linearship is deviated.[38]

$$\frac{1}{T_m} - \frac{1}{T_m^0} = \frac{T_m^0 - T_m}{T_m T_m^0} = -\left(\frac{R}{\Delta H_u}\right) \ln x_A \tag{2-9}$$

In Equation (2-9), T_m^0 is the melting temperature of an infinited long chain of homopolymer A, T_m is the melting temperature of a random copolymer AB, ΔH_u is the enthalpy of melting for repeating unit A and x_A is the molar fraction of the crystallizable unit A.

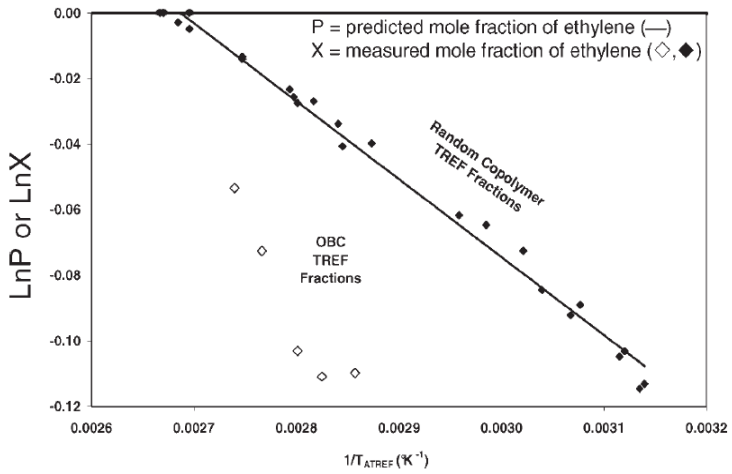

Figure 2-9. Flory theory.[38]

By using Pythagorean Theorem, Shan and Hazlitt[38] built two triangles as shown in Figure 2-10. T_x is the elution temperature measured by ATREF, X_x is the ethylene mole fraction measured by NMR, T_A is the ATREF elution temperature for the pure ‘‘hard segment’’, and P_A is the ethylene mole fraction for the pure ‘‘hard segment’’. T_A and P_A can be set to values for high density polyethylene homopolymer or it can be set to values corresponding to the actual hard segment, if known. The P_{AB} corresponds to the measured (NMR) ethylene mole fraction in the whole polymer prior to fractionation and the T_{AB} corresponds to the calculated random copolymer equivalent ATREF elution temperature based on the measured P_{AB}. From the measured ATREF elution temperature, T_X, the corresponding random ethylene mole fraction, P_{X0}, can also be calculated. Similarly, from the measured NMR composition, X_X, the corresponding random elution temperature, T_{X0}, can be calculated.

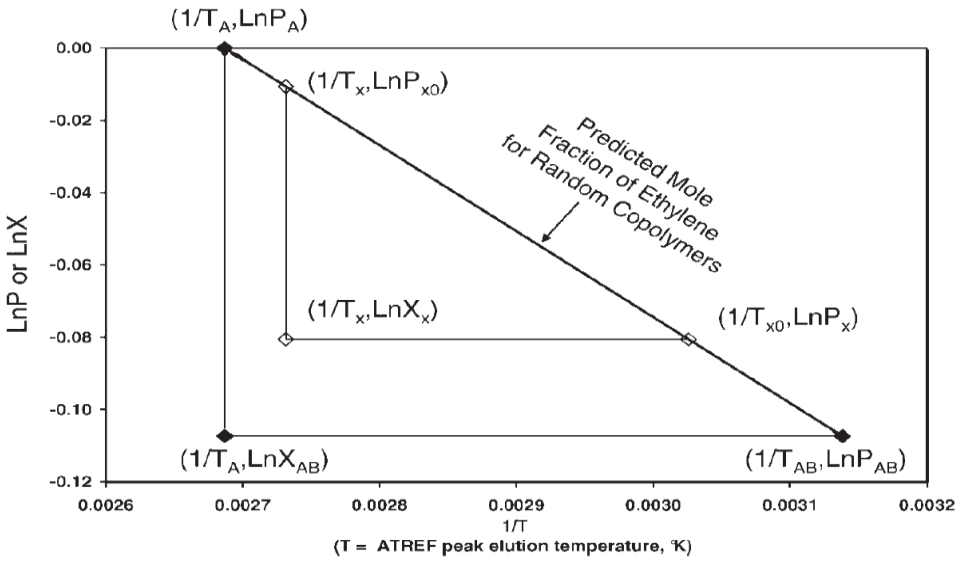

Figure 2-10. Definition of the block index.[38]

Shan and Hazlitt[38] defined the ratio of the area of the (T_X, X_x) triangle and the (T_A, X_{AB}) triangle, as the block index (BI). The BI is used to quantify the deviation of the peak temperature of analytical temperature rising elution fractionation (ATREF) profiles of OBCs from that of random copolymers with the same comonomer fraction. The BI can vary from zero to one: if BI = 0, the comonomer is randomly distributed in the copolymer; as the value of BI increases, the copolymer becomes "blockier".

$$BI = \frac{1/T_x - 1/T_{x0}}{1/T_A - 1/T_{AB}} \tag{2-10}$$

where T_x is the peak TREF elution temperature (T_e) of the OBC fraction of narrow chemical composition, T_{x0} is the elution temperature of the equivalent narrow composition random copolymer, T_A is the elution temperature of chains composed of a single hard block, and T_{AB} is the elution temperature of a random copolymer with the same average composition of the whole OBC. This parameter can be used to interpret the degree to which the intra-chain comonomer distribution is blocked—namely, the larger the BI, the "blockier" the polymer will be. The BI value can be used to shift the elution temperature from the expected elution temperature of the equivalent random ethylene/α-olefin copolymers (T_{x0}) to that of the OBC (T_x) as shown in Figure 2-11.

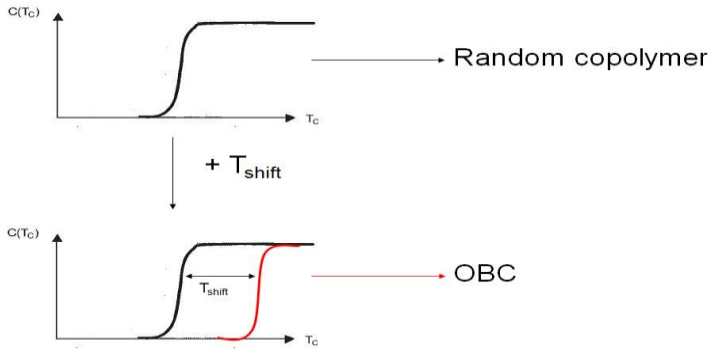

Figure 2-11. Melting temperature shifts in OBC.

Anantawaraskul et al.[39] developed a Monte Carlo simulation to describe the CRYSTAF profiles for OBC. The model was adapted from the CRYSTAF model for random ethylene/α-olefin copolymers, where the longest ethylene sequence (LES) depends on the molecular weight and the copolymer content. They used the BI definition and a linear relationship between the BI and comonomer content based on the equation developed by Shan and Hazlitt.[38] The effect of polymerization parameters (chain shuttling probability, propagation probability, and catalyst ratio) on the distribution of the longest ethylene sequence (LES) per chain and Crystaf profile was investigated. Anantawaraskul et al. found that when the chain shuttling probability increases from zero to 0.2306, the LES distribution moves from bimodal to unimodal.

$$BI = 4.7833 \times CC + 0.143 \tag{2-11}$$

In Equation (2-11), CC is the comonomer content that can be predicted by the Monte Carlo model. The degree of crystallinity of a random ethylene and α-olefin copolymer can be calculated by using the Avrami equation for the same monomer content and LES as each simulated from the Monte Carlo model. The BI estimated for each chain and the simulated results (i.e., comonomer contents and LES) can be used to shift the OBC chains' crystallization temperature and predict the CRYSTAF profile.

Anantawaraskul et al.[40] extended their previous model to study the effect of polymerization parameters (chain shuttling probability, propagation probability, and catalyst ratio) on the chemical composition distribution (CCD). They found that with small chain shuttling probability (P_s), the

LES and CCD distribution are bimodal distribution , but as P_s increases the bimodal distribution converts into a single distribution.

Mathematical models are required to help understand the complex microstructures of polymers made by chain shulling polymerization involving several catalysts, cocatalysts, CSAs, comonomers, and reactors. Several modeling techniques can be used to predict these microstructures from an assumed polymerization mechanism and conditions. Population balances can be used to describe the complete MWD of polymers based on molar balances for the concentration of living, dead, and dormant polymer chains of different lengths, but a large computational effort is required to solve the resulting set of simultaneous ordinary differential equations. The method of moments is a simple approach to modelling molecular weight averages because it only requires solving a few ordinary differential equations to obtain the 0^{th}, 1^{st}, and 2^{nd} (or higher) moment equations of the full MWD. The method of instantaneous distributions can also be used to describe the complete MWD, but distributions are not yet available for chain shuttling polymerization. Finally, Monte Carlo simulation is a powerful method based on reaction probabilities and randomly generated numbers that can be used to predict the complete MWD and other microstructural distributions of polymers made with chain shuttling polymerization without solving any differential or algebraic equations.[41]

Hustad et al.[42] described a model for chain shuttling polymerization to study the effects of reversibility of chain shuttling on the number and weight average molecular weight with a single catalyst in a semi-batch reactor. The model was based on population balances and the method of moments. The authors investigated three theoretical cases: irreversible chain shuttling (chain shuttling rate constant to CSA, $k_{CSA0} > 0$ and chain shuttling rate constant to dormant chain is zero, $k_{CSA} = 0$), reversible chain shuttling ($k_{CSA0} = k_{CSA} > 0$), and semi-reversible chain shuttling ($k_{CSA0} > 0$ and $k_{CSA} > 0$, but $k_{CSA0} \neq k_{CSA}$). They found that, in the case of irreversible chain shuttling, initially PDI increases dramatically above 2 and then drops to 2 as the polymerization goes on. In the case of reversible chain shuttling, the PDI first falls below 2 and then increases due to the accumulation of dead polymers in the reactor resulting from the chain transfer reaction. In the case of the semi-reversible chain shuttling, if $k_{CSA0} >> k_{CSA} > 0$, at the initial point of polymerization, the PDI increases dramatically above 2 and then drops to 2 as the polymerization proceeds. As k_{CSA} approaches k_{CSA0}, the PDI initially decreases below 2 and approaches 2 as the polymerization

proceeds. The model does not consider the effect of reversibility of chain shuttling on the chain microstructure of copolymerization using dual catalysts.

Zhang et al.[43] conducted a theoretical investigation of the validity of the Mayo-Lewis equation in chain shuttling copolymerization using one or two catalysts. They found that, in the presence of CSA, the Mayo-Lewis equation is valid only if one catalyst is used. However, if dual catalysts are used, the Mayo-Lewis equation is only valid if the rate of chain shuttling is smaller than the rate of propagation. But if this condition is violated (i.e., the rate of chain shuttling is higher than the rate of propagation), the Mayo-Lewis equation is not valid due to variations in the composition of the active center.

Zhang et al.[18] were the first to develop a kinetic model for the chain shuttling copolymerization of ethylene and α-olefin with dual catalysts in a single stirred-tank reactor using the method of moments. Only chain transfer to hydrogen was considered. The model assumed that the operation of the CSTR was homogeneous and isothermal. Their model predicted the average molecular weight properties and overall copolymer composition, which was validated using Arriolla et al.'s experimental data.[7] Different cases have been investigated, including the effect of the chain shuttling rate constant, chain shuttling feed rate, catalyst composition, and monomer composition on the overall polymer structure (see Table 2.1).

Table 2.1. Summary of Zhang et al.'s[18] model (block copolymers in a single CSTR).

Factor	The effect
Increase of chain shuttling rate constant.	• M_n decreases and reaches a constant value before increasing again. • Polydispersity decreases and approaches 2.
Increase of chain shuttling agent feed rate.	• M_n decreases. • Polydispersity decreases and approaches 2.
Increase of molar fraction of catalyst 1 (good comonomer incorporator).	• Octene conversion increases, and ethylene conversion decreases slightly. • Weight fraction of block 1 (generated by catalyst 1) increases. • M_n decreases significantly. • Polydispersity increases slightly above 2 and then drops to 2, where it remains for a wide range of catalyst 1 composition because of the nature of chain shuttling.
Increase of ethylene weight fraction.	• Molar fraction of ethylene in each block increases. • No change in the hard block (block 2 generated by catalyst 2). • Ethylene and octene conversion increases because the less reactive octene tends to decelerate the polymerization. • M_n increases. • Polydispersity remains around 2 because of the nature of chain shuttling.

Zhang et al.[44] extended their previous work to predict the average block structure, such as average number of blocks per chain, average block length, and the average number of linkage points between the soft and hard blocks on a chain. The effects of the relative chain shuttling rate constant and relative chain shuttle feed rate on the average block structure were also investigated. The relative chain shuttling rate constant is defined as the ratio between the chain shuttling rate constant

and a reference chain shuttling rate constant, while the relative chain shuttling feed rate is defined as the ratio between the chain shuttling feed rate and a reference chain shuttling feed rate. The effect of the relative chain shuttling rate constant can be defined in two regions: Below 1, the average number of linkages is close to zero, but as the relative chain shuttling rate constant increases, the average number of linkages and blocks per chain increases, and the average length of blocks 1 and 2 decreases. Almost the same phenomenon was observed with the relative chain shuttling feed rate. As the relative chain shuttling feed rate increases, the average number of linkages and blocks per chain initially increases to a certain point and then drops while the average length of both blocks decreases, thereby indicating the homogenization of the resulting polymers. The model predicted the overall properties, but failed to capture the detailed properties of the individual blocks and their time evolution.

Ahmadi et al.[45] also used population balances and the method of moments to predict the molecular weight average of the whole polymer. They used different process conditions than Zhang et al. did in their paper. Ahmadi et al. studied the effect of the reversibility of the chain transfer on the molecular weight averages of the final product. Their model did not identify the properties of individual blocks (Chapters 5 and 6 in this thesis covers these missing properties from Zhang et al.'s and Ahmadi et al.'s works).

Anantawaraskul et al. were the first to develop a Monte Carlo simulation to study the effect of different parameters' probabilities on the distribution of the number of blocks per chain made in CSTR operated at steady state. They found that, as the probabilities of chain shuttling and the probability of propagation increased, the distribution of the number of blocks per chain and the weight average number of blocks per chain increased.[37]

Mohammadi et al.[46] developed a detailed model for chain shuttling polymerization using dynamic Monte Carlo simulation. Their model used the process condition published in Zhang et al.'s paper.[18] The effects of CSA on the copolymerization were studied. The effect of hydrogen and CSA on the ethylene sequence length distribution (ESLD) and longest ethylene sequence length (LESL) was studied. They found that the introducing CSA in CSP using two catalysts converts the bimodal MWD and CCD to unimodal. They found that the formation of dead chains led to increase the width of MWD and CCD. If no chain transfer occured, the CSP would fallow the characteristic of living polymerization i.e M_n increases linearly and PDI reaches unity.

Recently, the same authors extended their previous work to investigate the microstructural evaluation of hard and soft block populations, such as the average number of blocks per chain, block averages, degree of polymerization, PDI and comonomer composition as a function of time. They also studied the microstructural distribution at the end of polymerization such as the distribution of the number of blocks per chain, block length distribution, CCD and ESLD.[47] The effects of process conditions such as CSA level, monomer composition, and catalyst composition on the microstructure of OBC at the end of polymerization, such as the number of blocks, the lengths of soft and hard blocks, the composition of the blocks (SB/HB ratio), CCD of the overall polymer, were also studied by Ahmadi et al.[48] They found that at high CSA levels, the shuttling reaction is rapid and the blocks are so short and the average ESL would be undistinguishable between hard and soft blocks, i.e., the ratio of ESL between hard and soft blocks approaches unity, and a random copolymer is formed. On the other hand, at low CSA levels, copolymer chains can be formed independently by individual catalyst without any shuttling reaction. Different CCDs are produced at low CSA levels. The bimodal distribution disappears at higher CSA levels and converts to a narrow peak at higher CSA levels. Similar behavior can be obtained with MWD as a function of the CSA level; however, the difference is more profound in CCD.

More recently, Tongtummachat et al.[49] developed a dynamic Monte Carlo simulation to describe the kinetic of chain shuttling copolymerization using two catalysts operated in a semi-batch reactor. They used the same process condition as appeared in Zhang et al.'s paper[18] to study the effect of the CSA concentration and chain shuttling constant on the evolution of chains with a different number of blocks as a function of time. They found that the properties of OBCs depend strongly on the CSA concentration and chains shuttling constant. However, the concentration of CSA significantly affected the average molecular weights, the molecular weight distribution, and the number fraction for chains with different numbers of blocks. As the CSA concentration increased, the molecular weight averages for overall polymer and for chains with different numbers of blocks decreased, because the CSA works as a reversible chain transfer agent and chain shuttling agent at the same time. Furthermore, the increase in CSA concentration increased the number fraction of multi-blocks and decreased the number fraction of chains with fewer blocks because as CSA concentration increased, the chain shuttling rate increased.

3. Simulation of Ethylene Chain Shuttling Polymerization in a Semi-Batch Reactor using the Method of Moments and a Dynamic Monte Carlo Model

3.1 Overview

We simulated the chain shuttling polymerization of ethylene with a single catalyst in a semi-batch reactor using the method of moments and a dynamic Monte Carlo model. The method of moments predicts molecular weight averages, while the dynamic Monte Carlo method predicts the complete chain length distribution (CLD) of polyethylene as a function of polymerization time. The objective of this study was to compare the results obtained with the dynamic Monte Carlo method with the method of moments, and to use both techniques to study the effect of process conditions and simulation parameters on the microstructure of polyethylene made with chain shuttling polymerization.

3.2 Ethylene Chain Shuttling Polymerization Mechanism

The mechanism used for ethylene chain shuttling polymerization consists of six steps: catalyst initiation with ethylene, chain propagation, chain transfer, catalyst deactivation, chain shuttling to virgin chain shuttling agent (CSA), and chain shuttling to polymeryl-CSA (dormant polyethylene chain bonded to a CSA molecule). Table 3-1 summarizes these polymerization steps. Additional model assumptions include: 1) instantaneous activation of catalyst by co-catalyst, 2) constant reaction volume, 3) constant polymerization temperature, 4) reaction rates independent of chain length, 5) initiation rate constant, k_i, equal to the propagation rate constant, k_p, 6) first-order catalyst decay kinetics, and 7) active sites resulting from β-hydride elimination, chain transfer to hydrogen, and chain shuttling to CSA that have the same behavior as those originally produced in the activation step. Chain transfer happens via two mechanisms: β-hydride elimination and chain transfer to hydrogen.

The polymerization mechanism in Table 3-1 is the same as the standard one for olefin polymerization with coordination catalysts, except for the steps involving CSA, as was explained in Chapter 2. During chain shuttling to virgin CSA, a growing polymer chain transfers to a CSA molecule, forms a dormant polymer chain and releases an active center that can form a new

polymer chain, as shown in Equation (3–7). Chain shuttling to dormant chain is a reversible reaction between living and dormant chains, as shown in Equation (3–8).[18]

Table 3-1. Mechanism for ethylene chain shuttling polymerization.

Description	Chemical equations	Rate constants	Equation
Initiation	$C + M \rightarrow P_1$	k_i	(3-1)
Propagation	$P_r + M \rightarrow P_{r+1}$	k_p	(3-2)
β-hydride elimination	$P_r \rightarrow D_r + C$	$k_{t\beta}$	(3-3)
Chain transfer to hydrogen	$P_r + H_2 \rightarrow D_r + C$	k_{tH}	(3-4)
Deactivation of growing chain	$P_r \rightarrow D_r + C_d$	k_d	(3-5)
Deactivation of active catalyst	$C \rightarrow C_d$	k_d	(3-6)
Chain shuttling to CSA	$P_r + S_0 \rightarrow SP_r + C$	k_{CSA0}	(3-7)
Chain shuttling to dormant chain	$P_r + SP_s \rightarrow P_s + SP_r$	k_{CSA}	(3-8)

C: active site, C_d: deactivated site, P_1: growing polymer chain of length 1, P_r: growing polymer chain of length r, P_s: growing polymer chain of length s, D_r: dead polymer chain of length r, SP_r: dormant polymer chain of length r, SP_s: dormant polymer chain of length s, M: ethylene, S_0: chain shuttling agent, H_2: hydrogen, k_i: initiation rate constant, k_p: propagation rate constant, $k_{t\beta}$: β-hydride elimination chain transfer rate constant, k_{tH}: chain transfer to hydrogen rate constant, k_d: deactivation rate constant, k_{CSA0}: chain shuttling rate constant to CSA, and k_{CSA}: chain shuttling rate constant to dormant chain.

3.3 The Method of Moments

We define the k^{th} moment, μ_k, of a generic distribution, $f(r)$, as,[50]

$$\mu_k = \sum_{r=1}^{\infty} r^k f(r) \tag{3-9}$$

This thesis uses the following conventions: Y_k is the k^{th} moment of living chains, SX_k is the k^{th} moment of dormant chains, and X_k is the k^{th} moment of dead chains,

$$Y_k = \sum_{r=1}^{\infty} r^k P_r \tag{3-10}$$

$$SX_k = \sum_{r=1}^{\infty} r^k SP_r \tag{3-11}$$

$$X_k = \sum_{r=1}^{\infty} r^k D_r \tag{3-12}$$

The population balance for living chains with length greater than 2 is,

$$\frac{dP_r}{dt} = k_p M\left(P_{r-1} - P_r\right) - \left(k_{t\beta} + k_{tH} H_2 + k_d + k_{CSA0} S_0 + k_{CSA}\left(SX_0\right)\right)P_r + k_{CSA} Y_0\left(SP_r\right) \tag{3-13}$$

and for living chains with length 1,

$$\frac{dP_1}{dt} = k_i CM - k_p P_1 M - \left(k_{t\beta} + k_{tH} H_2 + k_d + k_{CSA0} S_0 + k_{CSA}\left(SX_0\right)\right)P_1 + k_{CSA} Y_0\left(SP_1\right) \tag{3-14}$$

Similarly, the population balance for dormant chains is,

$$\frac{d\left(SP_r\right)}{dt} = k_{CSA0} S_0 P_r + k_{CSA}\left(SX_0\right)P_r - k_{CSA} Y_0\left(SP_r\right) \tag{3-15}$$

Finally, the population balance for dead chains is,

$$\frac{dD_r}{dt} = \left(k_{t\beta} + k_{tH} H_2 + k_d\right)P_r \tag{3-16}$$

Table 3-2 shows the equations for the 0^{th}, 1^{st}, and 2^{nd} moments, derived using the definitions in Equations (3–10) to (3–12) and the population balances in Equations (3–13) to (3–16). Table 3-3 lists the mole balances for catalyst, CSA, ethylene, and hydrogen. Appendix 3-A presents the derivations of these equations in detail. Table 3-4 summarizes the expressions for number and weight average chain lengths for overall, living, dormant, and dead polymer chains.[50]

Table 3-2. Moment equations for ethylene chain shuttling polymerization in a semi-batch reactor.

Description	Moment equations	Initial value
0^{th} Moment of living chains	$\frac{dY_0}{dt} = k_i MC - \left(k_{t\beta} + k_{tH}H_2 + k_d + k_{CSA0}S_0\right)Y_0$	0
1^{st} Moment of living chains	$\frac{dY_1}{dt} = k_i MC + k_p MY_0 - \left(k_{t\beta} + k_{tH}H_2 + k_d + k_{CSA0}S_0 + k_{CSA}(SX_0)\right)Y_1 + k_{CSA}(SX_1)Y_0$	0
2^{nd} Moment of living chains	$\frac{dY_2}{dt} = k_i MC + k_p M(Y_0 + 2Y_1) - \left(k_{t\beta} + k_{tH}H_2 + k_d + k_{CSA0}S_0 + k_{CSA}(SX_0)\right)Y_2 + k_{CSA}(SX_2)Y_0$	0
0^{th} Moment of dead chains	$\frac{dX_0}{dt} = \left(k_{t\beta} + k_{tH}H_2 + k_d\right)Y_0$	0
1^{st} Moment of dead chains	$\frac{dX_1}{dt} = \left(k_{t\beta} + k_{tH}H_2 + k_d\right)Y_1$	0
2^{nd} Moment of dead chains	$\frac{dX_2}{dt} = \left(k_{t\beta} + k_{tH}H_2 + k_d\right)Y_2$	0
0^{th} Moment of dormant chains	$\frac{d(SX_0)}{dt} = k_{CSA0}S_0Y_0$	0
1^{st} Moment of dormant chains	$\frac{d(SX_1)}{dt} = \left(k_{CSA0}S_0 + k_{CSA}(SX_0)\right)Y_1 - k_{CSA}(SX_1)Y_0$	0
2^{nd} Moment of dormant chains	$\frac{d(SX_2)}{dt} = \left(k_{CSA0}S_0 + k_{CSA}(SX_0)\right)Y_2 - k_{CSA}(SX_2)Y_0$	0

C: catalyst concentration, M: ethylene concentration, S_0: chain shuttling agent concentration, H_2: hydrogen concentration, Y_0: 0^{th} moments of living chains, Y_1: 1^{st} moments of living chains, Y_2: 2^{nd} moments of living chains, X_0: 0^{th} moments of dead chains, X_1: 1^{st} moments of dead chains, X_2: 2^{nd} moments of dead chains, SX_0: 0^{th} moments of dormant chains, SX_1: 1^{st} moments of dormant chains, and SX_2: 2^{nd} moments of dormant chains.

Table 3-3. Mole balance equations for ethylene chain shuttling polymerization in a semi-batch reactor.

Description	Molar equations	Initial value
Catalyst	$\frac{dC}{dt} = -(k_i M + k_d)C + (k_{t\beta} + k_{tH} H_2 + k_{CSA0} S_0) Y_0$	C
Chain shuttling agent (CSA)	$\frac{dS_0}{dt} = -k_{CSA0} Y_0 S_0$	CSA
Ethylene	$\frac{dM}{dt} = -(k_i C + k_p Y_0) M$	M
Hydrogen	$\frac{dH_2}{dt} = -k_{tH} Y_0 H_2$	H_2
Deactivated sites	$\frac{dC_d}{dt} = k_d (Y_0 + C)$	0
Ethylene consumption	$\frac{dM_p}{dt} = (k_i C + k_p Y_0) M$	0

Table 3-4. Average chain lengths.

Description	Number average chain length, r_n	Weight average chain length, r_w	Polydispersity, PDI
Overall polymer	$\frac{Y_1 + X_1 + SX_1}{Y_0 + X_0 + SX_0}$	$\frac{Y_2 + X_2 + SX_2}{Y_1 + X_1 + SX_1}$	$\frac{r_w^{overall}}{r_n^{overall}}$
Living polymer	$\frac{Y_1}{Y_0}$	$\frac{Y_2}{Y_1}$	$\frac{r_w^{living}}{r_n^{living}}$
Dormant polymer	$\frac{SX_1}{SX_0}$	$\frac{SX_2}{SX_1}$	$\frac{r_w^{dormant}}{r_n^{dormant}}$
Dead polymer	$\frac{X_1}{X_0}$	$\frac{X_2}{X_1}$	$\frac{r_w^{dead}}{r_n^{dead}}$

The number and weight average molecular weights, M_n and M_w, for all polymer types are calculated by multiplying the number and weight average chain lengths by the molecular weight of ethylene.

Finally, ethylene molar conversion is given by Equation (3-17),

$$x = \frac{M_p}{M + M_p} \tag{3-17}$$

The differential equations in Table 3-2 and Table 3-3 were solved simultaneously in Matlab using the stiff differential equation solver ode15s.[51]

3.4 Dynamic Monte Carlo Model

One of the advantages of dynamic Monte Carlo models is that one does not need to solve differential equations to obtain the complete chain length distribution (CLD) or any other polymer microstructural distribution, such as the chemical composition distribution (CCD) or the long chain branching distribution of polymers made in batch, semi-batch, or continuous reactors. The method requires: 1) the selection of a suitable control volume, 2) the transformation of macroscopic or experimental reaction rate constants (k^{exp}) to microscopic, or Monte Carlo, reaction rate constants (k^{MC}), and 3) the selection of several reaction steps using randomly generated numbers. The dynamic Monte Carlo model described below is based on the general simulation method developed by Gillespie.[52]

For a generic reaction, we can define Monte Carlo reaction rates and constants, R^{MC} and k^{MC},

$$R^{MC} = k^{MC} N_C \tag{3-18}$$

where N_C is the number of unique combinations between reactant molecules. Monte Carlo reaction rates and constants have units of reciprocal time. The number of combinations between reactant molecules depends on the type of reaction taking place, as explained below.

β-Hydride elimination and deactivation are unimolecular reactions. For instance, for β-hydride elimination, Equation (3-19) is obtained

$$P_r \xrightarrow{k_{t\beta}} D_r + C \tag{3-19}$$

For unimolecular reactions, the number of independent combinations equals the number of reactant molecules, n_P, as shown in Equation (3-20)

$$N_C = n_P \tag{3-20}$$

Initiation, propagation, transfer to hydrogen, and chain shuttling are bimolecular reactions between different molecules. For instance, the propagation reaction is given in Equation (3-21),

$$P_r + M \xrightarrow{k_p} P_{r+1} \tag{3-21}$$

We can determine the number of unique combinations between two different molecules using the expression,

$$N_C = n_M n_P \tag{3-22}$$

where n_M is the number of monomer molecules and n_P is the number of living chains present in the reactor at a given polymerization time.

Monte Carlo reaction rates for unimolecular reactions of molecule A are given by,

$$R^{MC} = k^{MC} n_A \quad (\mathrm{s}^{-1}) \tag{3-23}$$

and the macroscopic rate is,

$$R = kA \quad (\mathrm{mol/L.\ s}) \tag{3-24}$$

To compare these two equations, we must put them into the same unit basis. We can do this by dividing Equation (3–23) by $N_A V$, where $N_A = 6.02214 \times 10^{23}$ mol^{-1} is Avogadro's number and V is the simulation volume,

$$R = k^{MC} n_A \frac{1}{VN_A} \quad (\mathrm{mol/L.s}) \tag{3-25}$$

Since,

$$A = \frac{n_A}{VN_A} \tag{3-26}$$

then,

$$R = k^{MC} A \tag{3-27}$$

Comparing Equations (3–24) and (3–27), we conclude that, for unimolecular reactions,

$$k^{MC} = k \tag{3-28}$$

Monte Carlo reaction rates between molecules *A* and *B* are expressed as,

$$R^{MC} = k^{MC} n_A n_B \quad (\mathrm{s}^{-1}) \tag{3-29}$$

and the macroscopic rate by,

$$R = kAB \quad (\mathrm{mol/L.\ s}) \tag{3-30}$$

Altering Equation (3–29) to express it in units of mol/(L.s), we get,

$$R = k^{MC} n_A n_B \frac{1}{VN_A} \quad (\mathrm{mol/L.s}) \tag{3-31}$$

To compare Equation (3–30) with Equation (3–31), we need to express n_A and n_B as a function of the concentrations of *A* and *B* in the reaction medium,

$$n_A = AVN_A \tag{3-32}$$

$$n_B = BVN_A \tag{3-33}$$

Substituting Equations (3–32) and (3–33) into Equation (3–31), we obtain,

$$R = k^{MC} ABVN_A \tag{3-34}$$

Now we can compare Equations (3–30) and (3–34),

$$kAB = k^{MC} ABVN_A \tag{3-35}$$

to conclude that, for bimolecular reactions between different molecules,

$$k^{MC} = \frac{k}{VN_A} \tag{3-36}$$

The size of the simulation volume determines how smooth the results for a given simulation will be, but otherwise does not affect the simulation. The simulation volume should be large enough to generate statistically valid results.[53]

Similarly, the macroscopic concentration of catalyst, CSA, ethylene, and hydrogen must be transformed into the number of molecules of each species in the control volume, as defined by Equations (3–37) to (3–40). Table 3-5 summarizes all expressions needed for the dynamic Monte Carlo simulation of our system.

$$n_C = CN_A V \tag{3-37}$$

$$n_{S_0} = S_0 N_A V \tag{3-38}$$

$$n_M = MN_A V \tag{3-39}$$

$$n_{H_2} = H_2 N_A V \tag{3-40}$$

Table 3-5. Monte Carlo reaction rate and rate constants equations for chain shuttling polymerization.

Description	Chemical equations	k	R^{MC}, s^{-1}	k^{MC}, s^{-1}	Equation
Initiation	$C + M \rightarrow P_1$	k_i	$k_i^{MC} n_C n_M$	$\frac{k_i}{VN_A}$	(3-41)
Propagation	$P_r + M \rightarrow P_{r+1}$	k_p	$k_P^{MC} n_p n_M$	$\frac{k_p}{VN_A}$	(3-42)
β-hydride elimination	$P_r \rightarrow D_r + C$	$k_{t\beta}$	$k_{t\beta}^{MC} n_P$	$k_{t\beta}$	(3-43)
Chain transfer to hydrogen	$P_r + H_2 \rightarrow D_r + C$	k_{tH}	$k_{tH}^{MC} n_p n_{H_2}$	$\frac{k_{tH}}{VN_A}$	(3-44)
Deactivation of growing chain	$P_r \rightarrow D_r + C_d$	k_d	$k_d^{MC} n_P$	k_d	(3-45)
Deactivation of active catalyst	$C \rightarrow C_d$	k_d	$k_d^{MC} n_C$	k_d	(3-46)
Chain shuttling to CSA	$P_r + S_0 \rightarrow SP_r + C$	k_{CSA0}	$k_{CSA0}^{MC} n_p n_{S0}$	$\frac{k_{CSA0}}{VN_A}$	(3-47)
Chain shuttling to dormant chain	$P_r + SP_s \rightarrow P_s + SP_r$	k_{CSA}	$k_{CSA}^{MC} n_P n_{SP}$	$\frac{k_{CSA}}{VN_A}$	(3-48)

Thus, the sum of all reaction rates is,

$$R_T^{MC} = R_i^{MC} + R_p^{MC} + R_{t\beta}^{MC} + R_{tH}^{MC} + R_{dP}^{MC} + R_{dC}^{MC} + R_{CSA0}^{MC} + R_{CSA}^{MC} = \sum_{j=1}^{8} R_j^{MC} \tag{3-49}$$

The dynamic Monte Carlo algorithm requires the generation of two random numbers, r_1 and r_2, for each reaction step. The first number, r_1, selects the kind of reaction (k) that takes place according to the inequality,

$$\sum_{j=1}^{k-1} R_j^{MC} < r_1 R_T^{MC} \leq \sum_{j=1}^{k} R_j^{MC} \tag{3-50}$$

Figure 3-1 depicts a graphical analogy for this inequality.

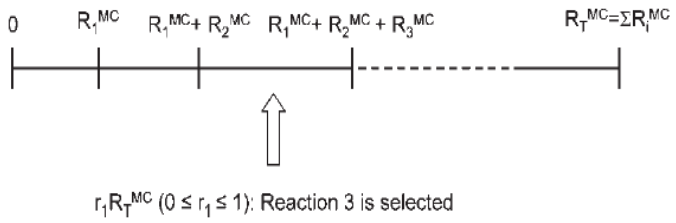

Figure 3-1. Schematic for reaction step selection in dynamic Monte Carlo.

The second random number, r_2, determines the time that elapsed between the consecutive reactions, as shown in the following expression,

$$\tau = \frac{1}{R_T^{MC}} \ln\left(\frac{1}{r_2}\right) \tag{3-51}$$

Figure 3-2 shows the dynamic Monte Carlo computation steps.

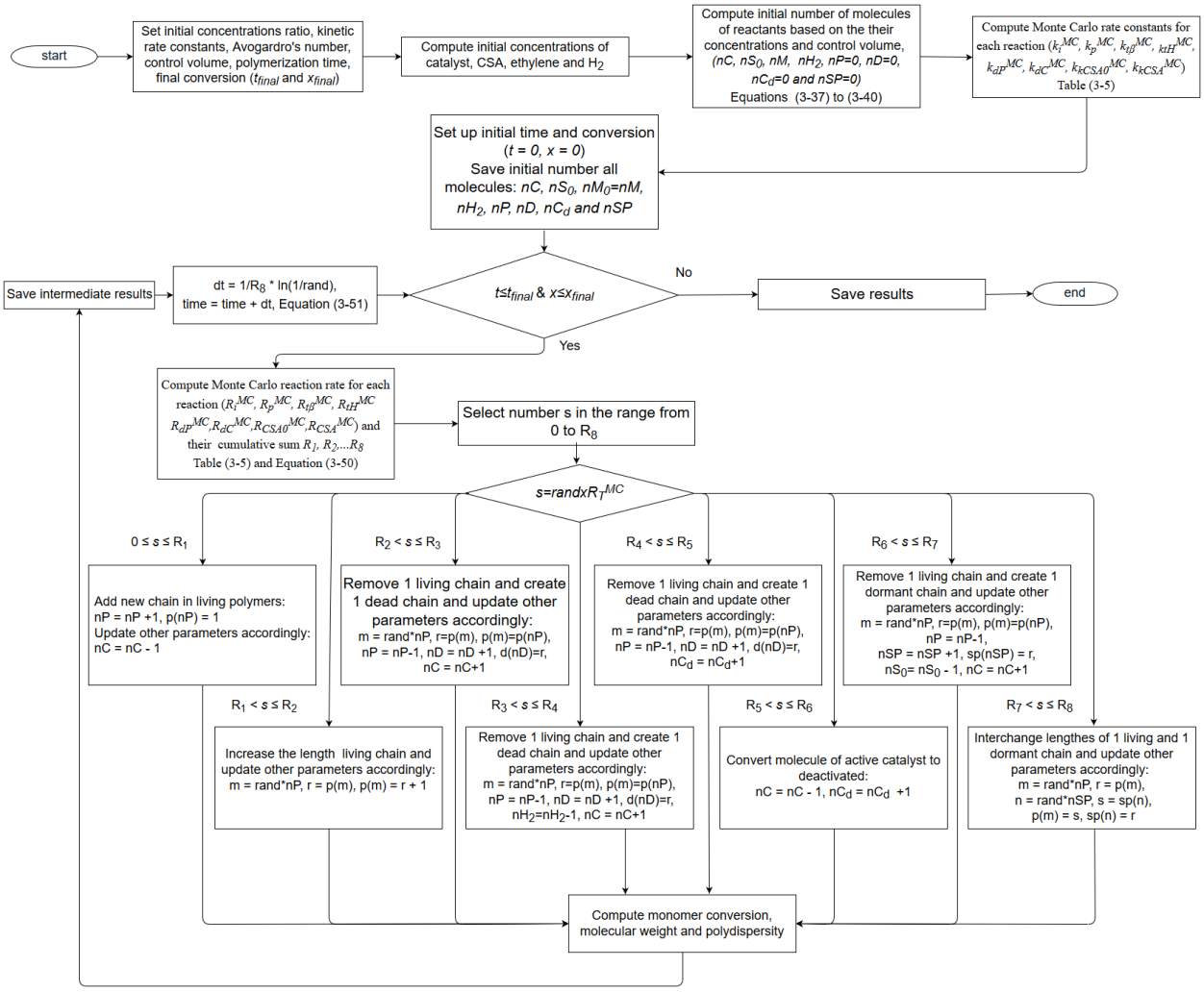

Figure 3-2. Dynamic Monte Carlo algorithm for ethylene chain shuttling polymerization in a semi-batch reactor.

We used Matlab to solve the dynamic Monte Carlo model summarized in Figure 3-2. The program starts at time t = 0, monomer conversion x = 0, and $nP = nSP = nD = nC_d = 0$, where nP is the number of living chains, nSP is the number of dormant chains, nD is the number of dead chains, and nC_d is the number of deactivated chains. Equations (3–37) to (3–40) are used to transform the concentrations of catalyst, CSA, ethylene, and hydrogen into the number of molecules in the control volume, and Equations (3–41) to (3–48) are used to transform all the macroscopic reaction rate constants into dynamic Monte Carlo reaction rate constants. After transforming all the required data, the simulation follows the steps below:

1. Calculate dynamic Monte Carlo reaction rate, $R_1^{MC}, R_1^{MC}, ..., R_8^{MC}$ and their sum $R_T^{MC} = \sum_{j=1}^{8} R_j^{MC}$.
2. Generate one random number, r_1, uniformly generated between 0 to 1, to determine the kind of reaction (k) that takes place according to Equation (3–50).
3. Generate a second random number, r_2, to determine the elapsed time between two successive reactions according to Equation (3–51).
4. Update the polymerization time with time increment, $t = t + \tau$, and calculate the monomer conversion, x.
5. If the conversion is higher than x_{final} or the polymerization time is higher than t_{final}, stop the simulation and save the polymer microstructures.

3.5 Results and Discussion

The objectives of the simulations in this chapter were: 1) to compare dynamic Monte Carlo and method of moments simulations to ensure both are working correctly, and 2) to investigate the effect of process conditions and simulation parameters on polyethylene microstructure using both simulation techniques.

Table 3-6 lists the kinetic rate constants used in all simulations, and Table 3-7 shows the process conditions used in the semi-batch reactor.

Table 3-6. Kinetic constants for ethylene chain shuttling polymerization.

Kinetic constants	Values	Units
Initiation rate constant, k_i	10000	L/mol.s
Propagation rate constant, k_p	10000	L/mol.s
β-hydride elimination, $k_{t\beta}$	25	s^{-1}
Chain transfer to hydrogen, k_{tH}	0	L/mol.s
Deactivation rate constant, k_d	0	s^{-1}
Chain shuttling rate constant to CSA, k_{CSA0}	$10\times k_p$	L/mol.s
Chain shuttling rate constant to dormant chain, k_{CSA}	$10\times k_p$	L/mol.s

Table 3-7. Process conditions for ethylene chain shuttling polymerization.

Reactants	Values	Units
Monomer concentration, $[M]$	2	mol/L
Catalyst concentration, $[Cat]$	7.78×10^{-7}	mol/L
Chain shuttling agent to catalyst concentration, $[CSA]/[Cat]$	1000	
Hydrogen to monomer concentration, $[H_2]/[M]$	0	
Polymerization time, t	600	s

3.5.1 Comparison of the Method of Moments and Monte Carlo Simulation

The size of the control volume affects the smoothness of the predicted chain length distributions (CLD). If $V = 1\times10^{-17}$ L, ethylene conversion, number average molecular weight (M_n), polydispersity index (PDI) predicted by dynamic Monte Carlo simulation differ from those calculated with the method of moments due to random fluctuations in the Monte Carlo method, but if the size of the control volume increases to 1×10^{-15} L, the two methods agree well, as depicted in Figure 3-3.

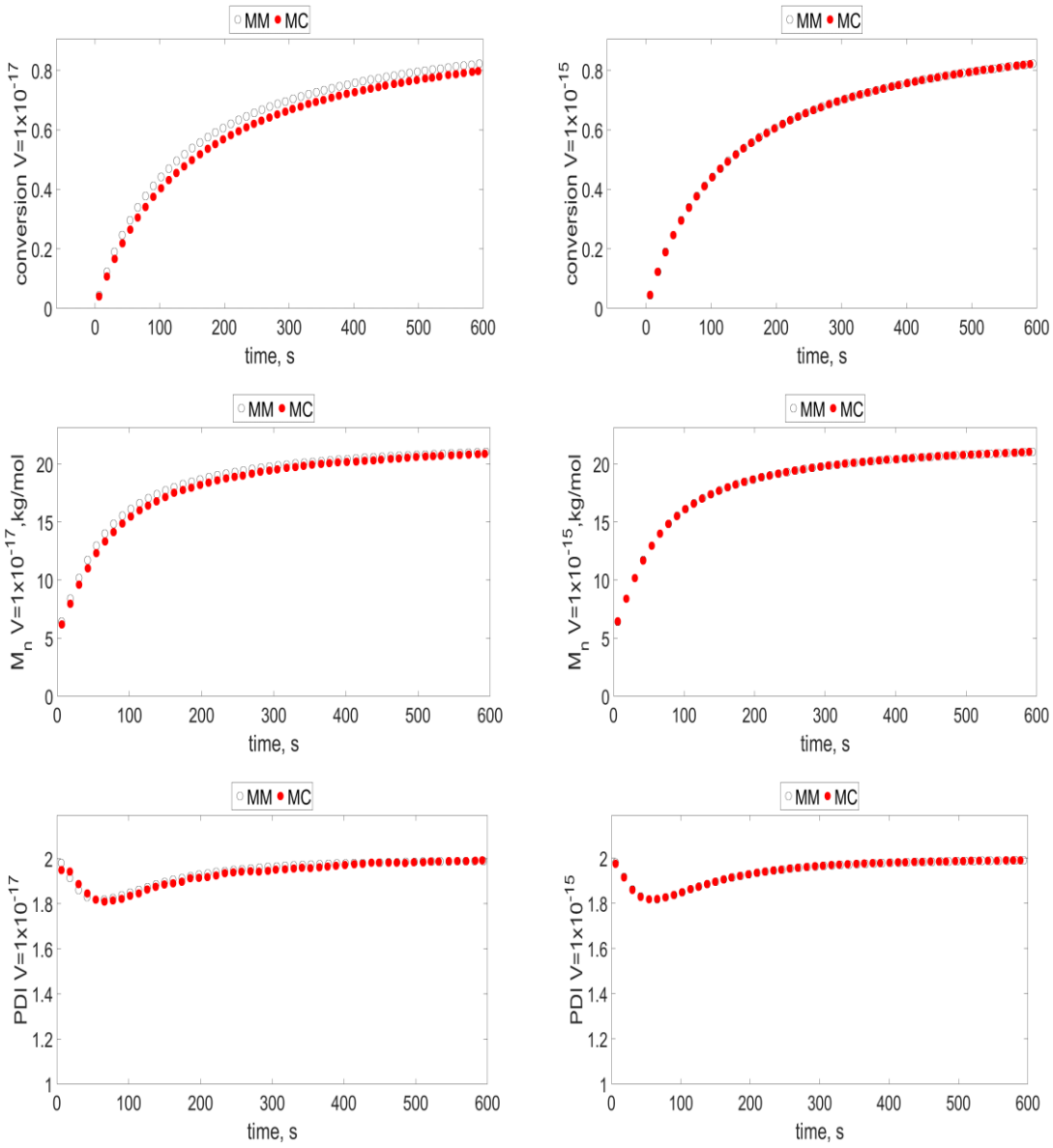

Figure 3-3. Effect of control volume size on ethylene conversion, M_n, and PDI predicted by the method of moments and dynamic Monte Carlo simulation.

3.5.2 Effect of Control Volume Size on CLD Predictions

Figure 3-4 compares the CLD for polyethylene produced at different polymerization times for several control volume sizes. The CLD predicted with the smallest volume ($V = 1\text{x}10^{-17}$ L) is noisy, especially at the beginning of polymerization (when there is little polymer) and is not adequate for an accurate representation of CLD. The two largest control volume sizes ($V = 1\times10^{-16}$ and 1×10^{-15} L) generate smooth CLDs, but at the expense of longer computation times. The computation times

are 26 minutes for $V = 1\times10^{-15}$ L and 5 minutes for $V = 1\times10^{-17}$ L in a microcomputer with the following characteristics: CPU: Intel Core i7-2600, 3.4GHz, 8GB RAM memory, Windows 10 operation system, 64-bit, and Matlab R2015b.

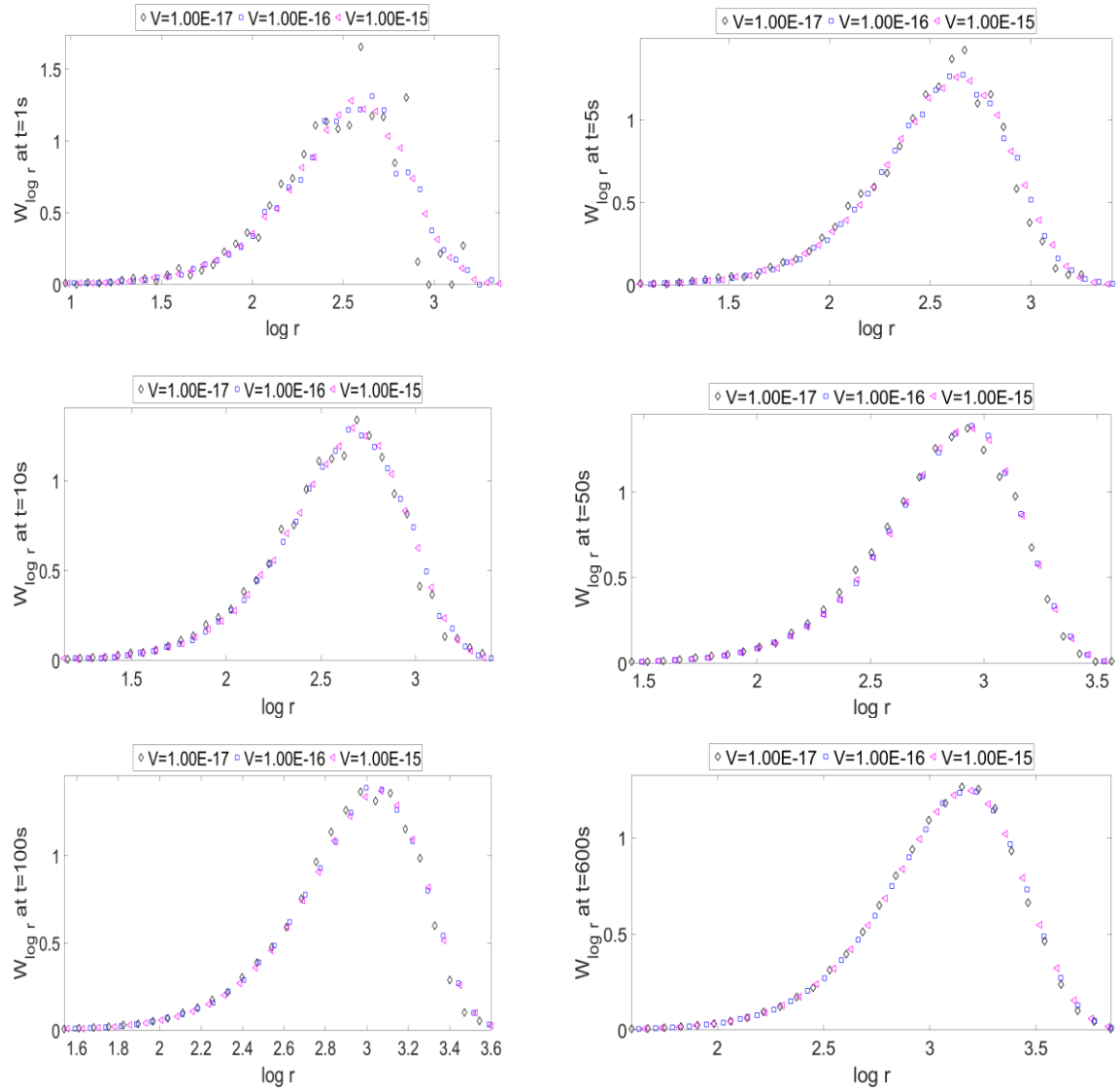

Figure 3-4. Effect of control volume size on the CLD of polyethylene at different polymerization times.

Figure 3-5 compares Flory's most probable distribution[54] with the CLD for polyethylene predicted with dynamic Monte Carlo simulation at different polymerization times. At short polymerization times, the CLD follows Flory's distribution, but after 10 seconds, the CLD becomes narrower than Flory's distribution as dormant chains are formed, broadening again and approaching Flory's

distribution at the end of the polymerization because of the accumulation of dead chains in the reactor.

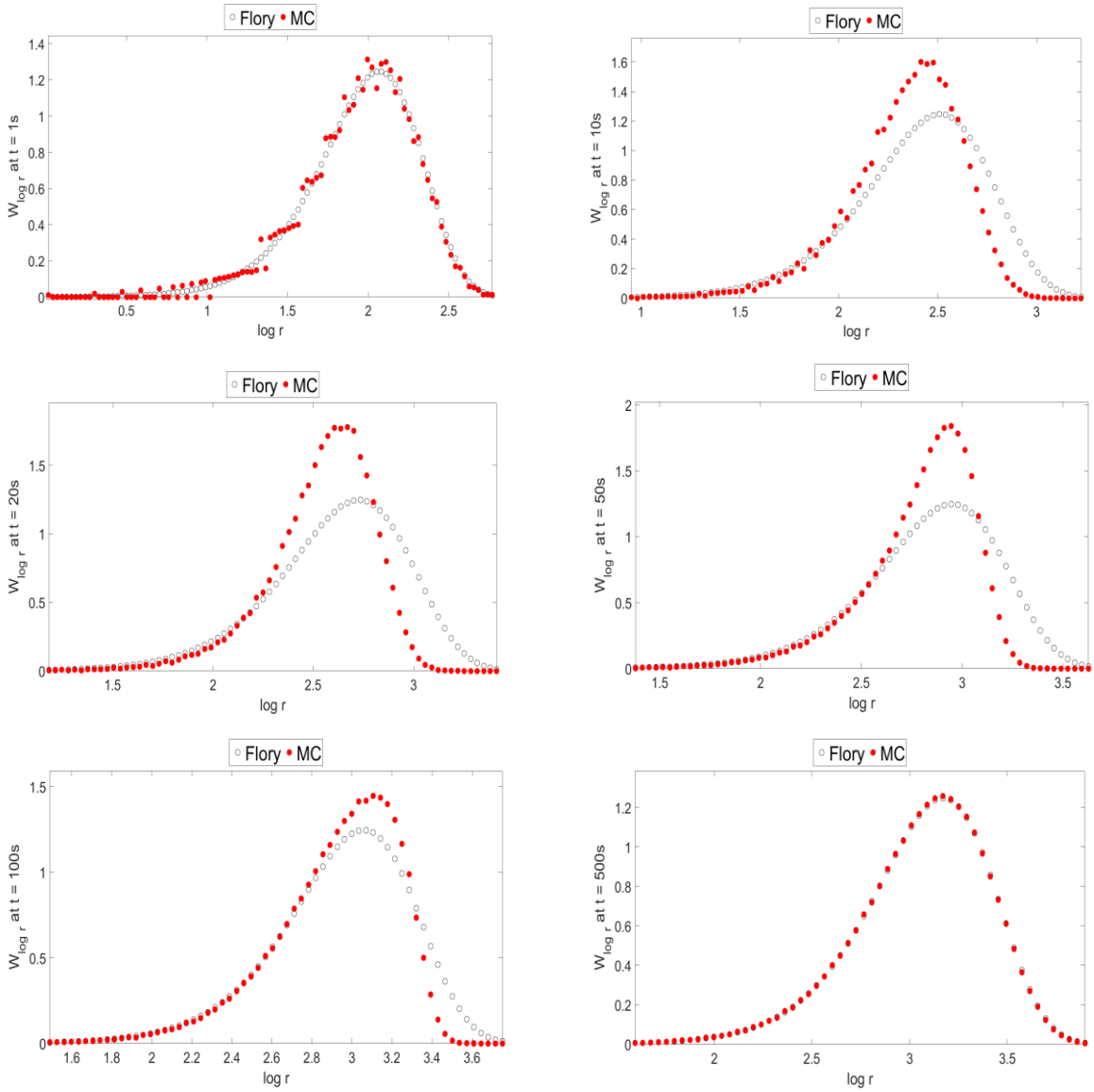

Figure 3-5. Comparison between the Flory distribution and CLD predicted by DMC at different polymerization times. (V = 1×10^{-15} L, $k_{CSA} = k_{CSA0} = 50k_p$, other variables as shown in Table 3-6 and Table 3-7.)

3.5.3 Effect of Polymerization Condition and Kinetic Constants

In the following simulations, we varied the chain shuttling to propagation rate constant ratios (k_{CSA0}/k_p and k_{CSA}/k_p) from 0 to 50 and set the CSA concentration to catalyst concentration ratio ([*CSA*]/[*Cat*]) to 1000, but kept all other variables constant, as shown in Table 3-6 and Table 3-7.

Figure 3-6 shows the effect of the chain shuttling rate on M_n and PDI. When no chain shuttling takes place ($k_{CSA}/k_p = 0$), M_n increases quickly to its steady state value and PDI reaches the theoretical value of 2.0 after a few seconds, as expected for regular coordination polymerization. Chain shuttling changes the polymerization behavior drastically. The value of M_n increases much more slowly as a function of polymerization time when $k_{CSA}/k_p > 0$ because the formation of dormant chains delays chain growth. Interestingly, for the same [*CSA*]/[*Cat*] ratio, changing the value of k_{CSA}/k_p has a minor effect on M_n at very short polymerization times, with higher k_{CSA}/k_p leading to a slower M_n increase, but at a longer polymerization time all M_n curves converge to the same value. The value of k_{CSA} regulates the frequency of chain exchange between dormant and living states while the value of k_p (for a given $k_{t\beta}$) controls M_n. Therefore, increasing k_{CSA}/k_p at constant k_p increases the frequency of living/dormant chain exchange, but that their final molecular weight averages will remain the same.

Polydispersity varies significantly with k_{CSA}/k_p ratio. Because of the quasi-living nature of chain shuttling polymerization, PDI is lower than 2.0 when $k_{CSA}/k_p > 0$. The PDI reaches its minimum value at early stages of polymerization, since termination reactions start playing a more important role for longer polymerization times. Note that $k_{t\beta}$ is not equal to zero in these simulations; therefore, dead chains will accumulate in the reactor as the polymerization proceeds, broadening the CLD of the overall polymer. Husted et al.[42] reported the same phenomenon. Figure 3-7 shows the effect of k_{CSA}/k_p on the CLD of polymer at different polymerization times. At early polymerization times, a higher k_{CSA}/k_p ratio produces a narrower CLD due to the effect of dormant chains. As the polymerization proceeds, all cases approach the same CLD due to the accumulation of the dead chains in the reactor.

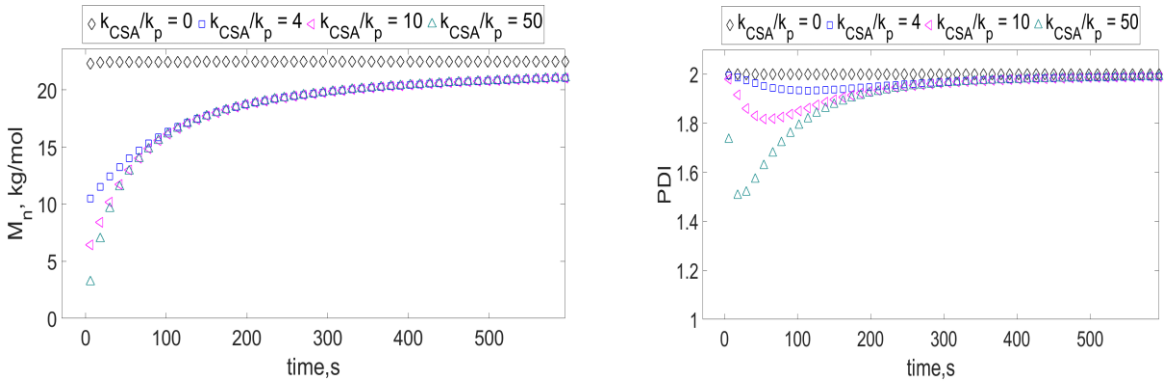

Figure 3-6. Effect of k_{CSA}/k_p on M_n and PDI of polyethylene made in a semi-batch reactor.

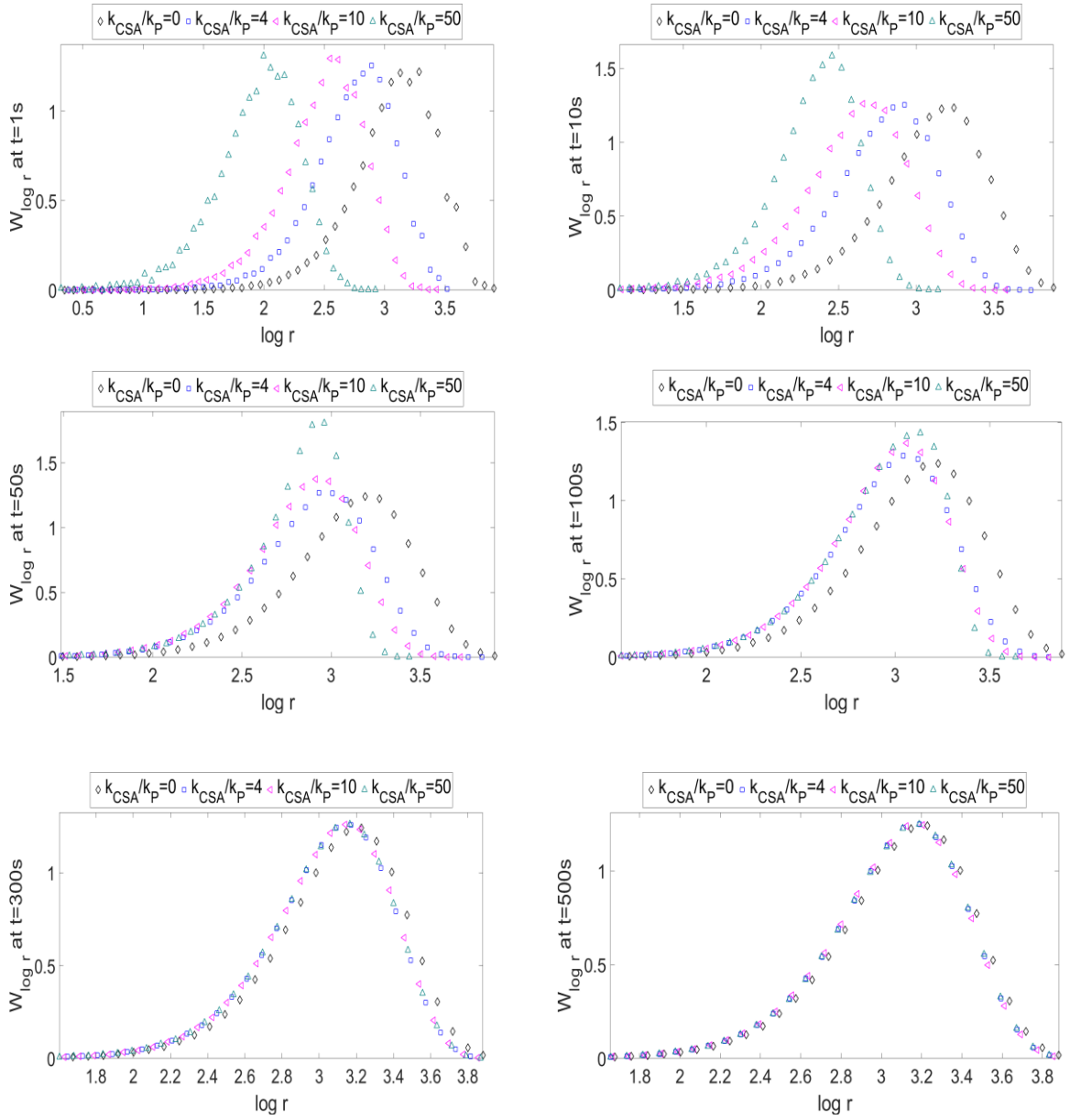

Figure 3-7. Effect of k_{CSA}/k_p on the CLD of polyethylene made in a semi-batch reactor at different polymerization times.

We carried out a complementary investigation on the effect of the propagation rate constant (k_p) to support the explanation proposed above by varying the propagation rate constant from 5000 to 20000 L/(mol.s) while keeping the chain shuttling rate constants (k_{CSA0} and k_{CSA}) at 100000 L/(mol.s) and the [*CSA*]/[*Cat*] ratio at 1000. As k_p increases, the value of M_n increases because the rate of ethylene insertion increases, as does M_n, but PDI remains the same (Figure 3-8). Figure 3-9 shows the effect of k_p on the CLD of the polymer at different polymerization times.

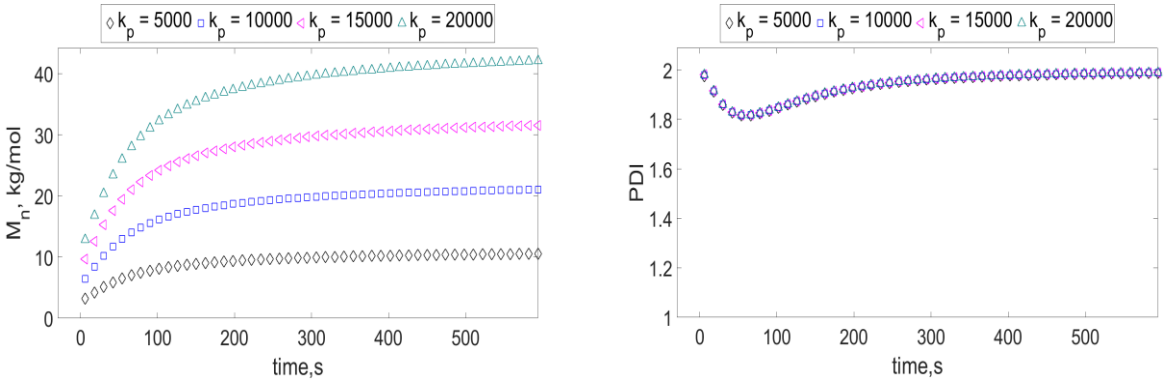

Figure 3-8. Effect of k_p on M_n and PDI of polyethylene made in a semi-batch reactor while keeping k_{CSA} constant.

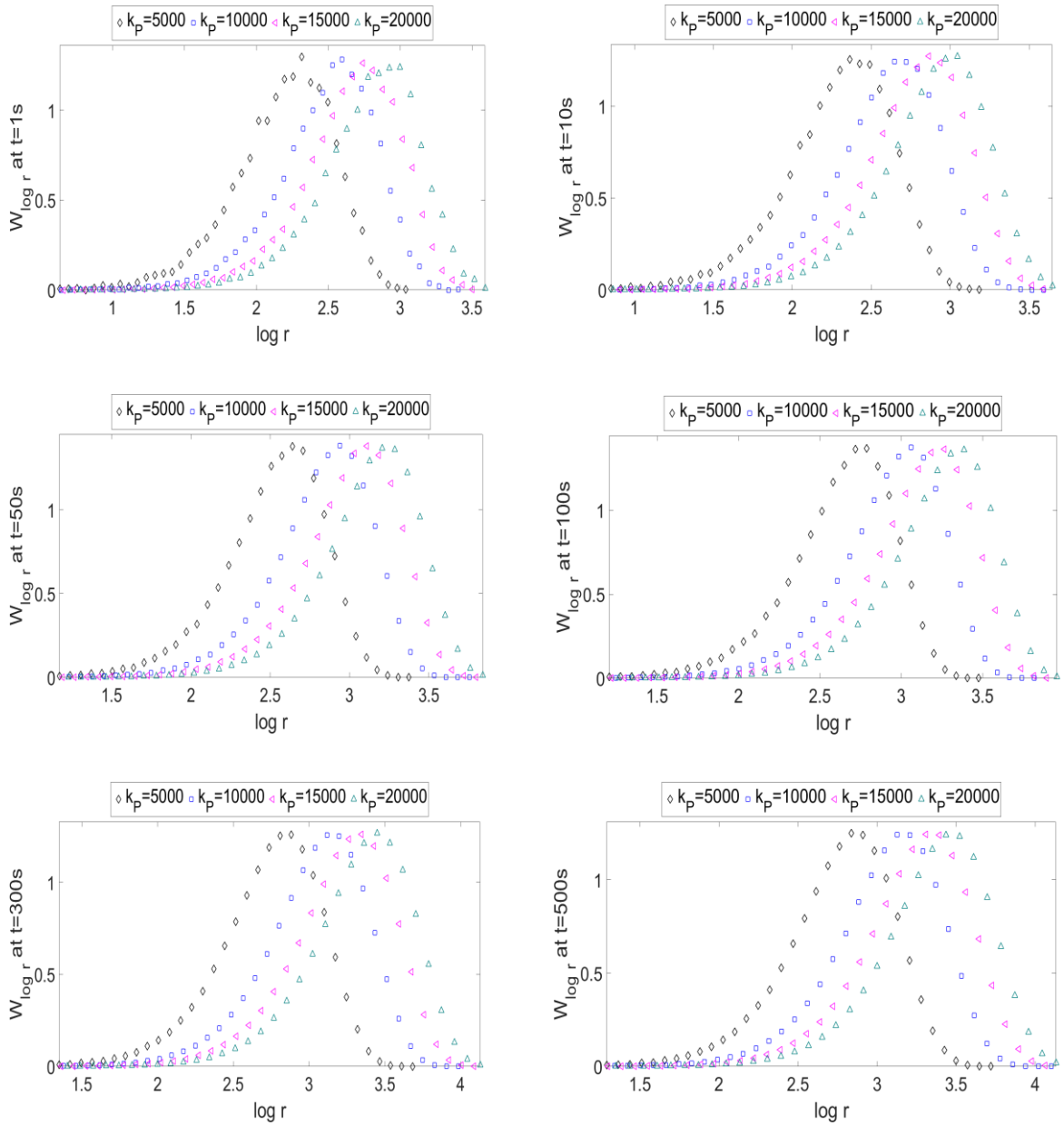

Figure 3-9. Effect of k_p on the CLD of polyethylene made in a semi-batch reactor at different polymerization times while keeping k_{CSA} constant.

The next simulations investigate why varying k_p did not affect PDI in the previous simulations by varying the propagation rate constant from 5000 to 20000 L/(mol.s) and changing the k_{CSA} to ensure that $k_{CSA}/k_p = 10$. Figure 3-10 shows that, as k_p increases, M_n also increases, but the PDI values do not remain the same. They differ for short polymerization times, reaching minimum values for the highest k_p value, which also correspond to the highest k_{CSA} value. Therefore, faster shuttling rates narrow the CLD of the polymer. Figure 3-11 shows the effect of k_p on the CLD of polymer at different polymerization times when $k_{CSA}/k_p = 10$. At early polymerization times, all cases have similar CLDs; as the polymerization time increases, the CLDs start differing from each other, reaching similar CLDs for all cases at the end of polymerization due the accumulation of the dead chains in the reactor.

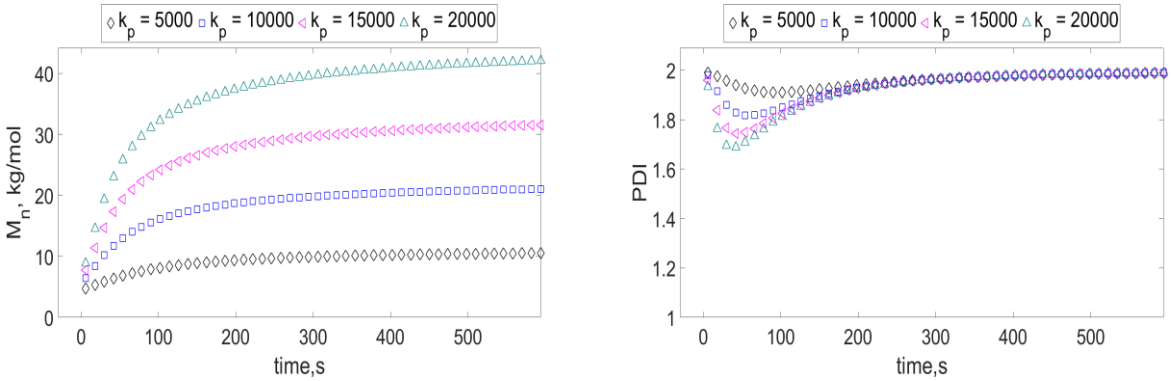

Figure 3-10. Effect of k_p on M_n and PDI of polyethylene made in a semi-batch reactor.

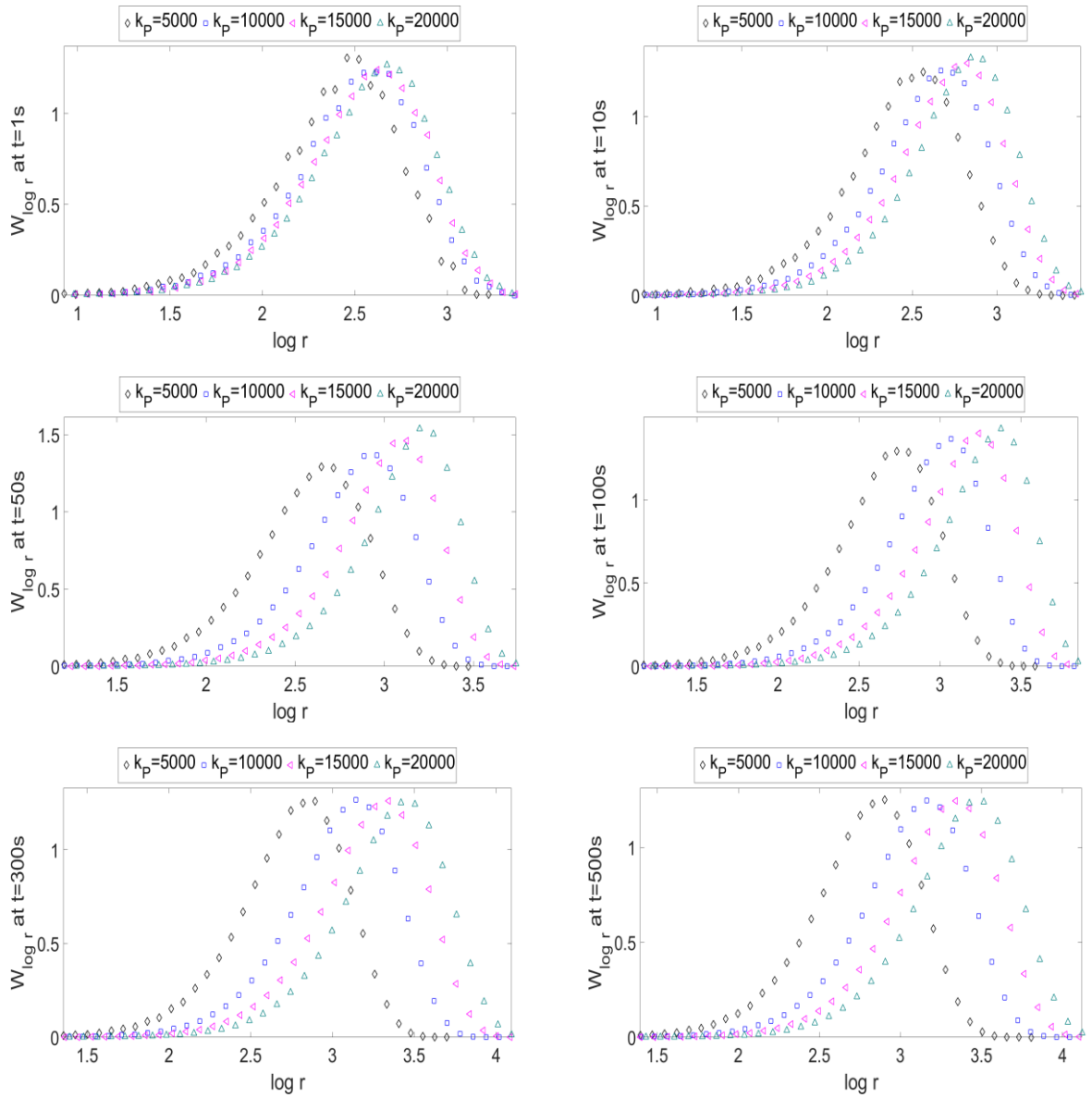

Figure 3-11. Effect of k_p on the CLD of polyethylene made in a semi-batch reactor at different polymerization times with $k_{CSA}/k_p = 10$.

The β-hydride elimination rate constant ($k_{t\beta}$) and the propagation rate constant (k_p) have a major effect on M_n. The following simulations investigated the effect of $k_{t\beta}$ on M_n and PDI. We varied the values of $k_{t\beta}$ from 0 to 25 s^{-1}, kept $k_{CSA0}/k_p = k_{CSA}/k_p = 10$, and $[CSA]/[Cat] = 1000$. Figure 3-12 shows the effect of $k_{t\beta}$ on M_n and PDI. The value of M_n decreases sharply as $k_{t\beta}$ increases, and the dynamic behavior of PDI also depends strongly on the value of $k_{t\beta}$. For higher $k_{t\beta}$ values, PDI rises faster due to the accumulation of dead chains in the reactor. The features of classic living polymerization (polymer has a PDI close to one, chain length distribution is close to Poisson distribution, and the average molecular weight increases linearly with polymerization time) are only approximated when $k_{t\beta} = 0$, as shown in Figure 3-12 and Figure 3-13. Figure 3-13 shows the effect of $k_{t\beta}$ on the CLD at different polymerization times. At short polymerization times, even without transfer, all the CLDs are similar, but at longer polymerization times, we observed different CLDs for distinct $k_{t\beta}$ values. In the case of no transfer ($k_{t\beta} = 0$), the CLD approaches Poisson distribution.

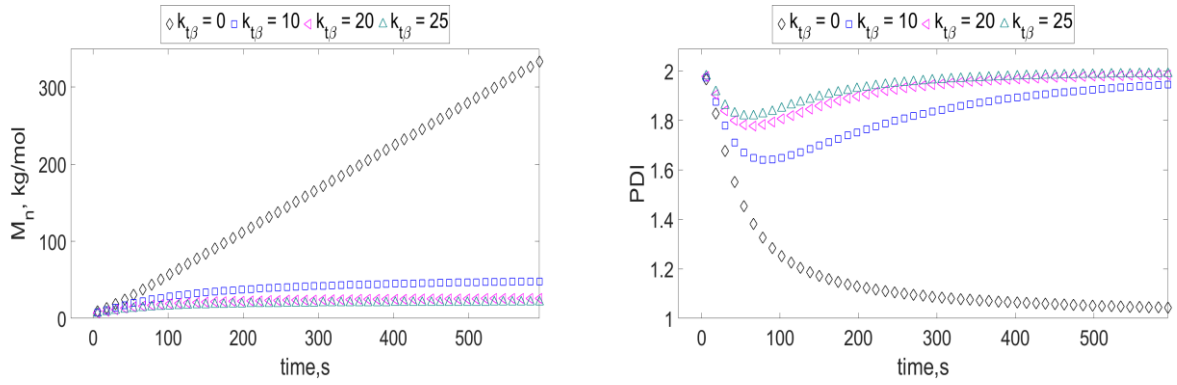

Figure 3-12. Effect of $k_{t\beta}$ on M_n and PDI of polyethylene made in a semi-batch reactor.

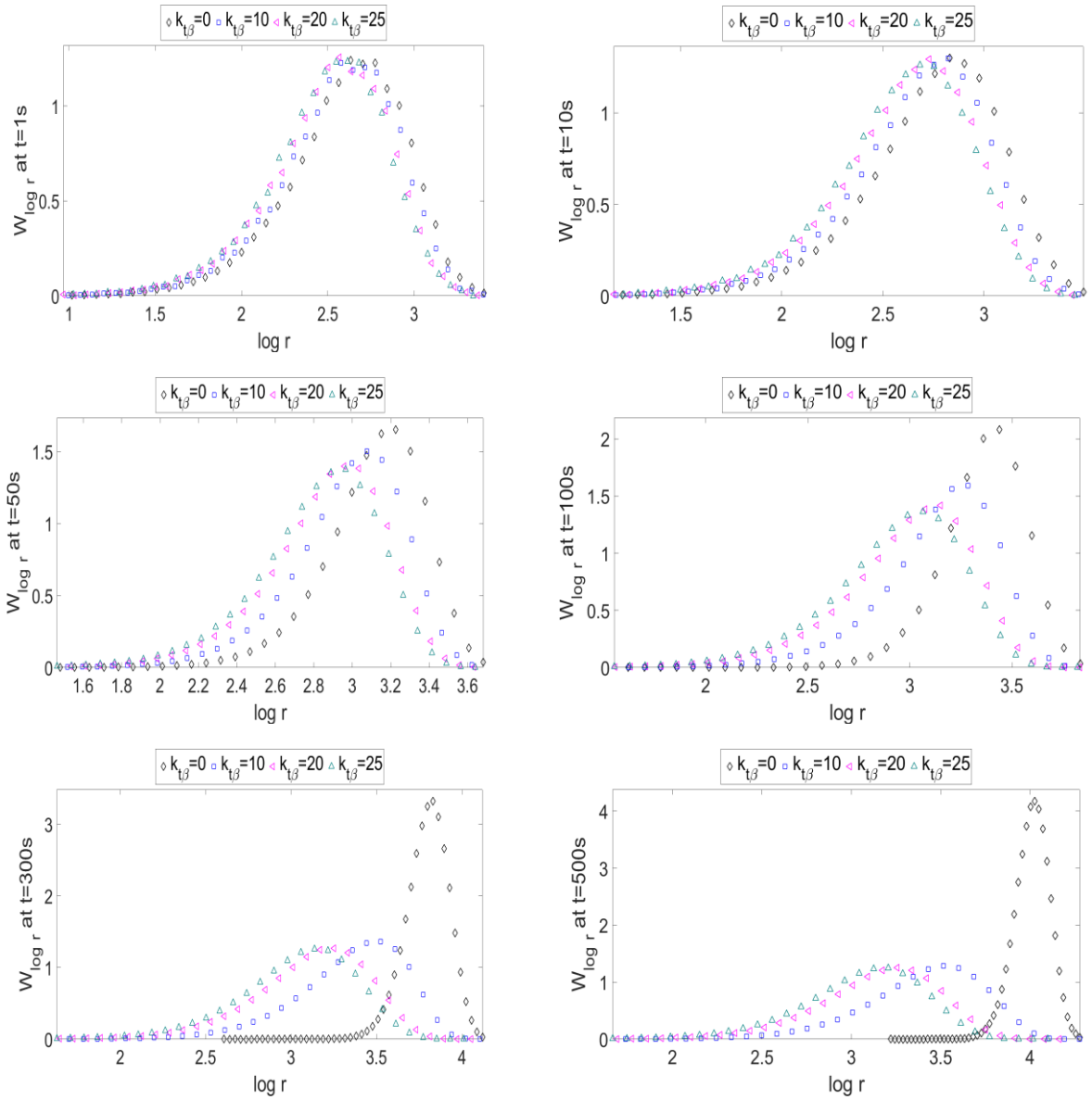

Figure 3-13. Effect of $k_{t\beta}$ on the CLD of polyethylene made in a semi-batch reactor at different polymerization times.

The following simulations analyze the effect of catalyst deactivation (k_d) on the polymer's average properties and CLD. Higher deactivation rates will lower the concentrations of the catalyst, living, dormant, and dead chains in the reactor. The immediate effect is a decrease in M_n. At short polymerization times, PDI decreases with the same rate, but as polymerization proceeds, PDI does not return to a value of 2 because less dead polymer accumulates in the reactor, as depicted in Figure 3-14. Figure 3-15 shows the effect of the deactivation rate on the CLD of polymers at different polymerization times. At longer polymerization times, we observed different CLDs for distinct k_d values.

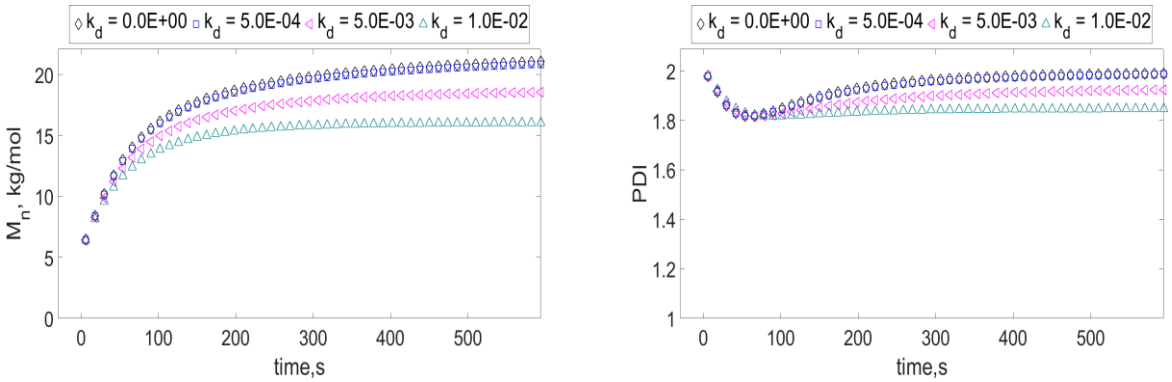

Figure 3-14. Effect of k_d on M_n and PDI of polyethylene made in a semi-batch reactor.

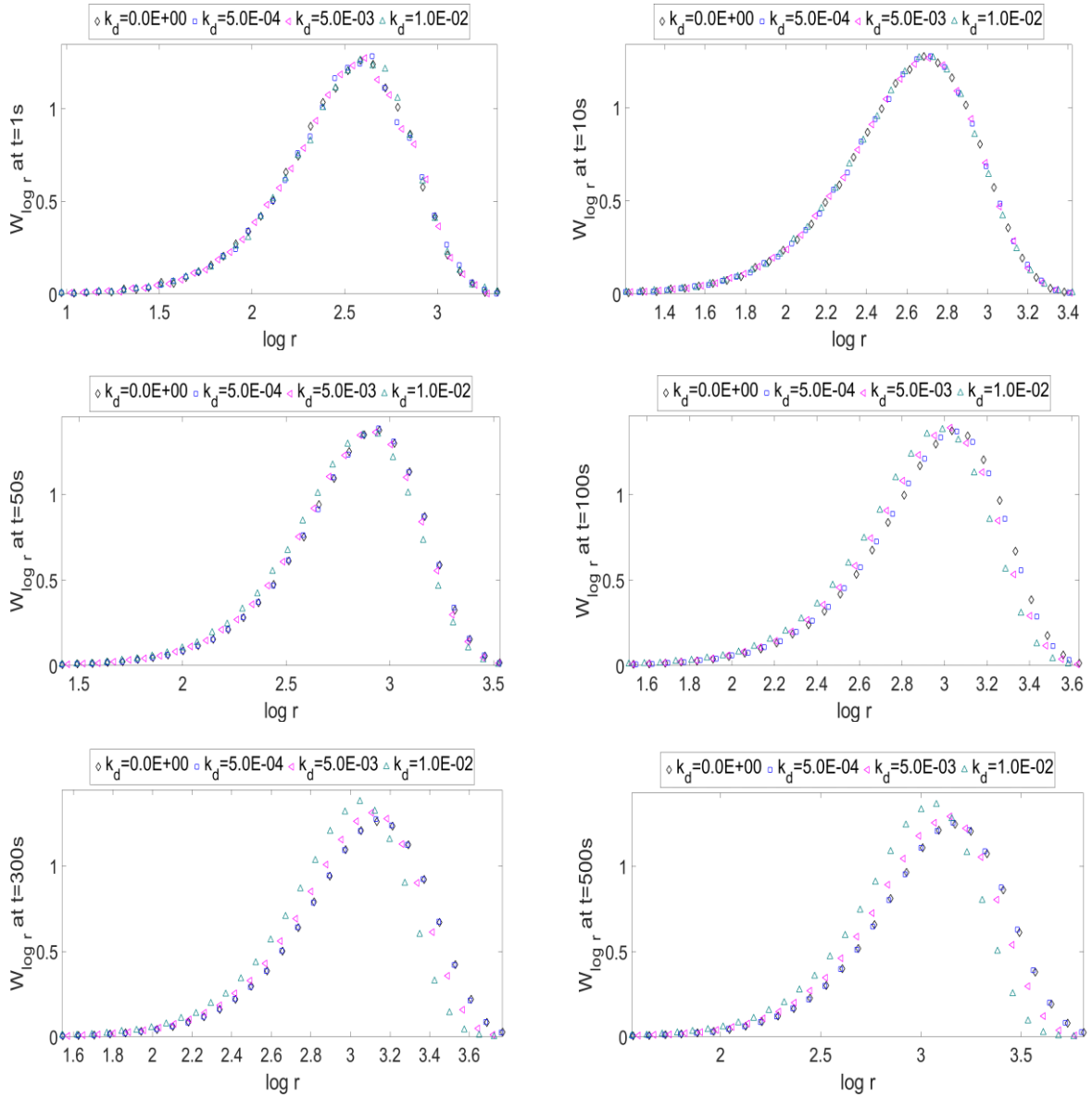

Figure 3-15. Effect of k_d on the CLD of polyethylene made in a semi-batch reactor at different polymerization times.

The concentration of CSA also has a marked effect on the time evolution of M_n and PDI of polyethylene made in a semi-batch reactor. In the following simulations, the [*CSA*]/[*Cat*] ratio varied from 500 to 2000, while $k_{CSA0}/k_p = k_{CSA}/k_p = 10$. As the [*CSA*]/[*Cat*] ratio increases, M_n drops sharply (see Figure 3-16). In the early stages of polymerization, PDI decreases at about the same rate in all cases, but as the polymerization proceeds, the PDI tends to the limiting value of 2.0 faster for the low [*CSA*]/[*Cat*] ratio. Since chain shuttling competes with chain termination, we expected PDI to remain smaller for a longer time for the high [*CSA*]/[*Cat*] ratio (see Figure 3-16). Figure 3-17 shows the effect of [*CSA*]/[*Cat*] on CLD at different polymerization times. At early polymerization times, the higher the [*CSA*]/[*Cat*] ratio, the narrower the CLD produced. As polymerization proceeds, all cases approach the same CLD due to the accumulation of dead chains in the reactor.

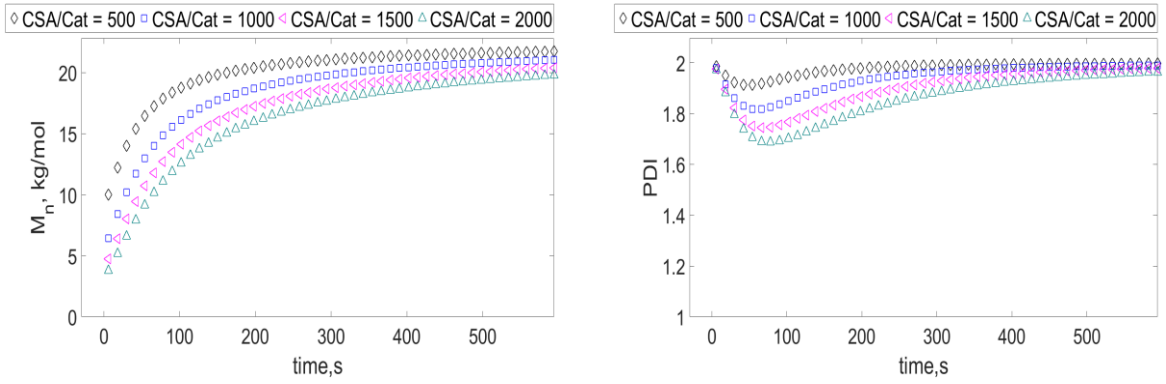

Figure 3-16. Effect of [*CSA*]/[*Cat*] on M_n and PDI of polyethylene made in a semi-batch reactor.

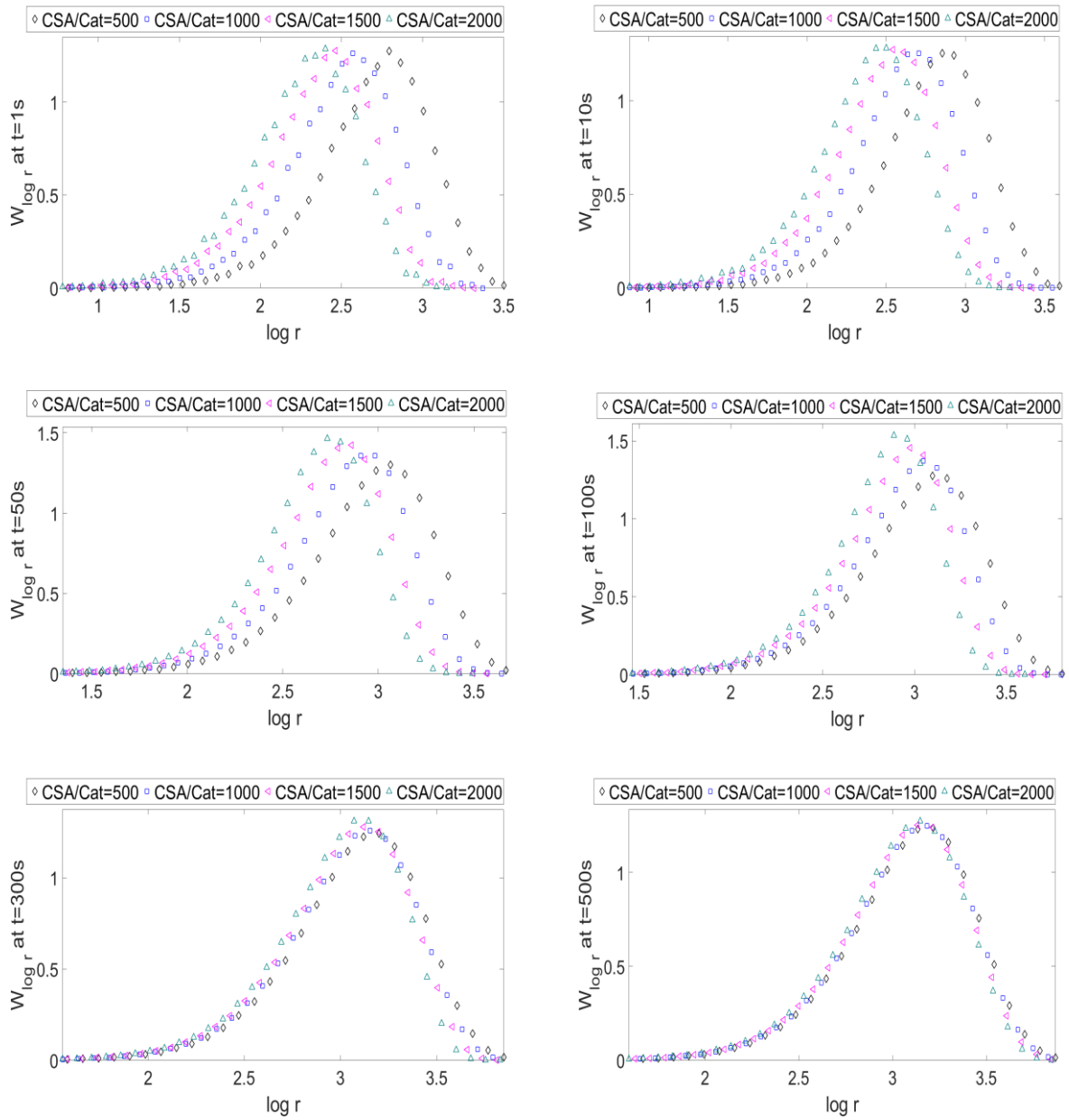

Figure 3-17. Effect of [*CSA*]/[*Cat*] on the CLD of polyethylene made in a semi-batch reactor at different polymerization times.

3.6 Conclusion

This study used the method of moments and dynamic Monte Carlo simulation to describe how the miscrostructure of polyethylene made by chain shuttling polymerization in a semi-batch reactor varied as a function of polymerization time. While the method of moments predicts average polymer properties, the dynamic Monte Carlo method predicts the complete CLD. When a large enough control volume is used, both methods give the same predictions for the chain length averages. The advantage of the method of moments is that it requires shorter simulation times; dynamic Monte Carlo simulations, although considerably longer, predict complete CLDs.

The concentration of CSA and the value of k_{CSA} affect CLD and M_n, but the influence of k_{CSA} on these properties is limited to only short polymerization times. The influence of CSA concentration on CLD and M_n is substantial even at longer polymerization times.

The value of k_p does not affect the shape of CLD, but it does affect its averages. If no chain transfer reaction occurs (not a realistic assumption in real chain shuttling polymerizations), M_n increases linearly with polymerization time and CLD follows Poisson distribution.

Finally, catalyst deactivation generates less polymer because few catalyst molecules are active in the reactor. At longer polymerization times, we observed different CLDs for distinct k_d values.

4. Simulation of Ethylene Chain Shuttling Polymerization in a Continuous Stirred Tank Reactor using the Method of Moments

4.1 Overview

We developed a model to simulate ethylene chain shuttling polymerization with a single catalyst using the method of moments in a continuous stirred tank reactor (CSTR) operated dynamically and at a steady state. The model predicts ethylene conversion, average molecular weights, and polydispersity. We used the model to quantify how polymerization conditions affect ethylene conversion and polymer properties by examining the effect of reactant flowrates and average residence time in the CSTR. We also investigated the effect of reactor type on the polyethylene properties by comparing CSTR and semi-batch reactor simulations described in Chapter 3.

4.2 Model Development for the Method of Moments in a Dynamic CSTR and at Steady State

The polymerization mechanism used in this chapter was described in Chapter 3. We modified the equations shown in Chapter 3 for moments and mole balances to include flow rates entering and leaving the CSTR. Table 4-1 and Table 4-2 show the moments equations in a dynamic CSTR and at steady state. Table 4-3 and Table 4-4 show the mole balance for catalyst, CSA, ethylene, and hydrogen in a dynamic CSTR and at steady state. Appendix 4-A presents the derivations of these equations.

Table 4-1. Moment equations for ethylene chain shuttling polymerization in a dynamic CSTR.

Description	Moment equations	Initial value
0th Moments of living chains	$\frac{dY_0}{dt} = k_i MC - \left(k_{t\beta} + k_{tH}H_2 + k_d + k_{CSA0}S_0 + s\right)Y_0$	0
1st Moments of living chains	$\frac{dY_1}{dt} = k_i MC + k_p MY_0 - \left(k_{t\beta} + k_{tH}H_2 + k_d + k_{CSA0}S_0 + k_{CSA}(SX_0) + s\right)Y_1 + k_{CSA}(SX_1)Y_0$	0
2nd Moments of living chains	$\frac{dY_2}{dt} = k_i MC + k_p M(Y_0 + 2Y_1) - \left(k_{t\beta} + k_{tH}H_2 + k_d + k_{CSA0}S_0 + k_{CSA}(SX_0) + s\right)Y_2 + k_{CSA}(SX_2)Y_0$	0
0th Moments of dead chains	$\frac{dX_0}{dt} = \left(k_{t\beta} + k_{tH}H_2 + k_d\right)Y_0 - sX_0$	0
1st Moments of dead chains	$\frac{dX_1}{dt} = \left(k_{t\beta} + k_{tH}H_2 + k_d\right)Y_1 - sX_1$	0
2nd Moment of dead chains	$\frac{dX_2}{dt} = \left(k_{t\beta} + k_{tH}H_2 + k_d\right)Y_2 - sX_2$	0
0th Moments of dormant chains	$\frac{d(SX_0)}{dt} = k_{CSA0}S_0Y_0 - s(SX_0)$	0
1st Moments of dormant chains	$\frac{d(SX_1)}{dt} = \left(k_{CSA0}S_0 + k_{CSA}(SX_0)\right)Y_1 - \left(k_{CSA}Y_0 + s\right)(SX_1)$	0
2nd Moments of dormant chains	$\frac{d(SX_2)}{dt} = \left(k_{CSA0}S_0 + k_{CSA}(SX_0)\right)Y_2 - \left(k_{CSA}Y_0 + s\right)(SX_2)$	0

Table 4-2. Moment equations for ethylene chain shuttling polymerization in a CSTR at steady state.

Description	Moment equations
0th Moments of living chains	$Y_0^2 + \left\{ \begin{array}{l} \dfrac{s}{k_{CSA0}} + \dfrac{[S_0]^{in}}{\left(k_{t\beta} + k_{tH}[H_2] + k_d + s\right)} \\ -\dfrac{k_i[C][M]}{\left(k_{t\beta} + k_{tH}[H_2] + k_d + s\right)} \end{array} \right\} Y_0 - \dfrac{k_i[C][M]s}{\left(k_{t\beta} + k_{tH}[H_2] + k_d + s\right)k_{CSA0}} = 0$
1st Moments of living chains	$Y_1 = \dfrac{k_i[C][M] + k_p[M]Y_0}{k_{t\beta} + k_{tH}[H_2] + k_d + s + \dfrac{k_{CSA0}[S_0]s}{k_{CSA}Y_0 + s} + \dfrac{k_{CSA}[SX_0]s}{k_{CSA}Y_0 + s}}$
2nd Moments of living chains	$Y_2 = \dfrac{k_i[C][M] + k_p[M]\left(Y_0 + 2Y_1\right)}{k_{t\beta} + k_{tH}[H_2] + k_d + s + \dfrac{k_{CSA0}[S_0]s}{k_{CSA}Y_0 + s} + \dfrac{k_{CSA}[SX_0]s}{k_{CSA}Y_0 + s}}$
0th Moments of dead chains	$[X_0] = \dfrac{\left(k_{t\beta} + k_{tH}[H_2] + k_d\right)Y_0}{s}$
1st Moments of dead chains	$[X_1] = \dfrac{\left(k_{t\beta} + k_{tH}[H_2] + k_d\right)Y_1}{s}$
2nd Moment of dead chains	$[X_2] = \dfrac{\left(k_{t\beta} + k_{tH}[H_2] + k_d\right)Y_2}{s}$
0th Moments of dormant chains	$[SX_0] = \dfrac{k_{CSA0}[S_0]Y_0}{s}$
1st Moments of dormant chains	$[SX_1] = \dfrac{\left(k_{CSA0}[S_0] + k_{CSA}[SX_0]\right)Y_1}{k_{CSA}Y_0 + s}$
2nd Moments of dormant chains	$[SX_2] = \dfrac{\left(k_{CSA0}[S_0] + k_{CSA}[SX_0]\right)Y_2}{k_{CSA}Y_0 + s}$

Table 4-3. Mole balance equations for ethylene chain shuttling polymerization in a dynamic CSTR.

Description	Molar equations	Initial value
Catalyst	$\frac{dC}{dt} = -(k_i M + k_d + s)C + (k_{t\beta} + k_{tH} H_2 + k_{CSA0} S_0) Y_0 + C^{in}$	0
Chain shuttling agent (CSA)	$\frac{dS_0}{dt} = -(k_{CSA0} Y_0 + s) S_0 + S_0^{in}$	0
Ethylene	$\frac{dM}{dt} = -(k_i C + k_p Y_0 + s) M + M^{in}$	0
Hydrogen	$\frac{dH_2}{dt} = -(k_{tH} Y_0 + s) H_2 + H_2^{in}$	0
Deactivated site	$\frac{dC_d}{dt} = k_d (Y_0 + C) - s C_d$	0
Ethylene consumption	$\frac{dM_p}{dt} = (k_i C + k_p Y_0) M - s M_p$	0

Table 4-4. Mole balance equations for ethylene chain shuttling polymerization in a CSTR at steady state.

Description	Molar equations
Catalyst	$[C] = \frac{[C]^{in} + (k_{t\beta} + k_{tH}[H_2] + k_{CSA0}[S_0]) Y_0}{k_d + k_i [M] + s}$
Chain shuttling agent (CSA)	$[S_0] = \frac{[S_0]^{in}}{k_{CSA0} Y_0 + s}$
Deactivated site	$C_d = \frac{k_d (Y_0 + C)}{s}$
Ethylene consumption	$M_p = \frac{(k_i C + k_p Y_0) M}{s}$

s: reciprocal of the average residence time in the CSTR.

The differential equations shown in Table 4-1 and Table 4-3 were solved in Matlab using the stiff differential equations solver ode15s. After manipulating the non-linear algebraic equations for CSTR shown in Table 4-2 and Table 4-4, we get Equations (4–1) and (4–2). The Matlab subroutine *vpasolve* was used to solve these two equations to obtain the 0^{th} moment (Y_0) of the living polymer

and the catalyst concentration, $[C]$, inside the CSTR. These results were then used to calculate all the other moments (living, dormant, and dead), reactant concentrations, monomer conversion, average molecular weights, and polydispersity.

$$Y_0^{\,2} + \left\{ \begin{array}{l} \dfrac{s}{k_{CSA0}} + \dfrac{[S_0]^{in}}{\left(k_{t\beta} + k_{tH}[H_2] + k_d + s\right)} \\ \quad - \dfrac{k_i[M]\left([C]^{in} + Y_0\left(k_{t\beta} + k_{tH}[H_2] + \dfrac{k_{CSA0}[S_0]^{in}}{k_{CSA0}Y_0 + s}\right)\right)}{(k_i[M] + k_d + s)\left(k_{t\beta} + k_{tH}[H_2] + k_d + s\right)} \end{array} \right\} Y_0 - \frac{k_i[M]s\left([C]^{in} + Y_0\left(k_{t\beta} + k_{tH}[H_2] + \dfrac{k_{CSA0}[S_0]^{in}}{k_{CSA0}Y_0 + s}\right)\right)}{(k_d + k_i[M] + s)\left(k_{t\beta} + k_{tH}[H_2] + k_d + s\right)k_{CSA0}} = 0 \tag{4-1}$$

$$[C]^{in} + \left\{ k_{t\beta} + k_{tH}[H_2] + \left(\frac{k_{CSA0}[S_0]^{in}}{k_{CSA0}Y_0 + s} \right) \right\} Y_0 - \left(k_d + k_i[M] + s\right)C = 0 \tag{4-2}$$

4.3 Results and Discussion

4.3.1 Effect of operation conditions

In the following simulations, we studied the effect of changing the operation conditions of a CSTR during 8 hours (28800 seconds) of operation. Table 4-5 and Table 4-6 show the kinetic constants and initial conditions used in the simulations. The average reactor residence time 600 seconds. The initial conditions for the CSTR appear in Table 4-6. After reaching a steady state, the CSTR conditions were changed according to the schedule shown in Table 4-7.

Table 4-5. Kinetic constants for ethylene chain shuttling polymerization.

Kinetic constants	Values	Units
Initiation rate constant, k_i	10000	L/mol.s
Propagation rate constant, k_p	10000	L/mol.s
β-hydride elimination, $k_{t\beta}$	0	s^{-1}
Chain transfer to hydrogen, k_{tH}	$0.1\times k_p$	L/mol.s
Deactivation rate constant, k_d	0	s^{-1}
Chain shuttling rate constant to CSA, k_{CSA0}	$10\times k_p$	L/mol.s
Chain shuttling rate constant to dormant chain, k_{CSA}	$10\times k_p$	L/mol.s

Table 4-6. Initial process conditions for ethylene chain shuttling polymerization in a dynamic CSTR.

Reactants	Values	Units
Monomer molar flow rate, M^{in}	2/600	mol/L.s
Catalyst molar flow rate, C^{in}	$7.78\times10^{-7}/600$	mol/L.s
Chain shuttling agent molar flow rate, S^{in}	$7.78\times10^{-4}/600$	mol/L.s
Hydrogen molar flow rate, H_2^{in}	0.005/600	mol/L.s
Average residence time, τ	600	s
Polymerization time, t	$5\times\tau$	s

When the CSTR reaches steady state, the ethylene molar flow rate increases from 2/600 to 4/600 mol/L.s; when CSTR reaches another steady state, then the CSA flow rate increases from $7.78\times10^{-4}/600$ to $15.56\times10^{-4}/600$ mol/L.s; when CSTR reaches yet another steady state, then the hydrogen flow rate increases from 0.005/600 to 0.01/600 mol/L.s. In the next step, the CSTR operates in order to go back to the initial conditions established. The hydrogen flow rate decreases from 0.01/600 to 0.005/600 mol/L.s; after CSTR reaches steady state, the CSA flow rate decreases from $15.56\times10^{-4}/600$ to $7.78\times10^{-4}/600$ mol/L.s and the ethylene flow rate decreases from 4/600 to 2/600 mol/L.s, as shown in Table 4-7.

Table 4-7. Process condition changes for ethylene chain shuttling polymerization in a dynamic CSTR.

Time, h	Condition before change (*mol/L.s*)	Condition after change (*mol/L.s*)
1	$M^{in} = 2/600$	$M^{in} = 4/600$
2	$S^{in} = 7.78\times10^{-4}/600$	$S^{in} = 15.56\times10^{-4}/600$
3	$H_2{}^{in} = 0.005/600$	$H_2{}^{in} = 0.01/600$
4	$H_2{}^{in} = 0.01/600$	$H_2{}^{in} = 0.005/600$
5	$S^{in} = 15.56\times10^{-4}/600$	$S^{in} = 7.78\times10^{-4}/600$
6	$M^{in} = 4/600$	$M^{in} = 2/600$

Figure 4-1 shows how ethylene, H_2, CSA, and catalyst concentrations vary as a function of time in a CSTR. All changes reflect the expected trends shown in Table 4-7. Note that the changes in catalyst concentration, [*C*], refer to ethylene-free active sites and do not include active sites attached to growing polymer chains. The changes in these concentrations will impact polymer properties, as discussed below.

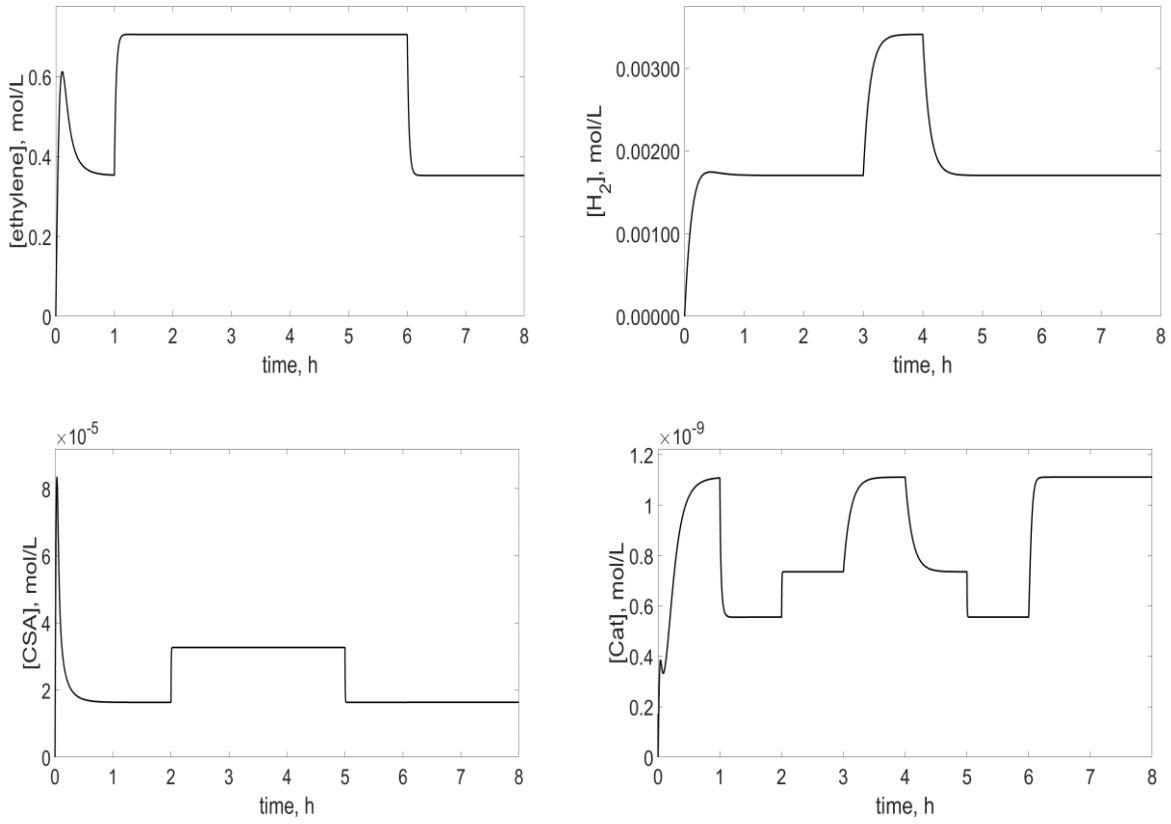

Figure 4-1. Ethylene, H_2, CSA, and catalyst profile for ethylene chain shuttling polymerization in a CSTR as a function of time.

Figure 4-2 shows how M_n and M_w vary for living, dormant, dead, and overall polymer chains. During reactor start-up, M_n and M_w increase sharply until they reach maximum values, then decrease to steady state values, following a trend similar to ethylene concentration in the reactor. At t = 1 h, the ethylene concentration doubles, causing M_n and M_w to increase as the polymerization rate increases but the transfer and chain shuttling rates remain the same; at t = 2 h, the CSA concentration increases, reducing M_n and M_w as more dormant chains form; at t = 3 h, the hydrogen concentration increases, reducing M_n and M_w due to increased chain transfer rates; finally, resetting the process conditions (ethylene, CSA and H_2 concentrations) to their original values causes M_n and M_w to return to the levels obtained at the beginning of the simulation. Molecular weight averages for the dead polymer trail behind those for living and dormant chains, as expected. This is just the consequence of chain shuttling polymerization, where the polymer chains take a certain time to become dead chains.

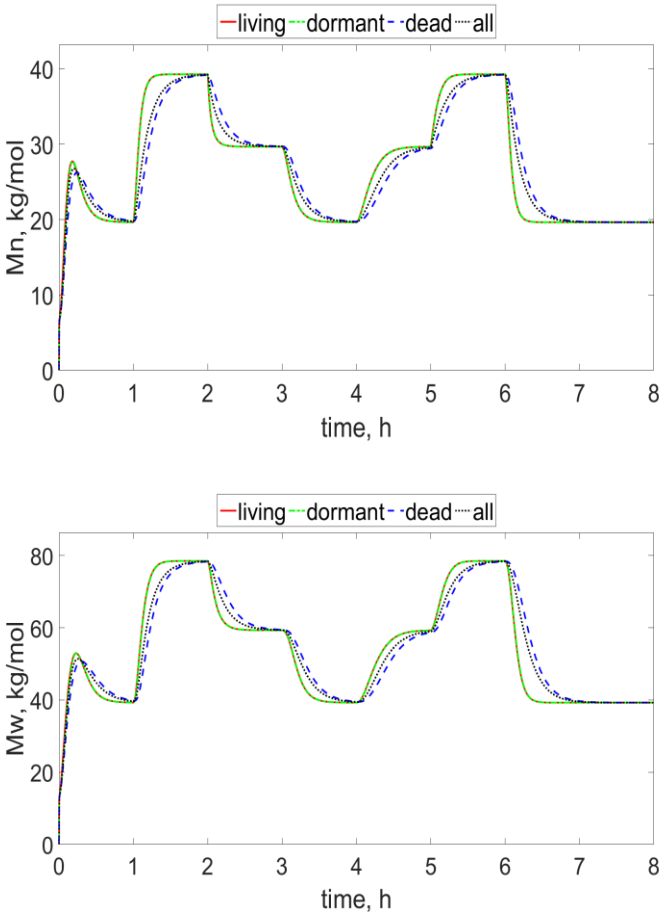

Figure 4-2. Number and weight average molecular weight profiles of different polyethylene chain populations.

Figure 4-3 shows how the polydispersity index (PDI) varies as a function of time and changes in operation conditions. Steady-state values converge to the expected value of 2.0, but deviate for a short time from 2.0 as different conditions in the CSTR change. Changing the operation conditions affects the PDI for a short time, but it eventually returns to 2.0, as is mandatory for a CSTR.

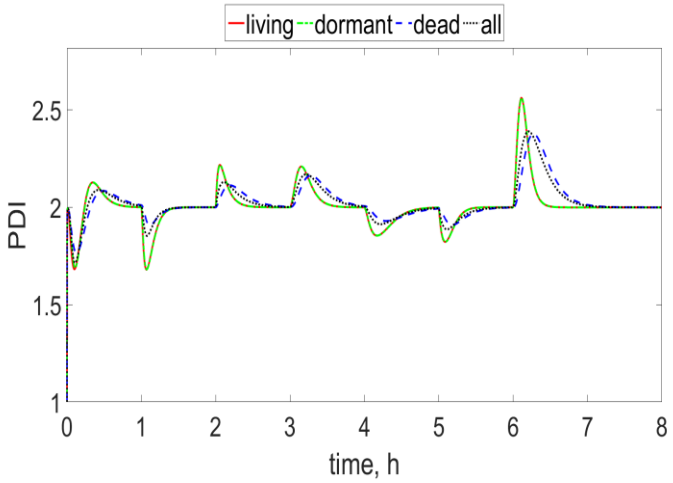

Figure 4-3. Polydispersity index profile of different polyethylene chain populations.

4.3.2 Comparison of semi-batch reactor and CSTR at a steady state

The following simulations study the effect of reactor type on the polymer properties at the end of polymerization. Table 4-8 and Table 4-9 show the kinetic rate constants and process conditions. The molar flow rate of catalyst and CSA to the CSTR was adjusted so that the concentration of catalyst and CSA in the CSTR was the same to the equivalent concentrations in the semi-batch reactor. Ethylene concentration was also kept the same in both reactors. For the comparisons discussed in this chapter, the polymerization time in the semi-batch reactor is equal to the average residence time in the CSTR.

Table 4-8. Kinetic constants for ethylene chain shuttling polymerization used for comparison of semi-batch reactor and CSTR.

Kinetic constants	Values	Units
Initiation rate constant, k_i	10000	L/mol.s
Propagation rate constant, k_p	10000	L/mol.s
β-hydride elimination, $k_{t\beta}$	25	s^{-1}
Chain transfer to hydrogen, k_{tH}	0	L/mol.s
Deactivation, k_d	0	s^{-1}
Chain shuttling rate constant to CSA, k_{CSA0}	$10\times k_p$	L/mol.s
Chain shuttling rate constant to dormant chain, k_{CSA}	$10\times k_p$	L/mol.s

Table 4-9. Process conditions for ethylene chain shuttling polymerization used for comparison of semi-batch reactor and CSTR.

Reactants	Values	Units
Monomer concentration, $[M]$	2	mol/L
Catalyst concentration, $[Cat]$	7.78×10^{-7}	mol/L
Chain shuttling agent to catalyst concentration, $[CSA]/[Cat]$	1000	
Hydrogen to monomer concentration, $[H_2]/[M]$	0	
Average residence time, τ	varied	
Polymerization time in semi-batch, t	τ	s

Figure 4-4 shows that ethylene conversion in the semi-batch reactor and CSTR at different times and at different $[CSA]/[Cat]$ ratios is the same. We expected this outcome as monomer conversion depends on catalyst concentration and polymerization time, which is the same for both modes of operation.

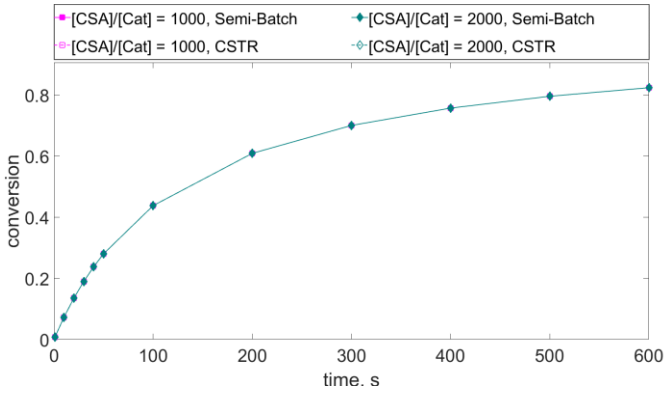

Figure 4-4. Effect of $[CSA]/[Cat]$ on ethylene conversion in a semi-batch reactor and CSTR. All other variables are constant (Table 4-8 and Table 4-9).

Figure 4-5 compares M_n for polymer made in a semi-batch reactor and a CSTR at different times and [*CSA*]/[*Cat*] ratios. M_n increases with time until reaching a plateau, because longer polymerization times allow for chains to grow longer. A plateau is reached because, after a certain time, chain transfer reactions start controlling the limiting value of M_n that can reach in this system. In addition, the CSTR produces polymers with slightly higher M_n because dormant chains are always present in a CSTR operated at a steady state, while they take a certain time to form in a semi-batch reactor. As the [*CSA*]/[*Cat*] ratio increases, M_n decreases in both reactors because the CSA works as a reversible chain transfer agent.

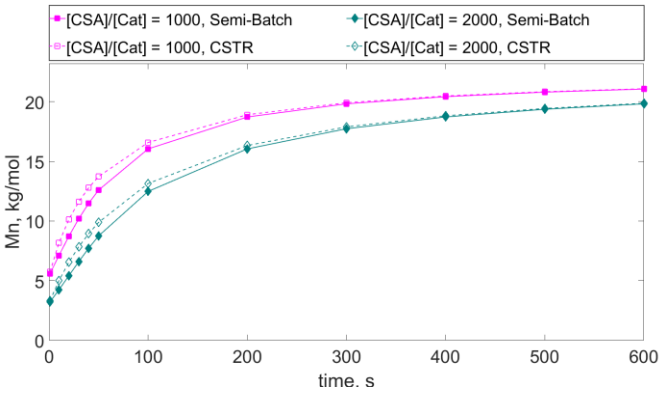

Figure 4-5. Effect of [*CSA*]/[*Cat*] on M_n for ethylene polymerization in a semi-batch reactor and CSTR. All other variables are constant (Table 4-8 and Table 4-9).

Figure 4-6 compares the PDI for polymers made under these two modes of operation. For the semi-batch reactor, the PDI decreases as polymerization time increases until achieving a minimum value; it then increases due to the accumulation of dead polymer chains. For the CSTR, the PDI is equal to 2 at any time due to the effect of the exponential residence time distribution in the CSTR. The [*CSA*]/[*Cat*] ratio does not affect the PDI of polymers made in the CSTR, but in a semi-batch reactor the PDI is smaller for high [*CSA*]/[*Cat*] ratios because of the competition between chain shuttling and chain termination.

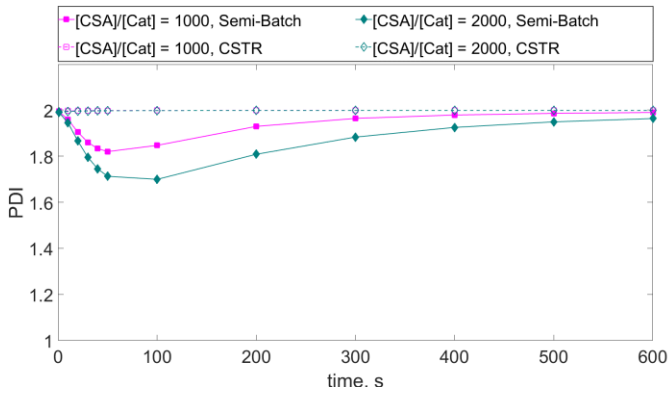

Figure 4-6. Effect of $[CSA]/[Cat]$ on PDI for ethylene polymerization in a semi-batch reactor and CSTR. All other variables are constant (Table 4-8 and Table 4-9).

Figure 4-7 compares the M_n of polymers made in a semi-batch reactor and CSTR at different times and k_{CSA}/k_p ratios. For the same $[CSA]/[Cat]$ ratio, changing the value of k_{CSA}/k_p has a minor effect on M_n at very short polymerization times. Higher k_{CSA}/k_p produces polymers for which the M_n increases more slowly, but at longer polymerization times all M_n curves converge to the same value. The value of k_{CSA} regulates the frequency of the chain exchange between dormant and living states whereas the value of k_p (for a given $k_{t\beta}$) controls M_n. Therefore, increasing k_{CSA}/k_p at constant k_p results in a more frequent exchange of chains between living and dormant states, but their final molecular weight averages will remain the same. The M_n for polymers made in CSTR is higher than in a semi-batch reactor in both cases, especially with small average residence time.

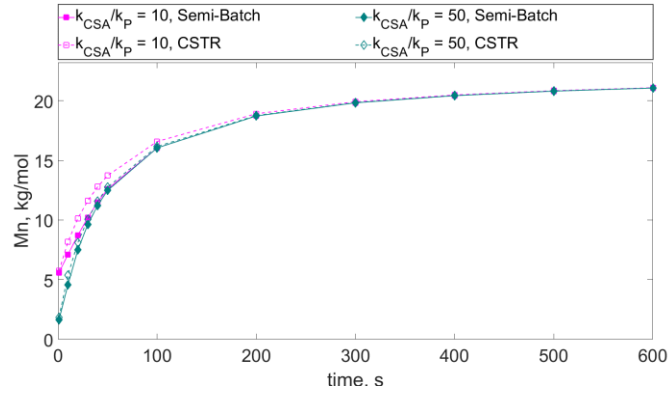

Figure 4-7. Effect of k_{CSA}/k_p on M_n for ethylene polymerization in a semi-batch reactor and CSTR. All other variables are constant (Table 4-8 and Table 4-9).

The PDI of polymers made in a semi-batch reactor varies significantly with the value of the k_{CSA}/k_p ratio (Figure 4-8). For the semi-batch reactor, because of the quasi-living nature of chain shuttling polymerization, PDI is lower than 2.0 when $k_{CSA}/k_p > 0$. The PDI reaches its minimum value at early stages of polymerization, since chain transfer reactions start playing a more important role for longer polymerization times. Note that $k_{t\beta}$ is not equal to zero in these simulations; therefore, dead chains will accumulate in the reactor as the polymerization proceeds, broadening the CLD of the polymer. For CSTR, the PDI is 2 in both cases due the effect of residence time distribution.

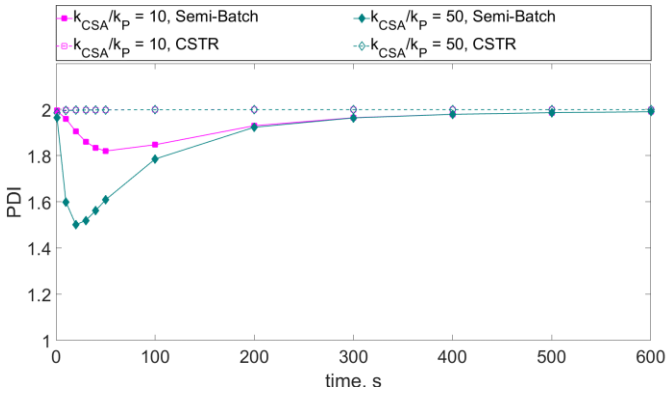

Figure 4-8. Effect of k_{CSA}/k_p on PDI for ethylene polymerization in a semi-batch reactor and CSTR. All other variables are constant (Table 4-8 and Table 4-9).

Figure 4-9 shows how M_n varies at different times with different k_p values while keeping the chain shuttling rate constants (k_{CSA0} and k_{CSA}) at 100000 L/(mol.s) and the [CSA]/[C] ratio at 1000. As k_p increases, the value of M_n increases, because ethylene insertion between catalyst and living chain increases, but PDI remains the same for all corresponding k_p values (Figure 4-10). The M_n for polymer made in CSTR is higher than in the semi-batch reactor in both cases, especially with small average residence time, while the PDI is 2 for both cases due the effect of residence time distribution.

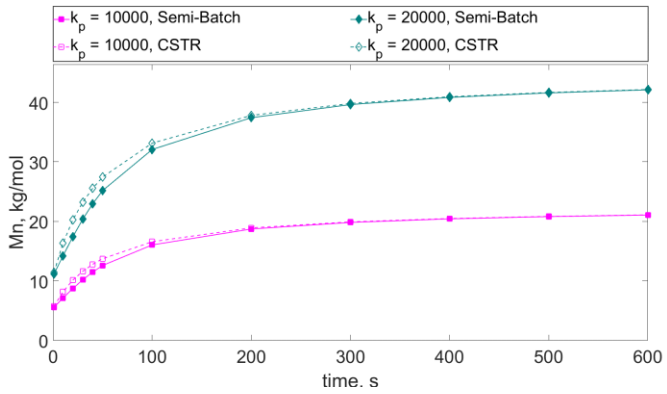

Figure 4-9. Effect of k_p on M_n for ethylene polymerization in a semi-batch reactor and CSTR while keeping k_{CSA} constant at 100000. All other variables are constant (Table 4-8 and Table 4-9).

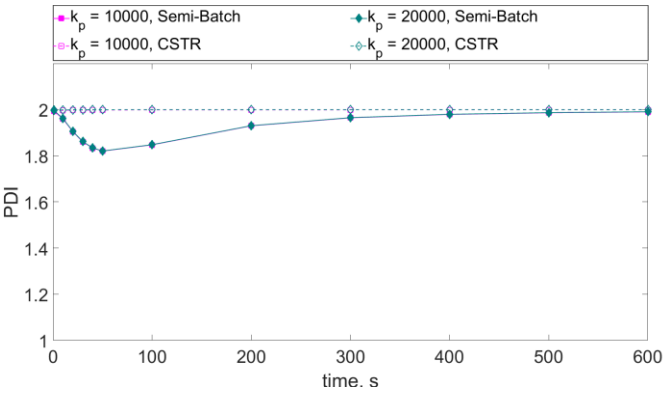

Figure 4-10. Effect of k_p on PDI for ethylene polymerization in a semi-batch and CSTR reactor while keeping k_{CSA} constant at 100000. All other variables are constant (Table 4-8 and Table 4-9).

As expected, the constants for β-hydride elimination ($k_{t\beta}$) and propagation (k_p) have a major effect on M_n. Figure 4-11 and Figure 4-12 show the effect of $k_{t\beta}$ on M_n and PDI. For both reactors, the value of M_n decreases sharply as $k_{t\beta}$ increases, and for the semi-batch reactor the dynamic behavior of PDI also depends strongly on the value of $k_{t\beta}$. For higher $k_{t\beta}$ values, PDI rises faster due to the accumulation of dead chains in the reactor. The features of classic living polymerization (polymer has a PDI close to one, chain length distribution is close to Poisson distribution, and the average molecular weight increases linearly with polymerization time) when $k_{t\beta} = 0$. The M_n for polymer made in CSTR is higher than in the semi-batch reactor in all cases while the PDI is 2 for all cases due the effect of residence time distribution.

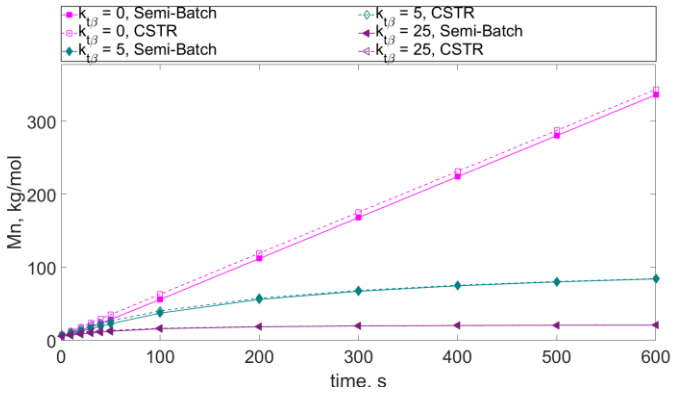

Figure 4-11. Effect of $k_{t\beta}$ on M_n for ethylene polymerization in a semi-batch reactor and CSTR. All other variables are constant (Table 4-8 and Table 4-9).

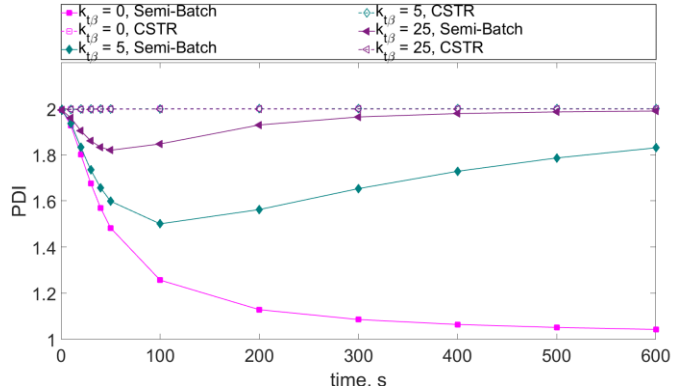

Figure 4-12. Effect of $k_{t\beta}$ on PDI for ethylene polymerization in a semi-batch reactor CSTR. All other variables are constant (Table 4-8 and Table 4-9).

4.4 Conclusion

Polyolefins are made commercially in CSTRs operated mostly under steady-state conditions, except during start up, shut down, or grade transitions. In this chapter, we compared dynamic and steady state solutions for the chain shuttling polymerization of ethylene in a CSTR. The dynamic solution converges to the steady-state solution, proving that our models and simulation programs are correct.

We also compared the properties of polyethylene made by chain shuttling polymerization in semi-batch reactors and CSTRs operated under steady state conditions. This comparison is important because we usually develop new resins in laboratory-scale semi-batch reactors before scaling up to CSTRs in pilot plants or industrial reactors. The properties of polymers made in semi-batch reactors will differ from those made in CSTRs; even if we operate both in the same conditions and for the same (average) polymerization time, it is very important in scaling up investigations.

Polymers made in CSTRs have higher M_n than those made in semi-batch reactors because dormant chains are always present in steady state CSTRs, while they take a certain time to form in semi-batch reactors. For CSTRs at a steady state, the molecular weight averages of living, dead, and dormant chains were all the same. In addition, the PDI of polymers made in CSTRs is always 2.0, even under perfect living polymerization conditions because of their broad residence time distribution.

5. Simulation of Chain Shuttling Copolymerization in a Semi-Batch Reactor using the Method of Moments and a Dynamic Monte Carlo Model

5.1 Overview

This chapter describes the method of moments and a dynamic Monte Carlo model that can predict the microstructure of ethylene/1-octene copolymers made with chain shuttling copolymerization using two single-site catalysts in a semi-batch reactor. One catalyst incorporates 1-octene well and produces chains with high comonomer content; the other catalyst is not an effective 1-octene incorporator and makes chains with low comonomer fraction. The chain shuttling agent acts as a reversible chain transfer agent, *shuttling* chains between the two catalyst types to produce linear olefin block copolymers (OBCs).

The population balance and dynamic Monte Carlo models predict the number and weight average chain lengths of polymer populations containing different numbers of blocks as a function of polymerization time. They also predict the weight and number fractions of the polymer populations. The dynamic Monte Carlo model predicts the complete distributions of chain length (CLD) and chemical composition (CCD) for the whole polymer and for chains with different numbers of blocks and their comonomer compositions.

5.2 Chain Shuttling Copolymerization Mechanism

The mechanism used for chain shuttling copolymerization consists of six steps, similar to the mechanism for ethylene homopolymerization presented in Chapter 3, but includes separate reactions for each comonomer type. For simplicity, the Bernoullian model for copolymerization was assumed, that is, the rates of reaction depend only on the type of comonomer reacting, not on the type of commoner last added to the polymer chain. The polymerization mechanism in Table 5-1 is the same as the standard one for olefin copolymerization with coordination catalysts based on Bernoullian statistics, except for the steps involving reactions with CSA. During chain shuttling to virgin CSA, a growing polymer chain transfers to a CSA molecule, forming a dormant polymer chain and releasing an active center capable of forming a new polymer chain, as shown in Equations (5–17) and (5–18).[18]

Table 5-1. Mechanism of chain shuttling copolymerization using two catalysts.

Description	Chemical equations	Rate constants	Equation
Initiation	$C_1 + A \rightarrow P_{1,1}$	k_{iA1}	(5-1)
	$C_1 + B \rightarrow P_{1,1}$	k_{iB1}	(5-2)
	$C_2 + A \rightarrow Q_{1,1}$	k_{iA2}	(5-3)
	$C_2 + B \rightarrow Q_{1,1}$	k_{iB2}	(5-4)
Propagation	$P_{r,i} + A \rightarrow P_{r+1,i}$	k_{pA1}	(5-5)
	$P_{r,i} + B \rightarrow P_{r+1,i}$	k_{pB1}	(5-6)
	$Q_{r,i} + A \rightarrow Q_{r+1,i}$	k_{pA2}	(5-7)
	$Q_{r,i} + B \rightarrow Q_{r+1,i}$	k_{pB2}	(5-8)
β-hydride elimination	$P_{r,i} \rightarrow D_{r,i} + C_1$	$k_{t\beta 1}$	(5-9)
	$Q_{r,i} \rightarrow D_{r,i} + C_2$	$k_{t\beta 2}$	(5-10)
Chain transfer to hydrogen	$P_{r,i} + H_2 \rightarrow D_{r,i} + C_1$	k_{tH1}	(5-11)
	$Q_{r,i} + H_2 \rightarrow D_{r,i} + C_2$	k_{tH2}	(5-12)
Deactivation of growing chain	$P_{r,i} \rightarrow D_{r,i} + C_{d1}$	k_{d1}	(5-13)
	$Q_{r,i} \rightarrow D_{r,i} + C_{d2}$	k_{d2}	(5-14)
Deactivation of active catalyst	$C_1 \rightarrow C_{d1}$	k_{d1}	(5-15)
	$C_2 \rightarrow C_{d2}$	k_{d2}	(5-16)
Chain shuttling to CSA	$P_{r,i} + S_0 \rightarrow SP_{r,i} + C_1$	k_{CSA01}	(5-17)
	$Q_{r,i} + S_0 \rightarrow SQ_{r,i} + C_2$	k_{CSA02}	(5-18)
Chain shuttling to dormant chain	$P_{r,i} + SP_{s,j} \rightarrow P_{s,j} + SP_{r,i}$	$k_{CSA1self}$	(5-19)
	$P_{r,i} + SQ_{s,j} \rightarrow P_{s,j+1} + SP_{r,i}$	$k_{CSA1cross}$	(5-20)
	$Q_{r,i} + SP_{s,j} \rightarrow Q_{s,j+1} + SQ_{r,i}$	$k_{CSA2cross}$	(5-21)
	$Q_{r,i} + SQ_{s,j} \rightarrow Q_{s,j} + SQ_{r,i}$	$k_{CSA2self}$	(5-22)

Subscripts r and s indicate the chain length. Subscripts i and j indicate the number of blocks. Subscripts 1 and 2 indicate the catalyst type P and Q. Thus, C_1 and C_2, respectively: active site from catalyst P and Q, A and B: ethylene and 1-octene, S_0: chain shuttling agent, H_2: hydrogen, $P_{1,1}$ and $Q_{1,1}$: living polymer chain of length 1 and number of block 1 made in catalyst type P and Q, $P_{r,i}$ and $Q_{r,i}$: living polymer chain of length r and number of block i made in catalyst type P and Q, $D_{r,i}$: dead polymer chain of length r and number of block i made in catalyst type P and Q, $SP_{r,i}$ and $SQ_{r,i}$: dormant polymer chain of length r and number of blocks i made in catalyst type P and Q, k_i: initiation rate constant, k_p: propagation rate constant, $k_{t\beta}$: β-hydride elimination rate constant, k_{tH}: chain transfer to hydrogen rate constant, k_{CSA0}: chain-shuttling rate constant to CSA, and k_{CSA}: chain-shuttling rate constant to dormant chain.

When the CSA reacts with the growing polymer chain, the latter becomes dormant. The dormant chain made by catalyst *P* attached to a CSA molecule, represented by $SP_{s,j}$, has two possibilities: 1) self-shuttling: CSA shuttles the dormant chain to catalyst *P*, represented by $P_{s,i}$, followed by a propagation step producing no new block (i.e., it will keep extending the length of the soft block, as shown in Equation (5–19)); and 2) cross-shuttling process: CSA shuttles the dormant chain to catalyst *Q*, followed by a propagation step, starting a new hard polymer block attached to the soft block made in catalyst *P*, as described in Equation (5–21). This process repeats several times until chain transfer eventually takes place or the polymerization stops. A similar process occurs for dormant chains made by catalyst *Q*, represented by $SQ_{s,j}$. Figure 5-1 illustrates this process.

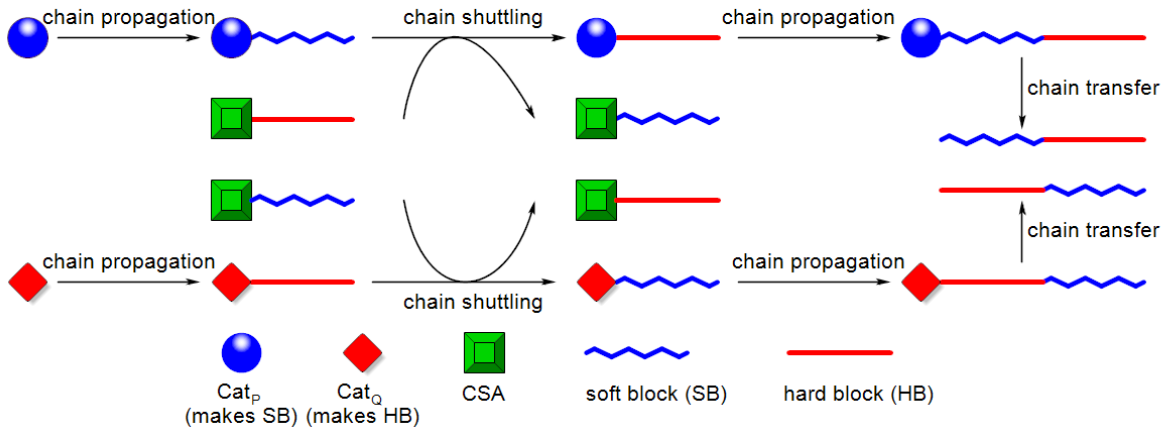

Figure 5-1. Mechanism of chain shuttling copolymerization using two catalysts.

5.3 The Method of Moments

Polymer populations were classified as living, dormant, and dead chains; polymer blocks were classified as soft (*S*), made by catalyst *P*, or hard (*H*), made by catalyst *Q*. Olefin block copolymers (OBCs) have alternating blocks, as depicted in Figure 5-2.

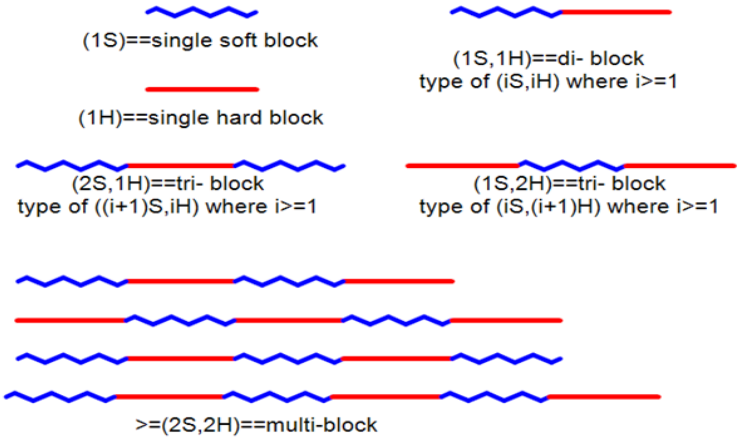

Figure 5-2. Types of olefin block copolymer chains.

The following expression gives the k^{th} moment for living, dormant, and dead chains of a generic distribution $f(r,i)$:[50]

$$\mu_{k,i} = \sum_{r=1}^{\infty} r^k f(r,i) \tag{5-23}$$

We adopted the following nomenclature for the moments:

1. $Y_{k,P}$ and $Y_{k,Q}$ are the k^{th} moments of the living chains growing in catalyst *P* and *Q*, respectively.
2. $SX_{k,P}$ and $SX_{k,Q}$ are the k^{th} moments of dormant chains for which catalyst *P* and *Q* made the last block, respectively.
3. $X_{k,P}$ and $X_{k,Q}$ are the k^{th} moments of dead chains for which catalyst *P* and *Q* made the last block, respectively.
4. $Y_{k,P,i}$ and $Y_{k,Q,i}$ are the k^{th} moments of living chains growing in catalyst *P* and *Q* having *i* blocks, respectively.

5. $SX_{k,P,i}$ and $SX_{k,Q,i}$ are the k^{th} moments of dormant chains having i blocks for which catalyst P and Q made the last block, respectively.
6. $X_{k,P,i}$ and $X_{k,Q,i}$ are the k^{th} moments of dead chains having i blocks for which catalyst P and Q made the last block, respectively.

These moments are defined using the following equations,

$$Y_{k,P} = \sum_{i=1}^{\infty}\sum_{r=1}^{\infty} r^k Y_{k,P,i} \tag{5-24}$$

$$Y_{k,Q} = \sum_{i=1}^{\infty}\sum_{r=1}^{\infty} r^k Y_{k,Q,i} \tag{5-25}$$

$$SX_{k,P} = \sum_{i=1}^{\infty}\sum_{r=1}^{\infty} r^k SX_{k,P,i} \tag{5-26}$$

$$SX_{k,Q} = \sum_{i=1}^{\infty}\sum_{r=1}^{\infty} r^k SX_{k,Q,i} \tag{5-27}$$

$$X_{k,P} = \sum_{i=1}^{\infty}\sum_{r=1}^{\infty} r^k X_{k,P,i} \tag{5-28}$$

$$X_{k,Q} = \sum_{i=1}^{\infty}\sum_{r=1}^{\infty} r^k X_{k,Q,i} \tag{5-29}$$

$$Y_{k,P,i} = \sum_{r=1}^{\infty} r^k P_{r,i} = P_{1,1} + \sum_{r=2}^{\infty} r^k P_{r,i} \tag{5-30}$$

$$Y_{k,Q,i} = \sum_{r=1}^{\infty} r^k Q_{r,i} = Q_{1,1} + \sum_{r=2}^{\infty} r^k Q_{r,i} \tag{5-31}$$

$$SX_{k,P,i} = \sum_{r=1}^{\infty} r^k SP_{r,i} = SP_{1,1} + \sum_{r=2}^{\infty} r^k SP_{r,i} \tag{5-32}$$

$$SX_{k,Q,i} = \sum_{r=1}^{\infty} r^k SQ_{r,i} = SQ_{1,1} + \sum_{r=2}^{\infty} r^k SQ_{r,i} \tag{5-33}$$

$$X_{k,P,i} = \sum_{r=1}^{\infty} r^k D_{r,i} = D_{1,1} + \sum_{r=2}^{\infty} r^k D_{r,i} \tag{5-34}$$

$$X_{k,Q,i} = \sum_{r=1}^{\infty} r^k D_{r,i} = D_{1,1} + \sum_{r=2}^{\infty} r^k D_{r,i} \tag{5-35}$$

Table 5-2 through Table 5-7 summarize the moment equations for living, dormant, and dead polymer populations, and Table 5-8 shows the molar balances for all reactants. The differential equations shown in Table 5-2 through Table 5-8 were solved in Matlab using the stiff differential equations solver ode15s.[51] Appendix 5-A shows the derivations of these equations in detail.

Table 5-9 shows the expressions for number and weight average chain lengths of polymer populations having different numbers of blocks. Table 5-10 shows their molar and weight fractions. Table 5-11 shows the equations for mole fraction for ethylene and 1-octene of polymer populations having different numbers of blocks. Table 5-12 shows the average number and weight of blocks per chain, comonomer composition for whole polymer, and overall conversion.

Table 5-2. Moment equations for chains made in catalyst P in a semi-batch reactor for the whole polymer.

Description	Moment equations	Initial value
0th Moment of living chains	$\frac{dY_{0,P}}{dt} = \left(k_{iA1}A + k_{iB1}B\right)C_1 - \left(k_{t\beta 1} + k_{tH1}H_2 + k_{d1} + k_{CSA01}S_0\right)Y_{0,P}$	0
1st Moment of living chains	$\frac{dY_{1,P}}{dt} = \left(k_{iA1}A + k_{iB1}B\right)C_1 + \left(k_{pA1}A + k_{pB1}B\right)Y_{0,P}$ $- \left(k_{t\beta 1} + k_{tH1}H_2 + k_{d1} + k_{CSA01}S_0 + k_{CSA1}\left(SX_{0,P}\right) + k_{CSA1}\left(SX_{0,Q}\right)\right)Y_{1,P} + \left(\left(SX_{1,P}\right) + \left(SX_{1,Q}\right)\right)k_{CSA1}Y_{0,P}$	0
2nd Moment of living chains	$\frac{dY_{2,P}}{dt} = \left(k_{iA1}A + k_{iB1}B\right)C_1 + \left(k_{pA1}A + k_{pB1}B\right)\left(Y_{0,P} + 2Y_{1,P}\right)$ $- \left(k_{t\beta 1} + k_{tH1}H_2 + k_{d1} + k_{CSA01}S_0 + k_{CSA1}\left(SX_{0,P}\right) + k_{CSA1}\left(SX_{0,Q}\right)\right)Y_{2,P} + \left(\left(SX_{2,P}\right) + \left(SX_{2,Q}\right)\right)k_{CSA1}Y_{0,P}$	0
0th Moment of dead chains	$\frac{dX_{0,P}}{dt} = \left(k_{t\beta 1} + k_{tH1}H_2 + k_{d1}\right)Y_{0,P}$	0
1st Moment of dead chains	$\frac{dX_{1,P}}{dt} = \left(k_{t\beta 1} + k_{tH1}H_2 + k_{d1}\right)Y_{1,P}$	0
2nd Moment of dead chains	$\frac{dX_{2,P}}{dt} = \left(k_{t\beta 1} + k_{tH1}H_2 + k_{d1}\right)Y_{2,P}$	0
0th Moment of dormant chains	$\frac{d\left(SX_{0,P}\right)}{dt} = \left(k_{CSA01}S_0 + k_{CSA1}\left(SX_{0,P}\right) + k_{CSA1}\left(SX_{0,Q}\right)\right)Y_{0,P} - \left(k_{CSA1}Y_{0,P} + k_{CSA2}Y_{0,Q}\right)\left(SX_{0,P}\right)$	0
1st Moment of dormant chains	$\frac{d\left(SX_{1,P}\right)}{dt} = \left(k_{CSA01}S_0 + k_{CSA1}\left(SX_{0,P}\right) + k_{CSA1}\left(SX_{0,Q}\right)\right)Y_{1,P} - \left(k_{CSA1}Y_{0,P} + k_{CSA2}Y_{0,Q}\right)\left(SX_{1,P}\right)$	0
2nd Moment of dormant chains	$\frac{d\left(SX_{2,P}\right)}{dt} = \left(k_{CSA01}S_0 + k_{CSA1}\left(SX_{0,P}\right) + k_{CSA1}\left(SX_{0,Q}\right)\right)Y_{2,P} - \left(k_{CSA1}Y_{0,P} + k_{CSA2}Y_{0,Q}\right)\left(SX_{2,P}\right)$	**0**

Table 5-3. Moment equations for chains made in catalyst Q in a semi-batch reactor for the whole polymer.

Description	Moment equations	Initial value
0th Moment of living chains	$\frac{dY_{0,Q}}{dt} = \left(k_{iA2}A + k_{iB2}B\right)C_2 - \left(k_{t\beta 2} + k_{tH2}H_2 + k_{d2} + k_{CSA02}S_0\right)Y_{0,Q}$	0
1st Moment of living chains	$\frac{dY_{1,Q}}{dt} = \left(k_{iA2}A + k_{iB2}B\right)C_2 + \left(k_{pA2}A + k_{pB2}B\right)Y_{0,Q}$ $- \left(k_{t\beta 2} + k_{tH2}H_2 + k_{d2} + k_{CSA02}S_0 + k_{CSA2}\left(SX_{0,P}\right) + k_{CSA2}\left(SX_{0,Q}\right)\right)Y_{1,Q} + \left(\left(SX_{1,P}\right) + \left(SX_{1,Q}\right)\right)k_{CSA2}Y_{0,Q}$	0
2nd Moment of living chains	$\frac{dY_{2,Q}}{dt} = \left(k_{iA2}A + k_{iB2}B\right)C_2 + \left(k_{pA2}A + k_{pB2}B\right)\left(Y_{0,Q} + 2Y_{1,Q}\right)$ $- \left(k_{t\beta 2} + k_{tH2}H_2 + k_{d2} + k_{CSA02}S_0 + k_{CSA2}\left(SX_{0,P}\right) + k_{CSA2}\left(SX_{0,Q}\right)\right)Y_{2,Q} + \left(\left(SX_{2,P}\right) + \left(SX_{2,Q}\right)\right)k_{CSA2}Y_{0,Q}$	0
0th Moment of dead chains	$\frac{dX_{0,Q}}{dt} = \left(k_{t\beta 2} + k_{tH2}H_2 + k_{d2}\right)Y_{0,Q}$	0
1st Moment of dead chains	$\frac{dX_{1,Q}}{dt} = \left(k_{t\beta 2} + k_{tH2}H_2 + k_{d2}\right)Y_{1,Q}$	0
2nd Moment of dead chains	$\frac{dX_{2,Q}}{dt} = \left(k_{t\beta 2} + k_{tH2}H_2 + k_{d2}\right)Y_{2,Q}$	0
0th Moment of dormant chains	$\frac{d\left(SX_{0,Q}\right)}{dt} = \left(k_{CSA02}S_0 + k_{CSA2}\left(SX_{0,P}\right) + k_{CSA2}\left(SX_{0,Q}\right)\right)Y_{0,Q} - \left(k_{CSA1}Y_{0,P} + k_{CSA2}Y_{0,Q}\right)\left(SX_{0,Q}\right)$	0
1st Moment of dormant chains	$\frac{d\left(SX_{1,Q}\right)}{dt} = \left(k_{CSA02}S_0 + k_{CSA2}\left(SX_{0,P}\right) + k_{CSA2}\left(SX_{0,Q}\right)\right)Y_{1,Q} - \left(k_{CSA1}Y_{0,P} + k_{CSA2}Y_{0,Q}\right)\left(SX_{1,Q}\right)$	0
2nd Moment of dormant chains	$\frac{d\left(SX_{2,Q}\right)}{dt} = \left(k_{CSA02}S_0 + k_{CSA2}\left(SX_{0,P}\right) + k_{CSA2}\left(SX_{0,Q}\right)\right)Y_{2,Q} - \left(k_{CSA1}Y_{0,P} + k_{CSA2}Y_{0,Q}\right)\left(SX_{2,Q}\right)$	**0**

Table 5-4. Moment equations for chains with a single block made in catalyst *P* in a semi-batch reactor.

Description	Moment equations	Initial value
0th Moment of living chains	$\frac{dY_{0,P,i}}{dt} = \left(k_{iA1}A + k_{iB1}B\right)C_1 - \left(k_{t\beta 1} + k_{tH1}H_2 + k_{d1} + k_{CSA01}S_0 + k_{CSA1}\left(SX_{0,P}\right) + k_{CSA1}\left(SX_{0,Q}\right)\right)Y_{0,P,i} + \left(SX_{0,P,i}\right)k_{CSA1}Y_{0,P}$	0
1st Moment of living chains	$\frac{dY_{1,P,i}}{dt} = \left(k_{iA1}A + k_{iB1}B\right)C_1 + \left(k_{pA1}A + k_{pB1}B\right)Y_{0,P,i}$ $-\left(k_{t\beta 1} + k_{tH1}H_2 + k_{d1} + k_{CSA01}S_0 + k_{CSA1}\left(SX_{0,P}\right) + k_{CSA1}\left(SX_{0,Q}\right)\right)Y_{1,P,i} + \left(SX_{1,P,i}\right)k_{CSA1}Y_{0,P}$	0
2nd Moment of living chains	$\frac{dY_{2,P,i}}{dt} = \left(k_{iA1}A + k_{iB1}B\right)C_1 + \left(k_{pA1}A + k_{pB1}B\right)\left(Y_{0,P,i} + 2Y_{1,P,i}\right)$ $-\left(k_{t\beta 1} + k_{tH1}H_2 + k_{d1} + k_{CSA01}S_0 + k_{CSA1}\left(SX_{0,P}\right) + k_{CSA1}\left(SX_{0,Q}\right)\right)Y_{2,P,i} + \left(SX_{2,P,i}\right)k_{CSA1}Y_{0,P}$	0
0th Moment of dead chains	$\frac{dX_{0,P,i}}{dt} = \left(k_{t\beta 1} + k_{tH1}H_2 + k_{d1}\right)Y_{0,P,i}$	0
1st Moment of dead chains	$\frac{dX_{1,P,i}}{dt} = \left(k_{t\beta 1} + k_{tH1}H_2 + k_{d1}\right)Y_{1,P,i}$	0
2nd Moment of dead chains	$\frac{dX_{2,P,i}}{dt} = \left(k_{t\beta 1} + k_{tH1}H_2 + k_{d1}\right)Y_{2,P,i}$	0
0th Moment of dormant chains	$\frac{d\left(SX_{0,P,i}\right)}{dt} = \left(k_{CSA01}S_0 + k_{CSA1}\left(SX_{0,P}\right) + k_{CSA1}\left(SX_{0,Q}\right)\right)Y_{0,P,i} - \left(k_{CSA1}Y_{0,P} + k_{CSA2}Y_{0,Q}\right)\left(SX_{0,P,i}\right)$	0
1st Moment of dormant chains	$\frac{d\left(SX_{1,P,i}\right)}{dt} = \left(k_{CSA01}S_0 + k_{CSA1}\left(SX_{0,P}\right) + k_{CSA1}\left(SX_{0,Q}\right)\right)Y_{1,P,i} - \left(k_{CSA1}Y_{0,P} + k_{CSA2}Y_{0,Q}\right)\left(SX_{1,P,i}\right)$	0
2nd Moment of dormant chains	$\frac{d\left(SX_{2,P,i}\right)}{dt} = \left(k_{CSA01}S_0 + k_{CSA1}\left(SX_{0,P}\right) + k_{CSA1}\left(SX_{0,Q}\right)\right)Y_{2,P,i} - \left(k_{CSA1}Y_{0,P} + k_{CSA2}Y_{0,Q}\right)\left(SX_{2,P,i}\right)$	0

Table 5-5. Moment equations for chains with a single block made in catalyst *Q* in a semi-batch reactor.

Description	Moment equations	Initial value
0th Moment of living chains	$\frac{dY_{0,Q,i}}{dt} = \left(k_{iA2}A + k_{iB2}B\right)C_2 - \left(k_{t\beta 2} + k_{tH2}H_2 + k_{d2} + k_{CSA02}S_0 + k_{CSA2}\left(SX_{0,P}\right) + k_{CSA2}\left(SX_{0,Q}\right)\right)Y_{0,Q,i} + \left(SX_{0,Q,i}\right)k_{CSA2}Y_{0,Q}$	0
1st Moment of living chains	$\frac{dY_{1,Q,i}}{dt} = \left(k_{iA2}A + k_{iB2}B\right)C_2 + \left(k_{pA2}A + k_{pB2}B\right)Y_{0,Q,i}$ $-\left(k_{t\beta 2} + k_{tH2}H_2 + k_{d2} + k_{CSA02}S_0 + k_{CSA2}\left(SX_{0,P}\right) + k_{CSA2}\left(SX_{0,Q}\right)\right)Y_{1,Q,i} + \left(SX_{1,Q,i}\right)k_{CSA2}Y_{0,Q}$	0
2nd Moment of living chains	$\frac{dY_{2,Q,i}}{dt} = \left(k_{iA2}A + k_{iB2}B\right)C_2 + \left(k_{pA2}A + k_{pB2}B\right)\left(Y_{0,Q,i} + 2Y_{1,Q,i}\right)$ $-\left(k_{t\beta 2} + k_{tH2}H_2 + k_{d2} + k_{CSA02}S_0 + k_{CSA2}\left(SX_{0,P}\right) + k_{CSA2}\left(SX_{0,Q}\right)\right)Y_{2,Q,i} + \left(SX_{2,Q,i}\right)k_{CSA2}Y_{0,Q}$	0
0th Moment of dead chains	$\frac{dX_{0,Q,i}}{dt} = \left(k_{t\beta 2} + k_{tH2}H_2 + k_{d2}\right)Y_{0,Q,i}$	0
1st Moment of dead chains	$\frac{dX_{1,Q,i}}{dt} = \left(k_{t\beta 2} + k_{tH2}H_2 + k_{d2}\right)Y_{1,Q,i}$	0
2nd Moment of dead chains	$\frac{dX_{2,Q,i}}{dt} = \left(k_{t\beta 2} + k_{tH2}H_2 + k_{d2}\right)Y_{2,Q,i}$	0
0th Moment of dormant chains	$\frac{d\left(SX_{0,Q,i}\right)}{dt} = \left(k_{CSA02}S_0 + k_{CSA2}\left(SX_{0,P}\right) + k_{CSA2}\left(SX_{0,Q}\right)\right)Y_{0,Q,i} - \left(k_{CSA1}Y_{0,P} + k_{CSA2}Y_{0,Q}\right)\left(SX_{0,Q,i}\right)$	0
1st Moment of dormant chains	$\frac{d\left(SX_{1,Q,i}\right)}{dt} = \left(k_{CSA02}S_0 + k_{CSA2}\left(SX_{0,P}\right) + k_{CSA2}\left(SX_{0,Q}\right)\right)Y_{1,Q,i} - \left(k_{CSA1}Y_{0,P} + k_{CSA2}Y_{0,Q}\right)\left(SX_{1,Q,i}\right)$	0
2nd Moment of dormant chains	$\frac{d\left(SX_{2,Q,i}\right)}{dt} = \left(k_{CSA02}S_0 + k_{CSA2}\left(SX_{0,P}\right) + k_{CSA2}\left(SX_{0,Q}\right)\right)Y_{2,Q,i} - \left(k_{CSA1}Y_{0,P} + k_{CSA2}Y_{0,Q}\right)\left(SX_{2,Q,i}\right)$	0

Table 5-6. Moment equations for OBC chains made in catalyst *P* in a semi-batch reactor for chains having two or more blocks.

Description	Moment equations	Initial value
0th Moment of living chains	$\frac{dY_{0,P,i}}{dt} = -\left(k_{t\beta 1} + k_{tH1}H_2 + k_{d1} + k_{CSA01}S_0 + k_{CSA1}\left(SX_{0,P}\right) + k_{CSA1}\left(SX_{0,Q}\right)\right)Y_{0,P,i} + \left(\left(SX_{0,P,i}\right) + \left(SX_{0,Q,i-1}\right)\right)k_{CSA1}Y_{0,P}$	0
1st Moment of living chains	$\frac{dY_{1,P,i}}{dt} = \left(k_{pA1}A + k_{pB1}B\right)Y_{0,P,i}$ $-\left(k_{t\beta 1} + k_{tH1}H_2 + k_{d1} + k_{CSA01}S_0 + k_{CSA1}\left(SX_{0,P}\right) + k_{CSA1}\left(SX_{0,Q}\right)\right)Y_{1,P,i} + \left(\left(SX_{1,P,i}\right) + \left(SX_{1,Q,i-1}\right)\right)k_{CSA1}Y_{0,P}$	0
2nd Moment of living chains	$\frac{dY_{2,P,i}}{dt} = \left(k_{pA1}A + k_{pB1}B\right)\left(Y_{0,P,i} + 2Y_{1,P,i}\right)$ $-\left(k_{t\beta 1} + k_{tH1}H_2 + k_{d1} + k_{CSA01}S_0 + k_{CSA1}\left(SX_{0,P}\right) + k_{CSA1}\left(SX_{0,Q}\right)\right)Y_{2,P,i} + \left(\left(SX_{2,P,i}\right) + \left(SX_{2,Q,i-1}\right)\right)k_{CSA1}Y_{0,P}$	0
0th Moment of dead chains	$\frac{dX_{0,P,i}}{dt} = \left(k_{t\beta 1} + k_{tH1}H_2 + k_{d1}\right)Y_{0,P,i}$	0
1st Moment of dead chains	$\frac{dX_{2,P,i}}{dt} = \left(k_{t\beta 1} + k_{tH1}H_2 + k_{d1}\right)Y_{2,P,i}$	0
2nd Moment of dead chains	$\frac{dX_{2,P,i}}{dt} = \left(k_{t\beta 1} + k_{tH1}H_2 + k_{d1}\right)Y_{2,P,i}$	0
0th Moment of dormant chains	$\frac{d\left(SX_{0,P,i}\right)}{dt} = \left(k_{CSA01}S_0 + k_{CSA1}\left(SX_{0,P}\right) + k_{CSA1}\left(SX_{0,Q}\right)\right)Y_{0,P,i} - \left(k_{CSA1}Y_{0,P} + k_{CSA2}Y_{0,Q}\right)\left(SX_{0,P,i}\right)$	0
1st Moment of dormant chains	$\frac{d\left(SX_{1,P,i}\right)}{dt} = \left(k_{CSA01}S_0 + k_{CSA1}\left(SX_{0,P}\right) + k_{CSA1}\left(SX_{0,Q}\right)\right)Y_{1,P,i} - \left(k_{CSA1}Y_{0,P} + k_{CSA2}Y_{0,Q}\right)\left(SX_{1,P,i}\right)$	0
2nd Moment of dormant chains	$\frac{d\left(SX_{2,P,i}\right)}{dt} = \left(k_{CSA01}S_0 + k_{CSA1}\left(SX_{0,P}\right) + k_{CSA1}\left(SX_{0,Q}\right)\right)Y_{2,P,i} - \left(k_{CSA1}Y_{0,P} + k_{CSA2}Y_{0,Q}\right)\left(SX_{2,P,i}\right)$	0

Table 5-7. Moment equations for OBC chains made in catalyst *Q* in a semi-batch reactor for chains having two or more blocks.

Description	Moment equations	Initial value
0th Moment of living chains	$\frac{dY_{0,Q,i}}{dt} = -\left(k_{t\beta 2} + k_{tH2}H_2 + k_{d2} + k_{CSA02}S_0 + k_{CSA2}\left(SX_{0,P}\right) + k_{CSA2}\left(SX_{0,Q}\right)\right)Y_{0,Q,i} + \left(\left(SX_{0,P,i-1}\right) + \left(SX_{0,Q,i}\right)\right)k_{CSA2}Y_{0,Q}$	0
1st Moment of living chains	$\frac{dY_{1,Q,i}}{dt} = \left(k_{pA2}A + k_{pB2}B\right)Y_{0,Q,i}$ $-\left(k_{t\beta 2} + k_{tH2}H_2 + k_{d2} + k_{CSA02}S_0 + k_{CSA2}\left(SX_{0,P}\right) + k_{CSA2}\left(SX_{0,Q}\right)\right)Y_{1,Q,i} + \left(\left(SX_{1,P,i-1}\right) + \left(SX_{1,Q,i}\right)\right)k_{CSA2}Y_{0,Q}$	0
2nd Moment of living chains	$\frac{dY_{2,Q,i}}{dt} = \left(k_{pA2}A + k_{pB2}B\right)\left(Y_{0,Q,i} + 2Y_{1,Q,i}\right)$ $-\left(k_{t\beta 2} + k_{tH2}H_2 + k_{d2} + k_{CSA02}S_0 + k_{CSA2}\left(SX_{0,P}\right) + k_{CSA2}\left(SX_{0,Q}\right)\right)Y_{2,Q,i} + \left(\left(SX_{2,P,i-1}\right) + \left(SX_{2,Q,i}\right)\right)k_{CSA2}Y_{0,Q}$	0
0th Moment of dead chains	$\frac{dX_{0,Q,i}}{dt} = \left(k_{t\beta 2} + k_{tH2}H_2 + k_{d2}\right)Y_{0,Q,i}$	0
1st Moment of dead chains	$\frac{dX_{1,Q,i}}{dt} = \left(k_{t\beta 2} + k_{tH2}H_2 + k_{d2}\right)Y_{1,Q,i}$	0
2nd Moment of dead chains	$\frac{dX_{2,Q,i}}{dt} = \left(k_{t\beta 2} + k_{tH2}H_2 + k_{d2}\right)Y_{2,Q,i}$	0
0th Moment of dormant chains	$\frac{d\left(SX_{0,Q,i}\right)}{dt} = \left(k_{CSA02}S_0 + k_{CSA2}\left(SX_{0,P}\right) + k_{CSA2}\left(SX_{0,Q}\right)\right)Y_{0,Q,i} - \left(k_{CSA1}Y_{0,P} + k_{CSA2}Y_{0,Q}\right)\left(SX_{0,Q,i}\right)$	0
1st Moment of dormant chains	$\frac{d\left(SX_{1,Q,i}\right)}{dt} = \left(k_{CSA02}S_0 + k_{CSA2}\left(SX_{0,P}\right) + k_{CSA2}\left(SX_{0,Q}\right)\right)Y_{1,Q,i} - \left(k_{CSA1}Y_{0,P} + k_{CSA2}Y_{0,Q}\right)\left(SX_{1,Q,i}\right)$	0
2nd Moment of dormant chains	$\frac{d\left(SX_{2,Q,i}\right)}{dt} = \left(k_{CSA02}S_0 + k_{CSA2}\left(SX_{0,P}\right) + k_{CSA2}\left(SX_{0,Q}\right)\right)Y_{2,Q,i} - \left(k_{CSA1}Y_{0,P} + k_{CSA2}Y_{0,Q}\right)\left(SX_{2,Q,i}\right)$	0

Table 5-8. Molar balance equations in a semi-batch reactor.

Description	Molar equations	Initial value
Catalyst *P*	$\frac{dC_1}{dt} = -(k_{iA1}A + k_{iB1}B)C_1 + (k_{t\beta 1} + k_{tH1}H_2 + k_{d1} + k_{CSA01}S_0)Y_{0,P}$	C_P
Catalyst *Q*	$\frac{dC_2}{dt} = -(k_{iA2}A + k_{iB2}B)C_2 + (k_{t\beta 2} + k_{tH2}H_2 + k_{d2} + k_{CSA02}S_0)Y_{0,Q}$	C_Q
Chain shuttling agent (CSA)	$\frac{dS_0}{dt} = -(k_{CSA01}Y_{0,P} + k_{CSA02}Y_{0,Q})S_0$	CSA
1-Octene	$\frac{dB}{dt} = -(k_{iB1}C_1 + k_{iB2}C_2 + k_{pB1}Y_{0,P} + k_{pB2}Y_{0,Q})B$	B
Hydrogen	$\frac{dH_2}{dt} = -(k_{tH1}Y_{0,P} + k_{tHB2}Y_{0,Q})H_2$	H_2
Deactivated site of catalyst *P*	$\frac{dC_{d1}}{dt} = k_{d1}(Y_{0,P} + C_1)$	0
Deactivated site of catalyst *Q*	$\frac{dC_{d2}}{dt} = k_{d2}(Y_{0,Q} + C_2)$	0
Ethylene consumption by catalysts *P* and *Q*	$\frac{dA_p}{dt} = (k_{iA1}C_1 + k_{iA2}C_2 + k_{pA1}Y_{0,P} + k_{pA2}Y_{0,Q})A$	0
1-Octene consumption by catalysts *P* and *Q*	$\frac{dB_p}{dt} = (k_{iB1}C_1 + k_{iB2}C_2 + k_{pB1}Y_{0,P} + k_{pB2}Y_{0,Q})B$	0
Ethylene consumption by catalyst *P*	$\frac{dA_{p,1}}{dt} = (k_{iA1}C_1 + k_{pA1}Y_{0,P})A$	0
Ethylene consumption by catalyst *Q*	$\frac{dA_{p,2}}{dt} = (k_{iA2}C_2 + k_{pA2}Y_{0,Q})A$	**0**
1-Octene consumption by catalyst *P*	$\frac{dB_{p,1}}{dt} = (k_{iB1}C_1 + k_{pB1}Y_{0,P})B$	**0**
1-octene consumption by catalyst Q	$\frac{dB_{p,2}}{dt} = (k_{iB2}C_2 + k_{pB2}Y_{0,Q})B$	**0**

Table 5-9. Average chain lengths.

Description	Number average chain length, r_n	Weight average chain length, r_w	PDI
Overall polymer	$\frac{Y_{1,P} + X_{1,P} + SX_{1,P} + Y_{1,Q} + X_{1,Q} + SX_{1,Q}}{Y_{0,P} + X_{0,P} + SX_{0,P} + Y_{0,Q} + X_{0,Q} + SX_{0,Q}}$	$\frac{Y_{2,P} + X_{2,P} + SX_{2,P} + Y_{2,Q} + X_{2,Q} + SX_{2,Q}}{Y_{1,P} + X_{1,P} + SX_{1,P} + Y_{1,Q} + X_{1,Q} + SX_{1,Q}}$	$\frac{r_w^{overall}}{r_n^{overall}}$
Block starts with S	$\frac{Y_{1,P,i} + X_{1,P,i} + SX_{1,P,i}}{Y_{0,P,i} + X_{0,P,i} + SX_{0,P,i}}$	$\frac{Y_{2,P,i} + X_{2,P,i} + SX_{2,P,i}}{Y_{1,P,i} + X_{1,P,i} + SX_{1,P,i}}$	$\frac{r_w^{((i+1)S,iH)}}{r_n^{((i+1)S,iH)}}$
Block starts with H	$\frac{Y_{1,Q,i} + X_{1,Q,i} + SX_{1,Q,i}}{Y_{0,Q,i} + X_{0,Q,i} + SX_{0,Q,i}}$	$\frac{Y_{2,Q,i} + X_{2,Q,i} + SX_{2,Q,i}}{Y_{1,Q,i} + X_{1,Q,i} + SX_{1,Q,i}}$	$\frac{r_w^{(iS,(i+1)H)}}{r_n^{(iS,(i+1)H)}}$
Even block	$\frac{Y_{1,P,i} + X_{1,P,i} + SX_{1,P,i} + Y_{1,Q,i} + X_{1,Q,i} + SX_{1,Q,i}}{Y_{0,P,i} + X_{0,P,i} + SX_{0,P,i} + Y_{0,Q,i} + X_{0,Q,i} + SX_{0,Q,i}}$	$\frac{Y_{2,P,i} + X_{2,P,i} + SX_{2,P,i} + Y_{2,Q,i} + X_{2,Q,i} + SX_{2,Q,i}}{Y_{1,P,i} + X_{1,P,i} + SX_{1,P,i} + Y_{1,Q,i} + X_{1,Q,i} + SX_{1,Q,i}}$	$\frac{r_w^{(iS,iH)}}{r_n^{(iS,iH)}}$

Table 5-10. Molar and weight fractions of polymer populations having different numbers of blocks.

Description	Number fraction	Weight fraction
Block starts with S	$\frac{Y_{0,P,i} + X_{0,P,i} + SX_{0,P,i}}{Y_{0,P} + X_{0,P} + SX_{0,P} + Y_{0,Q} + X_{0,Q} + SX_{0,Q}}$	$\frac{Y_{1,P,i} + X_{1,P,i} + SX_{1,P,i}}{Y_{1,P} + X_{1,P} + SX_{1,P} + Y_{1,Q} + X_{1,Q} + SX_{1,Q}}$
Block starts with H	$\frac{Y_{0,Q,i} + X_{0,Q,i} + SX_{0,Q,i}}{Y_{0,P} + X_{0,P} + SX_{0,P} + Y_{0,Q} + X_{0,Q} + SX_{0,Q}}$	$\frac{Y_{1,Q,i} + X_{1,Q,i} + SX_{1,Q,i}}{Y_{1,P} + X_{1,P} + SX_{1,P} + Y_{1,Q} + X_{1,Q} + SX_{1,Q}}$
Even block	$\frac{Y_{0,P,i} + X_{0,P,i} + SX_{0,P,i} + Y_{0,Q,i} + X_{0,Q,i} + SX_{0,Q,i}}{Y_{0,P} + X_{0,P} + SX_{0,P} + Y_{0,Q} + X_{0,Q} + SX_{0,Q}}$	$\frac{Y_{1,P,i} + X_{1,P,i} + SX_{1,P,i} + Y_{1,Q,i} + X_{1,Q,i} + SX_{1,Q,i}}{Y_{1,P} + X_{1,P} + SX_{1,P} + Y_{1,Q} + X_{1,Q} + SX_{1,Q}}$

Table 5-11. Ethylene and 1-octene mole fraction of polymer populations having different numbers of blocks.

Description	Catalyst *P*	Catalyst *Q*
Ethylene composition	$\frac{A_{P,1}}{A_{P,1} + B_{P,1}}$	$\frac{A_{P,2}}{A_{P,2} + B_{P,2}}$
1-Octene composition	$\frac{B_{P,1}}{A_{P,1} + B_{P,1}}$	$\frac{B_{P,2}}{A_{P,2} + B_{P,2}}$

Table 5-12. Average number and weight of blocks per chain, 1-octene mole fraction of whole polymer and overall conversion.

Description	Equation
Average number of blocks per chain	$\frac{\sum_{i=1}^{n} (Y_{0,P,i} + Y_{0,Q,i}) \times i}{\sum_{i=1}^{n} (Y_{0,P,i} + Y_{0,Q,i})}$
Average weight of blocks per chain	$\frac{\sum_{i=1}^{n} (Y_{0,P,i} + Y_{0,Q,i}) \times i^2}{\sum_{i=1}^{n} (Y_{0P,i} + Y_{0,Q,i}) \times i}$
1-Octene composition in whole polymer	$\frac{B_P}{A_P + B_P}$
Overall conversion	$\frac{A_p + B_p}{A + B + A_p + B_p}$

i = 1, 2, 3,... n, n: the number of blocks

5.4 Dynamic Monte Carlo Model

Similar to the procedure introduced in Chapter 3, the macroscopic concentrations of catalysts, CSA, monomers, and hydrogen must be transformed into the number of molecules of each species in the control volume, as defined by Equations (5–36) to (5–41).

$$n_{C1} = C_1 N_A V \tag{5-36}$$

$$n_{C2} = C_2 N_A V \tag{5-37}$$

$$n_{S_0} = S_0 N_A V \tag{5-38}$$

$$n_A = A N_A V \tag{5-39}$$

$$n_B = B N_A V \tag{5-40}$$

$$n_{H_2} = H_2 N_A V \tag{5-41}$$

Table 5-13 summarizes all expressions needed for the proposed dynamic Monte Carlo model and Figure 5-3 shows the flowsheet for the resulting simulation program.

Table 5-13. Dynamic Monte Carlo reaction rates and rate constants for chain shuttling copolymerization using two catalysts.

Description	Chemical equations	R^{MC}, s^{-1}	k^{MC}, s^{-1}	Equation
Initiation	$C_1 + A \rightarrow P_{1,1}$	$k_{iA1}{}^{MC} n_{C1} n_A$	$\frac{k_{iA1}}{VN_A}$	(5-42)
	$C_1 + B \rightarrow P_{1,1}$	$k_{iB1}{}^{MC} n_{C1} n_B$	$\frac{k_{iB1}}{VN_A}$	(5-43)
	$C_2 + A \rightarrow Q_{1,1}$	$k_{iA2}{}^{MC} n_{C2} n_A$	$\frac{k_{iA2}}{VN_A}$	(5-44)
	$C_2 + B \rightarrow Q_{1,1}$	$k_{iB2}{}^{MC} n_{C2} n_B$	$\frac{k_{iB2}}{VN_A}$	(5-45)
Propagation	$P_{r,i} + A \rightarrow P_{r+1,i}$	$k_{pA1}{}^{MC} n_P n_A$	$\frac{k_{pA1}}{VN_A}$	(5-46)
	$P_{r,i} + B \rightarrow P_{r+1,i}$	$k_{pB1}{}^{MC} n_P n_B$	$\frac{k_{pB1}}{VN_A}$	(5-47)
	$Q_{r,i} + A \rightarrow Q_{r+1,i}$	$k_{pA2}{}^{MC} n_Q n_A$	$\frac{k_{pA2}}{VN_A}$	(5-48)
	$Q_{r,i} + B \rightarrow Q_{r+1,i}$	$k_{pB2}{}^{MC} n_Q n_B$	$\frac{k_{pB2}}{VN_A}$	(5-49)
β-hydride elimination	$P_{r,i} \rightarrow D_{r,i} + C_1$	$k_{t\beta 1}{}^{MC} n_P$	$k_{t\beta 1}$	(5-50)
	$Q_{r,i} \rightarrow D_{r,i} + C_2$	$k_{t\beta 2}{}^{MC} n_Q$	$k_{t\beta 2}$	(5-51)
Chain transfer to hydrogen	$P_{r,i} + H_2 \rightarrow D_{r,i} + C_1$	$k_{tH1}{}^{MC} n_P n_{H_2}$	$\frac{k_{tH1}}{VN_A}$	(5-52)
	$Q_{r,i} + H_2 \rightarrow D_{r,i} + C_2$	$k_{tH2}{}^{MC} n_Q n_{H_2}$	$\frac{k_{tH2}}{VN_A}$	(5-53)
Deactivation of growing chain	$P_{r,i} \rightarrow D_{r,i} + C_{d1}$	$k_{d1}{}^{MC} n_P$	k_{d1}	(5-54)
	$Q_{r,i} \rightarrow D_{r,i} + C_{d2}$	$k_{d2}{}^{MC} n_Q$	k_{d2}	(5-55)
Deactivation of active catalyst	$C_1 \rightarrow C_{d1}$	$k_{d1}{}^{MC} n_{C1}$	k_{d1}	(5-56)
	$C_2 \rightarrow C_{d2}$	$k_{d2}{}^{MC} n_{C2}$	k_{d2}	(5-57)
Chain shuttling to CSA	$P_{r,i} + S_0 \rightarrow SP_{r,i} + C_1$	$k_{CSA01}{}^{MC} n_P n_{S0}$	$\frac{k_{CSA01}}{VN_A}$	(5-58)
	$Q_{r,i} + S_0 \rightarrow SQ_{r,i} + C_2$	$k_{CSA02}{}^{MC} n_Q n_{S0}$	$\frac{k_{CSA02}}{VN_A}$	(5-59)
Chain shuttling to dormant chain	$P_{r,i} + SP_{s,j} \rightarrow P_{s,j} + SP_{r,i}$	$k_{CSA1self}{}^{MC} n_P n_{SP}$	$\frac{k_{CSA1self}}{VN_A}$	(5-60)
	$P_{r,i} + SQ_{s,j} \rightarrow P_{s,j+1} + SP_{r,i}$	$k_{CSA1cross}{}^{MC} n_P n_{SQ}$	$\frac{k_{CSA1cross}}{VN_A}$	(5-61)
	$Q_{r,i} + SP_{s,j} \rightarrow Q_{s,j+1} + SQ_{r,i}$	$k_{CSA2cross}{}^{MC} n_Q n_{SP}$	$\frac{k_{CSA2cross}}{VN_A}$	(5-62)
	$Q_{r,i} + SQ_{s,j} \rightarrow Q_{s,j} + SQ_{r,i}$	$k_{CSA2self}{}^{MC} n_Q n_{SQ}$	$\frac{k_{CSA2self}}{VN_A}$	(5-63)

nP and *nQ*: number of living chains from catalyst *P* and *Q*; *nSP* and *nSQ*: number of dormant chains from catalyst *P* and *Q*; *nDP* and *nDQ*: number of dead chains from catalyst *P* and *Q*; *nCDp* and *nCDq*: number of deactivated chains from catalyst *P* and *Q*.

From inspection of Table 5-13, the sum of reaction rates is given by,

$$\begin{aligned} R^{MC} &= R_{iA1}^{MC} + R_{iB1}^{MC} + R_{iA2}^{MC} + R_{iB2}^{MC} + R_{pA1}^{MC} + R_{pB1}^{MC} + R_{pA2}^{MC} + R_{pB2}^{MC} \\ &+ R_{t\beta 1}^{MC} + R_{t\beta 2}^{MC} + R_{tH1}^{MC} + R_{tH2}^{MC} + R_{d1}^{MC} + R_{d2}^{MC} + R_{dC1}^{MC} + R_{dC2}^{MC} \\ &+ R_{CSA01}^{MC} + R_{CSA02}^{MC} + R_{CSA1self}^{MC} + R_{CSA1cross}^{MC} + R_{CSA2cross}^{MC} + R_{CSA2self}^{MC} = \sum_{j=1}^{22} R_j^{MC} \end{aligned} \tag{5-64}$$

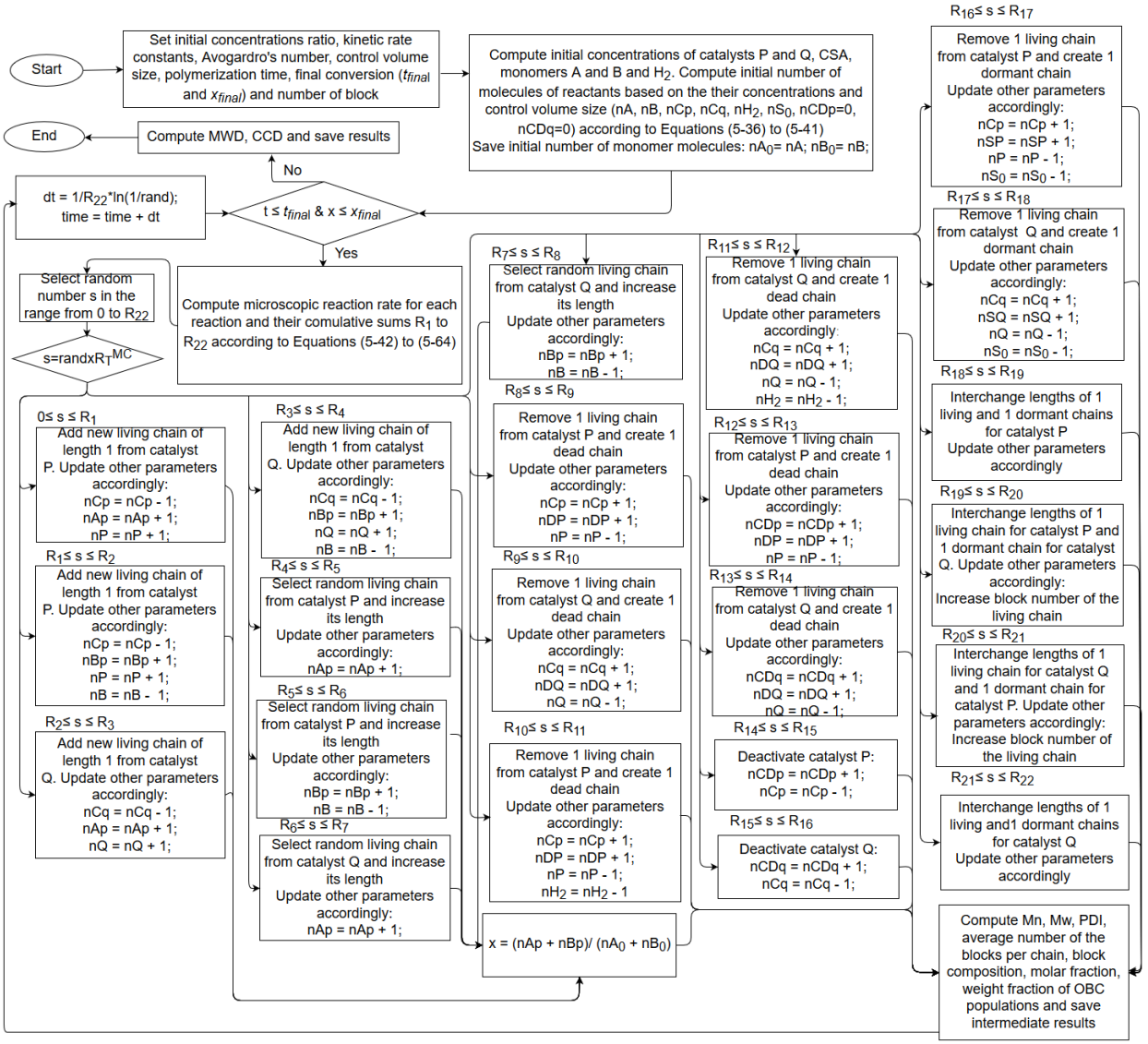

Figure 5-3. Flowsheet for dynamic Monte Carlo simulation of chain shuttling copolymerization using two catalysts.

5.5 Results and Discussion

The objectives of the simulations in this chapter were: 1) to compare simulations with the dynamic Monte Carlo model and the method of moments to ensure both are working correctly, and 2) to investigate how different polymerization kinetic rate constants and polymerization conditions affect the microstructure of OBCs.

Table 5-14 lists the polymerization kinetic rate constants, and Table 5-15 shows the process conditions used in all simulations.

I tried different propagation rate constants in order to get a reasonable average number of blocks per chain in the range of 2 to 10 blocks per chain. Wang et al.[55] reported that OBCs made by Dow Chemical Company had 2 to 10 blocks per chain. I kept the reactivity ratio for ethylene in catalyst that produced soft block (catalyst P), $r_1 = 5$ and the reactivity ratio for 1-octene in catalyst P, $r_2 = 0.2$ (Zhang et al.[18] used the reactivity ratio for ethylene in catalyst that produced soft block (catalyst 1), $r_1 = 5$ and the reactivity ratio for 1-octene in catalyst 1, $r_2 = 0.3$). I kept the ratio between the chain shuttling rate constant for both catalysts and propagation rate constant for catalyst P, $k_{CSA}/k_p^P = 10$ (Zhang et al.[18] used the same ratio). Finally, I assumed both catalysts had the same chain shuttling rate constant and the chain shuttling rate constant to CSA is equal the chain shuttling rate constant to dormant chain, $k_{CSA0} = k_{CSA}$, as suggested in literature.

Table 5-14. Polymerization kinetic constants for chain shuttling copolymerization.

Kinetic constants	Units	Catalyst P	Catalyst Q
Propagation rate constant for ethylene, k_{pA}^i	L/(mol.s)	10000	5000
Propagation rate constant for 1-octene, k_{pB}^i	L/(mol.s)	2000	100
Initiation rate constant for ethylene, k_{iA}^i	L/(mol.s)	k_{pA}^P	k_{pA}^Q
Initiation rate constant for 1-octene, k_{iB}^i	L/(mol.s)	k_{pB}^P	k_{pB}^Q
β-hydride elimination rate constant, $k_{t\beta}^i$	s^{-1}	5	10
Chain transfer to H_2 rate constant, k_{tH}^i	L/(mol.s)	0	0
Deactivation rate constant, k_d^i	s^{-1}	0	0
Chain shuttling rate constant to CSA, k_{CSA0}^i	L/(mol.s)	10× k_{pA}^P	10× k_{pA}^P
Chain shuttling rate constant to dormant chain, k_{CSA}^i	L/(mol.s)	10× k_{pA}^P	10× k_{pA}^P

Table 5-15. Process conditions for chain shuttling copolymerization.

Reactants	Units	Values
Total monomers concentration, $[M_{total}]$	mol/L	2
1-Octene mole fraction, x_B		0.5
Total catalysts concentration, $[C_{total}]$	mol/L	7.78×10^{-7}
Catalyst *P* mole fraction (make soft block), x_P		0.5
Ratio of CSA concentration to total catalysts, $[CSA]/[C_{total}]$		1000
Ratio of H_2 concentration to total monomers, $[H_2]/[M_{total}]$		0
Polymerization time, *t*	s	600

5.5.1 Comparison of the Method of Moments and Monte Carlo Simulation

Figure 5-4 shows that monomer conversion predicted using dynamic Monte Carlo and the method of moments simulations agree very well. The comonomer composition for the whole polymer predicted by both methods is also in good agreement, as depicted in Figure 5-5.

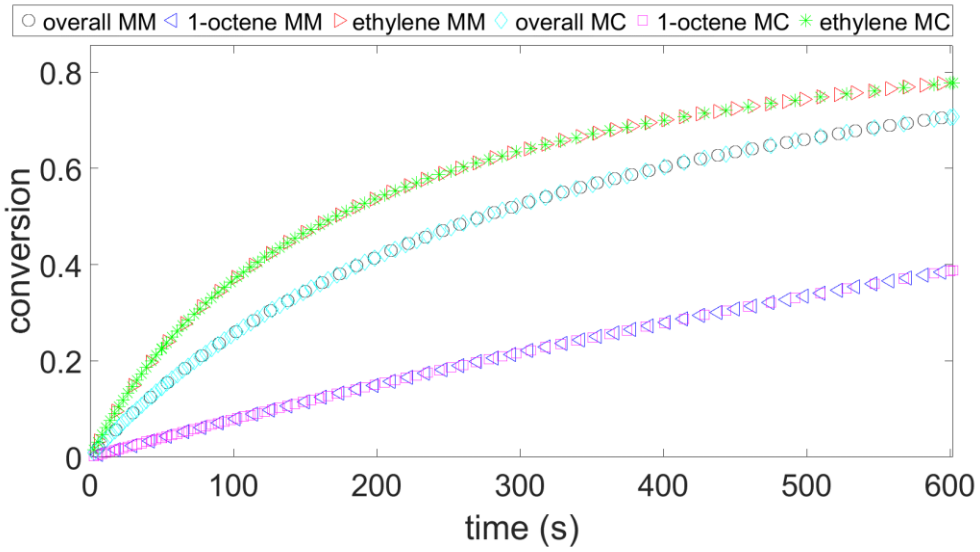

Figure 5-4. Comparison of simulations using dynamic Monte Carlo and method of moments for monomer conversion.

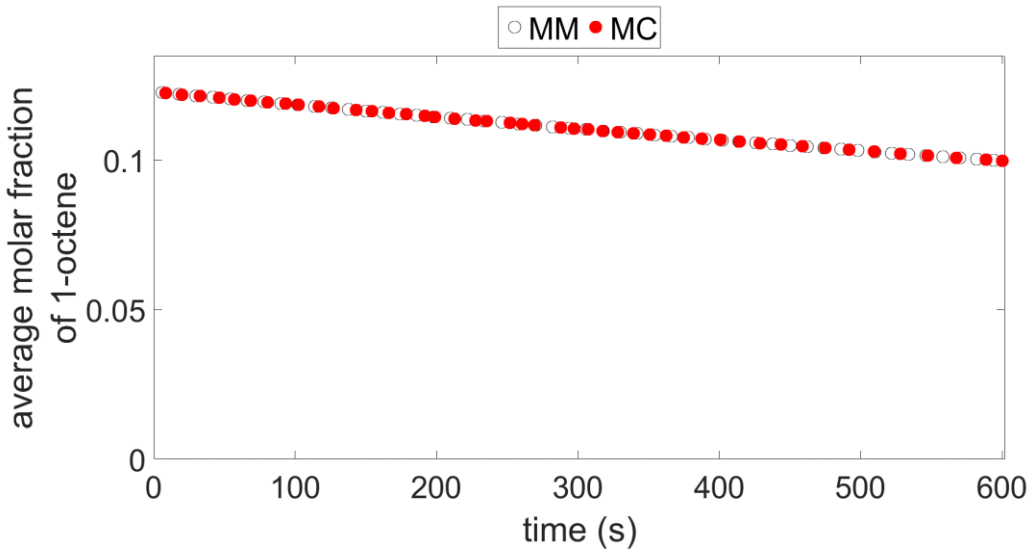

Figure 5-5 Comparison of simulations using dynamic Monte Carlo and method of moments for comonomer composition for whole copolymer.

The two methods predict the same r_n and PDI for the whole polymer and for polymer populations with different numbers of blocks (Figure 5-6 and Figure 5-7, respectively). Finally, Figure 5-8 shows that the two methods agree in their predictions for the fractions of the different chain populations.

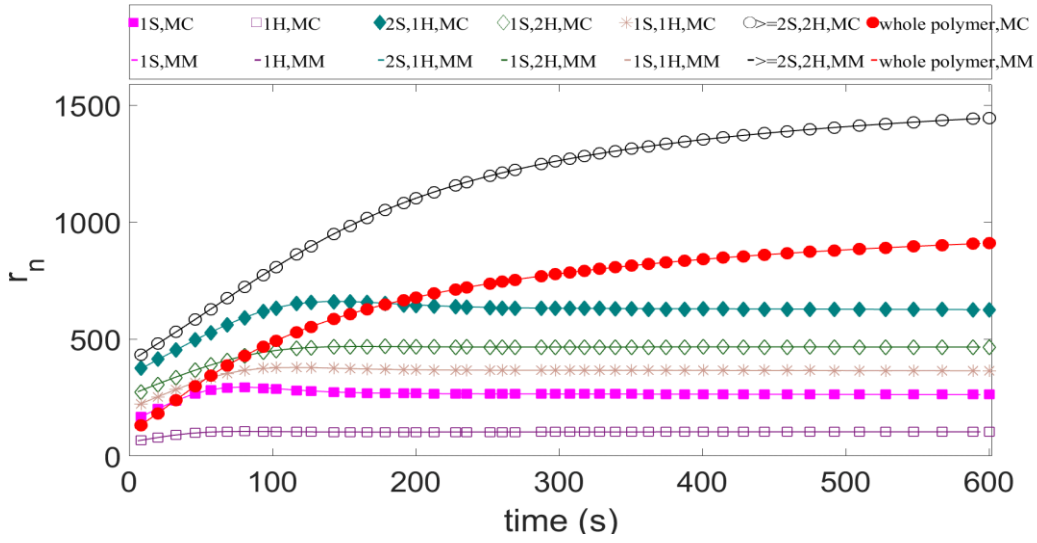

Figure 5-6. Comparison of simulations using dynamic Monte Carlo and method of moments for r_n.

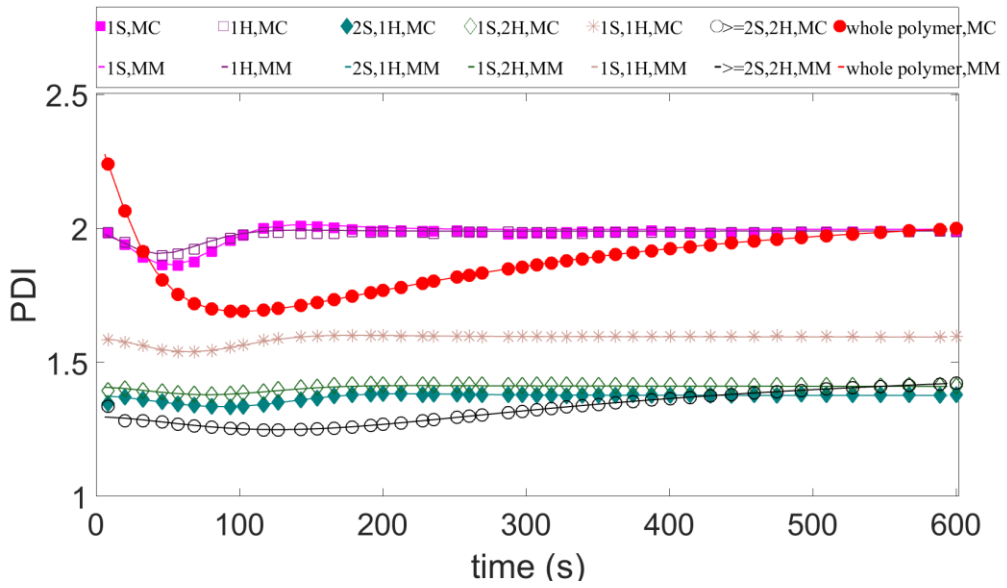

Figure 5-7. Comparison of simulations using dynamic Monte Carlo and method of moments for PDI.

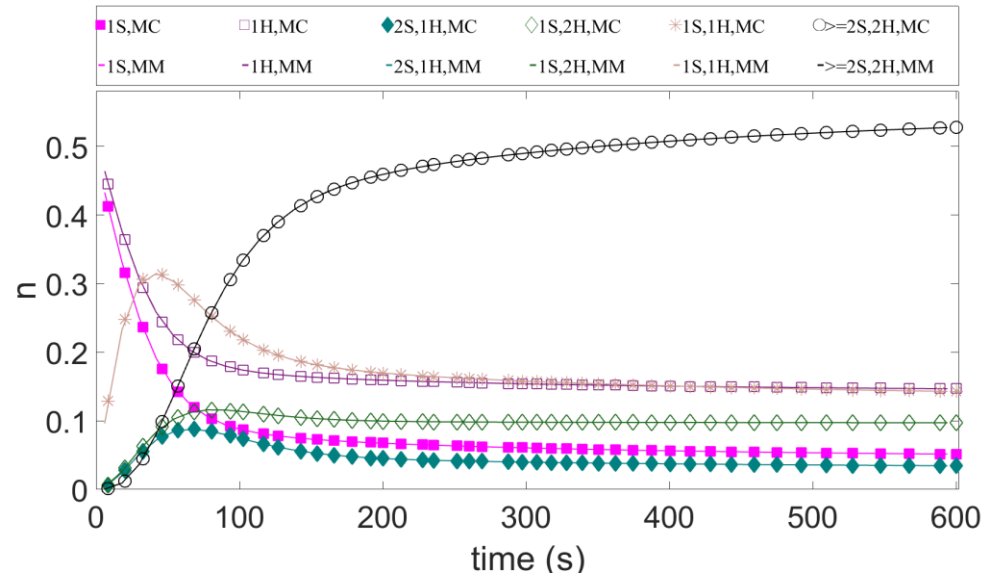

Figure 5-8. Comparison of simulations using dynamic Monte Carlo and method of moments for fractions different OBC populations.

These figures demonstrate that both models, using the method of moments or Monte Carlo techniques, predict the same average polymer property values and monomer conversion. Since these two models use entirely different simulation and modelling techniques, we can be confident that they are accurately describing the polymerization mechanism adopted for chain shuttling polymerization in this thesis (Table 5-1).

5.5.2 Effect of changing process conditions on chain length averages

Figure 5-9 illustrates how r_n of different OBC populations vary as a function of polymerization time. In the absence of chain transfer ($k_{t\beta} = 0$), the r_n of all populations increases linearly over time. The r_n for the whole polymer and for chains with 4 or more blocks ($\geq$ 2S,2H) keep increasing until the end of the polymerization, but the model stops calculating the r_n for populations with fewer blocks after a certain time because the concentration of these populations become vanishingly small, as chains with fewer blocks convert to chains with more blocks.

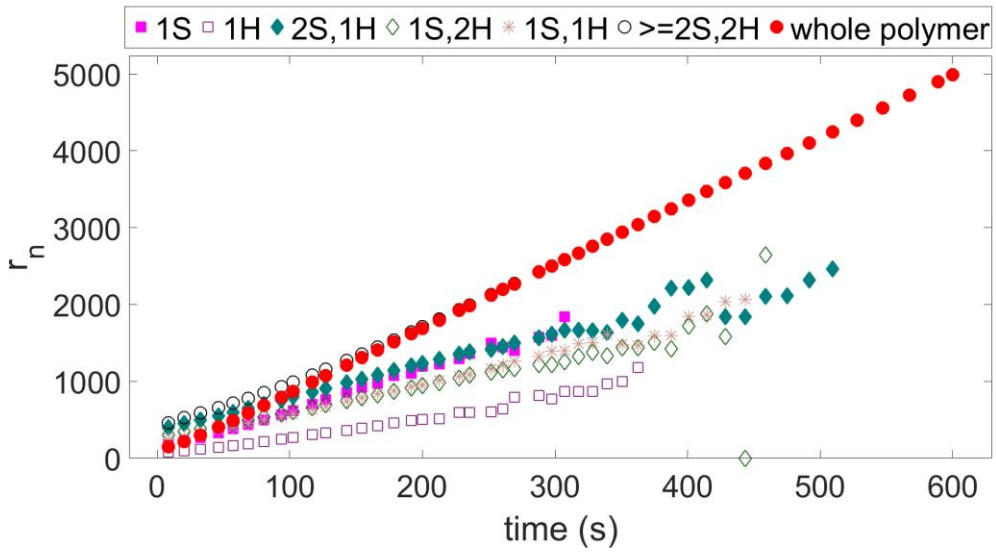

Figure 5-9. Number average chain length for different OBC populations ($k_{t\beta}$ = 0, $[CSA]/[C_{tot}]$ =1000).

If chain transfer takes place ($k_{t\beta} > 0$), the behavior of r_n changes drastically, as depicted in Figure 5-10. The r_n of the overall polymer and of different OBC populations increases until reaching a plateau, remaining constant until the end of the polymerization. The r_n increases in the order of (1H) < (1S) < (1S,1H) < (1S,2H) < (2S,1H) < ($\geq$ 2S,2H) because the catalyst that make the soft blocks (*P*) has a higher ratio of propagation to the chain transfer rate than the catalyst that makes the hard blocks (*Q*).

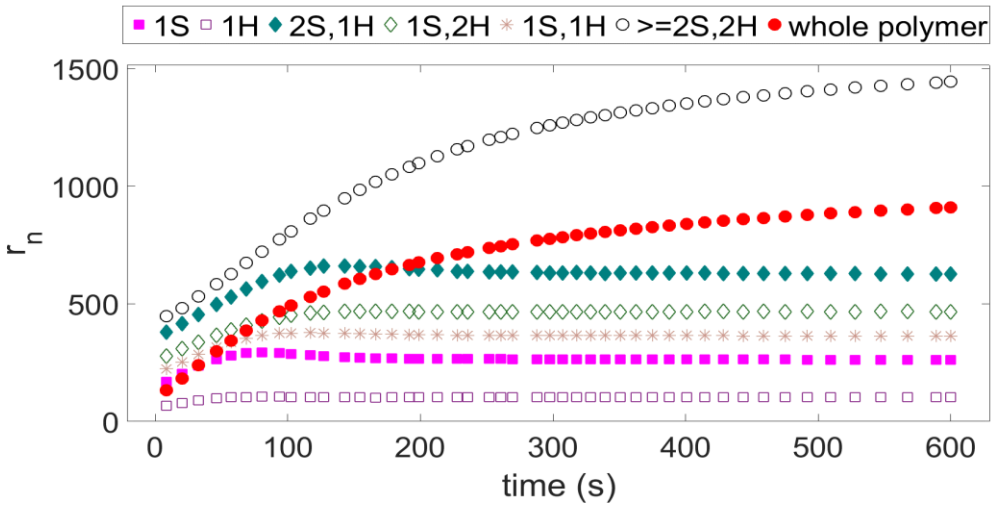

Figure 5-10. Number average chain length for different OBC populations ($k_{t\beta} > 0$, $[CSA]/[C_{tot}] = 1000$).

Increasing the $[CSA]/[C_{tot}]$ ratio from 1000 to 2000 (Figure 5-11) decreases the r_n of the OBC populations because the CSA acts as a reversible chain transfer agent (compare to Figure 5-10).

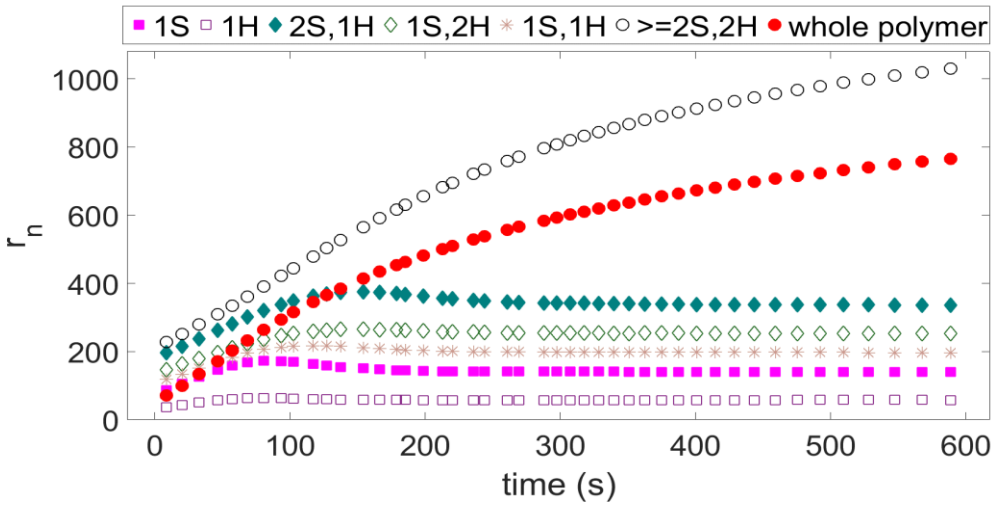

Figure 5-11. Number average chain length for different OBC populations ($k_{t\beta} > 0$, $[CSA]/[C_{tot}] = 2000$).

Figure 5-12 shows how the PDI for the different OBC populations evolves in time in the absence of chain transfer ($k_{t\beta} = 0$). The PDI of all populations decreases over time and approaches unity at the end of the polymerization as a result of the chains shuttling mechanism that randomly exchange chains of different lengths throughout the polymerization. This is an unlikely scenario in practical cases, since a certain degree of chain transfer is always observed in these systems.

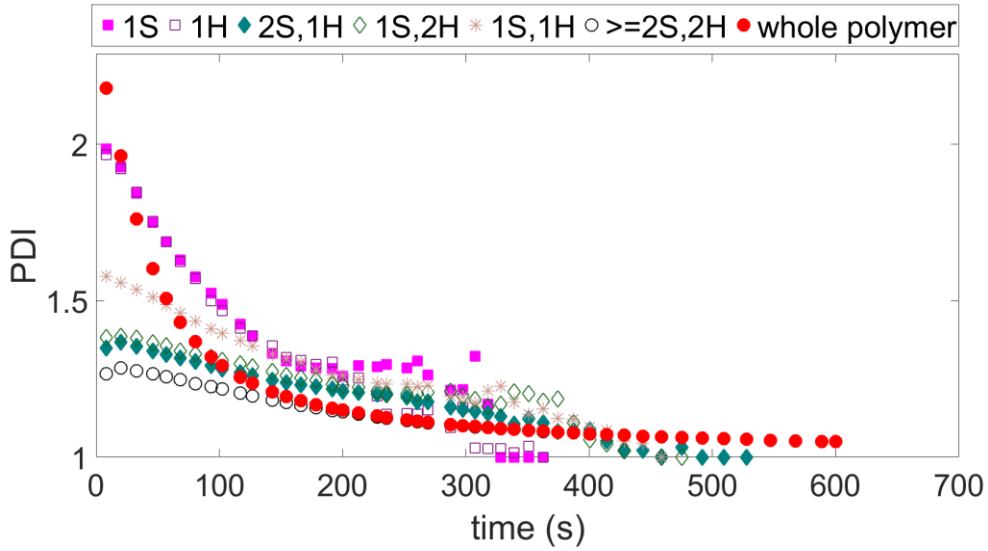

Figure 5-12. Polydispersity index for different OBC populations ($k_{t\beta} = 0$, $[CSA]/[C_{tot}] = 1000$).

Figure 5-13, on the other hand, examines how the PDI varies when chain transfer takes place ($k_{t\beta} > 0$). In this case, the PDI for the whole polymer and for single block populations (1H and 1S) falls below 2 at the beginning of the polymerization, but increases back to a value of 2 due to the accumulation of dead polymer chains formed by chain transfer. Note, however, that the PDI for the whole polymer is initially greater than 2 (because the polymer was being made by two catalysts before a substantial amount of chain transfer could take place), but converges to a value of 2 at the end of the polymerization, indicating that chain shuttling is effectively swapping polymer chains among the two catalyst types. The PDI of chains with single blocks follows the same trends as the whole polymer chain because these polymers consist of only one block. Populations with more than one block have lower PDIs due to the random averaging effect of chain shuttling.

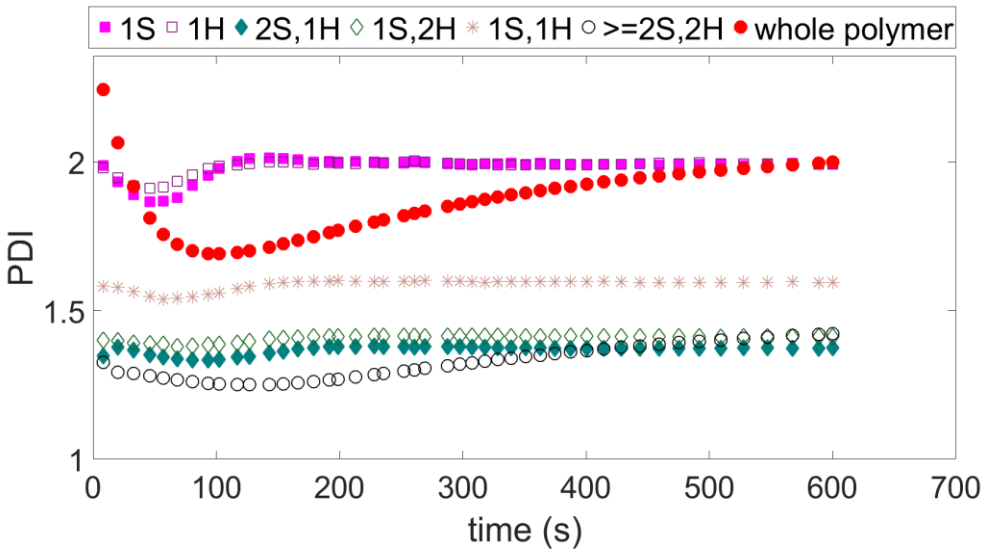

Figure 5-13. Polydispersity index for different OBC populations ($k_{t\beta} > 0$ and $[CSA]/[C_{tot}] = 1000$).

Figure 5-14 shows how the fraction of 1-octene in different OBC populations vary with time in the absence of chain transfer. The 1-octene molar fractions of populations decrease with time because 1-octene is fed only at the beginning of the polymerization (composition drift), as expected. Because the concentration of populations with few blocks becomes negligibly small after a certain polymerization time if no chain transfer takes place, the model stops calculating the 1-octene fraction in the copolymer after a certain limiting time. The molar fraction of 1-octene is the highest for uni-block populations made on catalyst *P* (1S), since this is the high 1-octene incorporator, while the lowest for uni-block populations made on catalyst *Q* (1H), the low 1-octene incorporator. The 1-octene concentration in OBC populations with more blocks fall in between these two limits, since they are different averages of these two uni-block populations.

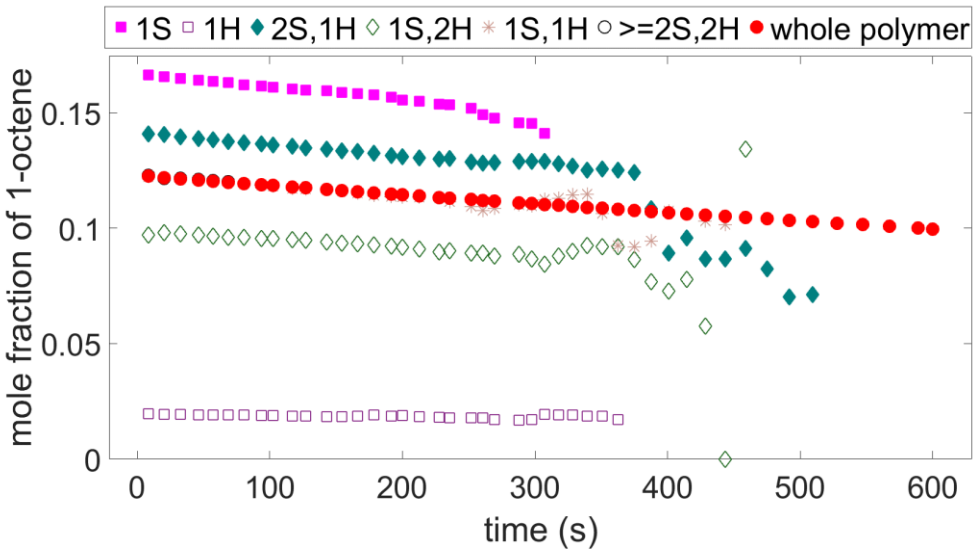

Figure 5-14. 1-Octene molar fraction in different OBC populations ($k_{t\beta} = 0$, $[CSA]/[C_{tot}] = 1000$).

Figure 5-15 shows a similar plot for the case when chain transfer is operative ($k_{t\beta} > 0$). The trends are the same as in Figure 5-14, but the 1-octene fractions are calculated for all OBC populations since chain transfer allow for the continuous production of uni-block populations throughout the polymerization.

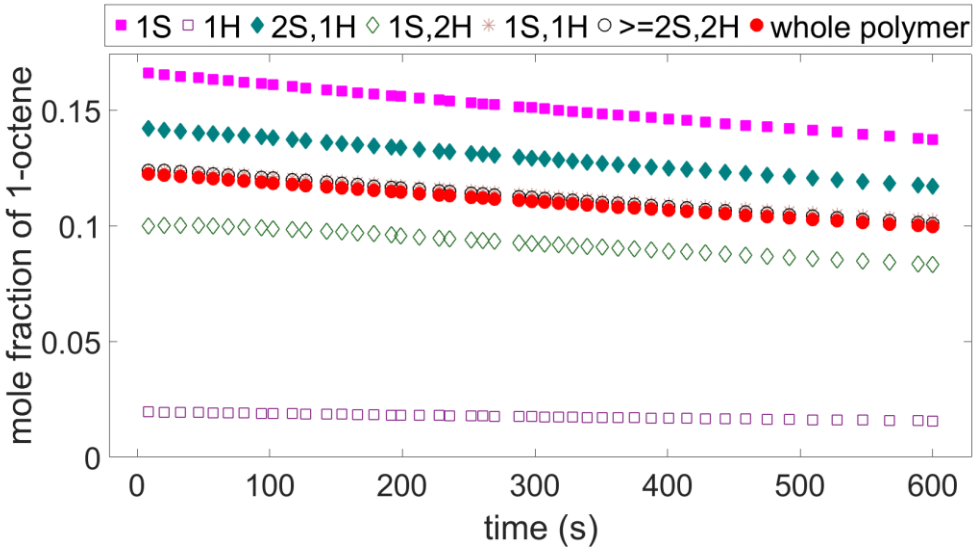

Figure 5-15. 1-Octene molar fraction in different OBC populations ($k_{t\beta} > 0$, $[CSA]/[C_{tot}] = 1000$).

Figure 5-16 shows that, without chain transfer, the fractions of uni-block populations approaches zero, whereas the fraction of di-block populations initially increase as uni-blocks become di-blocks, reach a maximum, then decrease as di-block chains react to from tri-block chains. A similar behavior is depicted for the two tri-block populations (2S,1H and 1S,2H), and the same would be observed for OBC populations with higher number of blocks, but since the model groups all these OBC chains in a single population (≥ 2S,2H), this profile increases continuously until reaching a value of 1.0, indicating that after a given time, all chains in the reactor would have 4 or more blocks. As mentioned above, this is an unlikely situation during the real production of OBCs.

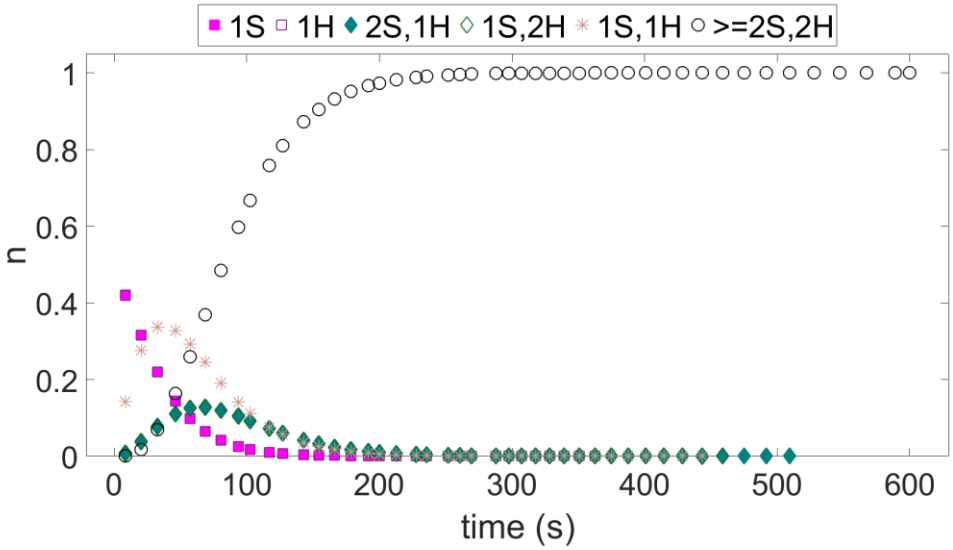

Figure 5-16. Time evolution of OBC populations ($k_{t\beta}$ = 0, [CSA]/[C_{tot}] = 1000).

As expected, the graph changes in the presence of chain transfer. The fraction of uni-block populations decreases with polymerization time but does not reach zero, as new uni-block chains are formed when polymer-free active sites are restored after chain transfer takes place. The same limiting behavior is observed for populations with 2 or more blocks. This picture is more consistent with our understanding of how chain shuttling polymerization works under usual experimental conditions (Figure 5-17).

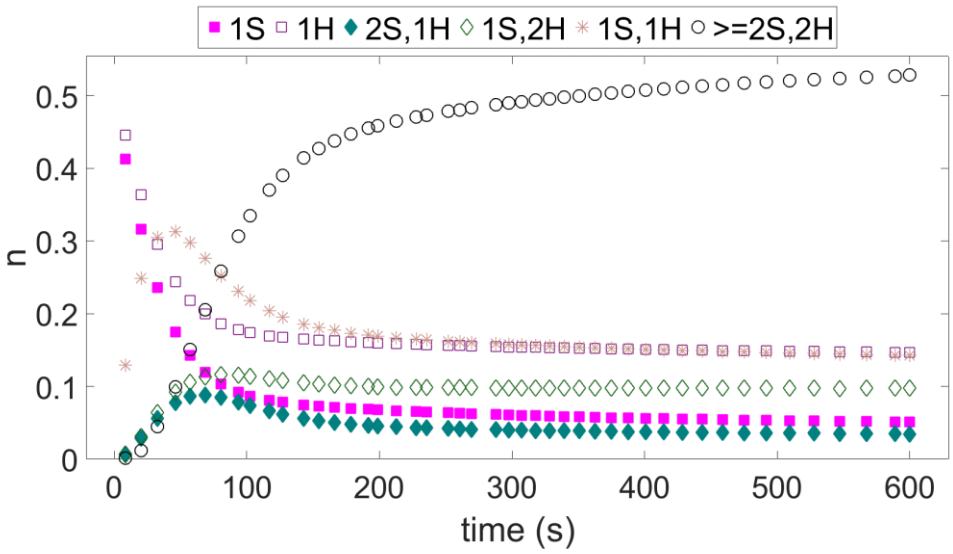

Figure 5-17. Time evolution of OBC populations ($k_{t\beta} > 0$, $[CSA]/[C_{tot}] = 1000$).

Increasing the $[CSA]/[C_{tot}]$ ratio affects relative amount of the distinct OBC populations: as this ratio increases from 1000 to 2000, the fractions of chains with fewer blocks decrease, and consequently the fraction of chains with more blocks (≥ 2S,2H) increases because of the higher chain shuttling frequency, as can be concluded by comparing Figure 5-18 with Figure 5-17. Tongtummachat et al.[49] reported a similar observation for semi-batch reactors.

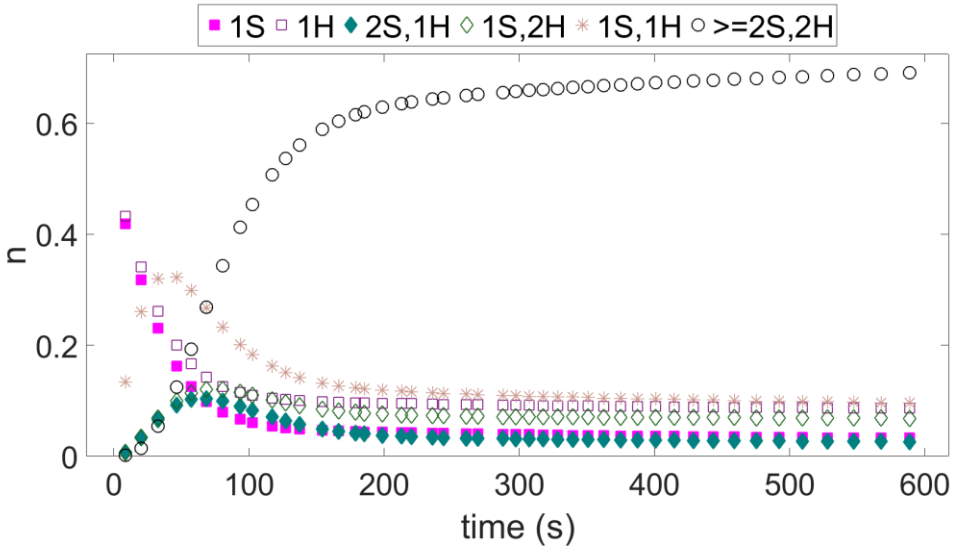

Figure 5-18. Time evolution of OBC populations ($k_{t\beta} > 0$, $[CSA]/[C_{tot}] = 2000$).

The effect of chain transfer in the average number of block in the whole polymer can be appreciated by comparing Figure 5-19a and Figure 5-19b. In the absence of transfer, the average number of blocks can increase up to 25 under the polymerization conditions considered in this simulation, and this number keeps increasing linearly as a function of polymerization time. On the other hand, the average number of blocks per chain stabilizes at a value of 6 under chain transfer conditions because chain transfer generates polymer-free active sites that can start forming uni-block chains any time during polymerization. Wang et al.[55] reported that the average number of blocks per chain for OBCs made by Dow Chemical Company was in the range of 2 to 10 blocks per chain. These two figures also compare Monte Carlo and method of moments simulations, confirming that their predictions are the same.

If one needs to make OBCs with a higher average number of blocks, one alternative would be to increase the $[CSA]/[C_{tot}]$ ratio, as demonstrated in Figure 5-19c. Higher $[CSA]/[C_{tot}]$ ratios increase the chain shuttling frequency, making OBCs with more blocks (but also with smaller average chain lengths). Zhang et al.[44] reported similar observation, noting that the average number of blocks per chain for the whole OBCs increased as CSA feed rate increased but for the CSTR.

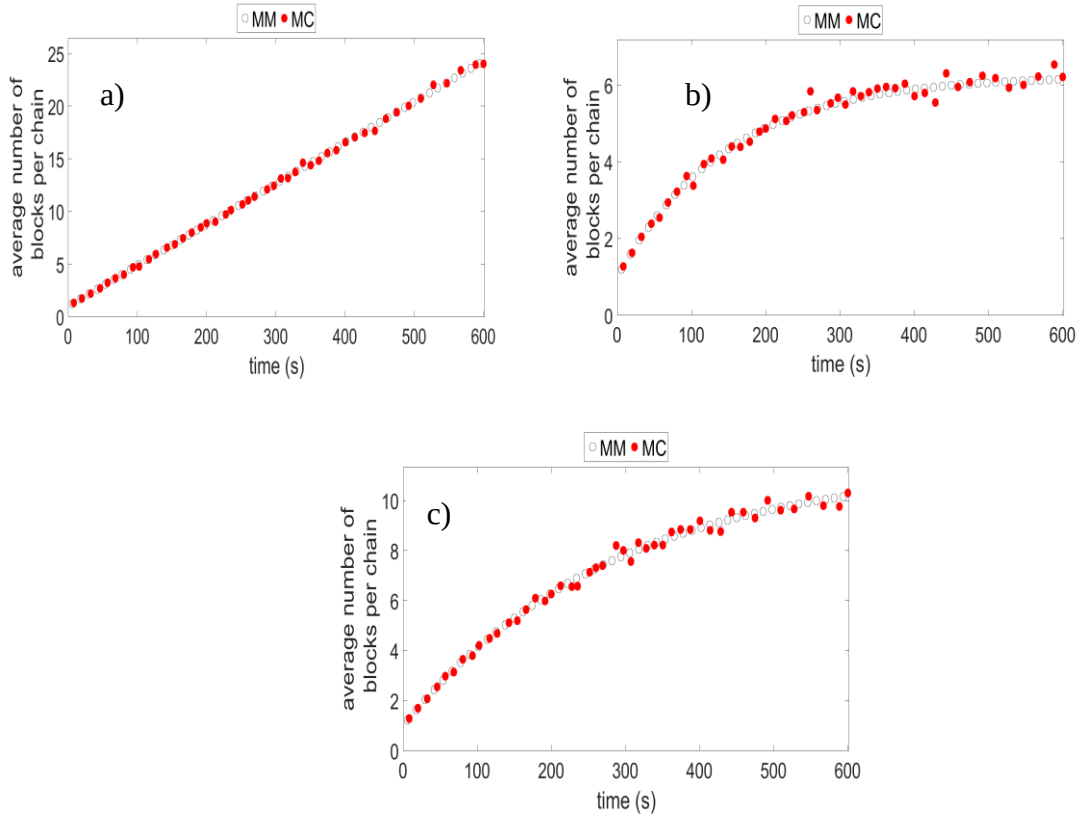

Figure 5-19. Average number of blocks per chain: a) $k_{t\beta}$ = 0, [*CSA*]/[C_{tot}] = 1000, b) $k_{t\beta}$ > 0, [*CSA*]/[C_{tot}] = 1000, c) $k_{t\beta}$ > 0, [*CSA*]/[C_{tot}] = 2000.

5.5.3 Effect of chain transfer on the distributions of chain length and chemical composition

Figure 5-20 illustrates how the CLD of the whole polymer changes as a function of polymerization time in the absence or presence of chain transfer reactions. In the beginning of polymerization, the CLD is broad (PDI > 2) because polymer chains are being formed by two catalysts that make polymers with distinct average chain lengths and no substantial chain shuttling has occurred yet. As polymerization proceeds in the absence of chain transfer, the CLDs become increasingly narrower over time, with PDIs approaching 1.0 because no dead polymer chains are formed. On the other hand, if chain transfer occurs, the CLD of the whole polymer becomes narrower via chain shuttling, but eventually converge to PDI values close to 2.0, which would be expected for either a single site catalyst, or for mixtures of single site catalysts in which substantial chain shuttling is taking place.

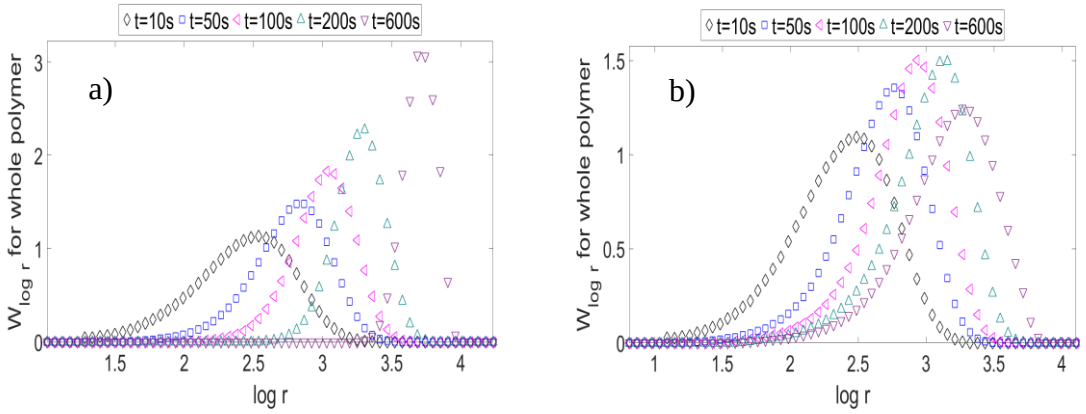

Figure 5-20. Effect of $k_{t\beta}$ on the CLD of whole OBCs: a) $k_{t\beta} = 0$, b) $k_{t\beta} > 0$.

One of the advantages of Monte Carlo method is that it allows us to look into the fine microstructural details of polymers. Figure 5-21 shows how CLDs of distinct OBC populations evolve in time in the absence or presence of chain transfer reactions. As polymerization proceeds, we can follow how the CLDs of OBCs with fewer blocks move into the CLDs of OBCs with more blocks, and track down the contribution of each population to the CLD of the whole polymer.

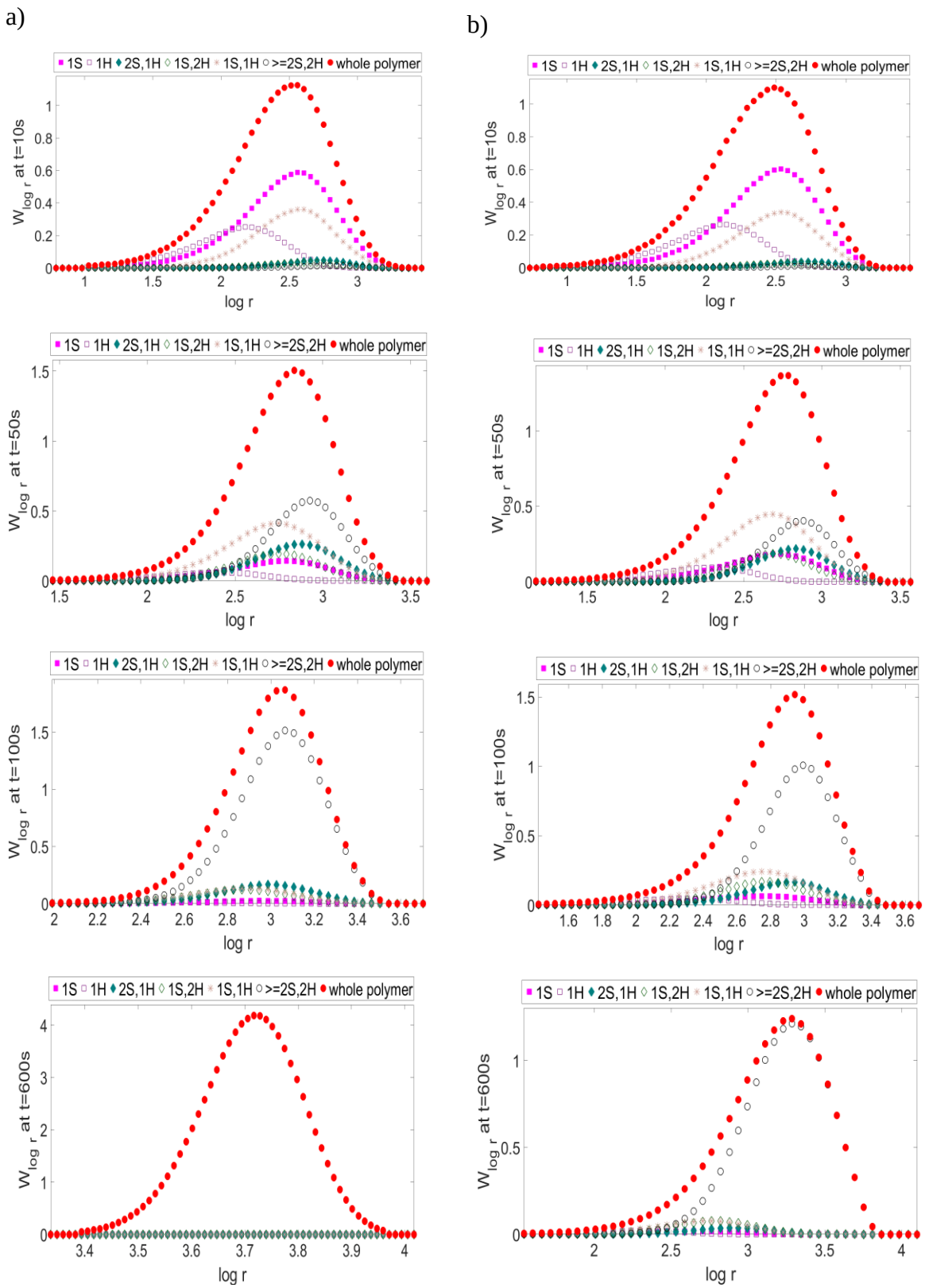

Figure 5-21. Effect of $k_{t\beta}$ on the CLD of different OBC populations: a) $k_{t\beta} = 0$, b) $k_{t\beta} > 0$.

A similar investigation can be conducted to track changes in the CCD of the whole polymer and its components as a function of polymerization time. Figure 5-22 illustrates how the CCD of the whole polymer changes from a bimodal distribution (clearly showing the individual compositions of the hard and soft uni-block chains) to a unimodal distribution as the polymerization proceeds and the effect of chain shuttling becomes more prevalent. If no chain transfer takes place at the end of polymerization, the CCD is narrow and unimodal, as expected for a multi-block product. If chain transfer is important, however, the CCD bimodality may be reduced, but not completely eliminated, since OBC populations with fewer blocks are constantly being formed after chain transfer events.

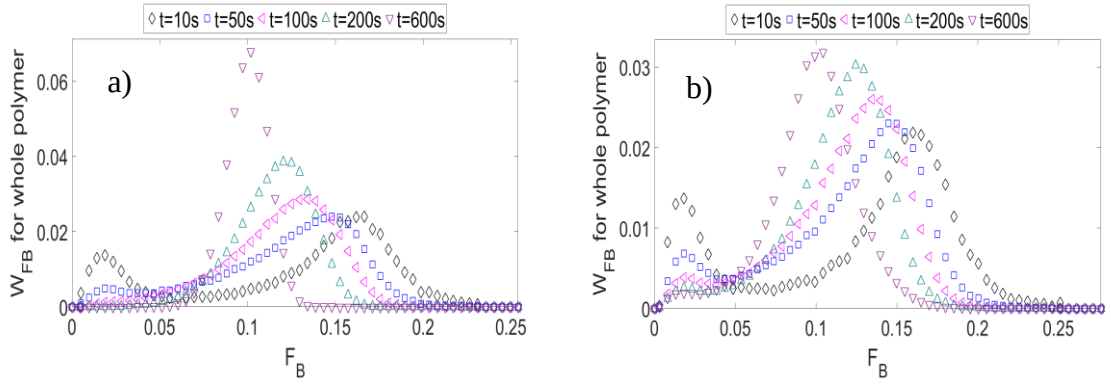

Figure 5-22. Effect of $k_{t\beta}$ on the CCD of the whole OBCs: a) $k_{t\beta} = 0$, b) $k_{t\beta} > 0$.

Figure 5-23 illustrates this phenomenon in more details, by breaking down the CCD into different populations containing distinct number of blocks. One clearly sees that the CCD of OBCs with more blocks becomes narrower and unimodal due to the random combination effect of the chain shuttling process.

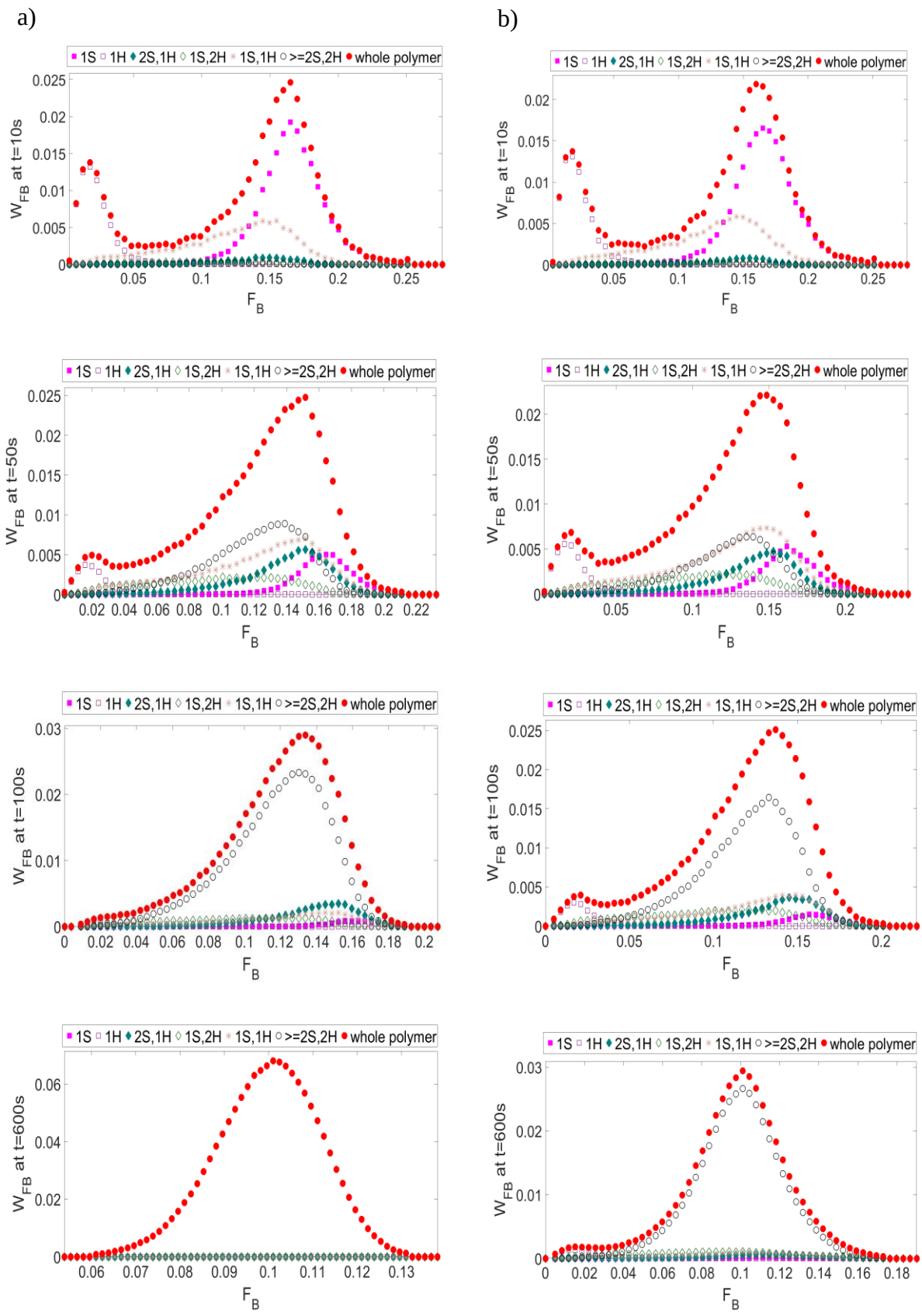

Figure 5-23. Effect of $k_{t\beta}$ on the CCD of different OBC populations: a) $k_{t\beta} = 0$, b) $k_{t\beta} > 0$.

5.5.4 Effect of CSA concentration on the distributions of chain length and chemical composition

Figure 5-24 illustrates how the CLD of the whole OBC evolves during the polymerization as the [*CSA*]/[C_{tot}] ratio changes from 1000 to 2000. As discussed for PDI, the CLDs are initially relatively broad (PDI > 2), but as polymerization proceeds, the CLDs becomes narrower and even more so for the higher [*CSA*]/[C_{tot}] of 2000, because the chain shuttling rate is higher in this case.

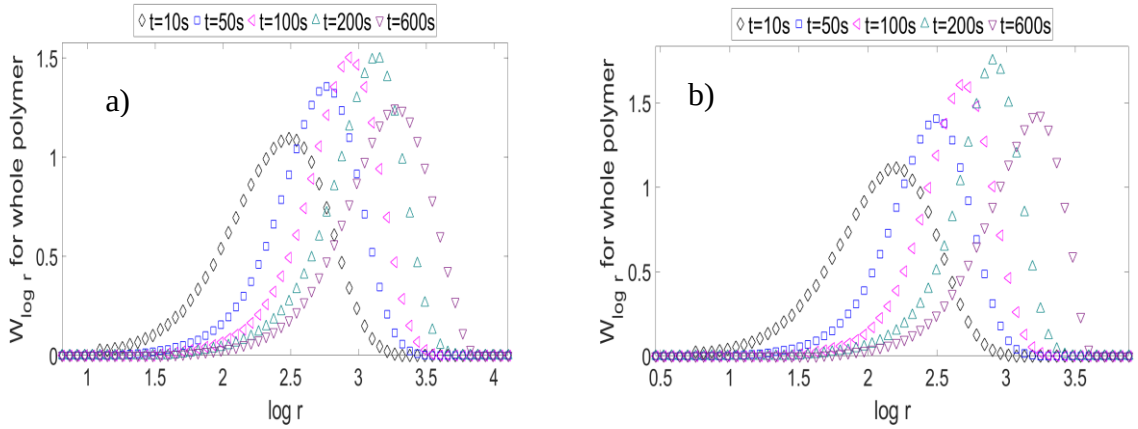

Figure 5-24. Effect of [*CSA*]/[C_{tot}] ratio on the CLD of the whole OBCs: a) [*CSA*]/[C_{tot}] = 1000, b) [*CSA*]/[C_{tot}] = 2000.

Figure 5-25 investigates the effect of the same change in [*CSA*]/[C_{tot}] on the CCD of the whole OBC. When the [*CSA*]/[C_{tot}] ratio is increased to 2000, the CCD narrows faster because of increase in chain shuttling frequency, but the position of the comonomer peaks remains the same. Ahmadi et la.[48] reported the same phenomena where the bimodality of CCD vanished at high CSA.

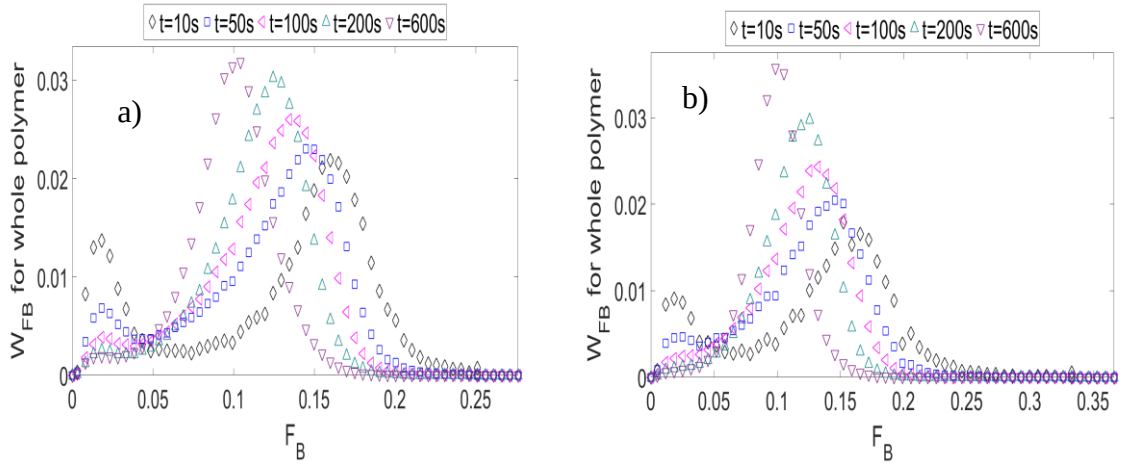

Figure 5-25. Effect of the [CSA]/[C_{tot}] on the CCD of the whole OBCs: a) [CSA]/[C_{tot}] = 1000, b) [CSA]/[C_{tot}] = 2000.

5.6 Conclusion

We have shown that simulation results obtained with a dynamic Monte Carlo model agree well with those predicted by the method of moments. In addition to microstructural averages, the dynamic Monte Carlo model can predict the temporal evolution of the distributions of chain length (CLD) and chemical composition (CCD) during polymerization in a semi-batch reactor, thus providing substantially more microstructural information than the method of moments.

The Monte Carlo model was used to investigate the effect of the chain transfer and chain shuttling agent (CSA) concentration on these microstructural distributions and their averages, for the whole OBC as well for populations with different number of blocks per chain.

Chain transfer has a substantial impact on the microstructure of OBCs. If chain transfer steps could be eliminated, multi-block OBCs would predominate for longer polymerization times, and their CLDs and CCDs would be unimodal and quite narrow. Unfortunately, this does not seem to be the case for most practical applications of chain shuttling polymerization, where chain shuttling reactions can compete, but cannot completely suppress chain transfer events. In such cases, chain shuttling polymerization makes OBCs with a broader CCDs with the perhaps unavoidable presence of populations with fewer blocks (uni-, di-, tri-blocks, etc.), but with CLDs with PDI converging to a value of 2.0 if chain shuttling is effective during the polymerization.

This tendency to form broader CCD can be overcome, in part, by increasing the ratio of chain shuttling agent to catalyst, $[CSA]/[C_{tot}]$, since this will increase the frequency of chain shuttling events and compete more effectively with chain transfer. But this occurs at a cost of making OBCs with lower average chain lengths, since chain shuttling agents, albeit being reversible, also act as chain transfer agents and retard chain growth. Note that, even though we did not examine this scenario in this chapter, a similar effect could be achieved by looking for catalysts with higher chain shuttling rates (k_{CSA}).

6. Mathematical Modeling of Chain Shuttling Copolymerization in a CSTR at Steady State using a Dual Catalyst

6.1 Overview

We developed a mathematical model to describe the microstructure of ethylene/1-octene olefin block copolymers made by chain shuttling copolymerization with a dual catalyst system in a CSTR operated at steady state using population balances and the method of moments. One catalyst incorporates 1-octene well and produces chains with high comonomer content; the other catalyst polymerizes 1-octene less effectively and makes chains with low comonomer content. The chain shuttling agent acts as a reversible chain transfer agent that "shuttles" chains between the two catalysts, producing linear olefin block copolymers (OBCs).

The population balance model predicts the number and weight average chain lengths of OBC populations containing different number of blocks and their fractions.

We used the proposed model to investigate the effect of chain shuttling agent concentration, chain shuttling rate constant, and average residence time for several ratios of the two catalysts on the microstructure of OBCs, and compared them to those of OBCs made in a semi-batch reactor described in Chapter 5.

6.2 Model Development

The polymerization mechanism used in this chapter was described in Chapter 5, but we modified the equations in Chapter 5 for moments and mole balances to include flow rates entering and leaving the CSTR. Table 6-1 through Table 6-6 summarize the moments equations for living, dormant, and dead OBC populations in a CSTR operated at steady state, and Table 6-7 lists the molar balances for all reactants. The resulting nonlinear algebraic system of equations shown in Table 6-1 through Table 6-7 was solved by Matlab using the function fsolve. Appendix 6-A presents the derivations of these equations in detail.

The equations used to calculate monomer conversion, average chain length, and PDI for the whole polymer and for OBC populations, fractions of OBC populations, average number of blocks per

chain, and mole fraction of ethylene and 1-octene for polymer populations having different numbers of blocks are the same used for the semi-batch reactor simulations discussed in Chapter 5.

Table 6-1. Moment equations for OBC chains made in catalyst *P* in a CSTR operated at steady state for the whole polymer.

Description	Moment equations
0th Moment of living chains	$Y_{0,P} = \frac{\left(k_{iA1}A + k_{iB1}B\right)C_1}{\left(k_{t\beta 1} + k_{tH1}H_2 + k_{d1} + k_{CSA01}S_0 + s\right)}$
1st Moment of living chains	$Y_{1,P} = \frac{\left(k_{iA1}A + k_{iB1}B\right)C_1 + \left(k_{pA1}A + k_{pB1}B\right)Y_{0,P} + \left(\left(SX_{1,P}\right) + \left(SX_{1,Q}\right)\right)k_{CSA1}Y_{0,P}}{\left(k_{t\beta 1} + k_{tH1}H_2 + k_{d1} + k_{CSA01}S_0 + k_{CSA1}\left(SX_{0,P}\right) + k_{CSA1}\left(SX_{0,Q}\right) + s\right)}$
2nd Moment of living chains	$Y_{2,P} = \frac{\left(k_{iA1}A + k_{iB1}B\right)C_1 + \left(k_{pA1}A + k_{pB1}B\right)\left(Y_{0,P} + 2Y_{1,P}\right) + \left(\left(SX_{2,P}\right) + \left(SX_{2,Q}\right)\right)k_{CSA1}Y_{0,P}}{\left(k_{t\beta 1} + k_{tH1}H_2 + k_{d1} + k_{CSA01}S_0 + k_{CSA1}\left(SX_{0,P}\right) + k_{CSA1}\left(SX_{0,Q}\right) + s\right)}$
0th Moment of dead chains	$X_{0,P} = \frac{\left(k_{t\beta 1} + k_{tH1}H_2 + k_{d1}\right)Y_{0,P}}{s}$
1st Moment of dead chains	$X_{1,P} = \frac{\left(k_{t\beta 1} + k_{tH1}H_2 + k_{d1}\right)Y_{1,P}}{s}$
2nd Moment of dead chains	$X_{2,P} = \frac{\left(k_{t\beta 1} + k_{tH1}H_2 + k_{d1}\right)Y_{2,P}}{s}$
0th Moment of dormant chains	$\left(SX_{0,P}\right) = \frac{\left(k_{CSA01}S_0 + k_{CSA1}\left(SX_{0,Q}\right)\right)Y_{0,P}}{\left(k_{CSA2}Y_{0,Q} + s\right)}$
1st Moment of dormant chains	$\left(SX_{1,P}\right) = \frac{\left(k_{CSA01}S_0 + k_{CSA1}\left(SX_{0,P}\right) + k_{CSA1}\left(SX_{0,Q}\right)\right)Y_{1,P}}{\left(k_{CSA1}Y_{0,P} + k_{CSA2}Y_{0,Q} + s\right)}$
2nd Moment of dormant chains	$\left(SX_{2,P}\right) = \frac{\left(k_{CSA01}S_0 + k_{CSA1}\left(SX_{0,P}\right) + k_{CSA1}\left(SX_{0,Q}\right)\right)Y_{2,P}}{\left(k_{CSA1}Y_{0,P} + k_{CSA2}Y_{0,Q} + s\right)}$

Table 6-2. Moment equations for OBC chains made in catalyst *Q* in a CSTR operated at steady state for the whole polymer.

Description	Moment equations
0th Moment of living chains	$Y_{0,Q} = \frac{\left(k_{iA2}A + k_{iB2}B\right)C_2}{\left(k_{t\beta 2} + k_{tH2}H_2 + k_{d2} + k_{CSA02}S_0 + s\right)}$
1st Moment of living chains	$Y_{1,Q} = \frac{\left(k_{iA2}A + k_{iB2}B\right)C_2 + \left(k_{pA2}A + k_{pB2}B\right)Y_{0,Q} + \left(\left(SX_{1,P}\right) + \left(SX_{1,Q}\right)\right)k_{CSA2}Y_{0,Q}}{\left(k_{t\beta 2} + k_{tH2}H_2 + k_{d2} + k_{CSA02}S_0 + k_{CSA2}\left(SX_{0,P}\right) + k_{CSA2}\left(SX_{0,Q}\right) + s\right)}$
2nd Moment of living chains	$Y_{2,Q} = \frac{\left(k_{iA2}A + k_{iB2}B\right)C_2 + \left(k_{pA2}A + k_{pB2}B\right)\left(Y_{0,Q} + 2Y_{1,Q}\right) + \left(\left(SX_{2,P}\right) + \left(SX_{2,Q}\right)\right)k_{CSA2}Y_{0,Q}}{\left(k_{t\beta 2} + k_{tH2}H_2 + k_{d2} + k_{CSA02}S_0 + k_{CSA2}\left(SX_{0,P}\right) + k_{CSA2}\left(SX_{0,Q}\right) + s\right)}$
0th Moment of dead chains	$X_{0,Q} = \frac{\left(k_{t\beta 2} + k_{tH2}H_2 + k_{d2}\right)Y_{0,Q}}{s}$
1st Moment of dead chains	$X_{1Q} = \frac{\left(k_{t\beta 2} + k_{tH2}H_2 + k_{d2}\right)Y_{1,Q}}{s}$
2nd Moment of dead chains	$X_{2,Q} = \frac{\left(k_{t\beta 2} + k_{tH2}H_2 + k_{d2}\right)Y_{2,Q}}{s}$
0th Moment of dormant chains	$\left(SX_{0,Q}\right) = \frac{\left(k_{CSA02}S_0 + k_{CSA2}\left(SX_{0,P}\right)\right)Y_{0,Q}}{\left(k_{CSA1}Y_{0,P} + s\right)}$
1st Moment of dormant chains	$\left(SX_{1,Q}\right) = \frac{\left(k_{CSA02}S_0 + k_{CSA2}\left(SX_{0,P}\right) + k_{CSA2}\left(SX_{0,Q}\right)\right)Y_{1,Q}}{\left(k_{CSA1}Y_{0,P} + k_{CSA2}Y_{0,Q} + s\right)}$
2nd Moment of dormant chains	$\left(SX_{2,Q}\right) = \frac{\left(k_{CSA02}S_0 + k_{CSA2}\left(SX_{0,P}\right) + k_{CSA2}\left(SX_{0,Q}\right)\right)Y_{2,Q}}{\left(k_{CSA1}Y_{0,P} + k_{CSA2}Y_{0,Q} + s\right)}$

Table 6-3. Moment equations for chains with a single block made in catalyst *P* in a CSTR operated at steady state.

Description	Moment equations
0th Moment of living chains	$Y_{0,P,i} = \frac{\left(k_{iA1}A + k_{iB1}B\right)C_1 + \left(SX_{0,P,i}\right)k_{CSA1}Y_{0,P}}{\left(k_{t\beta 1} + k_{tH1}H_2 + k_{d1} + k_{CSA01}S_0 + k_{CSA1}\left(SX_{0,P}\right) + k_{CSA1}\left(SX_{0,Q}\right) + s\right)}$
1st Moment of living chains	$Y_{1,P,i} = \frac{\left(k_{iA1}A + k_{iB1}B\right)C_1 + \left(k_{pA1}A + k_{pB1}B\right)Y_{0,P,i} + \left(SX_{1,P,i}\right)k_{CSA1}Y_{0,P}}{\left(k_{t\beta 1} + k_{tH1}H_2 + k_{d1} + k_{CSA01}S_0 + k_{CSA1}\left(SX_{0,P}\right) + k_{CSA1}\left(SX_{0,Q}\right) + s\right)}$
2nd Moment of living chains	$Y_{2,P,i} = \frac{\left(k_{iA1}A + k_{iB1}B\right)C_1 + \left(k_{pA1}A + k_{pB1}B\right)\left(Y_{0,P,i} + 2Y_{1,P,i}\right) + \left(SX_{2,P,i}\right)k_{CSA1}Y_{0,P}}{\left(k_{t\beta 1} + k_{tH1}H_2 + k_{d1} + k_{CSA01}S_0 + k_{CSA1}\left(SX_{0,P}\right) + k_{CSA1}\left(SX_{0,Q}\right) + s\right)}$
0th Moment of dead chains	$X_{0,P,i} = \frac{\left(k_{t\beta 1} + k_{tH1}H_2 + k_{d1}\right)Y_{0,P,i}}{s}$
1st Moment of dead chains	$X_{1,P,i} = \frac{\left(k_{t\beta 1} + k_{tH1}H_2 + k_{d1}\right)Y_{1,P,i}}{s}$
2nd Moment of dead chains	$X_{2,P,i} = \frac{\left(k_{t\beta 1} + k_{tH1}H_2 + k_{d1}\right)Y_{2,P,i}}{s}$
0th Moment of dormant chains	$\left(SX_{0,P,i}\right) = \frac{\left(k_{CSA01}S_0 + k_{CSA1}\left(SX_{0,P}\right) + k_{CSA1}\left(SX_{0,Q}\right)\right)Y_{0,P,i}}{\left(k_{CSA1}Y_{0,P} + k_{CSA2}Y_{0,Q} + s\right)}$
1st Moment of dormant chains	$\left(SX_{1,P,i}\right) = \frac{\left(k_{CSA01}S_0 + k_{CSA1}\left(SX_{0,P}\right) + k_{CSA1}\left(SX_{0,Q}\right)\right)Y_{1,P,i}}{\left(k_{CSA1}Y_{0,P} + k_{CSA2}Y_{0,Q} + s\right)}$
2nd Moment of dormant chains	$\left(SX_{2,P,i}\right) = \frac{\left(k_{CSA01}S_0 + k_{CSA1}\left(SX_{0,P}\right) + k_{CSA1}\left(SX_{0,Q}\right)\right)Y_{2,P,i}}{\left(k_{CSA1}Y_{0,P} + k_{CSA2}Y_{0,Q} + s\right)}$

Table 6-4. Moment equations for chains with a single block made in catalyst Q in a CSTR operated at steady state.

Description	Moment equations
0th Moment of living chains	$Y_{0,Q,i} = \frac{\left(k_{iA2}A + k_{iB2}B\right)C_2 + \left(SX_{0,Q,i}\right)k_{CSA2}Y_{0,Q}}{\left(k_{t\beta 2} + k_{tH2}H_2 + k_{d2} + k_{CSA02}S_0 + k_{CSA2}\left(SX_{0,P}\right) + k_{CSA2}\left(SX_{0,Q}\right) + s\right)}$
1st Moment of living chains	$Y_{1,Q,i} = \frac{\left(k_{iA2}A + k_{iB2}B\right)C_2 + \left(k_{pA2}A + k_{pB2}B\right)Y_{0,Q,i} + \left(SX_{1,Q,i}\right)k_{CSA2}Y_{0,Q}}{\left(k_{t\beta 2} + k_{tH2}H_2 + k_{d2} + k_{CSA02}S_0 + k_{CSA2}\left(SX_{0,P}\right) + k_{CSA2}\left(SX_{0,Q}\right) + s\right)}$
2nd Moment of living chains	$Y_{2,Q,i} = \frac{\left(k_{iA2}A + k_{iB2}B\right)C_2 + \left(k_{pA2}A + k_{pB2}B\right)\left(Y_{0,Q,i} + 2Y_{1,Q,i}\right) + \left(SX_{2,Q,i}\right)k_{CSA2}Y_{0,Q}}{\left(k_{t\beta 2} + k_{tH2}H_2 + k_{d2} + k_{CSA02}S_0 + k_{CSA2}\left(SX_{0,P}\right) + k_{CSA2}\left(SX_{0,Q}\right) + s\right)}$
0th Moment of dead chains	$X_{0,Q,i} = \frac{\left(k_{t\beta 2} + k_{tH2}H_2 + k_{d2}\right)Y_{0,Q,i}}{s}$
1st Moment of dead chains	$X_{1,Q,i} = \frac{\left(k_{t\beta 2} + k_{tH2}H_2 + k_{d2}\right)Y_{1,Q,i}}{s}$
2nd Moment of dead chains	$X_{2,Q,i} = \frac{\left(k_{t\beta 2} + k_{tH2}H_2 + k_{d2}\right)Y_{2,Q,i}}{s}$
0th Moment of dormant chains	$\left(SX_{0,Q,i}\right) = \frac{\left(k_{CSA02}S_0 + k_{CSA2}\left(SX_{0,P}\right) + k_{CSA2}\left(SX_{0,Q}\right)\right)Y_{0,Q,i}}{\left(k_{CSA1}Y_{0,P} + k_{CSA2}Y_{0,Q} + s\right)}$
1st Moment of dormant chains	$\left(SX_{1,Q,i}\right) = \frac{\left(k_{CSA02}S_0 + k_{CSA2}\left(SX_{0,P}\right) + k_{CSA2}\left(SX_{0,Q}\right)\right)Y_{1,Q,i}}{\left(k_{CSA1}Y_{0,P} + k_{CSA2}Y_{0,Q} + s\right)}$
2nd Moment of dormant chains	$\left(SX_{2,Q,i}\right) = \frac{\left(k_{CSA02}S_0 + k_{CSA2}\left(SX_{0,P}\right) + k_{CSA2}\left(SX_{0,Q}\right)\right)Y_{2,Q,i}}{\left(k_{CSA1}Y_{0,P} + k_{CSA2}Y_{0,Q} + s\right)}$

Table 6-5. Moment equations for OBC chains made in catalyst *P* in a CSTR operated at steady state for chains having two or more blocks.

Description	Moment equations
0th Moment of living chains	$Y_{0,P,i} = \frac{\left(\left(SX_{0,P,i}\right)+\left(SX_{0,Q,i-1}\right)\right)k_{CSA1}Y_{0,P}}{\left(k_{t\beta 1}+k_{tH1}H_2+k_{d1}+k_{CSA01}S_0+k_{CSA1}\left(SX_{0,P}\right)+k_{CSA1}\left(SX_{0,Q}\right)+s\right)}$
1st Moment of living chains	$Y_{1,P,i} = \frac{\left(k_{pA1}A+k_{pB1}B\right)Y_{0,P,i}+\left(\left(SX_{1,P,i}\right)+\left(SX_{1,Q,i-1}\right)\right)k_{CSA1}Y_{0,P}}{\left(k_{t\beta 1}+k_{tH1}H_2+k_{d1}+k_{CSA01}S_0+k_{CSA1}\left(SX_{0,P}\right)+k_{CSA1}\left(SX_{0,Q}\right)+s\right)}$
2nd Moment of living chains	$Y_{2,P,i} = \frac{\left(k_{pA1}A+k_{pB1}B\right)\left(Y_{0,P,i}+2Y_{1,P,i}\right)+\left(\left(SX_{2,P,i}\right)+\left(SX_{2,Q,i-1}\right)\right)k_{CSA1}Y_{0,P}}{\left(k_{t\beta 1}+k_{tH1}H_2+k_{d1}+k_{CSA01}S_0+k_{CSA1}\left(SX_{0,P}\right)+k_{CSA1}\left(SX_{0,Q}\right)+s\right)}$
0th Moment of dead chains	$X_{0,P,i} = \frac{\left(k_{t\beta 1}+k_{tH1}H_2+k_{d1}\right)Y_{0,P,i}}{s}$
1st Moment of dead chains	$X_{1,P,i} = \frac{\left(k_{t\beta 1}+k_{tH1}H_2+k_{d1}\right)Y_{1,P,i}}{s}$
2nd Moment of dead chains	$X_{2,P,i} = \frac{\left(k_{t\beta 1}+k_{tH1}H_2+k_{d1}\right)Y_{2,P,i}}{s}$
0th Moment of dormant chains	$\left(SX_{0,P,i}\right) = \frac{\left(k_{CSA01}S_0+k_{CSA1}\left(SX_{0,P}\right)+k_{CSA1}\left(SX_{0,Q}\right)\right)Y_{0,P,i}}{\left(k_{CSA1}Y_{0,P}+k_{CSA2}Y_{0,Q}+s\right)}$
1st Moment of dormant chains	$\left(SX_{1,P,i}\right) = \frac{\left(k_{CSA01}S_0+k_{CSA1}\left(SX_{0,P}\right)+k_{CSA1}\left(SX_{0,Q}\right)\right)Y_{1,P,i}}{\left(k_{CSA1}Y_{0,P}+k_{CSA2}Y_{0,Q}+s\right)}$
2nd Moment of dormant chains	$\left(SX_{2,P,i}\right) = \frac{\left(k_{CSA01}S_0+k_{CSA1}\left(SX_{0,P}\right)+k_{CSA1}\left(SX_{0,Q}\right)\right)Y_{2,P,i}}{\left(k_{CSA1}Y_{0,P}+k_{CSA2}Y_{0,Q}+s\right)}$

Table 6-6. Moment equations for OBC chains made in catalyst *Q* in a CSTR operated at steady state for chains having two or more blocks.

Description	Moment equations
0th Moment of living chains	$Y_{0,Q,i} = \frac{\left(\left(SX_{0,P,i-1}\right)+\left(SX_{0,Q,i}\right)\right)k_{CSA2}Y_{0,Q}}{\left(k_{t\beta 2}+k_{tH2}H_2+k_{d2}+k_{CSA02}S_0+k_{CSA2}\left(SX_{0,P}\right)+k_{CSA2}\left(SX_{0,Q}\right)+s\right)}$
1st Moment of living chains	$Y_{1,Q,i} = \frac{\left(k_{pA2}A+k_{pB2}B\right)Y_{0,Q,i}+\left(\left(SX_{1,P,i-1}\right)+\left(SX_{1,Q,i}\right)\right)k_{CSA2}Y_{0,Q}}{\left(k_{t\beta 2}+k_{tH2}H_2+k_{d2}+k_{CSA02}S_0+k_{CSA2}\left(SX_{0,P}\right)+k_{CSA2}\left(SX_{0,Q}\right)+s\right)}$
2nd Moment of living chains	$Y_{2,Q,i} = \frac{\left(k_{pA2}A+k_{pB2}B\right)\left(Y_{0,Q,i}+2Y_{1,Q,i}\right)+\left(\left(SX_{2,P,i-1}\right)+\left(SX_{2,Q,i}\right)\right)k_{CSA2}Y_{0,Q}}{\left(k_{t\beta 2}+k_{tH2}H_2+k_{d2}+k_{CSA02}S_0+k_{CSA2}\left(SX_{0,P}\right)+k_{CSA2}\left(SX_{0,Q}\right)+s\right)}$
0th Moment of dead chains	$X_{0,Q,i} = \frac{\left(k_{t\beta 2}+k_{tH2}H_2+k_{d2}\right)Y_{0,Q,i}}{s}$
1st Moment of dead chains	$X_{1,Q,i} = \frac{\left(k_{t\beta 2}+k_{tH2}H_2+k_{d2}\right)Y_{1,Q,i}}{s}$
2nd Moment of dead chains	$X_{2,Q,i} = \frac{\left(k_{t\beta 2}+k_{tH2}H_2+k_{d2}\right)Y_{2,Q,i}}{s}$
0th Moment of dormant chains	$\left(SX_{0,Q,i}\right) = \frac{\left(k_{CSA02}S_0+k_{CSA2}\left(SX_{0,P}\right)+k_{CSA2}\left(SX_{0,Q}\right)\right)Y_{0,Q,i}}{\left(k_{CSA1}Y_{0,P}+k_{CSA2}Y_{0,Q}+s\right)}$
1st Moment of dormant chains	$\left(SX_{1,Q,i}\right) = \frac{\left(k_{CSA02}S_0+k_{CSA2}\left(SX_{0,P}\right)+k_{CSA2}\left(SX_{0,Q}\right)\right)Y_{1,Q,i}}{\left(k_{CSA1}Y_{0,P}+k_{CSA2}Y_{0,Q}+s\right)}$
2nd Moment of dormant chains	$\left(SX_{2,Q,i}\right) = \frac{\left(k_{CSA02}S_0+k_{CSA2}\left(SX_{0,P}\right)+k_{CSA2}\left(SX_{0,Q}\right)\right)Y_{2,Q,i}}{\left(k_{CSA1}Y_{0,P}+k_{CSA2}Y_{0,Q}+s\right)}$

Table 6-7. Molar balance equations in a CSTR operated at steady state.

Description	Molar equations
Catalyst *P*	$C_1 = \frac{\left(k_{t\beta 1} + k_{tH1}H_2 + k_{d1} + k_{CSA01}S_0\right)Y_{0,P} + C_1^{in}}{\left(k_{iA1}A + k_{iB1}B + s\right)}$
Catalyst *Q*	$C_2 = \frac{\left(k_{t\beta 2} + k_{tH2}H_2 + k_{d2} + k_{CSA02}S_0\right)Y_{0,Q} + C_2^{in}}{\left(k_{iA2}A + k_{iB2}B + s\right)}$
Chain shuttling agent (CSA)	$S_0 = \frac{S_0^{in}}{\left(k_{CSA01}Y_{0,P} + k_{CSA02}Y_{0,Q} + s\right)}$
Deactivated site of catalyst *P*	$C_{d1} = \frac{k_{d1}\left(Y_{0,P} + C_1\right)}{s}$
Deactivated site of catalyst *Q*	$C_{d2} = \frac{k_{d2}\left(Y_{0,Q} + C_2\right)}{s}$
Ethylene consumption by catalysts *P* and *Q*	$A_p = \frac{\left(k_{iA1}C_1 + k_{iA2}C_2 + k_{pA1}Y_{0,P} + k_{pA2}Y_{0,Q}\right)A}{s}$
1-Octene consumption by catalysts *P* and *Q*	$B_p = \frac{\left(k_{iB1}C_1 + k_{iB2}C_2 + k_{pB1}Y_{0,P} + k_{pB2}Y_{0,Q}\right)B}{s}$
Ethylene consumption by catalyst *P*	$A_{p,1} = \frac{\left(k_{iA1}C_1 + k_{pA1}Y_{0,P}\right)A}{s}$
Ethylene consumption by catalyst *Q*	$A_{p,2} = \frac{\left(k_{iA2}C_2 + k_{pA2}Y_{0,Q}\right)A}{s}$
1-Octene consumption by catalyst *P*	$B_{p,1} = \frac{\left(k_{iB1}C_1 + k_{pB1}Y_{0,P}\right)B}{s}$
1-octene consumption by catalyst Q	$B_{p,2} = \frac{\left(k_{iB2}C_2 + k_{pB2}Y_{0,Q}\right)B}{s}$

s: reciprocal of the average residence time in the CSTR

6.3 Results and Discussion

Table 6-8 lists the polymerization kinetic rate constants, and Table 6-9 shows the polymerization conditions used in all simulations.

Table 6-8. Polymerization kinetic constants.

Kinetic constants	Units	Catalyst P	Catalyst Q
Propagation rate constant for ethylene, $k_{pA}{}^{i}$	L/(mol.s)	10000	5000
Propagation rate constant for 1-octene, $k_{pB}{}^{i}$	L/(mol.s)	2000	100
Initiation rate constant for ethylene, $k_{iA}{}^{i}$	L/(mol.s)	$k_{pA}{}^{P}$	$k_{pA}{}^{Q}$
Initiation rate constant for 1-octene, $k_{iB}{}^{i}$	L/(mol.s)	$k_{pB}{}^{P}$	$k_{pB}{}^{Q}$
β-hydride elimination rate constant, $k_{t\beta}{}^{i}$	s^{-1}	5	10
Chain transfer to H_2 rate constant, $k_{tH}{}^{i}$	L/(mol.s)	0	0
Deactivation rate constant, $k_{d}{}^{i}$	s^{-1}	0	0
Chain shuttling rate constant to CSA, $k_{CSA0}{}^{i}$	L/(mol.s)	10× $k_{pA}{}^{P}$	10× $k_{pA}{}^{P}$
Chain shuttling rate constant to dormant chain, $k_{CSA}{}^{i}$	L/(mol.s)	10× $k_{pA}{}^{P}$	10× $k_{pA}{}^{P}$

Table 6-9. Polymerization conditions.

Reactants	Units	Values
Total monomers concentration, $[M_{tot}]$	mol/L	2
1-Octene mole fraction, x_B		0.5
Total catalysts concentration, $[C_{tot}]$	mol/L	7.78×10^{-7}
Catalyst *P* mole fraction (make soft block), x_P		0.5
Ratio of CSA concentration to total catalysts, $[CSA]/[C_{tot}]$		1000
Ratio of H_2 concentration to total monomers, $[H_2]/[M_{tot}]$		0
Average residence time, τ	s	600

The total molar flow rate of catalysts and CSA to the CSTR was adjusted so that the total concentration of catalyst and CSA in the CSTR was the same to the equivalent concentrations in the semi-batch reactor. Ethylene and 1-octene concentrations were also kept the same in both reactors. For the comparisons discussed in this chapter, the polymerization time in the semi-batch reactor is equal to the average residence time in the CSTR.

6.3.1 Effect of CSA concentration on the microstructure of OBCs made in CSTRs and semi-batch reactors

Figure 6-1a compares the number fraction (n) of the different OBC populations made in CSTR and a semi-batch reactor under equivalent conditions as a function of the mole fraction of the catalyst that makes the soft blocks (x_P).

As x_P increases, the fractions of OBCs having two or more blocks – (1S,1H), (2S,1H), (1S,2H) and (≥ 2S,2H) – increase until reaching a maximum value, then decrease. As x_p increases, the fraction of chains with a single soft block, (1S), increases, while that of chains with a single hard block, (1H), decreases, as expected. OBC chains with 2 blocks (1S,1H) reach a relatively flat plateau, provided that both catalysts are present in the reactor, but chains with three blocks, (1S,2H) and (2S,1H) achieve maximum fraction when the catalyst that makes two of its blocks is present in higher molar fraction. Finally, multiblock chains with 4 or more blocks, (≥ 2S,2H), are favored when an almost equimolar concentration of the two catalysts is introduced in the reactor. These results agree with our expectations, but nonetheless provide useful information for the design of OBCs with controlled microstructures.

The fraction of chains with 4 or more blocks in the CSTR is lower than that obtained in the semi-batch reactor, while the opposite is observed for chains with fewer blocks, because fresh catalyst (without any blocks) is constantly fed to the CSTR. Note also that the differences are more pronounced for higher $[CSA]/[C_{tot}]$ ratios (Figure 6-1b). As the $[CSA]/[C_{tot}]$ ratio increases, the fraction of chains with 4 or more blocks increases, while the fraction of chains with fewer blocks decreases in both modes of operation due to the increase chain shuttling rate. Tongtummachat et al.[49] reported a similar observation for semi-batch reactors but did not extend their analysis to CSTRs.

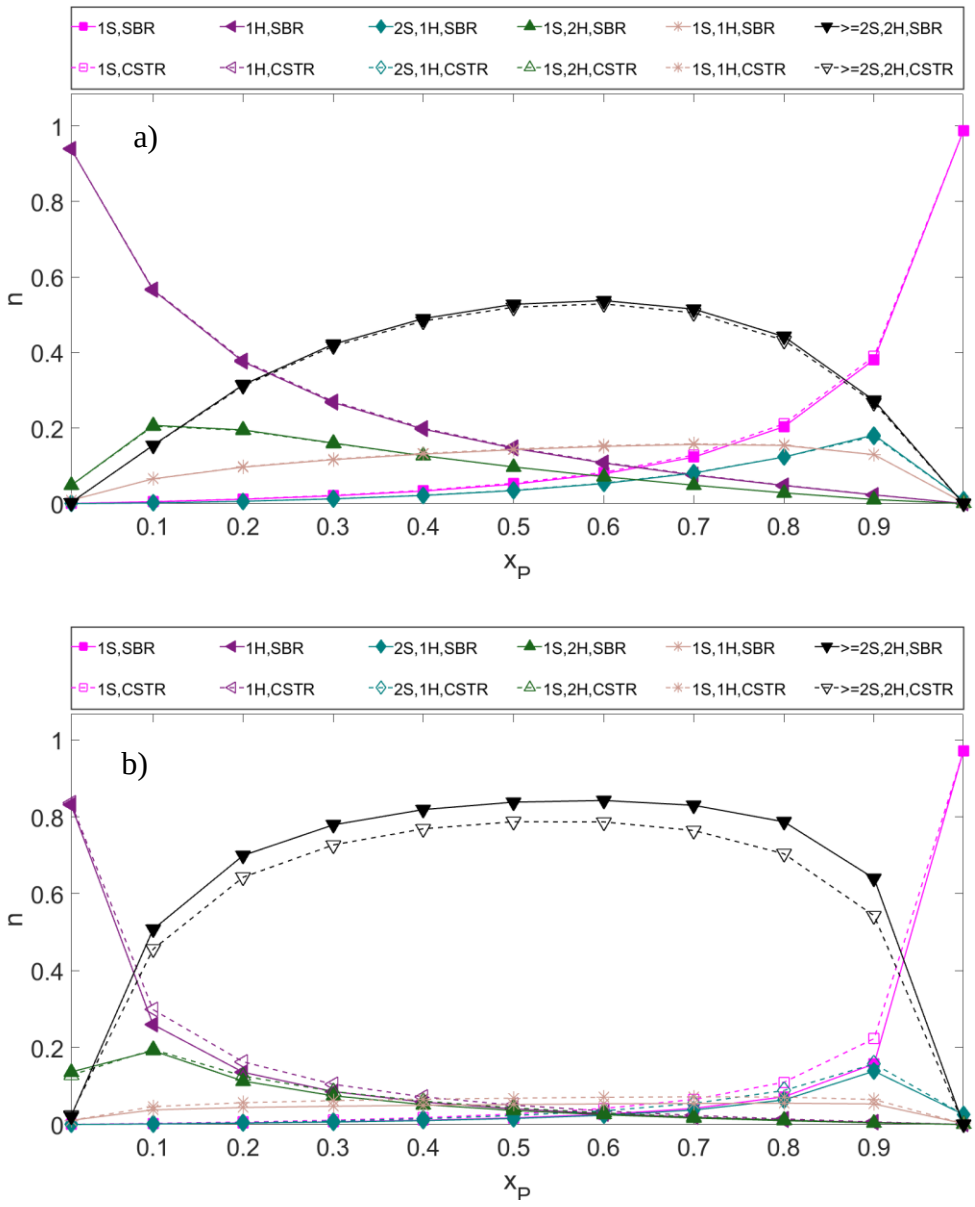

Figure 6-1. Number fractions of different OBC populations: a) $[CSA]/[C_{tot}]$ = 1000 and b) $[CSA]/[C_{tot}]$ = 5000 (Semi-batch reactor: solid lines; CSTR: dashed lines).

Figure 6-2a shows that as x_P increases, the r_n of chains with a single soft block (1S) increases and the r_n for chains with a single hard block (1H) decreases. This simply reflects the fact that when more catalyst *P* is present in the reactor, it is more likely that a dormant chain made in catalyst *P* will shuttle back to another catalyst *P* molecule, further extending its length, than shuttling to catalyst *Q* to form a chain with 2 blocks (1S,1H). A similar rationale explains the variations for seen for the other OBC populations.

Under the investigated simulation conditions, the r_n of OBC populations made in the semi-batch reactor or CSTR are very similar. Chains with 4 of more blocks made in the CSTR have slightly higher r_n than those produced in the semi-batch reactor, but this behavior is reversed for chains with fewer blocks, which can be accounted for by the continuous feed of fresh catalyst to the CSTR.

As the $[CSA]/[C_{tot}]$ ratio increases, the r_n of all OBC populations decreases in both reactors because the chain shuttling agent acts as a reversible chain transfer agent. The difference between the r_n in both reactors becomes more obvious at higher $[CSA]/[C_{tot}]$, as shown in Figure 6-2b compared to Figure 6-2a.

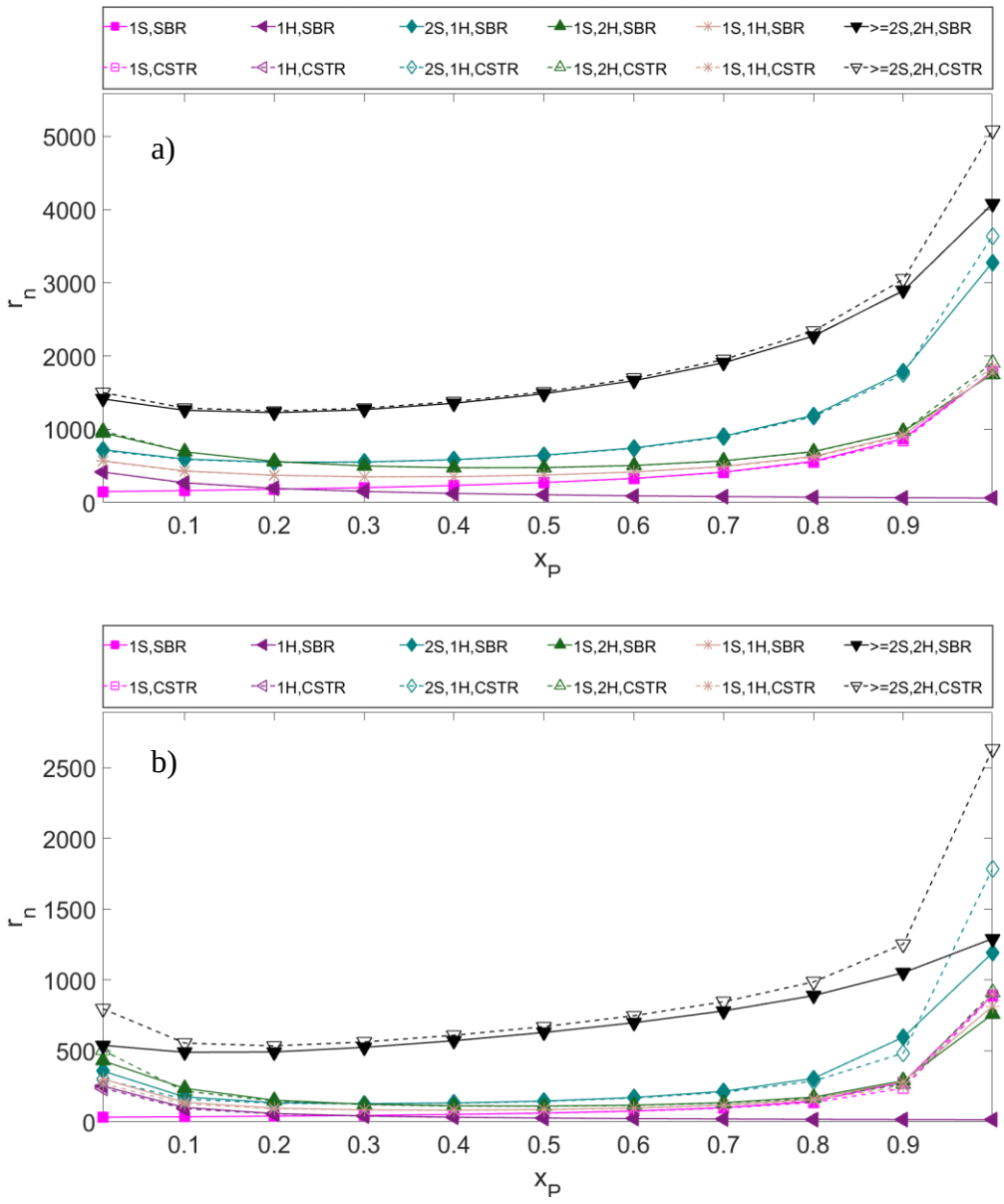

Figure 6-2. Number average chain lengths of different OBC populations: a) $[CSA]/[C_{tot}]$ = 1000 and b) $[CSA]/[C_{tot}]$ = 5000 (Semi-batch reactor: solid lines; CSTR: dashed lines).

Figure 6-3a shows that as x_P increases, the r_n of the whole polymer also increases because the propagation to chain transfer ratio for catalyst *P* is higher than that for catalyst *Q*. The r_n of the whole polymer made in the CSTR have slightly higher r_n than those produced in the semi-batch reactor. This is because the fraction of chains with fewer blocks made in the CSTR is higher than that made in the semi-batch reactor, while the fraction of chains with 4 of more blocks made in the CSTR is lower than that produced in the semi-batch reactor. These two effects cancel each other out, making the r_n of the whole polymer made in both reactors the same.

Even though the r_n for the whole polymer made on both reactor is almost the same, the r_w for the whole OBC is not the same, since OBCs made in a CSTR will have PDI equal to 2.0 due to the exponential residence time distribution of a CSTR as shown in Figure 6-3b.

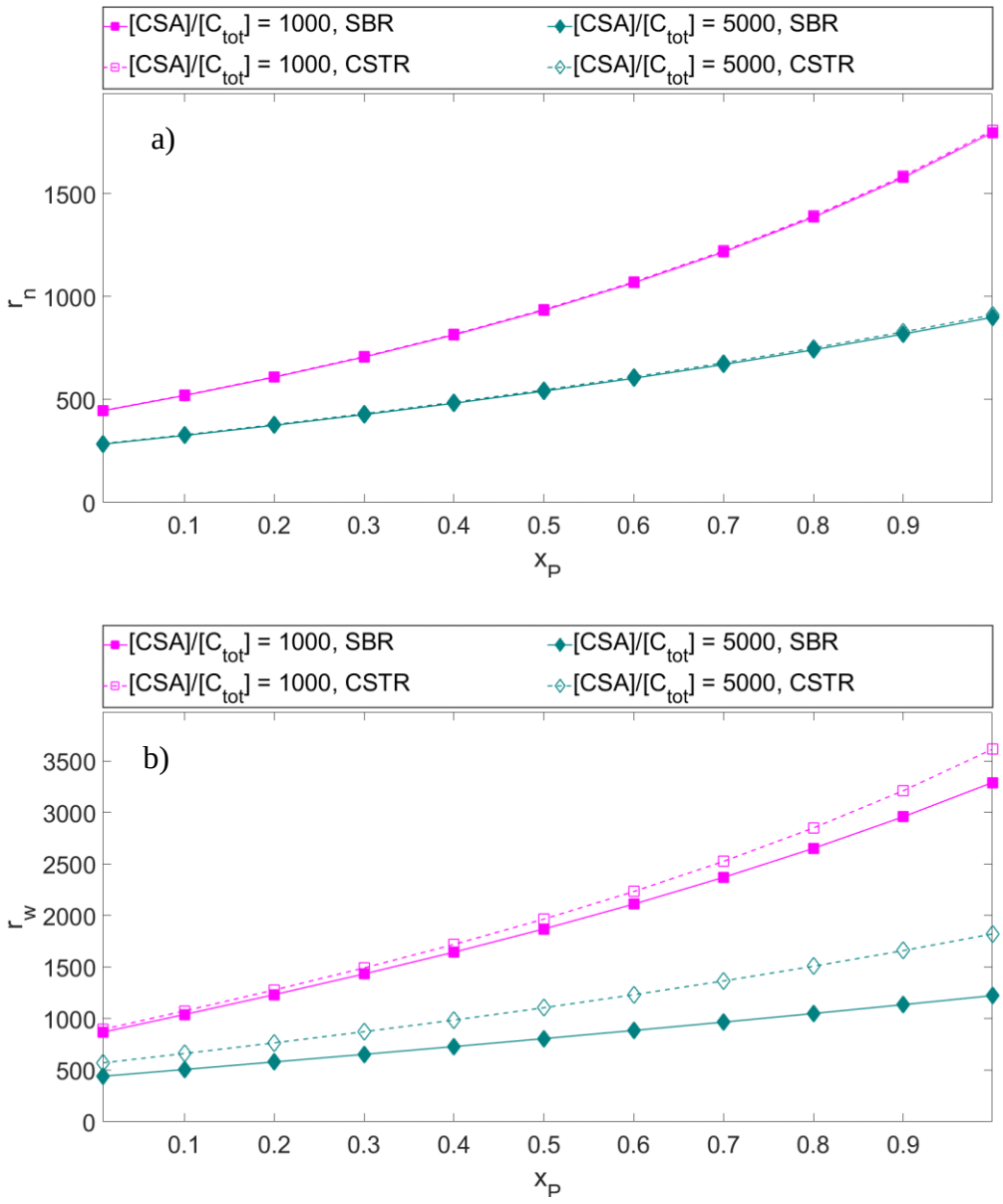

Figure 6-3. Effect of $[CSA]/[C_{tot}]$ ratio on the whole polymer: a) r_n and b) r_w (Semi-batch reactor: solid lines; CSTR: dashed lines).

6.3.2 Effect of chain shuttling rate constant on the microstructure of OBCs made in CSTRs and semi-batch reactors

Figure 6-4a to Figure 6-4f compare the effect of the k_{CSA}/k_{pA}^{P} ratio on the number fraction of different OBC populations made in a CSTR and a semi-batch reactor. As k_{CSA}/k_{pA}^{P} increases (keeping k_{pA}^{P} the same), the fraction of OBCs with 4 or more blocks increases, while the fractions of OBCs with fewer blocks decrease due to higher chain shuttling frequency. The difference between the fractions in both reactor becomes smaller by increasing the k_{CSA}/k_{pA}^{P} ratio.

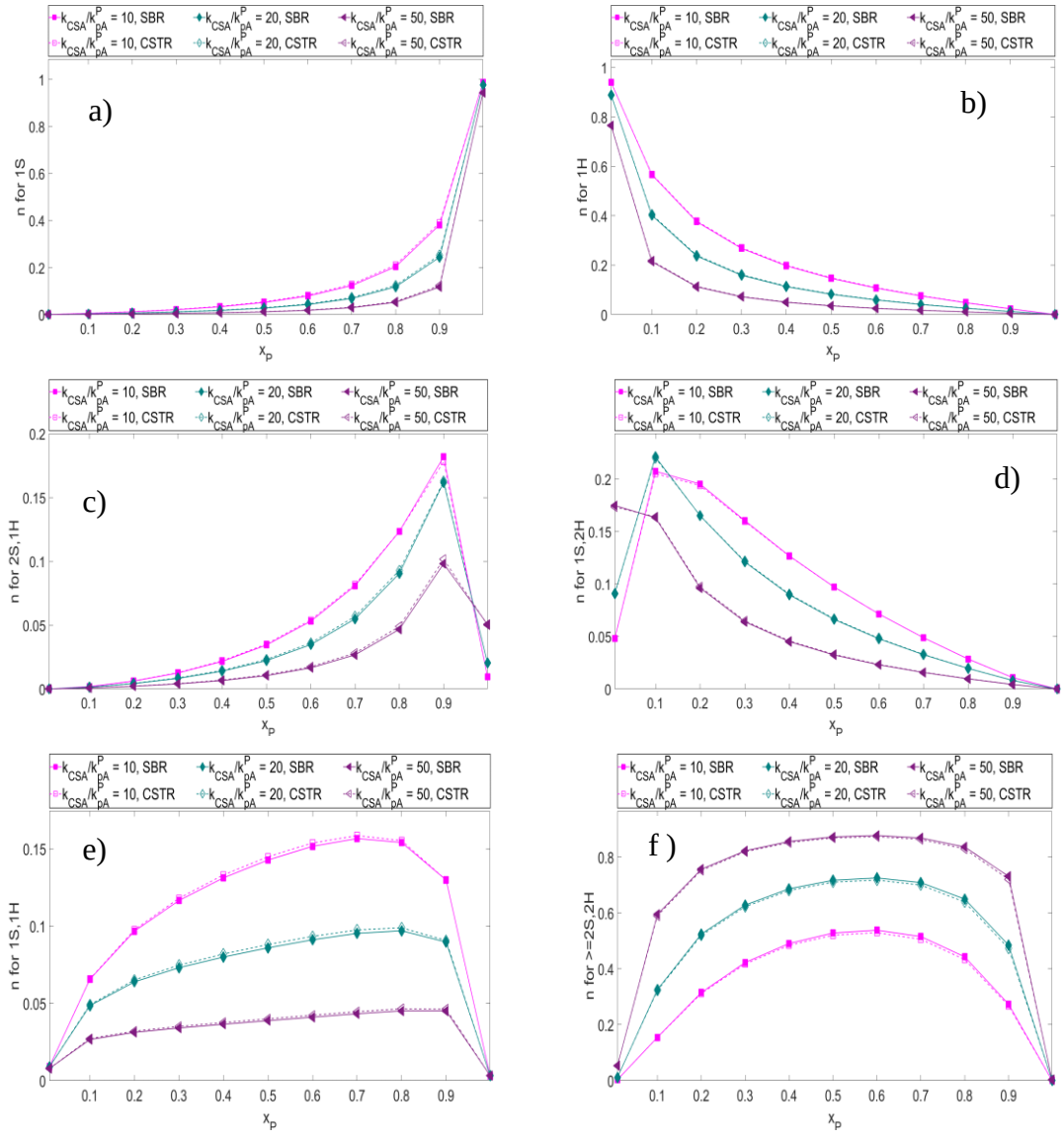

Figure 6-4. Effect of the k_{CSA}/k_{pA}^{P} ratio on the fraction of different OBC populations (Semi-batch reactor: solid lines; CSTR: dashed lines).

Although the increase of the k_{CSA}/k_{pA}^{P} ratio does not affect the r_n of the whole polymer (Figure 6-5), it affects the r_n of the OBC populations (Figure 6-6a through Figure 6-6f). As the k_{CSA}/k_{pA}^{P} ratio increases, the r_n for OBC populations decreases in both reactors, since higher k_{CSA} values increases the frequency of exchange between living and dormant polymer chains. Thus, the higher the k_{CSA}, the faster the exchange between the two polymer chains (i.e., living and dormant) and the lower the average chain length for OBC populations while the whole polymer is not affected. Tongtummachat et al.[49] reported a similar observation for semi-batch reactors but did not extend their analysis to CSTRs. They found that for the same chain shuttling concentration, changing the value of k_{CSA}/k_p has a minor effect on the number average molecular weight (M_n) at very short polymerization times, with higher k_{CSA}/k_p leading to a slower M_n increase, but with a longer polymerization time, all M_n curves converge to the same value because the chain transfer becomes dominant. The same behavior was observed for ethylene chain shuttling polymerization as discussed in Chapter 3. The difference between the r_n in both reactors becomes small at higher k_{CSA}/k_{pA}^{P} ratio.

The difference between the polymer populations made in both reactors becomes large at high CSA concentration and small at high chain shuttling rate constant (k_{CSA}). This can be explained by the effect that CSA works as chain transfer and chain shuttling agent in the same time in both reactors while the fresh CSA is fed to CSTR continuously.

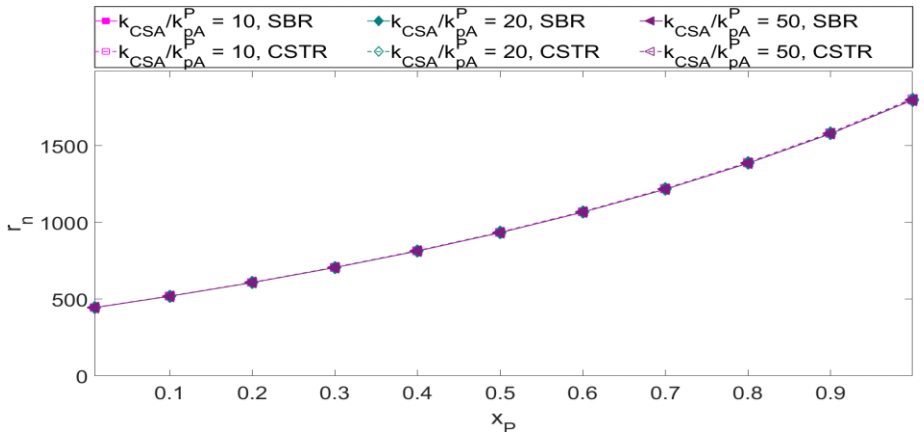

Figure 6-5. Effect of the k_{CSA}/k_{pA}^{P} ratio on the r_n of the whole polymer (Semi-batch reactor: solid lines; CSTR: dashed lines).

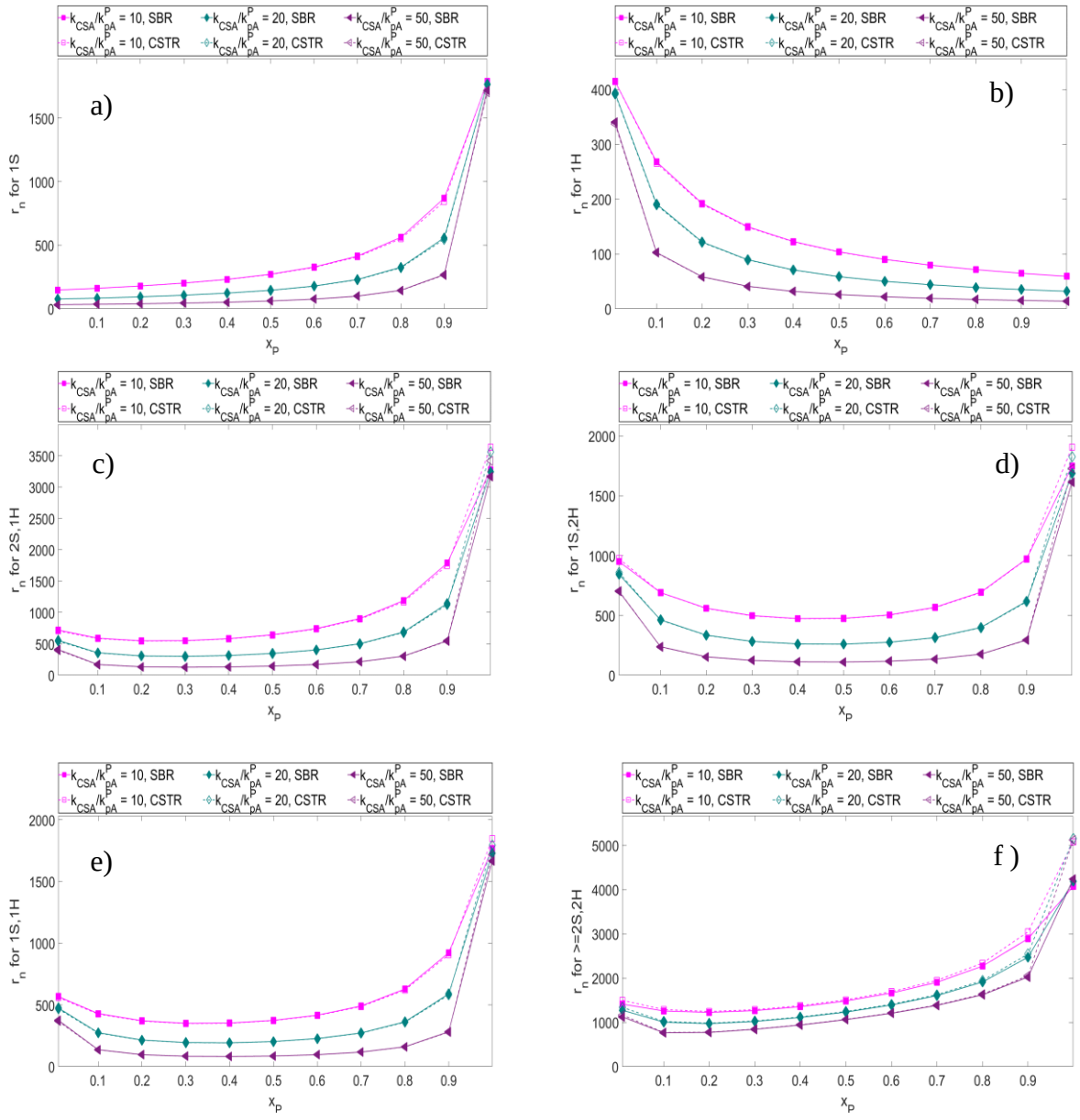

Figure 6-6. Effect of the $k_{CSA}/k_{pA}{}^{P}$ ratio on the r_n of different OBC populations (Semi-batch reactor: solid lines; CSTR: dashed lines).

6.3.3 Effect of reactor average residence time on the microstructure of OBCs made in CSTRs and in semi-batch reactors

Figure 6-7a to Figure 6-7f compare the effect of the average residence time (τ) on the number fraction of different OBC populations made in a CSTR and in a semi-batch reactor. The plot for the fraction of chains with single soft blocks (1S) is a mirror image of the plot for the fraction of chains with single hard blocks (1H); the same behavior is seen for the two tri-blocks OBCs, (2S,1H) and (1S,2H). The fraction of chains with two blocks (1S,1H) and 4 or more blocks ($\geq$ 2S,2H) passes through a maximum value as x_P varies from 0 to 1.0.

It is important to highlight a few trends. As the reactor average residence time (or polymerization time) increases: 1) the fraction of chains with a single block decrease, 2) those with 2 and 3 blocks initially increase, pass through a maximum, then decrease, and 3) those with 4 or more blocks increase continuously. This is consistent with the increased number of chain shuttling events that take place when the polymerization time increases. Finally, OBCs made in semi-batch reactors at all times will have a higher fraction of multiblock chains, as already observed above for other simulations.

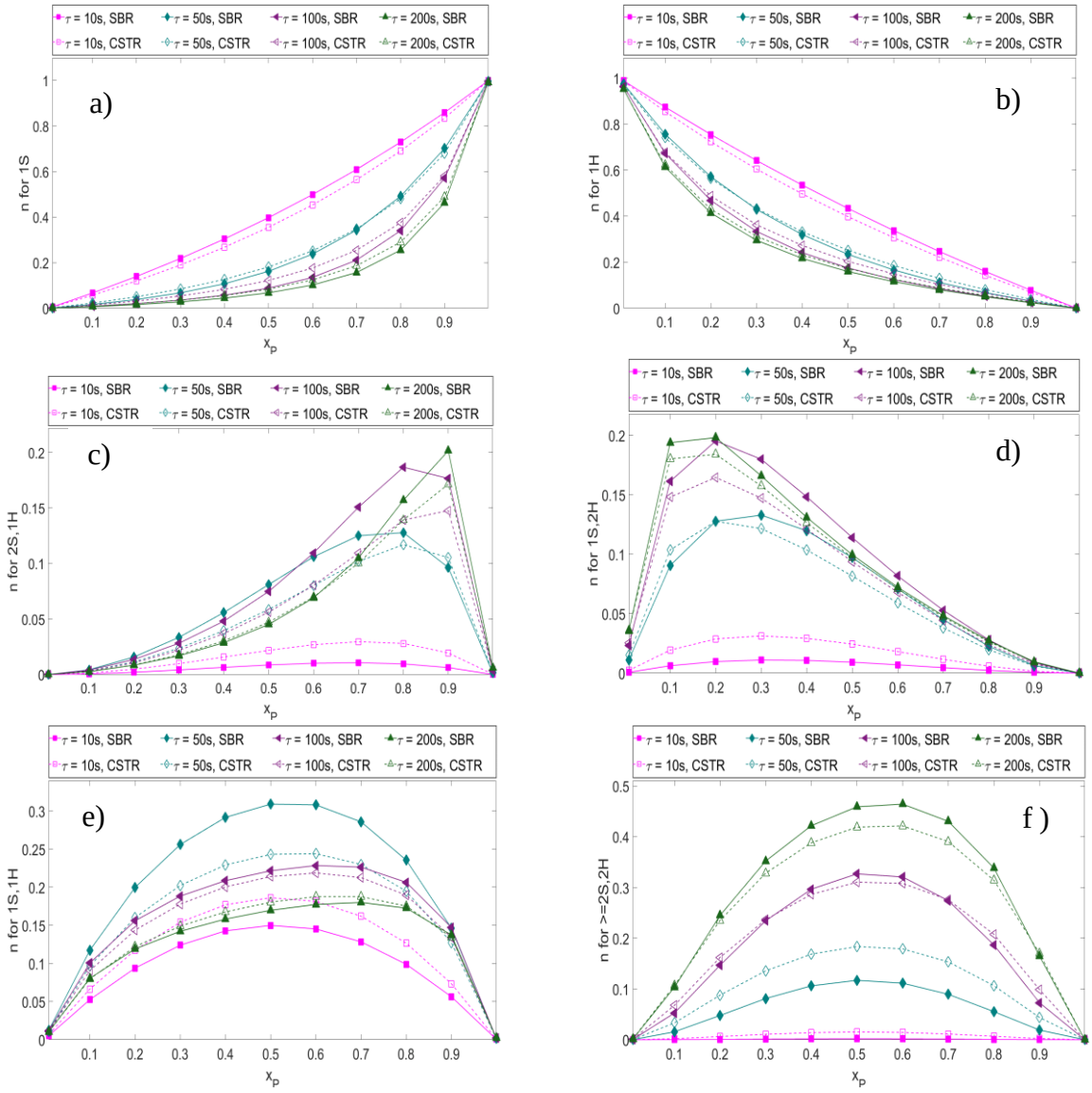

Figure 6-7. Effect of average residence time on the fraction of different OBC populations (Semi-batch reactor: solid lines; CSTR: dashed lines).

Figure 6-8 and Figure 6-9 (a to f) compare the effect of the average residence time (τ) on the r_n of the whole polymer and OBC populations, respectively. The values of r_n for the whole OBC increase with τ, since longer polymerization times allow for more extensive chain shuttling, and consequently make longer OBC chains. (Figure 6-8). OBCs made in the CSTR have slightly higher r_n since dormant chains are always present in the CSTR, allowing the fresh catalysts to start shuttling with them as soon as they enter the reactor. In a semi-batch reactor, on the other hand, at time $t = 0$ there are no dormant chains, only fresh catalysts, and it takes a certain length time until the dormant chains of different lengths are formed and accumulate in the reactor.

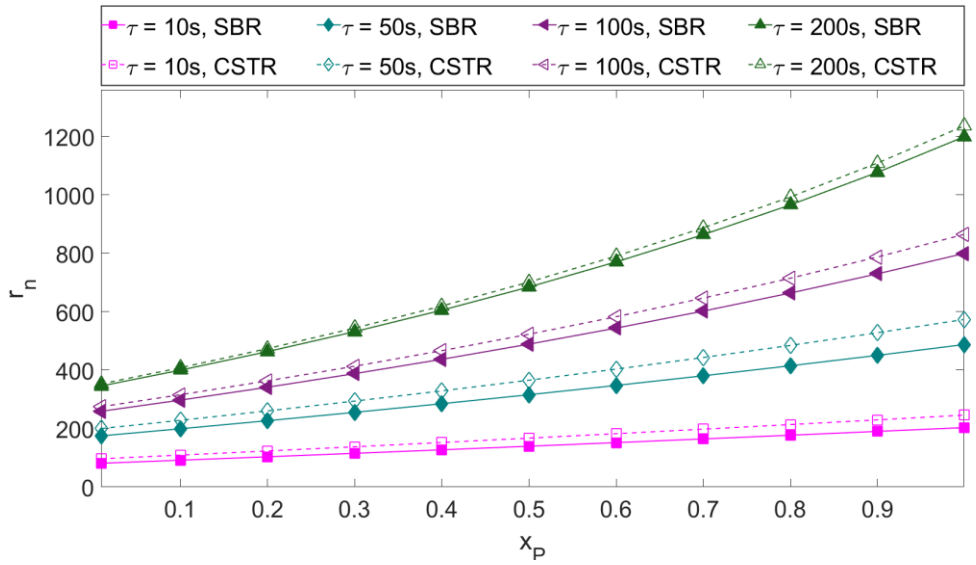

Figure 6-8. Effect of average residence time on the r_n of whole polymer (Semi-batch reactor: solid lines; CSTR: dashed lines).

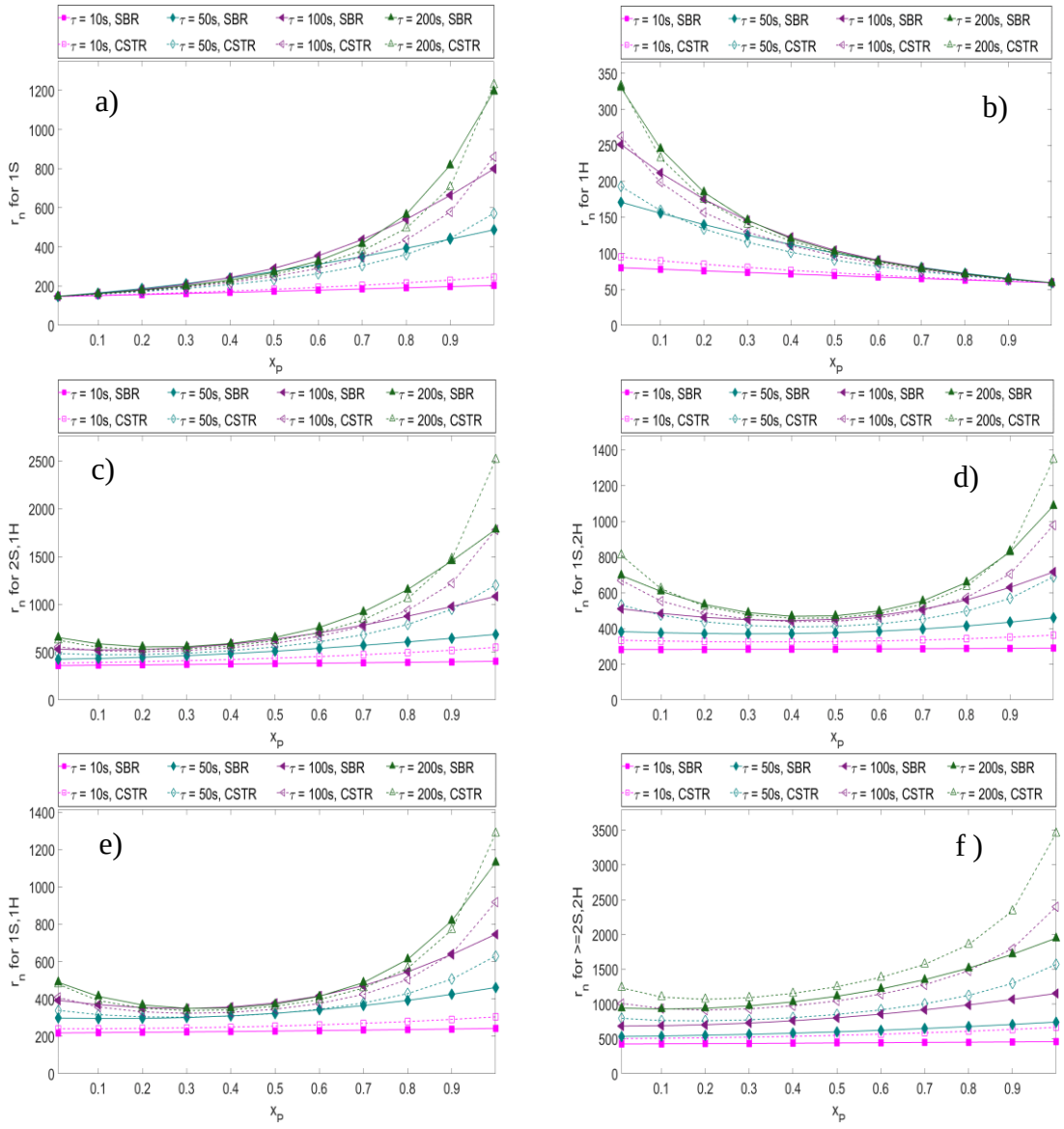

Figure 6-9. Effect of average residence time on the r_n of different OBC populations (Semi-batch reactor: solid lines; CSTR: dashed lines).

6.3.4 Effect of reactor mode of operation on the average number of blocks per chain

Figure 6-10 illustrates how the average number of blocks per chain passes through a maximum value as x_P varies from 0 to 1.0, as expected since to form blocks both catalysts must be present in the reactor (the average number of blocks per chain = 1 at $x_P = 0$ or $x_P = 1.0$). The average number of blocks per chain made in the CSTR is lower than that obtained in the semi-batch reactor also because fresh catalysts (no blocks) are fed continuously to the CSTR. This finding is important for polymer properties because it shows that, even though n and r_n for the chain populations does not differ much for polymers made in semi-batch reactors and CSTRs (Figure 6-1 and Figure 6-2), the average number of blocks of these materials may be substantially different, as will be their final properties.

As the $[CSA]/[C_{tot}]$ ratio increases, the average number of blocks per chain increases in both reactors due to the increase in the chain shuttling rate (Figure 6-10a). We observe the same behavior if the $k_{CSA}/k_{pA}{}^P$ increases at constant $k_{pA}{}^P$ (Figure 6-10b) and if τ increases (Figure 6-10c).

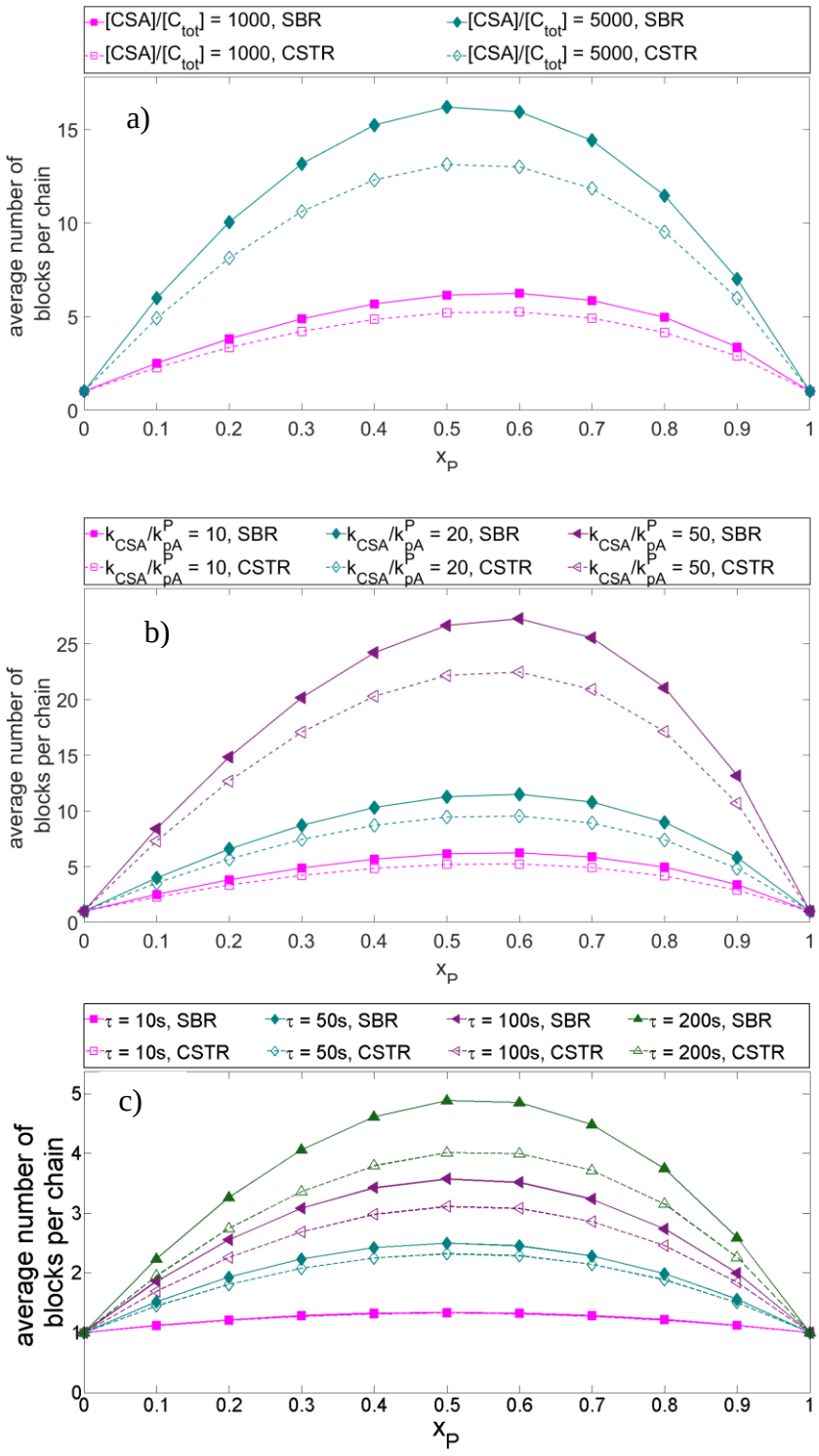

Figure 6-10. Average number of blocks per chain: effect of a) $[CSA]/[C_{tot}]$, b) $k_{CSA}/k_{pA}{}^{P}$ and c) τ (Semi-batch reactor: solid lines; CSTR: dashed lines).

6.4 Conclusion

We carried out a comprehensive comparison of chain shuttling copolymerization in a CSTR operated at a steady state and in a semi-batch reactor. We investigated the effect of CSA concentration, chain shuttling rate constant and average residence time as a function of the mole fraction of the catalyst that makes soft blocks.

Reactor type influences the average number of blocks per chain, fraction of OBC populations, and average chain length of the different OBC populations. The average number of blocks per chain made in the CSTR is lower than that made in the semi-batch reactor. The fraction of chains with multi-blocks made in the CSTR is lower than that produced in the semi-batch reactor, while the reverse is observed for chain with fewer blocks.

The effect of reactor type on the number average chain length of OBC populations is opposite to its effect on the fractions. Interestingly, the reactor type has no effect on the number average chain length of the whole polymer at higher average residence time. The difference between the polymer populations made in both reactor becomes large at high CSA concentration and at low chain shuttling rate constant.

7. Main Contributions and Recommendations for Future Work

7.1 Contributions

The following points summarize the major contributions of this thesis:

1. Development of a mathematical model for chain shuttling polymerization in a semi-batch reactor using the method of moments covering the properties of chains having 1, 2, 3 and 4 or more blocks as a function of time.
2. Development of a mathematical model for chain shuttling polymerization in dynamic and steady-state CSTR using the method of moments describing the properties of chains having 1, 2, 3, and 4 or more blocks.
3. Development of a dynamic Monte Carlo simulation model for chain shuttling polymerization in a semi-batch reactor covering the properties of chains having 1, 2, 3 and 4 or more blocks as a function of time.
4. Use of these models to quantify how different polymerization conditions and reactor operation modes affected the microstructure of olefin block copolymers.

7.2 Recommendations for future work

Based on the extensive simulation work performed in this thesis, the following additional modelling work is recommended to further increase the understanding of olefin block copolyemrs:

1. Extend the proposed polymerization models from Bernoullian to Terminal model.
2. Verify whether the pseudo-kinetic model applies to chain shuttling polymerization, which would make the development of Terminal models much easier to implement.
3. Perform polymerization experiments, including the experimental determination of chain shuttling constants, to test the proposed model.
4. Look for a possible analytical solution to describe the microstructure of olefin block copolymers made instantaneously in any reactor type.
5. Find analytical methods to characterize the detailed microstructure of olefin block copolymers. These methods are essential for model validation and to establish property-structure relationships for these materials.

References

1. Soares, J. B. P., and McKenna, T. F. L. *Polyolefin Reaction Engineering*. *Wiley-VCH Verlag & Co. KGaA* (2012).

2. Mayo, F. R. & Walling, C. Copolymerization. *Chem. Rev.* **46,** 191–287 (1950).

3. Zhu, S. & Hamielec, A. *Polymerization Kinetic Modeling and Macromolecular Reaction Engineering*. *Polymer Science: A Comprehensive Reference, 10 Volume Set* **4,** (Elsevier B.V., 2012).

4. Tian, J., Hustad, P. D. & Coates, G. W. A New Catalyst for Highly Syndiospecific Living Olefin Polymerization: Homopolymers and Block Copolymers from Ethylene and Propylene. *J. Am. Chem. Soc.* **123,** 5134–5135 (2001).

5. Al-harthi, M. Mathematical Modeling of Atom Transfer Radical Polymerization. (2006).

6. Mishra, V. & Kumar, R. Living Radical Polymerization: a Review. *J. Sci. Res.* **56,** 141–176 (2012).

7. Arriola, D. J., Carnahan, E. M., Hustad, P. D., Kuhlman, R. L. & Wenzel, T. T. Catalytic production of olefin block copolymers via chain shuttling polymerization. *Science* **312,** 714–719 (2006).

8. Wenzel, T. T., Arriola, D. J., Carnahan, E. M., Hustad, P. D. & Kuhlman, R. L. in *Metal Catalysts in Olefin Polymerization* **3,** 699–737 (Elsevier, 2008).

9. Shamiri, A. *et al.* The influence of Ziegler-Natta and metallocene catalysts on polyolefin structure, properties, and processing ability. *Materials (Basel).* **7,** 5069–5108 (2014).

10. Kaminsky, W. Discovery of Methylaluminoxane as Cocatalyst for Olefin Polymerization. *Macromolecules* **45,** 3289–3297 (2012).

11. Hustad, P. D., Kuhlman, R. L., Arriola, D. J., Carnahan, E. M. & Wenzel, T. T. Continuous Production of Ethylene-Based Diblock Copolymers Using Coordinative Chain

Transfer Polymerization. *Macromolecules* **40,** 7061–7064 (2007).

12. Zintl, M. & Rieger, B. Novel olefin block copolymers through chain-shuttling polymerization. *Angew. Chemie - Int. Ed.* **46,** 333–335 (2007).

13. Kuhlman, R. L. & Wenzel, T. T. Investigations of chain shuttling olefin polymerization using deuterium labeling. *Macromolecules* **41,** 4090–4094 (2008).

14. Mehdiabadi, S., Soares, J. B. P. & Dekmezian, A. H. Simulation of polymerization and long chain branch formation in a semi-batch reactor using two single-site catalysts. *Macromol. React. Eng.* **2,** 37–57 (2008).

15. Li, S. *Structure and Properties of Novel Homopolymers and Block Copolymers Synthesized by Ring-Opening Metathesis Polymerization or Chain Shuttling Polymerization*. (2013).

16. Dung, B. T. New segmented block copolymers based on hard and soft segments using selectively reacting bifunctional coupling agents. (2007).

17. Santos, L. S. What do we know about reaction mechanism? The electrospray ionization mass spectrometry approach. *J. Braz. Chem. Soc.* **22,** 1827–1840 (2011).

18. Zhang, M., Karjala, T. W. & Jain, P. Modeling of α-olefin copolymerization with chain-shuttling chemistry using dual catalysts in stirred-tank reactors: Molecular weight distributions and copolymer composition. *Ind. Eng. Chem. Res.* **49,** 8135–8146 (2010).

19. Kaminsky, W. Trends in polyolefin chemistry. *Macromol. Chem. Phys.* **209,** 459–466 (2008).

20. Malpass, D. B. *Introduction to Polymers of Ethylene 1.1*. **1933,** (2010).

21. Wang, W. Effect of Diethylzinc on the Activity of Ethylene Polymerization by Metallocene Catalyst. *Macromol. React. Eng.* **9,** 333–338 (2015).

22. Makio, H., Kashiwa, N. & Fujita, T. FI Catalysts:A New Family of High Performance Catalysts for Olefin Polymerization. *Adv. Synth. Catal.* **344,** 477–493 (2002).

23. Tian, J. & Coates, G. W. Development of a diversity-based approach for the discovery of stereoselective polymerization catalysts: Identification of a catalyst for the synthesis of syndiotactic polypropylene. *Angew. Chemie - Int. Ed.* **39,** 3626–3629 (2000).

24. Takeuchi, D. Recent progress in olefinpolymerization catalyzed by transition metal complexes: new catalysts and new reactions. *Dalt. Trans.* **39,** 311–328 (2010).

25. Froese, R. D. J., Hustad, P. D., Kuhlman, R. L. & Wenzel, T. T. Mechanism of activation of a hafnium pyridyl-amide olefin polymerization catalyst: Ligand modification by monomer. *J. Am. Chem. Soc.* **129,** 7831–7840 (2007).

26. Martins, R., Quinello, L., Souza, G. & Marques, M. Polymerization of ethylene with catalyst mixture in the presence of chain shuttling agent. *Chem. Chem. Technol.* **6,** 153–162 (2012).

27. Xiao, A. *et al.* A novel linear-hyperbranched multiblock polyethylene produced from ethylene monomer alone via chain walking and chain shuttling polymerization. *Macromolecules* **42,** 1834–1837 (2009).

28. Van Meurs, M., Britovsek, G. J. P., Gibson, V. C. & Cohen, S. a. Polyethylene chain growth on zinc catalyzed by olefin polymerization catalysts: A comparative investigation of highly active catalyst systems across the transition series. *J. Am. Chem. Soc.* **127,** 9913–9923 (2005).

29. Xiao, A., Wang, L., Liu, Q. & Ding, J. Propylene Polymerization Catalyzed by rac-$Et(Ind)_2ZrCl_2$/Cp_2ZrCl_2 in the Presence of $ZnEt_2$. *Des. Monomers Polym.* **12,** 425–431 (2009).

30. Chien, J. C. W., Iwamoto, Y. & Rausch, M. D. Homogeneous binary zirconocenium catalysts for propylene polymerization. II. Mixtures of isospecific and syndiospecific zirconocene systems. *J. Polym. Sci. Part A Polym. Chem.* **37,** 2439–2445 (1999).

31. Chien, J. C. W., Iwamoto, Y., Rausch, M. D., Wedler, W. & Winter, H. H. Homogeneous Binary Zirconocenium Catalyst Systems for Propylene Polymerization. 1. Isotactic/Atactic Interfacial Compatibilized Polymers Having Thermoplastic Elastomeric Properties ⊥.

Macromolecules **30,** 3447–3458 (1997).

32. Przybyla, C. & Fink, G. Two different, on the same silica supported metallocene catalysts, activated by various trialkylaluminums – a kinetic and morphological study as well as an experimental investigation for building stereoblock polymers. *Acta Polym*. **50,** 77–83 (1999).

33. Lieber, S. & Brintzinger, H. H. Propene polymerization with catalyst mixtures containing different ansa-zirconocenes: chain transfer to alkylaluminum cocatalysts and formation of stereoblock polymers. *Macromolecules* **33,** 9192–9199 (2000).

34. Tynys, A., Eilertsen, J. L., Seppälä, J. V. & Rytter, E. Propylene polymerizations with a binary metallocene system—Chain shuttling caused by trimethylaluminium between active catalyst centers. *J. Polym. Sci. Part A Polym. Chem.* **45,** 1364–1376 (2007).

35. Pan, L., Zhang, K., Nishiura, M. & Hou, Z. Chain-shuttling polymerization at two different scandium sites: Regio- and stereospecific 'one-pot' block copolymerization of styrene, isoprene, and butadiene. *Angew. Chemie - Int. Ed.* **50,** 12012–12015 (2011).

36. Valente, A., Mortreux, A., Visseaux, M. & Zinck, P. Coordinative Chain Transfer Polymerization. *Chem. Rev*. **113,** 3836–3857 (2013).

37. Anantawaraskul, S., Somnukguande, P. & Soares, J. B. P. Monte Carlo Simulation of the Microstructure of Linear Olefin Block Copolymers. *Macromol. Symp.* **312,** 167–173 (2012).

38. Shan, C. L. P. & Hazlitt, L. G. Block index for characterizing olefin block copolymers. *Macromol. Symp.* **257,** 80–93 (2007).

39. Anantawaraskul, S., Somnukguande, P. & Soares, J. B. P. Simulation of crystallization analysis fractionation (Crystaf) of linear olefin block copolymers. *Macromol. Symp.* **282,** 205–215 (2009).

40. Anantawaraskul, S., Sottesakul, S., Siriwongsarn, E. & Soares, J. B. P. Chemical composition distribution and temperature rising elution fractionation of linear olefin block copolymers. *Macromol. Symp.* **330,** 123–131 (2013).

41. Brandão, A. L. T., Soares, J. B. P., Pinto, J. C. & Alberton, A. L. When Polymer Reaction Engineers Play Dice: Applications of Monte Carlo Models in PRE. *Macromol. React. Eng.* **9,** 141–185 (2015).

42. Hustad, P. D., Kuhlman, R. E., Carnahan, E. M., Wenzel, T. T. & Arriola, D. J. An exploration of the effects of reversibility in chain transfer to metal in olefin polymerization. *Macromolecules* **41,** 4081–4089 (2008).

43. Zhang, M., Carnahan, E. M., Karjala, T. W. & Jain, P. Theoretical analysis of the copolymer composition equation in chain shuttling copolymerization. *Macromolecules* **42,** 8013–8016 (2009).

44. Zhang, M., Karjala, T. W., Jain, P. & Villa, C. Theoretical Modeling of Average Block Structure in Chain-Shuttling α–Olefin Copolymerization Using Dual Catalysts. *Macromolecules* **46,** 4847–4853 (2013).

45. Ahmadi, M. & Nasresfahani, A. Realistic Representation of Kinetics and Microstructure Development During Chain Shuttling Polymerization of Olefin Block Copolymers. *Macromol. Theory Simulations* **24,** 311–321 (2015).

46. Mohammadi, Y. *et al.* A detailed model on kinetics and microstructure evolution during copolymerization of ethylene and 1-octene: From coordinative chain transfer to chain shuttling polymerization. *Macromolecules* **47,** 4778–4789 (2014).

47. Saeb, M. R., Khorasani, M. M., Ahmadi, M., Mohammadi, Y. & Stadler, F. J. A unified picture of hard-soft segmental development along olefin chain shuttling copolymerization. *Polym. (United Kingdom)* **76,** 245–253 (2015).

48. Ahmadi, M., Saeb, M. R., Mohammadi, Y., Khorasani, M. M. & Stadler, F. J. A Perspective on Modeling and Characterization of Transformations in the Blocky Nature of Olefin Block Copolymers. *Ind. Eng. Chem. Res.* **54,** 8867–8873 (2015).

49. Tongtummachat, T., Anantawaraskul, S. & Soares, J. B. P. Understanding the Formation of Linear Olefin Block Copolymers with Dynamic Monte Carlo Simulation. *Macromol. React. Eng.* 1–16 (2016). doi:10.1002/mren.201600002

50. Ray, W. H. On the Mathematical Modeling of Polymerization Reactors. *J. Macromol. Sci. Part C* **8,** 1–56 (1972).

51. Shampine, L. F. & Reichelt, M. W. The MATLAB ODE Suite. *SIAM J. Sci. Comput*. **18,** 1–22 (1997).

52. Gillespie, D. T. Exact stochastic simulation of coupled chemical reactions. *J. Phys. Chem*. **81,** 2340–2361 (1977).

53. Soares, J. B. P. & Hamielec, A. E. Chain length distributions of polyolefins made in stopped-flow reactors for non-instantaneous site activation. *Macromol. React. Eng.* **2,** 115–125 (2008).

54. Flory, P. J. Role of Crystallization in Polymers and Proteins. *Science* **124,** 53–60 (1956).

55. Wang, H. P. *et al.* Characterization of some new olefinic block copolymers. *Macromolecules* **40,** 2852–2862 (2007).

Appendices

Appendix 3-A

Population Balance for M

$$\frac{d[M]}{dt} = -k_i[C][M] - k_p \sum_{r=1}^{\infty}[P_r][M] \tag{1}$$

Now substituting $Y_0 = \sum_{r=1}^{\infty}[P_r]$ into Equation (1):

$$\frac{d[M]}{dt} = -k_i[C][M] - k_p Y_0[M] \tag{2}$$

Population Balance for *C*

$$\frac{d[C]}{dt} = -k_i[C][M] - k_d[C] + (k_{t\beta} + k_{tH}[H_2]) \sum_{r=1}^{\infty}[P_r] + k_{CSA0} \sum_{r=1}^{\infty}[P_r][S_0] \tag{3}$$

Simplified Equation (3):

$$\frac{d[C]}{dt} = -(k_i[M] + k_d)[C] + (k_{t\beta} + k_{tH}[H_2] + k_{CSA0}[S_0])Y_0 \tag{4}$$

Population Balance for S_0

$$\frac{d[S_0]}{dt} = -k_{CSA0} \sum_{r=1}^{\infty}[P_r][S_0] \tag{5}$$

Simplified Equation (5):

$$\frac{d[S_0]}{dt} = -k_{CSA0} Y_0[S_0] \tag{6}$$

Population Balance for P_1 ($r = 1$)

$$\frac{d[P_1]}{dt} = k_i[C][M] - k_p[P_1][M] - k_{t\beta}[P_1] - k_{tH}[H_2][P_1] - k_d[P_1] - k_{CSA0}[P_1][S_0] - k_{CSA}[P_1] \sum_{\substack{s=1 \\ s \neq r}}^{\infty}[S_0 D_s] + k_{CSA} \sum_{\substack{s=1 \\ s \neq r}}^{\infty}[P_s][S_0 D_1] \tag{7}$$

Now substituting $[SX_0] \cong \sum_{\substack{s=1 \\ s\neq r}}^{\infty}[SP_s]$ and $Y_0 \cong \sum_{\substack{s=1 \\ s\neq r}}^{\infty}[P_s]$ into Equation (7):

$$\frac{d[P_1]}{dt} = k_i[C][M] - k_p[P_1][M] - (k_{t\beta} + k_{tH}[H_2] + k_d + k_{CSA0}[S_0] + k_{CSA}[SX_0])[P_1] + k_{CSA}Y_0[SP_1] \quad (8)$$

Population Balance for P_r where $(r \geq 2)$:

$$\frac{d[P_r]}{dt} = k_p[P_{r-1}][M] - k_p[P_r][M] - k_{t\beta}[P_r] - k_{tH}[H_2][P_r] - k_d[P_r] - k_{CSA0}[P_r][S_0] + k_{CSA}\sum_{\substack{s=1 \\ s\neq r}}^{\infty}[P_s][SP_r] - k_{CSA}\sum_{\substack{s=1 \\ s\neq r}}^{\infty}[SP_s][P_r] \quad (9)$$

Simplified Equation (9):

$$\frac{d[P_r]}{dt} = k_p[M]([P_{r-1}] - [P_r]) - (k_{t\beta} + k_{tH}[H_2] + k_d + k_{CSA0}[S_0] + k_{CSA}[SX_0])[P_r] + k_{CSA}Y_0[SP_r] \quad (10)$$

Population Balance for D_r where $(r \geq 2)$:

$$\frac{d[D_r]}{dt} = (k_{t\beta} + k_{tH}[H_2])[P_r] + k_d[P_r] = (k_{t\beta} + k_{tH}[H_2] + k_d)[P_r] \quad (11)$$

Population Balance for SP_r where $(r \geq 2)$:

$$\frac{d[SP_r]}{dt} = k_{CSA0}[S_0][P_r] + k_{CSA}\sum_{\substack{s=1 \\ s\neq r}}^{\infty}[SP_s][P_r] - k_{CSA}\sum_{\substack{s=1 \\ s\neq r}}^{\infty}[P_s][SP_r] \quad (12)$$

Simplified Equation (12):

$$\frac{d[SP_r]}{dt} = k_{CSA0}[S_0][P_r] + k_{CSA}[SX_0][P_r] - k_{CSA}Y_0[SP_r] \quad (13)$$

The 0th moment of living polymer chain,

$$Y_0 = \sum_{r=1}^{\infty}[P_r] = [P_1] + \sum_{r=2}^{\infty}[P_r] \quad (14)$$

Taking the first derivative of Equation (14):

$$\frac{dY_0}{dt} = \frac{dP_1}{dt} + \sum_{r=2}^{\infty} \frac{d[P_r]}{dt} \tag{15}$$

Now substituting Equations (8) and (10) into Equation (15):

$$\frac{dY_0}{dt} = k_i[C][M] - k_p[P_1][M] - (k_{t\beta} + k_{tH}[H_2] + k_d + k_{CSA0}[S_0] + k_{CSA}[SX_0])[P_1] + k_{CSA}Y_0[SP_1] + k_p[M](\sum_{r=2}^{\infty}[P_{r-1}] - \sum_{r=2}^{\infty}[P_r]) - (k_{t\beta} + k_{tH}[H_2] + k_d + k_{CSA0}[S_0] + k_{CSA}[SX_0])\sum_{r=2}^{\infty}[P_r] + k_{CSA}Y_0\sum_{r=2}^{\infty}[SP_r] \tag{16}$$

The term $\sum_{r=2}^{\infty}[P_{r-1}]$ in Equation (16) must be expressed as a function of moments by using:

$$\sum_{r=2}^{\infty}[P_{r-1}] = [P_1] + [P_2] + [P_3] + ... = \sum_{r=1}^{\infty}[P_r] = Y_0 \tag{17}$$

$$[P_1] + \sum_{r=2}^{\infty}[P_r] = \sum_{r=1}^{\infty}[P_r] = Y_0 \tag{18}$$

$$[SP_1] + \sum_{r=2}^{\infty}[SP_r] = \sum_{r=1}^{\infty}[SP_r] = [SX_0] \tag{19}$$

$$\frac{dY_0}{dt} = k_i[C][M] - (k_{t\beta} + k_{tH}[H_2] + k_d + k_{CSA0}[S_0])Y_0 \tag{20}$$

The 1st moment of living polymer chain,

$$Y_1 = \sum_{r=1}^{\infty} r[P_r] = [P_1] + \sum_{r=2}^{\infty} r[P_r] \tag{21}$$

Taking the first derivative of Equation (21):

$$\frac{dY_1}{dt} = \frac{d[P]_1}{dt} + \sum_{r=2}^{\infty} r\frac{d[P_r]}{dt} \tag{22}$$

Now substituting Equations (8) and (10) into Equation (22):

$$\frac{dY_1}{dt} = k_i[C][M] - k_p[P_1][M - (k_{t\beta} + k_{tH}[H_2] + k_d + k_{CSA0}[S_0] + k_{CSA}[SX_0])[P_1] + k_{CSA}Y_0[SP_1] + k_pM](\sum_{r=2}^{\infty} r[P_{r-1}] - \sum_{r=2}^{\infty} r[P_r]) - (k_{t\beta} + k_{tH}[H_2] + k_d + k_{CSA0}[S_0] + k_{CSA}[SX_0])\sum_{r=2}^{\infty} r[P_r] + k_{CSA}Y_0\sum_{r=2}^{\infty} r[SP_r] \tag{23}$$

The term $\sum_{r=2}^{\infty} r[P_{r-1}]$ in Equation (23) must be expressed as a function of moments by using:

$$\sum_{r=2}^{\infty} r[P_{r-1}] = 2[P_1] + 3[P_2] + 4[P_3] + ... + ... = \sum_{r=1}^{\infty} [P_r] + \sum_{r=1}^{\infty} r[P_r] = Y_0 + Y_1 \tag{24}$$

$$[P_1] + \sum_{r=2}^{\infty} r[P_r] = [P_1] + 2[P_2] + 3[P_3] + 4[P_4] + ... = \sum_{r=1}^{\infty} r[P_r] = Y_1 \tag{25}$$

$$[SP_1] + \sum_{r=2}^{\infty} r[SP_r] = [SP_1] + 2[SP_2] + 3[SP_3] + 4[SP_4] + ... = \sum_{r=1}^{\infty} r[SP_r] = [SX_1] \tag{26}$$

$$\frac{dY_1}{dt} = k_i[C][M] + k_p[M]Y_0 - (k_{t\beta} + k_{tH}[H_2] + k_d + k_{CSA0}[S_0] + k_{CSA}[SX_0])\, Y_1 + k_{CSA}Y_0[SX_1] \tag{27}$$

The 2nd moment of living polymer chain,

$$Y_2 = \sum_{r=1}^{\infty} r^2[P_r] = [P_1] + \sum_{r=2}^{\infty} r^2[P_r] \tag{28}$$

Taking the first derivative of Equation (28):

$$\frac{dY_2}{dt} = \frac{d[P_1]}{dt} + \sum_{r=2}^{\infty} r^2 \frac{d[P_r]}{dt} \tag{29}$$

Now substituting Equations (8) and (10) into Equation (29):

$$\begin{aligned} \frac{dY_2}{dt} &= k_i[C][M] - k_p[P_1][M - (k_{t\beta} + k_{tH}[H_2] + k_d + k_{CSA0}[S_0] + k_{CSA}[SX_0])[P_1] + k_{CSA}Y_0[SP_1] + \\ & k_p M](\sum_{r=2}^{\infty} r^2[P_{r-1}] - \sum_{r=2}^{\infty} r^2[P_r]) - (k_{t\beta} + k_{tH}[H_2] + k_d + k_{CSA0}[S_0] + k_{CSA}[SX_0])\sum_{r=2}^{\infty} r^2[P_r] + k_{CSA}Y_0\sum_{r=2}^{\infty} r^2[SP_r] \end{aligned} \tag{30}$$

The term $\sum_{r=2}^{\infty} r^2[P_{r-1}]$ in Equation (30) must be expressed as a function of moments by using:

$$\begin{aligned} \sum_{r=2}^{\infty} r^2[P_{r-1}] = 4[P_2] + 9[P_3] + 16[P_4] + ... &= \sum_{r=1}^{\infty} (r+1)^2[P_r] = \sum_{r=1}^{\infty} (r^2 + 2r + 1)[P_r] \\ &= \sum_{r=1}^{\infty} [P_r] + 2\sum_{r=1}^{\infty} r[P_r] + \sum_{r=1}^{\infty} r^2[P_r] = Y_0 + 2Y_1 + Y_2 \end{aligned} \tag{31}$$

$$[P_1]+\sum_{r=2}^{\infty} r^2[P_r]=[P_1]+4[P_2]+9[P_3]+16[P_4]+.....=\sum_{r=1}^{\infty} r^2[P_r]=Y_2 \tag{32}$$

$$[SP_1]+\sum_{r=2}^{\infty} r^2[SP_r]=[SP_1]+4[SP_2]+9[SP_3]+16[SP_4]+.....=\sum_{r=1}^{\infty} r^2[SP_r]=[SX_2] \tag{33}$$

$$\frac{dY_2}{dt}=k_i[C][M]+k_p[M](Y_0+2Y_1)-(k_{t\beta}+k_{tH}[H_2]+k_d+k_{CSA0}[S_0]+k_{CSA}[SX_0])\,Y_2+k_{CSA}Y_0[SX_2] \tag{34}$$

The 0th moment of dead polymer chain,

$$[X_0]=\sum_{r=2}^{\infty}[D_r] \tag{35}$$

Taking the first derivative of Equation (35):

$$\frac{d[X_0]}{dt}=\sum_{r=2}^{\infty}\frac{d[D_r]}{dt} \tag{36}$$

Take summation the both side of the equation (11):

$$\sum_{r=2}^{\infty}\frac{d[D_r]}{dt}=(k_{t\beta}+k_{tH}[H_2]+k_d)\sum_{r=2}^{\infty}[P_r]=(k_{t\beta}+k_{tH}[H_2]+k_d)(Y_0-P_1)\cong\ (k_{t\beta}+k_{tH}[H_2]+k_d)Y_0 \tag{37}$$

Now substituting Equation (36) into Equation (37):

$$\frac{d[X_0]}{dt}=(k_{t\beta}+k_{tH}[H_2]+k_d)Y_0 \tag{38}$$

The 1st moment of dead polymer chain,

$$[X_1]=\sum_{r=2}^{\infty} r[D_r] \tag{39}$$

Taking the first derivative of Equation (39):

$$\frac{d[X_1]}{dt}=\sum_{r=2}^{\infty} r\frac{d[D_r]}{dt} \tag{40}$$

Take summation the both side of the equation (11):

$$\sum_{r=2}^{\infty} r\frac{d[D_r]}{dt} = (k_{t\beta} + k_{tH}[H_2] + k_d)\sum_{r=2}^{\infty} r[P_r] = (k_{t\beta} + k_{tH}[H_2] + k_d)(Y_1 - P_1) \cong (k_{t\beta} + k_{tH}[H_2] + k_d)Y_1 \quad (41)$$

Now substituting Equation (40) into Equation (41):

$$\frac{d[X_1]}{dt} = (k_{t\beta} + k_{tH}[H_2] + k_d)Y_1 \quad (42)$$

The 2nd moment of dead polymer chain,

$$[X_2] = \sum_{r=2}^{\infty} r^2[D_r] \quad (43)$$

Taking the first derivative of Equation (43):

$$\frac{d[X_2]}{dt} = \sum_{r=2}^{\infty} r^2\frac{d[D_r]}{dt} \quad (44)$$

Take summation the both side of the equation (11):

$$\sum_{r=2}^{\infty} r^2\frac{d[D_r]}{dt} = (k_{t\beta} + k_{tH}[H_2] + k_d)\sum_{r=2}^{\infty} r^2[P_r] = (k_{t\beta} + k_{tH}[H_2] + k_d)(Y_2 - P_1) \cong (k_{t\beta} + k_{tH}[H_2] + k_d)Y_2 \quad (45)$$

Now substituting Equation (44) into Equation (45):

$$\frac{d[X_2]}{dt} = (k_{t\beta} + k_{tH}[H_2] + k_d)Y_2 \quad (46)$$

The 0th moment of dormant polymer chain,

$$[SX_0] = \sum_{r=1}^{\infty}[SP_r] \quad (47)$$

Taking the first derivative of Equation (47):

$$\frac{d[SX_0]}{dt} = \sum_{r=1}^{\infty}\frac{d[SP_r]}{dt} \quad (48)$$

Take summation the both side of equation (13):

$$\sum_{r=1}^{\infty}\frac{d[SP_r]}{dt} = k_{CSA0}[S_0]\sum_{r=1}^{\infty}[P_r] + k_{CSA}[SX_0]\sum_{r=1}^{\infty}[P_r] - k_{CSA}Y_0\sum_{r=1}^{\infty}[SP_r] \quad (49)$$

Now substituting Equation (48) into Equation (49) and simplified:

$$\frac{d[SX_0]}{dt} = k_{CSA0}[S_0]Y_0 + k_{CSA}[SX_0]Y_0 - k_{CSA}Y_0[SX_0] \tag{50}$$

$$\frac{d[SX_0]}{dt} = k_{CSA0}[S_0]Y_0 \tag{51}$$

The 1st moment of dormant polymer chain,

$$[SX_1] = \sum_{r=1}^{\infty} r[SP_r] \tag{52}$$

Taking the first derivative of Equation (52):

$$\frac{d[SX_1]}{dt} = \sum_{r=1}^{\infty} r\frac{d[SP_r]}{dt} \tag{53}$$

Take summation the both side of equation (13):

$$\sum_{r=1}^{\infty} r\frac{d[SP_r]}{dt} = k_{CSA0}[S_0]\sum_{r=1}^{\infty} r[P_r] + k_{CSA}[SX_0]\sum_{r=1}^{\infty} r[P_r] - k_{CSA}Y_0\sum_{r=1}^{\infty} r[SP_r] \tag{54}$$

Now substituting Equation (53) into Equation (54) and simplified:

$$\frac{d[SX_1]}{dt} = k_{CSA0}[S_0]Y_1 + k_{CSA}Y_1[SX_0] - k_{CSA}Y_0[SX_1] \tag{55}$$

Rearrange the above equation:

$$\frac{d[SX_1]}{dt} = (k_{CSA0}[S_0] + k_{CSA}[SX_0])Y_1 - k_{CSA}Y_0[SX_1] \tag{56}$$

The 2nd moment of dormant polymer chain,

$$[SX_2] = \sum_{r=1}^{\infty} r^2[SP_r] \tag{57}$$

Taking the first derivative of Equation (57):

$$\frac{d[SX_2]}{dt} = \sum_{r=1}^{\infty} r^2\frac{d[SP_r]}{dt} \tag{58}$$

Take summation the both side of equation (13):

$$\sum_{r=1}^{\infty} r^2 \frac{d[SP_r]}{dt} = k_{CSA0}[S_0]\sum_{r=1}^{\infty} r^2[P_r] + k_{CSA}[SX_0]\sum_{r=1}^{\infty} r^2[P_r] - k_{CSA}Y_0\sum_{r=1}^{\infty} r^2[SP_r] \tag{59}$$

Now substituting Equation (59) into Equation (58) and simplified:

$$\frac{d[SX_2]}{dt} = k_{CSA0}[S_0]Y_2 + k_{CSA}Y_2[SX_0] - k_{CSA}Y_0[SX_2] \tag{60}$$

Rearrange the above equation:

$$\frac{d[SX_2]}{dt} = (k_{CSA0}[S_0] + k_{CSA}[SX_0])Y_2 - k_{CSA}Y_0[SX_2] \tag{61}$$

Appendix 4-A

Population Balance for M

$$\frac{d[M]}{dt} = -k_i[C][M] - k_p \sum_{r=1}^{\infty}[P_r][M] - s[M] + [M]^{in} \tag{1}$$

Now substituting $Y_0 = \sum_{r=1}^{\infty}[P_r]$ into Equation (1):

$$\frac{d[M]}{dt} = -(k_i[C] + k_p Y_0 + s)[M] + [M]^{in} \tag{2}$$

Population Balance for C

$$\frac{d[C]}{dt} = -k_i[C][M] - k_d[C] - s[C] + (k_{t\beta} + k_{tH}[H_2])\sum_{r=1}^{\infty}[P_r] + k_{CSA0}\sum_{r=1}^{\infty}[P_r][S_0] + [C]^{in} \tag{3}$$

Simplified Equation (3):

$$\frac{d[C]}{dt} = -(k_i[M] + k_d + s)[C] + (k_{t\beta} + k_{tH}[H_2] + k_{CSA0}[S_0])Y_0 + [C]^{in} \tag{4}$$

Population Balance for S_0

$$\frac{d[S_0]}{dt} = -k_{CSA0}\sum_{r=1}^{\infty}[P_r][S_0] - s[S_0] + [S_0]^{in} \tag{5}$$

Simplified Equation (5):

$$\frac{d[S_0]}{dt} = -(k_{CSA0}Y_0 + s)[S_0] + [S_0]^{in} \tag{6}$$

Population Balance for P_1 ($r = 1$)

$$\begin{aligned}\frac{d[P_1]}{dt} &= k_i[C][M] - k_p[P_1][M] - k_{t\beta}[P_1] - k_{tH}[H_2][P_1] - k_d[P_1] - k_{CSA0}[P_1][S_0] \\ &- k_{CSA}[P_1]\sum_{\substack{s=1 \\ s\neq r}}^{\infty}[S_0 D_s] + k_{CSA}\sum_{\substack{s=1 \\ s\neq r}}^{\infty}[P_s][S_0 D_1] - s[P_1]\end{aligned} \tag{7}$$

Now substituting $[SX_0] \cong \sum_{\substack{s=1 \\ s\neq r}}^{\infty}[SP_s]$ and $Y_0 \cong \sum_{\substack{s=1 \\ s\neq r}}^{\infty}[P_s]$ into Equation (7):

$$\frac{d[P_1]}{dt} = k_i[C][M] - k_p[P_1][M] - (k_{t\beta} + k_{tH}[H_2] + k_d + k_{CSA0}[S_0] + k_{CSA}[SX_0] + s)[P_1] + k_{CSA}Y_0[SP_1] \tag{8}$$

Population Balance for P_r where $(r \geq 2)$:

$$\frac{d[P_r]}{dt} = k_p[P_{r-1}][M] - k_p[P_r][M] - k_{t\beta}[P_r] - k_{tH}[H_2][P_r] - k_d[P_r] - k_{CSA0}[P_r][S_0] + k_{CSA}\sum_{\substack{s=1 \\ s\neq r}}^{\infty}[P_s][SP_r] - k_{CSA}\sum_{\substack{s=1 \\ s\neq r}}^{\infty}[SP_s][P_r] - s[P_r] \tag{9}$$

Simplified Equation (9):

$$\frac{d[P_r]}{dt} = k_p[M]([P_{r-1}] - [P_r]) - (k_{t\beta} + k_{tH}[H_2] + k_d + k_{CSA0}[S_0] + k_{CSA}[SX_0] + s)[P_r] + k_{CSA}Y_0[SP_r] \tag{10}$$

Population Balance for D_r where $(r \geq 2)$:

$$\frac{d[D_r]}{dt} = (k_{t\beta} + k_{tH}[H_2])[P_r] + k_d[P_r] - s[D_r] = (k_{t\beta} + k_{tH}[H_2] + k_d)[P_r] - s[D_r] \tag{11}$$

Population Balance for SP_r where $(r \geq 2)$:

$$\frac{d[SP_r]}{dt} = k_{CSA0}[S_0][P_r] + k_{CSA}\sum_{\substack{s=1 \\ s\neq r}}^{\infty}[SP_s][P_r] - k_{CSA}\sum_{\substack{s=1 \\ s\neq r}}^{\infty}[P_s][SP_r] - s[SP_r] \tag{12}$$

Simplified Equation (12):

$$\frac{d[SP_r]}{dt} = k_{CSA0}[S_0][P_r] + k_{CSA}[SX_0][P_r] - k_{CSA}Y_0[SP_r] - s[SP_r] \tag{13}$$

The 0th moment of living polymer chain,

$$Y_0 = \sum_{r=1}^{\infty}[P_r] = [P_1] + \sum_{r=2}^{\infty}[P_r] \tag{14}$$

Taking the first derivative of Equation (14):

$$\frac{dY_0}{dt} = \frac{dP_1}{dt} + \sum_{r=2}^{\infty}\frac{d[P_r]}{dt} \tag{15}$$

Now substituting Equations (8) and (10) into Equation (15):

$$\frac{dY_0}{dt} = k_i[C][M] - k_p[P_1][M] - (k_{t\beta} + k_{tH}[H_2] + k_d + k_{CSA0}[S_0] + k_{CSA}[SX_0] + s)[P_1] + k_{CSA}Y_0[SP_1] + k_p[M](\sum_{r=2}^{\infty}[P_{r-1}] - \sum_{r=2}^{\infty}[P_r]) - (k_{t\beta} + k_{tH}[H_2] + k_d + k_{CSA0}[S_0] + k_{CSA}[SX_0] + s)\sum_{r=2}^{\infty}[P_r] + k_{CSA}Y_0\sum_{r=2}^{\infty}[SP_r] \quad (16)$$

The term $\sum_{r=2}^{\infty}[P_{r-1}]$ in Equation (16) must be expressed as a function of moments by using:

$$\sum_{r=2}^{\infty}[P_{r-1}] = [P_1] + [P_2] + [P_3] + ... = \sum_{r=1}^{\infty}[P_r] = Y_0 \quad (17)$$

$$[P_1] + \sum_{r=2}^{\infty}[P_r] = \sum_{r=1}^{\infty}[P_r] = Y_0 \quad (18)$$

$$[SP_1] + \sum_{r=2}^{\infty}[SP_r] = \sum_{r=1}^{\infty}[SP_r] = [SX_0] \quad (19)$$

$$\frac{dY_0}{dt} = k_i[C][M] - (k_{t\beta} + k_{tH}[H_2] + k_d + k_{CSA0}[S_0] + s)Y_0 \quad (20)$$

The 1st moment of living polymer chain,

$$Y_1 = \sum_{r=1}^{\infty} r[P_r] = [P_1] + \sum_{r=2}^{\infty} r[P_r] \quad (21)$$

Taking the first derivative of Equation (21):

$$\frac{dY_1}{dt} = \frac{d[P]_1}{dt} + \sum_{r=2}^{\infty} r\frac{d[P_r]}{dt} \quad (22)$$

Now substituting Equations (8) and (10) into Equation (22):

$$\frac{dY_1}{dt} = k_i[C][M] - k_p[P_1][M - (k_{t\beta} + k_{tH}[H_2] + k_d + k_{CSA0}[S_0] + k_{CSA}[SX_0] + s)[P_1] + k_{CSA}Y_0[SP_1] + k_pM](\sum_{r=2}^{\infty} r[P_{r-1}] - \sum_{r=2}^{\infty} r[P_r]) - (k_{t\beta} + k_{tH}[H_2] + k_d + k_{CSA0}[S_0] + k_{CSA}[SX_0] + s)\sum_{r=2}^{\infty} r[P_r] + k_{CSA}Y_0\sum_{r=2}^{\infty} r[SP_r] \quad (23)$$

The term $\sum_{r=2}^{\infty} r[P_{r-1}]$ in Equation (23) must be expressed as a function of moments by using:

$$\sum_{r=2}^{\infty} r[P_{r-1}] = 2[P_1] + 3[P_2] + 4[P_3] + ... + ... = \sum_{r=1}^{\infty}[P_r] + \sum_{r=1}^{\infty} r[P_r] = Y_0 + Y_1 \tag{24}$$

$$[P_1] + \sum_{r=2}^{\infty} r[P_r] = [P_1] + 2[P_2] + 3[P_3] + 4[P_4] + ... = \sum_{r=1}^{\infty} r[P_r] = Y_1 \tag{25}$$

$$[SP_1] + \sum_{r=2}^{\infty} r[SP_r] = [SP_1] + 2[SP_2] + 3[SP_3] + 4[SP_4] + ... = \sum_{r=1}^{\infty} r[SP_r] = [SX_1] \tag{26}$$

$$\frac{dY_1}{dt} = k_i[C][M] + k_p[M]Y_0 - (k_{t\beta} + k_{tH}[H_2] + k_d + k_{CSA0}[S_0] + k_{CSA}[SX_0] + s)Y_1 + k_{CSA}Y_0[SX_1] \tag{27}$$

The 2nd moment of living polymer chain,

$$Y_2 = \sum_{r=1}^{\infty} r^2[P_r] = [P_1] + \sum_{r=2}^{\infty} r^2[P_r] \tag{28}$$

Taking the first derivative of Equation (28):

$$\frac{dY_2}{dt} = \frac{d[P_1]}{dt} + \sum_{r=2}^{\infty} r^2 \frac{d[P_r]}{dt} \tag{29}$$

Now substituting Equations (8) and (10) into Equation (29):

$$\begin{aligned}\frac{dY_2}{dt} &= k_i[C][M] - k_p[P_1][M - (k_{t\beta} + k_{tH}[H_2] + k_d + k_{CSA0}[S_0] + k_{CSA}[SX_0] + s)[P_1] + k_{CSA}Y_0[SP_1] + \\ &k_pM](\sum_{r=2}^{\infty} r^2[P_{r-1}] - \sum_{r=2}^{\infty} r^2[P_r]) - (k_{t\beta} + k_{tH}[H_2] + k_d + k_{CSA0}[S_0] + k_{CSA}[SX_0] + s)\sum_{r=2}^{\infty} r^2[P_r] + k_{CSA}Y_0\sum_{r=2}^{\infty} r^2[SP_r]\end{aligned} \tag{30}$$

The term $\sum_{r=2}^{\infty} r^2[P_{r-1}]$ in Equation (30) must be expressed as a function of moments by using:

$$\begin{aligned}\sum_{r=2}^{\infty} r^2[P_{r-1}] = 4[P_2] + 9[P_3] + 16[P_4] + ... &= \sum_{r=1}^{\infty}(r+1)^2[P_r] = \sum_{r=1}^{\infty}(r^2 + 2r + 1)[P_r] \\ &= \sum_{r=1}^{\infty}[P_r] + 2\sum_{r=1}^{\infty} r[P_r] + \sum_{r=1}^{\infty} r^2[P_r] = Y_0 + 2Y_1 + Y_2\end{aligned} \tag{31}$$

$$[P_1] + \sum_{r=2}^{\infty} r^2[P_r] = [P_1] + 4[P_2] + 9[P_3] + 16[P_4] + ... = \sum_{r=1}^{\infty} r^2[P_r] = Y_2 \tag{32}$$

$$[SP_1]+\sum_{r=2}^{\infty} r^2[SP_r]=[SP_1]+4[SP_2]+9[SP_3]+16[SP_4]+.....=\sum_{r=1}^{\infty} r^2[SP_r]=[SX_2] \tag{33}$$

$$\frac{dY_2}{dt}=k_i[C][M]+k_p[M](Y_0+2Y_1)-(k_{t\beta}+k_{tH}[H_2]+k_d+k_{CSA0}[S_0]+k_{CSA}[SX_0]+s)Y_2+k_{CSA}Y_0[SX_2] \tag{34}$$

The 0th moment of dead polymer chain,

$$[X_0]=\sum_{r=2}^{\infty}[D_r] \tag{35}$$

Taking the first derivative of Equation (35):

$$\frac{d[X_0]}{dt}=\sum_{r=2}^{\infty}\frac{d[D_r]}{dt} \tag{36}$$

Take summation the both side of the equation (11):

$$\sum_{r=2}^{\infty}\frac{d[D_r]}{dt}=(k_{t\beta}+k_{tH}[H_2]+k_d)\sum_{r=2}^{\infty}[P_r]-s\sum_{r=2}^{\infty}[D_r]= \\ (k_{t\beta}+k_{tH}[H_2]+k_d)(Y_0-P_1)-s_1[X_0]\cong (k_{t\beta}+k_{tH}[H_2]+k_d)Y_0-s[X_0] \tag{37}$$

Now substituting Equation (36) into Equation (37):

$$\frac{d[X_0]}{dt}=(k_{t\beta}+k_{tH}[H_2]+k_d)Y_0-s[X_0] \tag{38}$$

The 1st moment of dead polymer chain,

$$[X_1]=\sum_{r=2}^{\infty} r[D_r] \tag{39}$$

Taking the first derivative of Equation (39):

$$\frac{d[X_1]}{dt}=\sum_{r=2}^{\infty} r\frac{d[D_r]}{dt} \tag{40}$$

Take summation the both side of the equation (11):

$$\sum_{r=2}^{\infty} r\frac{d[D_r]}{dt}=(k_{t\beta}+k_{tH}[H_2]+k_d)\sum_{r=2}^{\infty} r[P_r]-s\sum_{r=2}^{\infty} r[D_r]=(k_{t\beta}+k_{tH}[H_2]+k_d)(Y_1-P_1)-s[X_1]\cong \\ (k_{t\beta}+k_{tH}[H_2]+k_d)Y_1-s[X_1] \tag{41}$$

Now substituting Equation (40) into Equation (41):

$$\frac{d[X_1]}{dt} = (k_{t\beta} + k_{tH}[H_2] + k_d)Y_1 - s[X_1] \tag{42}$$

The 2nd moment of dead polymer chain,

$$[X_2] = \sum_{r=2}^{\infty} r^2 [D_r] \tag{43}$$

Taking the first derivative of Equation (43):

$$\frac{d[X_2]}{dt} = \sum_{r=2}^{\infty} r^2 \frac{d[D_r]}{dt} \tag{44}$$

Take summation the both side of the equation (11):

$$\sum_{r=2}^{\infty} r^2 \frac{d[D_r]}{dt} = (k_{t\beta} + k_{tH}[H_2] + k_d)\sum_{r=2}^{\infty} r^2 [P_r] - s\sum_{r=2}^{\infty} r^2 [D_r] = \\ (k_{t\beta} + k_{tH}[H_2] + k_d)(Y_2 - P_1) - s[X_2] \cong (k_{t\beta} + k_{tH}[H_2] + k_d)Y_2 - s[X_2] \tag{45}$$

Now substituting Equation (44) into Equation (45):

$$\frac{d[X_2]}{dt} = (k_{t\beta} + k_{tH}[H_2] + k_d)Y_2 - s[X_2] \tag{46}$$

The 0th moment of dormant polymer chain,

$$[SX_0] = \sum_{r=1}^{\infty} [SP_r] \tag{47}$$

Taking the first derivative of Equation (47):

$$\frac{d[SX_0]}{dt} = \sum_{r=1}^{\infty} \frac{d[SP_r]}{dt} \tag{48}$$

Take summation the both side of equation (13):

$$\sum_{r=1}^{\infty} \frac{d[SP_r]}{dt} = k_{CSA0}[S_0]\sum_{r=1}^{\infty} [P_r] + k_{CSA}[SX_0]\sum_{r=1}^{\infty} [P_r] - k_{CSA}Y_0 \sum_{r=1}^{\infty} [SP_r] - s\sum_{r=1}^{\infty} [SP_r] \tag{49}$$

Now substituting Equation (48) into Equation (49) and simplified:

$$\frac{d[SX_0]}{dt} = k_{CSA0}[S_0]Y_0 + k_{CSA}[SX_0]Y_0 - k_{CSA}Y_0[SX_0] - s[SX_0] \tag{50}$$

$$\frac{d[SX_0]}{dt} = k_{CSA0}[S_0]Y_0 - s[SX_0] \tag{51}$$

The 1st moment of dormant polymer chain,

$$[SX_1] = \sum_{r=1}^{\infty} r[SP_r] \tag{52}$$

Taking the first derivative of Equation (52):

$$\frac{d[SX_1]}{dt} = \sum_{r=1}^{\infty} r\frac{d[SP_r]}{dt} \tag{53}$$

Take summation the both side of equation (13):

$$\sum_{r=1}^{\infty} r\frac{d[SP_r]}{dt} = k_{CSA0}[S_0]\sum_{r=1}^{\infty} r[P_r] + k_{CSA}[SX_0]\sum_{r=1}^{\infty} r[P_r] - k_{CSA}Y_0\sum_{r=1}^{\infty} r[SP_r] - s\sum_{r=1}^{\infty} r[SP_r] \tag{54}$$

Now substituting Equation (53) into Equation (54) and simplified:

$$\frac{d[SX_1]}{dt} = k_{CSA0}[S_0]Y_1 + k_{CSA}Y_1[SX_0] - k_{CSA}Y_0[SX_1] - s[SX_1] \tag{55}$$

Rearrange the above equation:

$$\frac{d[SX_1]}{dt} = (k_{CSA0}[S_0] + k_{CSA}[SX_0])Y_1 - (k_{CSA}Y_0 + s)[SX_1] \tag{56}$$

The 2nd moment of dormant polymer chain,

$$[SX_2] = \sum_{r=1}^{\infty} r^2[SP_r] \tag{57}$$

Taking the first derivative of Equation (57):

$$\frac{d[SX_2]}{dt} = \sum_{r=1}^{\infty} r^2\frac{d[SP_r]}{dt} \tag{58}$$

Take summation the both side of equation (13):

$$\sum_{r=1}^{\infty} r^2 \frac{d[SP_r]}{dt} = k_{CSA0}[S_0]\sum_{r=1}^{\infty} r^2[P_r] + k_{CSA}[SX_0]\sum_{r=1}^{\infty} r^2[P_r] - k_{CSA}Y_0\sum_{r=1}^{\infty} r^2[SP_r] - s\sum_{r=1}^{\infty} r^2[SP_r] \quad (59)$$

Now substituting Equation (59) into Equation (58) and simplified:

$$\frac{d[SX_2]}{dt} = k_{CSA0}[S_0]Y_2 + k_{CSA}Y_2[SX_0] - k_{CSA}Y_0[SX_2] - s[SX_2] \quad (60)$$

Rearrange the above equation:

$$\frac{d[SX_2]}{dt} = (k_{CSA0}[S_0] + k_{CSA}[SX_0])Y_2 - (k_{CSA}Y_0 + s)[SX_2] \quad (61)$$

Appendix 5-A

The following expression gives the k^{th} moment for living, dormant, and dead chains of a generic distribution $f(r,i)$:

$$\mu_{k,i} = \sum_{r=1}^{\infty} r^k f(r,i) \tag{1}$$

We adopted the following nomenclature for the moments:

1. $Y_{k,P}$ and $Y_{k,Q}$ are the k^{th} moments of the living chains growing in catalyst P and Q, respectively.
2. $SX_{k,P}$ and $SX_{k,Q}$ are the k^{th} moments of dormant chains for which catalyst P and Q made the last block, respectively.
3. $X_{k,P}$ and $X_{k,Q}$ are the k^{th} moments of dead chains for which catalyst P and Q made the last block, respectively.
4. $Y_{k,P,i}$ and $Y_{k,Q,i}$ are the k^{th} moments of living chains growing in catalyst P and Q having i blocks, respectively.
5. $SX_{k,P,i}$ and $SX_{k,Q,i}$ are the k^{th} moments of dormant chains having i blocks for which catalyst P and Q made the last block, respectively.
6. $X_{k,P,i}$ and $X_{k,Q,i}$ are the k^{th} moments of dead chains having i blocks for which catalyst P and Q made the last block, respectively.

These moments are defined using the following equations,

$$Y_{k,P} = \sum_{i=1}^{\infty}\sum_{r=1}^{\infty} r^k Y_{k,P,i} \tag{2}$$

$$Y_{k,Q} = \sum_{i=1}^{\infty}\sum_{r=1}^{\infty} r^k Y_{k,Q,i} \tag{3}$$

$$SX_{k,P} = \sum_{i=1}^{\infty}\sum_{r=1}^{\infty} r^k SX_{k,P,i} \tag{4}$$

$$SX_{k,Q} = \sum_{i=1}^{\infty}\sum_{r=1}^{\infty} r^k SX_{k,Q,i} \tag{5}$$

$$X_{k,P} = \sum_{i=1}^{\infty}\sum_{r=1}^{\infty} r^k X_{k,P,i} \tag{6}$$

$$X_{k,Q} = \sum_{i=1}^{\infty}\sum_{r=1}^{\infty} r^k X_{k,Q,i} \tag{7}$$

$$Y_{k,P,i} = \sum_{r=1}^{\infty} r^k P_{r,i} = P_{1,1} + \sum_{r=2}^{\infty} r^k P_{r,i} \tag{8}$$

$$Y_{k,Q,i} = \sum_{r=1}^{\infty} r^k Q_{r,i} = Q_{1,1} + \sum_{r=2}^{\infty} r^k Q_{r,i} \tag{9}$$

$$SX_{k,P,i} = \sum_{r=1}^{\infty} r^k SP_{r,i} = SP_{1,1} + \sum_{r=2}^{\infty} r^k SP_{r,i} \tag{10}$$

$$SX_{k,Q,i} = \sum_{r=1}^{\infty} r^k SQ_{r,i} = SQ_{1,1} + \sum_{r=2}^{\infty} r^k SQ_{r,i} \tag{11}$$

$$X_{k,P,i} = \sum_{r=1}^{\infty} r^k D_{r,i} = D_{1,1} + \sum_{r=2}^{\infty} r^k D_{r,i} \tag{12}$$

$$X_{k,Q,i} = \sum_{r=1}^{\infty} r^k D_{r,i} = D_{1,1} + \sum_{r=2}^{\infty} r^k D_{r,i} \tag{13}$$

Where: k: 0th, 1st, and 2nd moments, i: block number, r: chain length and P and Q: catalyst type.

Moment Equation for Living Chains

Two living polymer chains with length larger than 2 ($r \geq 2$) and with a number of blocks greater than 1 ($i > 1$) made by catalyst type P ($P_{r,i}$) and made by catalyst type Q ($Q_{r,i}$) were produced in the reactor. The population balance for living polymer chain made by catalyst P of block i, $P_{r,i}$, is expressed by:

$$\begin{aligned}\frac{dP_{r,i}}{dt} &= k_{pA1}A\left(P_{r-1,i} - P_{r,i}\right) + k_{pB1}B\left(P_{r-1,i} - P_{r,i}\right) \\ &-\left(k_{t\beta 1} + k_{tH1}H_2 + k_{d1} + k_{CSA01}S_0 + k_{CSA1}SX_{0,P} + k_{CSA1}SX_{0,Q}\right)P_{r,i} + \left(SP_{r,i} + SQ_{r,i-1}\right)k_{CSA1}Y_{0,P}\end{aligned} \tag{14}$$

A slightly different equation is applied for chain length 1, $P_{1,1}$:

$$\frac{dP_{1,1}}{dt} = (k_{iA1}A + k_{iB1}B)C_1 - k_{pA1}P_{1,1}A - k_{pB1}P_{1,1}B \\ -(k_{t\beta 1} + k_{tH1}H_2 + k_{d1} + k_{CSA01}S_0 + k_{CSA1}SX_{0,P} + k_{CSA1}SX_{0,Q})P_{1,1} + k_{CSA1}(SP_{1,1})Y_{0,P} \quad (15)$$

The k^{th} moment of living chains made by catalyst type P for block i is given by:

$$\frac{dY_{k,P,i}}{dt} = \sum_{r=1}^{\infty} r^k \frac{dP_{r,i}}{dt} = \frac{dP_{1,1}}{dt} + \sum_{r=2}^{\infty} r^k \frac{dP_{r,i}}{dt} \quad (16)$$

Substituting Equations (14) and (15) into Equation (16) and by using Equations (2) to (13) with simplifying, the 0th, 1st, and 2nd moments of living chains made by catalyst type P for block i are given by the following equations:

$$\frac{dY_{0,P,i}}{dt} = (k_{iA1}A + k_{iB1}B)C_1 - (k_{t\beta 1} + k_{tH1}H_2 + k_{d1} + k_{CSA01}S_0 + k_{CSA1}(SX_{0,P}) + k_{CSA1}(SX_{0,Q}))Y_{0,P,i} \\ + ((SX_{0,P,i}) + (SX_{0,Q,i-1}))k_{CSA1}Y_{0,P} \quad (17)$$

$$\frac{dY_{1,P,i}}{dt} = (k_{iA1}A + k_{iB1}B)C_1 + (k_{pA1}A + k_{pB1}B)Y_{0,P,i} \\ -(k_{t\beta 1} + k_{tH1}H_2 + k_{d1} + k_{CSA01}S_0 + k_{CSA1}(SX_{0,P}) + k_{CSA1}(SX_{0,Q}))Y_{1,P,i} + ((SX_{1,P,i}) + (SX_{1,Q,i-1}))k_{CSA1}Y_{0,P} \quad (18)$$

$$\frac{dY_{2,P,i}}{dt} = (k_{iA1}A + k_{iB1}B)C_1 + (k_{pA1}A + k_{pB1}B)(Y_{0,P,i} + 2Y_{1,P,i}) \\ -(k_{t\beta 1} + k_{tH1}H_2 + k_{d1} + k_{CSA01}S_0 + k_{CSA1}(SX_{0,P}) + k_{CSA1}(SX_{0,Q}))Y_{2,P,i} + ((SX_{2,P,i}) + (SX_{2,Q,i-1}))k_{CSA1}Y_{0,P} \quad (19)$$

For the moment equations for 1 block made by catalyst P, the dormant term for block i made by catalyst Q will be omitted, i.e, $SX_{0,Q,i-1}$ =0 in the Equations (17) to (19). For the moment equations for more than 1 block made by catalyst P, the initiation part will be omitted, i.e, $(k_{iA1}*A+k_{iB1}*B)*C_1$=0 in the Equations (17) to (19).

To find the moment equations for the overall living polymer chain made by catalyst P, we need to define a new population balance for P_r and P_1

The population balance for overall living polymer chain made by catalyst P, P_r, is expressed by:

$$\frac{dP_r}{dt} = k_{pA1}A(P_{r-1} - P_r) + k_{pB1}B(P_{r-1} - P_r) \\ -(k_{t\beta 1} + k_{tH1}H_2 + k_{d1} + k_{CSA01}S_0 + k_{CSA1}SX_{0,P} + k_{CSA1}SX_{0,Q})P_r + (SP_r + SQ_r)k_{CSA1}Y_{0,P} \quad (20)$$

A slightly different equation is applied for chain length 1, P_1:

$$\frac{dP_1}{dt} = \left(k_{iA1}A + k_{iB1}B\right)C_1 - k_{pA1}P_1A - k_{pB1}P_1B \\ -\left(k_{t\beta 1} + k_{tH1}H_2 + k_{d1} + k_{CSA01}S_0 + k_{CSA1}SX_{0,P} + k_{CSA1}SX_{0,Q}\right)P_1 + k_{CSA1}\left(SP_1\right)Y_{0,P} \tag{21}$$

The k[th] moment of overall living polymer chain made by catalyst type *P* is given by:

$$\frac{dY_{k,P}}{dt} = \sum_{r=1}^{\infty} r^k \frac{dP_r}{dt} = \frac{dP_1}{dt} + \sum_{r=2}^{\infty} r^k \frac{dP_r}{dt} \tag{22}$$

Substituting Equations (20) and (21) into Equation (22) with simplifying, the 0[th], 1[st], and 2[nd] moments of overall living polymer chain made by catalyst type *P* are given by the following equations:

$$\frac{dY_{0,P}}{dt} = \left(k_{iA1}A + k_{iB1}B\right)C_1 - \left(k_{t\beta 1} + k_{tH1}H_2 + k_{d1} + k_{CSA01}S_0\right)Y_{0,P} \tag{23}$$

$$\frac{dY_{1,P}}{dt} = \left(k_{iA1}A + k_{iB1}B\right)C_1 + \left(k_{pA1}A + k_{pB1}B\right)Y_{0,P} \\ -\left(k_{t\beta 1} + k_{tH1}H_2 + k_{d1} + k_{CSA01}S_0 + k_{CSA1}\left(SX_{0,P}\right) + k_{CSA1}\left(SX_{0,Q}\right)\right)Y_{1,P} + \left(\left(SX_{1,P}\right) + \left(SX_{1,Q}\right)\right)k_{CSA1}Y_{0,P} \tag{24}$$

$$\frac{dY_{2,P}}{dt} = \left(k_{iA1}A + k_{iB1}B\right)C_1 + \left(k_{pA1}A + k_{pB1}B\right)\left(Y_{0,P,i} + 2Y_{1,P}\right) \\ -\left(k_{t\beta 1} + k_{tH1}H_2 + k_{d1} + k_{CSA01}S_0 + k_{CSA1}\left(SX_{0,P}\right) + k_{CSA1}\left(SX_{0,Q}\right)\right)Y_{2,P} + \left(\left(SX_{2,P}\right) + \left(SX_{2,Q}\right)\right)k_{CSA1}Y_{0,P} \tag{25}$$

The population balance living polymer chain made by catalyst *Q* of block *i*, $Q_{r,i}$, is expressed by:

$$\frac{dQ_{r,i}}{dt} = k_{pA2}A\left(Q_{r-1,i} - Q_{r,i}\right) + k_{pB2}B\left(Q_{r-1,i} - Q_{r,i}\right) \\ -\left(k_{t\beta 2} + k_{tH2}H_2 + k_{d2} + k_{CSA02}S_0 + k_{CSA2}SX_{0,P} + k_{CSA2}SX_{0,Q}\right)Q_{r,i} + \left(SP_{r,i-1} + SQ_{r,i}\right)k_{CSA2}Y_{0,Q} \tag{26}$$

For $Q_{1,1}$:

$$\frac{dQ_{1,1}}{dt} = \left(k_{iA2}A + k_{iB2}B\right)C_2 - k_{pA2}Q_{1,1}A - k_{pB2}Q_{1,1}B \\ -\left(k_{t\beta 2} + k_{tH2}H_2 + k_{d2} + k_{CSA02}S_0 + k_{CSA2}SX_{0,P} + k_{CSA2}SX_{0,Q}\right)Q_{1,1} + k_{CSA2}\left(SQ_{1,1}\right)Y_{0,Q} \tag{27}$$

The k[th] moment of living chains made by catalyst type Q for block i is given by:

$$\frac{dY_{k,Q,i}}{dt} = \sum_{r=1}^{\infty} r^k \frac{dQ_{r,i}}{dt} = \frac{dQ_{1,1}}{dt} + \sum_{r=2}^{\infty} r^k \frac{dQ_{r,i}}{dt} \tag{28}$$

Substituting Equations (26) and (27) into Equation (28) and by using Equations (2) to (13) with simplifying, the 0th, 1st, and 2nd moments of living chains made by catalyst type *Q* for block *i* are given by the following equations:

$$\begin{aligned}\frac{dY_{0,Q,i}}{dt} &= \left(k_{iA2}A + k_{iB2}B\right)C_2 - \left(k_{t\beta 2} + k_{tH2}H_2 + k_{d2} + k_{CSA02}S_0 + k_{CSA2}\left(SX_{0,P}\right) + k_{CSA2}\left(SX_{0,Q}\right)\right)Y_{0,Q,i} \\ &+ \left(\left(SX_{0,P,i-1}\right) + \left(SX_{0,Q,i}\right)\right)k_{CSA2}Y_{0,Q}\end{aligned} \tag{29}$$

$$\begin{aligned}\frac{dY_{1,Q,i}}{dt} &= \left(k_{iA2}A + k_{iB2}B\right)C_2 + \left(k_{pA2}A + k_{pB2}B\right)Y_{0,Q,i} \\ &- \left(k_{t\beta 2} + k_{tH2}H_2 + k_{d2} + k_{CSA02}S_0 + k_{CSA2}\left(SX_{0,P}\right) + k_{CSA2}\left(SX_{0,Q}\right)\right)Y_{1,Q,i} + \left(\left(SX_{1,P,i-1}\right) + \left(SX_{1,Q,i}\right)\right)k_{CSA2}Y_{0,Q}\end{aligned} \tag{30}$$

$$\begin{aligned}\frac{dY_{2,Q,i}}{dt} &= \left(k_{iA2}A + k_{iB2}B\right)C_2 + \left(k_{pA2}A + k_{pB2}B\right)\left(Y_{0,Q,i} + 2Y_{1,Q,i}\right) \\ &- \left(k_{t\beta 2} + k_{tH2}H_2 + k_{d2} + k_{CSA02}S_0 + k_{CSA2}\left(SX_{0,P}\right) + k_{CSA2}\left(SX_{0,Q}\right)\right)Y_{2,Q,i} + \left(\left(SX_{2,P,i-1}\right) + \left(SX_{2,Q,i}\right)\right)k_{CSA2}Y_{0,Q}\end{aligned} \tag{31}$$

For the moment equations for 1 block made by catalyst *Q*, the dormant term for block *i* made by catalyst *P* will be omitted, i.e, $SX_{0,P,i-1}=0$ in the Equations (29) to (31). The moment equations for more than 1 block made by catalyst *Q*, the initiation part will be omitted, i.e, $(k_{iA2}*A+k_{iB2}*B)*C_2=0$ in the Equations (29) to (31).

To find the moment equations for the overall living polymer chain made by catalyst *Q*, we need to define a new population balance for Q_r and Q_1

The population balance for overall living polymer chain made by catalyst *Q*, Q_r, is expressed by:

$$\begin{aligned}\frac{dQ_r}{dt} &= k_{pA2}A\left(Q_{r-1} - Q_r\right) + k_{pB2}B\left(Q_{r-1} - Q_r\right) \\ &- \left(k_{t\beta 2} + k_{tH2}H_2 + k_{d2} + k_{CSA02}S_0 + k_{CSA2}SX_{0,P} + k_{CSA2}SX_{0,Q}\right)Q_r + \left(SP_r + SQ_r\right)k_{CSA2}Y_{0,Q}\end{aligned} \tag{32}$$

For Q_1:

$$\begin{aligned}\frac{dQ_1}{dt} &= \left(k_{iA2}A + k_{iB2}B\right)C_2 - k_{pA2}Q_1A - k_{pB2}Q_1B \\ &- \left(k_{t\beta 2} + k_{tH2}H_2 + k_{d2} + k_{CSA02}S_0 + k_{CSA2}SX_{0,P} + k_{CSA2}SX_{0,Q}\right)Q_1 + k_{CSA2}\left(SQ_1\right)Y_{0,Q}\end{aligned} \tag{33}$$

The k^{th} moment of overall living polymer chain made by catalyst type Q is given by:

$$\frac{dY_{k,Q}}{dt} = \sum_{r=1}^{\infty} r^k \frac{dQ_r}{dt} = \frac{dQ_1}{dt} + \sum_{r=2}^{\infty} r^k \frac{dQ_r}{dt} \tag{34}$$

Substituting Equations (32) and (33) into Equation (34) with simplifying, the 0^{th}, 1^{st}, and 2^{nd} moments of overall living polymer chain made by catalyst type *Q* are given by the following equations:

$$\frac{dY_{0,Q}}{dt} = \left(k_{iA2}A + k_{iB2}B\right)C_2 - \left(k_{t\beta 2} + k_{tH2}H_2 + k_{d2} + k_{CSA02}S_0\right)Y_{0,Q} \tag{35}$$

$$\begin{aligned}\frac{dY_{1,Q}}{dt} &= \left(k_{iA2}A + k_{iB2}B\right)C_2 + \left(k_{pA2}A + k_{pB2}B\right)Y_{0,Q} \\ &- \left(k_{t\beta 2} + k_{tH2}H_2 + k_{d2} + k_{CSA02}S_0 + k_{CSA2}\left(SX_{0,P}\right) + k_{CSA2}\left(SX_{0,Q}\right)\right)Y_{1,Q} + \left(\left(SX_{1,P}\right) + \left(SX_{1,Q}\right)\right)k_{CSA2}Y_{0,Q}\end{aligned} \tag{36}$$

$$\begin{aligned}\frac{dY_{2,Q}}{dt} &= \left(k_{iA2}A + k_{iB2}B\right)C_2 + \left(k_{pA2}A + k_{pB2}B\right)\left(Y_{0,Q} + 2Y_{1,Q}\right) \\ &- \left(k_{t\beta 2} + k_{tH2}H_2 + k_{d2} + k_{CSA02}S_0 + k_{CSA2}\left(SX_{0,P}\right) + k_{CSA2}\left(SX_{0,Q}\right)\right)Y_{2,Q} + \left(\left(SX_{2,P}\right) + \left(SX_{2,Q}\right)\right)k_{CSA2}Y_{0,Q}\end{aligned} \tag{37}$$

Moment Equation for Dormant Chains

The presence of two catalysts and chain shuttling agent in the system generated two different types of dormant chains with chain length larger than 2 ($r \geq 2$) and with number of blocks greater than 1 ($i > 1$) made by catalyst type *P* ($SP_{r,i}$) and by catalyst type *Q* ($SQ_{r,i}$). The population balance for $SP_{r,i}$ is expressed by:

$$\frac{d\left(SP_{r,i}\right)}{dt} = \left(k_{CSA01}S_0 + k_{CSA1}SX_{0,P} + k_{CSA1}SX_{0,Q}\right)P_{r,i} - \left(k_{CSA1}Y_{0,P} + k_{CSA2}Y_{0,Q}\right)\left(SP_{r,i}\right) \tag{38}$$

The k^{th} moment of dormant chains made by catalyst type P for block i is given by:

$$\frac{dSX_{k,P,i}}{dt} = \sum_{r=1}^{\infty} r^k \frac{dSP_{r,i}}{dt} = \frac{dSP_{1,1}}{dt} + \sum_{r=2}^{\infty} r^k \frac{dSP_{r,i}}{dt} \tag{39}$$

Substituting Equation (38) into Equation (39) and by using Equations (2) to (13), the 0^{th}, 1^{st}, and 2^{nd} moments of dormant chains made by catalyst type *P* for block *i* are given by:

$$\frac{d(SX_{0,P,i})}{dt} = (k_{CSA01}S_0 + k_{CSA1}(SX_{0,P}) + k_{CSA1}(SX_{0,Q}))Y_{0,P,i} - (k_{CSA1}Y_{0,P} + k_{CSA2}Y_{0,Q})(SX_{0,P,i}) \quad (40)$$

$$\frac{d(SX_{1,P,i})}{dt} = (k_{CSA01}S_0 + k_{CSA1}(SX_{0,P}) + k_{CSA1}(SX_{0,Q}))Y_{1,P,i} - (k_{CSA1}Y_{0,P} + k_{CSA2}Y_{0,Q})(SX_{1,P,i}) \quad (41)$$

$$\frac{d(SX_{2,P,i})}{dt} = (k_{CSA01}S_0 + k_{CSA1}(SX_{0,P}) + k_{CSA1}(SX_{0,Q}))Y_{2,P,i} - (k_{CSA1}Y_{0,P} + k_{CSA2}Y_{0,Q})(SX_{2,P,i}) \quad (42)$$

The population balance for $SQ_{r,i}$ is expressed by:

$$\frac{d(SQ_{r,i})}{dt} = (k_{CSA02}S_0 + k_{CSA2}SX_{0,P} + k_{CSA2}SX_{0,Q})Q_{r,i} - (k_{CSA1}Y_{0,P} + k_{CSA2}Y_{0,Q})(SQ_{r,i}) \quad (43)$$

The k^{th} moment of dormant chains made by catalyst type Q for block i is given by:

$$\frac{dSX_{k,Q,i}}{dt} = \sum_{r=1}^{\infty} r^k \frac{dSQ_{r,i}}{dt} = \frac{dSQ_{1,1}}{dt} + \sum_{r=2}^{\infty} r^k \frac{dSQ_{r,i}}{dt} \quad (44)$$

Substituting Equation (43) into Equation (44) and by using Equations (2) to (13), the 0^{th}, 1^{st}, and 2^{nd} moments of dormant chains made by catalyst type Q for block i are given by:

$$\frac{d(SX_{0,Q,i})}{dt} = (k_{CSA02}S_0 + k_{CSA2}(SX_{0,P}) + k_{CSA2}(SX_{0,Q}))Y_{0,Q,i} - (k_{CSA1}Y_{0,P} + k_{CSA2}Y_{0,Q})(SX_{0,Q,i}) \quad (45)$$

$$\frac{d(SX_{1,Q,i})}{dt} = (k_{CSA02}S_0 + k_{CSA2}(SX_{0,P}) + k_{CSA2}(SX_{0,Q}))Y_{1,Q,i} - (k_{CSA1}Y_{0,P} + k_{CSA2}Y_{0,Q})(SX_{1,Q,i}) \quad (46)$$

$$\frac{d(SX_{2,Q,i})}{dt} = (k_{CSA02}S_0 + k_{CSA2}(SX_{0,P}) + k_{CSA2}(SX_{0,Q}))Y_{2,Q,i} - (k_{CSA1}Y_{0,P} + k_{CSA2}Y_{0,Q})(SX_{2,Q,i}) \quad (47)$$

The moment equations for the overall dormant polymer chain made by catalyst P, and Q cane be given by:

$$\frac{d(SX_{0,P})}{dt} = (k_{CSA01}S_0 + k_{CSA1}(SX_{0,P}) + k_{CSA1}(SX_{0,Q}))Y_{0,P} - (k_{CSA1}Y_{0,P} + k_{CSA2}Y_{0,Q})(SX_{0,P}) \quad (48)$$

$$\frac{d(SX_{1,P})}{dt} = (k_{CSA01}S_0 + k_{CSA1}(SX_{0,P}) + k_{CSA1}(SX_{0,Q}))Y_{1,P} - (k_{CSA1}Y_{0,P} + k_{CSA2}Y_{0,Q})(SX_{1,P}) \quad (49)$$

$$\frac{d(SX_{2,P})}{dt} = (k_{CSA01}S_0 + k_{CSA1}(SX_{0,P}) + k_{CSA1}(SX_{0,Q}))Y_{2,P} - (k_{CSA1}Y_{0,P} + k_{CSA2}Y_{0,Q})(SX_{2,P}) \quad (50)$$

$$\frac{d(SX_{0,Q})}{dt} = (k_{CSA02}S_0 + k_{CSA2}(SX_{0,P}) + k_{CSA2}(SX_{0,Q}))Y_{0,Q} - (k_{CSA1}Y_{0,P} + k_{CSA2}Y_{0,Q})(SX_{0,Q}) \quad (51)$$

$$\frac{d(SX_{1,Q})}{dt} = (k_{CSA02}S_0 + k_{CSA2}(SX_{0,P}) + k_{CSA2}(SX_{0,Q}))Y_{1,Q} - (k_{CSA1}Y_{0,P} + k_{CSA2}Y_{0,Q})(SX_{1,Q}) \quad (52)$$

$$\frac{d(SX_{2,Q})}{dt} = (k_{CSA02}S_0 + k_{CSA2}(SX_{0,P}) + k_{CSA2}(SX_{0,Q}))Y_{2,Q} - (k_{CSA1}Y_{0,P} + k_{CSA2}Y_{0,Q})(SX_{2,Q}) \quad (53)$$

Moment Equation for Dead Chains

The derivation of population balance and moments equations for dead polymer follows the same way used for living and dormant chains. The final expressions are shown below.

$$\frac{dX_{0,i}}{dt} = (k_{t\beta 1} + k_{tH1}H_2 + k_{d1})Y_{0,P,i} + (k_{t\beta 2} + k_{tH2}H_2 + k_{d2})Y_{0,Q,i} \quad (54)$$

$$\frac{dX_{1,i}}{dt} = (k_{t\beta 1} + k_{tH1}H_2 + k_{d1})Y_{1,P,i} + (k_{t\beta 2} + k_{tH2}H_2 + k_{d2})Y_{1,Q,i} \quad (55)$$

$$\frac{dX_{2,i}}{dt} = (k_{t\beta 1} + k_{tH1}H_2 + k_{d1})Y_{2,P,i} + (k_{t\beta 2} + k_{tH2}H_2 + k_{d2})Y_{2,Q,i} \quad (56)$$

The moment equations for the overall dead polymer chain cane be given by:

$$\frac{dX_0}{dt} = (k_{t\beta 1} + k_{tH1}H_2 + k_{d1})Y_{0,P} + (k_{t\beta 2} + k_{tH2}H_2 + k_{d2})Y_{0,Q} \quad (57)$$

$$\frac{dX_1}{dt} = (k_{t\beta 1} + k_{tH1}H_2 + k_{d1})Y_{1,P} + (k_{t\beta 2} + k_{tH2}H_2 + k_{d2})Y_{1,Q} \quad (58)$$

$$\frac{dX_2}{dt} = (k_{t\beta 1} + k_{tH1}H_2 + k_{d1})Y_{2,P} + (k_{t\beta 2} + k_{tH2}H_2 + k_{d2})Y_{2,Q} \quad (59)$$

Reactants molar balance:

The molar balance for catalyst active site 1, C_1

$$\frac{dC_1}{dt} = -k_{iA1}C_1A - k_{iB1}C_1A + k_{t\beta 1}\sum_{i=1}^{\infty}\sum_{r=1}^{\infty}P_{r,i} + k_{tH1}H_2\sum_{i=1}^{\infty}\sum_{r=1}^{\infty}P_{r,i} + k_{d1}\sum_{i=1}^{\infty}\sum_{r=1}^{\infty}P_{r,i} + k_{CSA01}S_0\sum_{i=1}^{\infty}\sum_{r=1}^{\infty}P_{r,i} \quad (60)$$

Substituting equations (2) and (13) in equation (60):

$$\frac{dC_1}{dt} = -\left(k_{iA1}A + k_{iB1}B\right)C_1 + \left(k_{t\beta 1} + k_{tH1}H_2 + k_{d1} + k_{CSA01}S_0\right)Y_{0,P} \tag{61}$$

The molar balance for catalyst active site 2, C_2

$$\frac{dC_2}{dt} = -k_{iA2}C_2A - k_{iB2}C_2B + k_{t\beta 2}\sum_{i=1}^{\infty}\sum_{r=1}^{\infty}Q_{r,i} + k_{tH2}H_2\sum_{i=1}^{\infty}\sum_{r=1}^{\infty}Q_{r,i} + k_{d2}\sum_{i=1}^{\infty}\sum_{r=1}^{\infty}Q_{r,i} + k_{CSA02}S_0\sum_{i=1}^{\infty}\sum_{r=1}^{\infty}Q_{r,i} \tag{62}$$

Substituting equations (2) and (13) in equation (62):

$$\frac{dC_2}{dt} = -\left(k_{iA2}A + k_{iB2}B\right)C_2 + \left(k_{t\beta 2} + k_{tH2}H_2 + k_{d2} + k_{CSA02}S_0\right)Y_{0,Q} \tag{63}$$

The molar balance for chain shuttling agent, S_0

$$\frac{dS_0}{dt} = -k_{CSA01}S_0\sum_{i=1}^{\infty}\sum_{r=1}^{\infty}P_{r,i} - k_{CSA02}S_0\sum_{j=1}^{\infty}\sum_{s=1}^{\infty}Q_{s,j} \tag{64}$$

Substituting equations (2) to and (13) in equation (64):

$$\frac{dS_0}{dt} = -\left(k_{CSA01}Y_{0,P} + k_{CSA02}Y_{0,Q}\right)S_0 \tag{65}$$

The molar balance for monomer A is given by

$$\frac{dA}{dt} = -k_{iA1}C_1A - k_{iA2}C_2A - k_{pA1}A\sum_{i=1}^{\infty}\sum_{r=1}^{\infty}P_{r,i} - k_{pA2}A\sum_{i=1}^{\infty}\sum_{r=1}^{\infty}Q_{r,i} \tag{66}$$

Substituting equations (2) to (13) in equation (66):

$$\frac{dA}{dt} = -\left(k_{iA1}C_1 + k_{iA2}C_2 + k_{pA1}Y_{0,P} + k_{pA2}Y_{0,Q}\right)A \tag{67}$$

The molar balance for monomer B is given by

$$\frac{dB}{dt} = -k_{iB1}C_1B - k_{iB2}C_2B - k_{pB1}B\sum_{i=1}^{\infty}\sum_{r=1}^{\infty}P_{r,i} - k_{pB2}B\sum_{i=1}^{\infty}\sum_{r=1}^{\infty}Q_{r,i} \tag{68}$$

Substituting equations (2) to (13) in equation (68):

$$\frac{dB}{dt} = -\left(k_{iB1}C_1 + k_{iB2}C_2 + k_{pB1}Y_{0,P} + k_{pB2}Y_{0,Q}\right)B \tag{69}$$

Appendix 6-A

The following expression gives the k^{th} moment for living, dormant, and dead chains of a generic distribution $f(r,i)$:

$$\mu_{k,i} = \sum_{r=1}^{\infty} r^k f(r,i) \tag{1}$$

We adopted the following nomenclature for the moments:

1. $Y_{k,P}$ and $Y_{k,Q}$ are the k^{th} moments of the living chains growing in catalyst P and Q, respectively.
2. $SX_{k,P}$ and $SX_{k,Q}$ are the k^{th} moments of dormant chains for which catalyst P and Q made the last block, respectively.
3. $X_{k,P}$ and $X_{k,Q}$ are the k^{th} moments of dead chains for which catalyst P and Q made the last block, respectively.
4. $Y_{k,P,i}$ and $Y_{k,Q,i}$ are the k^{th} moments of living chains growing in catalyst P and Q having i blocks, respectively.
5. $SX_{k,P,i}$ and $SX_{k,Q,i}$ are the k^{th} moments of dormant chains having i blocks for which catalyst P and Q made the last block, respectively.
6. $X_{k,P,i}$ and $X_{k,Q,i}$ are the k^{th} moments of dead chains having i blocks for which catalyst P and Q made the last block, respectively.

These moments are defined using the following equations,

$$Y_{k,P} = \sum_{i=1}^{\infty}\sum_{r=1}^{\infty} r^k Y_{k,P,i} \tag{2}$$

$$Y_{k,Q} = \sum_{i=1}^{\infty}\sum_{r=1}^{\infty} r^k Y_{k,Q,i} \tag{3}$$

$$SX_{k,P} = \sum_{i=1}^{\infty}\sum_{r=1}^{\infty} r^k SX_{k,P,i} \tag{4}$$

$$SX_{k,Q} = \sum_{i=1}^{\infty}\sum_{r=1}^{\infty} r^k SX_{k,Q,i} \tag{5}$$

$$X_{k,P} = \sum_{i=1}^{\infty}\sum_{r=1}^{\infty} r^k X_{k,P,i} \tag{6}$$

$$X_{k,Q} = \sum_{i=1}^{\infty}\sum_{r=1}^{\infty} r^k X_{k,Q,i} \tag{7}$$

$$Y_{k,P,i} = \sum_{r=1}^{\infty} r^k P_{r,i} = P_{1,1} + \sum_{r=2}^{\infty} r^k P_{r,i} \tag{8}$$

$$Y_{k,Q,i} = \sum_{r=1}^{\infty} r^k Q_{r,i} = Q_{1,1} + \sum_{r=2}^{\infty} r^k Q_{r,i} \tag{9}$$

$$SX_{k,P,i} = \sum_{r=1}^{\infty} r^k SP_{r,i} = SP_{1,1} + \sum_{r=2}^{\infty} r^k SP_{r,i} \tag{10}$$

$$SX_{k,Q,i} = \sum_{r=1}^{\infty} r^k SQ_{r,i} = SQ_{1,1} + \sum_{r=2}^{\infty} r^k SQ_{r,i} \tag{11}$$

$$X_{k,P,i} = \sum_{r=1}^{\infty} r^k D_{r,i} = D_{1,1} + \sum_{r=2}^{\infty} r^k D_{r,i} \tag{12}$$

$$X_{k,Q,i} = \sum_{r=1}^{\infty} r^k D_{r,i} = D_{1,1} + \sum_{r=2}^{\infty} r^k D_{r,i} \tag{13}$$

Where: k: 0th, 1st, and 2nd moments, i: block number, r: chain length and P and Q: catalyst type.

Moment Equation for Living Chains

Two living polymer chains with length larger than 2 ($r \geq 2$) and with a number of blocks greater than 1 ($i > 1$) made by catalyst type P ($P_{r,i}$) and made by catalyst type Q ($Q_{r,i}$) were produced in the reactor. The population balance for living polymer chain made by catalyst P of block i, $P_{r,i}$, is expressed by:

$$\frac{dP_{r,i}}{dt} = k_{pA1}A\left(P_{r-1,i} - P_{r,i}\right) + k_{pB1}B\left(P_{r-1,i} - P_{r,i}\right)$$
$$-\left(k_{t\beta 1} + k_{tH1}H_2 + k_{d1} + k_{CSA01}S_0 + k_{CSA1}SX_{0,P} + k_{CSA1}SX_{0,Q} + s\right)P_{r,i} + \left(SP_{r,i} + SQ_{r,i-1}\right)k_{CSA1}Y_{0,P} \tag{14}$$

A slightly different equation is applied for chain length 1, $P_{1,1}$:

$$\frac{dP_{1,1}}{dt} = (k_{iA1}A + k_{iB1}B)C_1 - k_{pA1}P_{1,1}A - k_{pB1}P_{1,1}B \\ -(k_{t\beta 1} + k_{tH1}H_2 + k_{d1} + k_{CSA01}S_0 + k_{CSA1}SX_{0,P} + k_{CSA1}SX_{0,Q} + s)P_{1,1} + k_{CSA1}(SP_{1,1})Y_{0,P} \quad (15)$$

The k^{th} moment of living chains made by catalyst type P for block i is given by:

$$\frac{dY_{k,P,i}}{dt} = \sum_{r=1}^{\infty} r^k \frac{dP_{r,i}}{dt} = \frac{dP_{1,1}}{dt} + \sum_{r=2}^{\infty} r^k \frac{dP_{r,i}}{dt} \quad (16)$$

Substituting Equations (14) and (15) into Equation (12) and by using Equations (2) to (13) with simplifying, the 0th, 1st, and 2nd moments of living chains made by catalyst type P for block i are given by the following equations:

$$\frac{dY_{0,P,i}}{dt} = (k_{iA1}A + k_{iB1}B)C_1 - (k_{t\beta 1} + k_{tH1}H_2 + k_{d1} + k_{CSA01}S_0 + k_{CSA1}(SX_{0,P}) + k_{CSA1}(SX_{0,Q}) + s)Y_{0,P,i} \\ + ((SX_{0,P,i}) + (SX_{0,Q,i-1}))k_{CSA1}Y_{0,P} \quad (17)$$

$$\frac{dY_{1,P,i}}{dt} = (k_{iA1}A + k_{iB1}B)C_1 + (k_{pA1}A + k_{pB1}B)Y_{0,P,i} \\ -(k_{t\beta 1} + k_{tH1}H_2 + k_{d1} + k_{CSA01}S_0 + k_{CSA1}(SX_{0,P}) + k_{CSA1}(SX_{0,Q}) + s)Y_{1,P,i} + ((SX_{1,P,i}) + (SX_{1,Q,i-1}))k_{CSA1}Y_{0,P} \quad (18)$$

$$\frac{dY_{2,P,i}}{dt} = (k_{iA1}A + k_{iB1}B)C_1 + (k_{pA1}A + k_{pB1}B)(Y_{0,P,i} + 2Y_{1,P,i}) \\ -(k_{t\beta 1} + k_{tH1}H_2 + k_{d1} + k_{CSA01}S_0 + k_{CSA1}(SX_{0,P}) + k_{CSA1}(SX_{0,Q}) + s)Y_{2,P,i} + ((SX_{2,P,i}) + (SX_{2,Q,i-1}))k_{CSA1}Y_{0,P} \quad (19)$$

Solve Equations (17) to (19) at steady state:

$$Y_{0,P,i} = \frac{(k_{iA1}A + k_{iB1}B)C_1 + ((SX_{0,P,i}) + (SX_{0,Q,i-1}))k_{CSA1}Y_{0,P}}{(k_{t\beta 1} + k_{tH1}H_2 + k_{d1} + k_{CSA01}S_0 + k_{CSA1}(SX_{0,P}) + k_{CSA1}(SX_{0,Q}) + s)} \quad (20)$$

$$Y_{1,P,i} = \frac{(k_{iA1}A + k_{iB1}B)C_1 + (k_{pA1}A + k_{pB1}B)Y_{0,P,i} + ((SX_{1,P,i}) + (SX_{1,Q,i-1}))k_{CSA1}Y_{0,P}}{(k_{t\beta 1} + k_{tH1}H_2 + k_{d1} + k_{CSA01}S_0 + k_{CSA1}(SX_{0,P}) + k_{CSA1}(SX_{0,Q}) + s)} \quad (21)$$

$$Y_{2,P,i} = \frac{(k_{iA1}A + k_{iB1}B)C_1 + (k_{pA1}A + k_{pB1}B)(Y_{0,P,i} + 2Y_{1,P,i}) + ((SX_{2,P,i}) + (SX_{2,Q,i-1}))k_{CSA1}Y_{0,P}}{(k_{t\beta 1} + k_{tH1}H_2 + k_{d1} + k_{CSA01}S_0 + k_{CSA1}(SX_{0,P}) + k_{CSA1}(SX_{0,Q}) + s)} \quad (22)$$

For the moment equations for 1 block made by catalyst P, the dormant term for block i made by catalyst Q will be omitted, i.e, $SX_{0,Q,i-1}=0$ in the Equations (17) to (22). For the moment equations for more than 1 block made by catalyst P, the initiation part will be omitted, i.e, $(k_{iA1}*A+k_{iB1}*B)*C_1=0$ in the Equations (17) to (22).

To find the moment equations for the overall living polymer chain made by catalyst P, we need to define a new population balance for P_r and P_1

The population balance for overall living polymer chain made by catalyst P, P_r, is expressed by:

$$\frac{dP_r}{dt} = k_{pA1}A(P_{r-1} - P_r) + k_{pB1}B(P_{r-1} - P_r) - (k_{t\beta 1} + k_{tH1}H_2 + k_{d1} + k_{CSA01}S_0 + k_{CSA1}SX_{0,P} + k_{CSA1}SX_{0,Q} + s)P_r + (SP_r + SQ_r)k_{CSA1}Y_{0,P} \quad (23)$$

A slightly different equation is applied for chain length 1, P_1:

$$\frac{dP_1}{dt} = (k_{iA1}A + k_{iB1}B)C_1 - k_{pA1}P_1A - k_{pB1}P_1B - (k_{t\beta 1} + k_{tH1}H_2 + k_{d1} + k_{CSA01}S_0 + k_{CSA1}SX_{0,P} + k_{CSA1}SX_{0,Q} + s)P_1 + k_{CSA1}(SP_1)Y_{0,P} \quad (24)$$

The kth moment of overall living polymer chain made by catalyst type P is given by:

$$\frac{dY_{k,P}}{dt} = \sum_{r=1}^{\infty} r^k \frac{dP_r}{dt} = \frac{dP_1}{dt} + \sum_{r=2}^{\infty} r^k \frac{dP_r}{dt} \quad (25)$$

Substituting Equations (23) and (24) into Equation (25) with simplifying, the 0th, 1st, and 2nd moments of overall living polymer chain made by catalyst type P are given by the following equations:

$$\frac{dY_{0,P}}{dt} = (k_{iA1}A + k_{iB1}B)C_1 - (k_{t\beta 1} + k_{tH1}H_2 + k_{d1} + k_{CSA01}S_0 + s)Y_{0,P} \quad (26)$$

$$\frac{dY_{1,P}}{dt} = (k_{iA1}A + k_{iB1}B)C_1 + (k_{pA1}A + k_{pB1}B)Y_{0,P} - (k_{t\beta 1} + k_{tH1}H_2 + k_{d1} + k_{CSA01}S_0 + k_{CSA1}(SX_{0,P}) + k_{CSA1}(SX_{0,Q}) + s)Y_{1,P} + ((SX_{1,P}) + (SX_{1,Q}))k_{CSA1}Y_{0,P} \quad (27)$$

$$\frac{dY_{2,P}}{dt} = \left(k_{iA1}A + k_{iB1}B\right)C_1 + \left(k_{pA1}A + k_{pB1}B\right)\left(Y_{0,P,i} + 2Y_{1,P}\right) - \left(k_{t\beta 1} + k_{tH1}H_2 + k_{d1} + k_{CSA01}S_0 + k_{CSA1}\left(SX_{0,P}\right) + k_{CSA1}\left(SX_{0,Q}\right) + s\right)Y_{2,P} + \left(\left(SX_{2,P}\right) + \left(SX_{2,Q}\right)\right)k_{CSA1}Y_{0,P} \quad (28)$$

Solve Equations (26) to (28) at steady state:

$$Y_{0,P} = \frac{\left(k_{iA1}A + k_{iB1}B\right)C_1}{\left(k_{t\beta 1} + k_{tH1}H_2 + k_{d1} + k_{CSA01}S_0 + s\right)} \quad (29)$$

$$Y_{1,P} = \frac{\left(k_{iA1}A + k_{iB1}B\right)C_1 + \left(k_{pA1}A + k_{pB1}B\right)Y_{0,P} + \left(\left(SX_{1,P}\right) + \left(SX_{1,Q}\right)\right)k_{CSA1}Y_{0,P}}{\left(k_{t\beta 1} + k_{tH1}H_2 + k_{d1} + k_{CSA01}S_0 + k_{CSA1}\left(SX_{0,P}\right) + k_{CSA1}\left(SX_{0,Q}\right) + s\right)} \quad (30)$$

$$Y_{2,P} = \frac{\left(k_{iA1}A + k_{iB1}B\right)C_1 + \left(k_{pA1}A + k_{pB1}B\right)\left(Y_{0,P,i} + 2Y_{1,P}\right) + \left(\left(SX_{2,P}\right) + \left(SX_{2,Q}\right)\right)k_{CSA1}Y_{0,P}}{\left(k_{t\beta 1} + k_{tH1}H_2 + k_{d1} + k_{CSA01}S_0 + k_{CSA1}\left(SX_{0,P}\right) + k_{CSA1}\left(SX_{0,Q}\right) + s\right)} \quad (31)$$

The population balance living polymer chain made by catalyst Q of block i, $Q_{r,i}$, is expressed by:

$$\frac{dQ_{r,i}}{dt} = k_{pA2}A\left(Q_{r-1,i} - Q_{r,i}\right) + k_{pB2}B\left(Q_{r-1,i} - Q_{r,i}\right) - \left(k_{t\beta 2} + k_{tH2}H_2 + k_{d2} + k_{CSA02}S_0 + k_{CSA2}SX_{0,P} + k_{CSA2}SX_{0,Q} + s\right)Q_{r,i} + \left(SP_{r,i-1} + SQ_{r,i}\right)k_{CSA2}Y_{0,Q} \quad (32)$$

For $Q_{1,1}$:

$$\frac{dQ_{1,1}}{dt} = \left(k_{iA2}A + k_{iB2}B\right)C_2 - k_{pA2}Q_{1,1}A - k_{pB2}Q_{1,1}B - \left(k_{t\beta 2} + k_{tH2}H_2 + k_{d2} + k_{CSA02}S_0 + k_{CSA2}SX_{0,P} + k_{CSA2}SX_{0,Q} + s\right)Q_{1,1} + k_{CSA2}\left(SQ_{1,1}\right)Y_{0,Q} \quad (33)$$

The k^{th} moment of living chains made by catalyst type Q for block i is given by:

$$\frac{dY_{k,Q,i}}{dt} = \sum_{r=1}^{\infty} r^k \frac{dQ_{r,i}}{dt} = \frac{dQ_{1,1}}{dt} + \sum_{r=2}^{\infty} r^k \frac{dQ_{r,i}}{dt} \quad (34)$$

Substituting Equations (32) and (33) into Equation (34) and by using Equations (2) to (13) with simplifying, the 0^{th}, 1^{st}, and 2^{nd} moments of living chains made by catalyst type Q for block i are given by the following equations:

$$\frac{dY_{0,Q,i}}{dt} = \left(k_{iA2}A + k_{iB2}B\right)C_2 - \left(k_{t\beta 2} + k_{tH2}H_2 + k_{d2} + k_{CSA02}S_0 + k_{CSA2}\left(SX_{0,P}\right) + k_{CSA2}\left(SX_{0,Q}\right) + s\right)Y_{0,Q,i} + \left(\left(SX_{0,P,i-1}\right) + \left(SX_{0,Q,i}\right)\right)k_{CSA2}Y_{0,Q} \tag{35}$$

$$\frac{dY_{1,Q,i}}{dt} = \left(k_{iA2}A + k_{iB2}B\right)C_2 + \left(k_{pA2}A + k_{pB2}B\right)Y_{0,Q,i} - \left(k_{t\beta 2} + k_{tH2}H_2 + k_{d2} + k_{CSA02}S_0 + k_{CSA2}\left(SX_{0,P}\right) + k_{CSA2}\left(SX_{0,Q}\right) + s\right)Y_{1,Q,i} + \left(\left(SX_{1,P,i-1}\right) + \left(SX_{1,Q,i}\right)\right)k_{CSA2}Y_{0,Q} \tag{36}$$

$$\frac{dY_{2,Q,i}}{dt} = \left(k_{iA2}A + k_{iB2}B\right)C_2 + \left(k_{pA2}A + k_{pB2}B\right)\left(Y_{0,Q,i} + 2Y_{1,Q,i}\right) - \left(k_{t\beta 2} + k_{tH2}H_2 + k_{d2} + k_{CSA02}S_0 + k_{CSA2}\left(SX_{0,P}\right) + k_{CSA2}\left(SX_{0,Q}\right) + s\right)Y_{2,Q,i} + \left(\left(SX_{2,P,i-1}\right) + \left(SX_{2,Q,i}\right)\right)k_{CSA2}Y_{0,Q} \tag{37}$$

Solve Equations (35) to (37) at steady state:

$$Y_{0,Q,i} = \frac{\left(k_{iA2}A + k_{iB2}B\right)C_2 + \left(\left(SX_{0,P,i-1}\right) + \left(SX_{0,Q,i}\right)\right)k_{CSA2}Y_{0,Q}}{\left(k_{t\beta 2} + k_{tH2}H_2 + k_{d2} + k_{CSA02}S_0 + k_{CSA2}\left(SX_{0,P}\right) + k_{CSA2}\left(SX_{0,Q}\right) + s\right)} \tag{38}$$

$$Y_{1,Q,i} = \frac{\left(k_{iA2}A + k_{iB2}B\right)C_2 + \left(k_{pA2}A + k_{pB2}B\right)Y_{0,Q,i} + \left(\left(SX_{1,P,i-1}\right) + \left(SX_{1,Q,i}\right)\right)k_{CSA2}Y_{0,Q}}{\left(k_{t\beta 2} + k_{tH2}H_2 + k_{d2} + k_{CSA02}S_0 + k_{CSA2}\left(SX_{0,P}\right) + k_{CSA2}\left(SX_{0,Q}\right) + s\right)} \tag{39}$$

$$Y_{2,Q,i} = \frac{\left(k_{iA2}A + k_{iB2}B\right)C_2 + \left(k_{pA2}A + k_{pB2}B\right)\left(Y_{0,Q,i} + 2Y_{1,Q,i}\right) + \left(\left(SX_{2,P,i-1}\right) + \left(SX_{2,Q,i}\right)\right)k_{CSA2}Y_{0,Q}}{\left(k_{t\beta 2} + k_{tH2}H_2 + k_{d2} + k_{CSA02}S_0 + k_{CSA2}\left(SX_{0,P}\right) + k_{CSA2}\left(SX_{0,Q}\right) + s\right)} \tag{40}$$

For the moment equations for 1 block made by catalyst *Q*, the dormant term for block *i* made by catalyst *P* will be omitted, i.e, $SX_{0,P,i-1} = 0$ in the Equations (35) to (40). The moment equations for more than 1 block made by catalyst *Q*, the initiation part will be omitted, i.e, $(k_{iA2}*A + k_{iB2}*B)*C_2 = 0$ in the Equations (35) to (40).

To find the moment equations for the overall living polymer chain made by catalyst *Q*, we need to define a new population balance for Q_r and Q_1

The population balance for overall living polymer chain made by catalyst *Q*, Q_r, is expressed by:

$$\frac{dQ_r}{dt} = k_{pA2}A(Q_{r-1} - Q_r) + k_{pB2}B(Q_{r-1} - Q_r)$$
$$-\left(k_{t\beta 2} + k_{tH2}H_2 + k_{d2} + k_{CSA02}S_0 + k_{CSA2}SX_{0,P} + k_{CSA2}SX_{0,Q} + s\right)Q_r + (SP_r + SQ_r)k_{CSA2}Y_{0,Q} \quad (41)$$

For Q_1:

$$\frac{dQ_1}{dt} = \left(k_{iA2}A + k_{iB2}B\right)C_2 - k_{pA2}Q_1A - k_{pB2}Q_1B$$
$$-\left(k_{t\beta 2} + k_{tH2}H_2 + k_{d2} + k_{CSA02}S_0 + k_{CSA2}SX_{0,P} + k_{CSA2}SX_{0,Q} + s\right)Q_1 + k_{CSA2}(SQ_1)Y_{0,Q} \quad (42)$$

The k^{th} moment of overall living polymer chain made by catalyst type Q is given by:

$$\frac{dY_{k,Q}}{dt} = \sum_{r=1}^{\infty} r^k \frac{dQ_r}{dt} = \frac{dQ_1}{dt} + \sum_{r=2}^{\infty} r^k \frac{dQ_r}{dt} \quad (43)$$

Substituting Equations (41) and (42) into Equation (43) with simplifying, the 0th, 1st, and 2nd moments of overall living polymer chain made by catalyst type *Q* are given by the following equations:

$$\frac{dY_{0,Q}}{dt} = \left(k_{iA2}A + k_{iB2}B\right)C_2 - \left(k_{t\beta 2} + k_{tH2}H_2 + k_{d2} + k_{CSA02}S_0 + s\right)Y_{0,Q} \quad (44)$$

$$\frac{dY_{1,Q}}{dt} = \left(k_{iA2}A + k_{iB2}B\right)C_2 + \left(k_{pA2}A + k_{pB2}B\right)Y_{0,Q}$$
$$-\left(k_{t\beta 2} + k_{tH2}H_2 + k_{d2} + k_{CSA02}S_0 + k_{CSA2}\left(SX_{0,P}\right) + k_{CSA2}\left(SX_{0,Q}\right) + s\right)Y_{1,Q} + \left(\left(SX_{1,P}\right) + \left(SX_{1,Q}\right)\right)k_{CSA2}Y_{0,Q} \quad (45)$$

$$\frac{dY_{2,Q}}{dt} = \left(k_{iA2}A + k_{iB2}B\right)C_2 + \left(k_{pA2}A + k_{pB2}B\right)\left(Y_{0,Q} + 2Y_{1,Q}\right)$$
$$-\left(k_{t\beta 2} + k_{tH2}H_2 + k_{d2} + k_{CSA02}S_0 + k_{CSA2}\left(SX_{0,P}\right) + k_{CSA2}\left(SX_{0,Q}\right) + s\right)Y_{2,Q} + \left(\left(SX_{2,P}\right) + \left(SX_{2,Q}\right)\right)k_{CSA2}Y_{0,Q} \quad (46)$$

Solve Equations (44) to (46) at steady state:

$$Y_{0,Q} = \frac{\left(k_{iA2}A + k_{iB2}B\right)C_2}{\left(k_{t\beta 2} + k_{tH2}H_2 + k_{d2} + k_{CSA02}S_0 + s\right)} \quad (47)$$

$$Y_{1,Q} = \frac{\left(k_{iA2}A + k_{iB2}B\right)C_2 + \left(k_{pA2}A + k_{pB2}B\right)Y_{0,Q} + \left(\left(SX_{1,P}\right) + \left(SX_{1,Q}\right)\right)k_{CSA2}Y_{0,Q}}{\left(k_{t\beta 2} + k_{tH2}H_2 + k_{d2} + k_{CSA02}S_0 + k_{CSA2}\left(SX_{0,P}\right) + k_{CSA2}\left(SX_{0,Q}\right) + s\right)} \quad (48)$$

$$Y_{2,Q} = \frac{(k_{iA2}A + k_{iB2}B)C_2 + (k_{pA2}A + k_{pB2}B)(Y_{0,Q} + 2Y_{1,Q}) + ((SX_{2,P}) + (SX_{2,Q}))k_{CSA2}Y_{0,Q}}{(k_{t\beta 2} + k_{tH2}H_2 + k_{d2} + k_{CSA02}S_0 + k_{CSA2}(SX_{0,P}) + k_{CSA2}(SX_{0,Q}) + s)} \quad (49)$$

Moment Equation for Dormant Chains

The presence of two catalysts and chain shuttling agent in the system generated two different types of dormant chains with chain length larger than 2 ($r \geq 2$) and with number of blocks greater than 1 ($i > 1$) made by catalyst type P ($SP_{r,i}$) and by catalyst type Q ($SQ_{r,i}$). The population balance for $SP_{r,i}$ is expressed by:

$$\frac{d(SP_{r,i})}{dt} = (k_{CSA01}S_0 + k_{CSA1}SX_{0,P} + k_{CSA1}SX_{0,Q})P_{r,i} - (k_{CSA1}Y_{0,P} + k_{CSA2}Y_{0,Q} + s)(SP_{r,i}) \quad (50)$$

The kth moment of dormant chains made by catalyst type P for block i is given by:

$$\frac{dSX_{k,P,i}}{dt} = \sum_{r=1}^{\infty} r^k \frac{dSP_{r,i}}{dt} = \frac{dSP_{1,1}}{dt} + \sum_{r=2}^{\infty} r^k \frac{dSP_{r,i}}{dt} \quad (51)$$

Substituting Equation (50) into Equation (51) and by using Equations (2) to (13), the 0th, 1st, and 2nd moments of dormant chains made by catalyst type P for block i are given by:

$$\frac{d(SX_{0,P,i})}{dt} = (k_{CSA01}S_0 + k_{CSA1}(SX_{0,P}) + k_{CSA1}(SX_{0,Q}))Y_{0,P,i} - (k_{CSA1}Y_{0,P} + k_{CSA2}Y_{0,Q} + s)(SX_{0,P,i}) \quad (52)$$

$$\frac{d(SX_{1,P,i})}{dt} = (k_{CSA01}S_0 + k_{CSA1}(SX_{0,P}) + k_{CSA1}(SX_{0,Q}))Y_{1,P,i} - (k_{CSA1}Y_{0,P} + k_{CSA2}Y_{0,Q} + s)(SX_{1,P,i}) \quad (53)$$

$$\frac{d(SX_{2,P,i})}{dt} = (k_{CSA01}S_0 + k_{CSA1}(SX_{0,P}) + k_{CSA1}(SX_{0,Q}))Y_{2,P,i} - (k_{CSA1}Y_{0,P} + k_{CSA2}Y_{0,Q} + s)(SX_{2,P,i}) \quad (54)$$

Solve Equations (52) to (54) at steady state:

$$(SX_{0,P,i}) = \frac{(k_{CSA01}S_0 + k_{CSA1}(SX_{0,P}) + k_{CSA1}(SX_{0,Q}))Y_{0,P,i}}{(k_{CSA1}Y_{0,P} + k_{CSA2}Y_{0,Q} + s)} \quad (55)$$

$$(SX_{1,P,i}) = \frac{(k_{CSA01}S_0 + k_{CSA1}(SX_{0,P}) + k_{CSA1}(SX_{0,Q}))Y_{1,P,i}}{(k_{CSA1}Y_{0,P} + k_{CSA2}Y_{0,Q} + s)} \quad (56)$$

$$\left(SX_{2,P,i}\right)=\frac{\left(k_{CSA01}S_0+k_{CSA1}\left(SX_{0,P}\right)+k_{CSA1}\left(SX_{0,Q}\right)\right)Y_{2,P,i}}{\left(k_{CSA1}Y_{0,P}+k_{CSA2}Y_{0,Q}+s\right)} \tag{57}$$

The population balance for $SQ_{r,i}$ is expressed by:

$$\frac{d\left(SQ_{r,i}\right)}{dt}=\left(k_{CSA02}S_0+k_{CSA2}SX_{0,P}+k_{CSA2}SX_{0,Q}\right)Q_{r,i}\ -\left(k_{CSA1}Y_{0,P}+k_{CSA2}Y_{0,Q}+s\right)\left(SQ_{r,i}\right) \tag{58}$$

The k^{th} moment of dormant chains made by catalyst type Q for block i is given by:

$$\frac{dSX_{k,Q,i}}{dt}=\sum_{r=1}^{\infty}r^k\frac{dSQ_{r,i}}{dt}=\frac{dSQ_{1,1}}{dt}+\sum_{r=2}^{\infty}r^k\frac{dSQ_{r,i}}{dt} \tag{59}$$

Substituting Equation (58) into Equation (59) and by using Equations (2) to (13), the 0^{th}, 1^{st}, and 2^{nd} moments of dormant chains made by catalyst type Q for block i are given by:

$$\frac{d\left(SX_{0,Q,i}\right)}{dt}=\left(k_{CSA02}S_0+k_{CSA2}\left(SX_{0,P}\right)+k_{CSA2}\left(SX_{0,Q}\right)\right)Y_{0,Q,i}-\left(k_{CSA1}Y_{0,P}+k_{CSA2}Y_{0,Q}+s\right)\left(SX_{0,Q,i}\right) \tag{60}$$

$$\frac{d\left(SX_{1,Q,i}\right)}{dt}=\left(k_{CSA02}S_0+k_{CSA2}\left(SX_{0,P}\right)+k_{CSA2}\left(SX_{0,Q}\right)\right)Y_{1,Q,i}-\left(k_{CSA1}Y_{0,P}+k_{CSA2}Y_{0,Q}+s\right)\left(SX_{1,Q,i}\right) \tag{61}$$

$$\frac{d\left(SX_{2,Q,i}\right)}{dt}=\left(k_{CSA02}S_0+k_{CSA2}\left(SX_{0,P}\right)+k_{CSA2}\left(SX_{0,Q}\right)\right)Y_{2,Q,i}-\left(k_{CSA1}Y_{0,P}+k_{CSA2}Y_{0,Q}+s\right)\left(SX_{2,Q,i}\right) \tag{62}$$

Solve Equations (60) to (62) at steady state:

$$\left(SX_{0,Q,i}\right)=\frac{\left(k_{CSA02}S_0+k_{CSA2}\left(SX_{0,P}\right)+k_{CSA2}\left(SX_{0,Q}\right)\right)Y_{0,Q,i}}{\left(k_{CSA1}Y_{0,P}+k_{CSA2}Y_{0,Q}+s\right)} \tag{63}$$

$$\left(SX_{1,Q,i}\right)=\frac{\left(k_{CSA02}S_0+k_{CSA2}\left(SX_{0,P}\right)+k_{CSA2}\left(SX_{0,Q}\right)\right)Y_{1,Q,i}}{\left(k_{CSA1}Y_{0,P}+k_{CSA2}Y_{0,Q}+s\right)} \tag{64}$$

$$\left(SX_{2,Q,i}\right)=\frac{\left(k_{CSA02}S_0+k_{CSA2}\left(SX_{0,P}\right)+k_{CSA2}\left(SX_{0,Q}\right)\right)Y_{2,Q,i}}{\left(k_{CSA1}Y_{0,P}+k_{CSA2}Y_{0,Q}+s\right)} \tag{65}$$

The moment equations for the overall dormant polymer chain made by catalyst P, and Q cane be given by:

$$\frac{d(SX_{0,P})}{dt} = (k_{CSA01}S_0 + k_{CSA1}(SX_{0,P}) + k_{CSA1}(SX_{0,Q}))Y_{0,P} - (k_{CSA1}Y_{0,P} + k_{CSA2}Y_{0,Q} + s)(SX_{0,P}) \quad (66)$$

$$\frac{d(SX_{1,P})}{dt} = (k_{CSA01}S_0 + k_{CSA1}(SX_{0,P}) + k_{CSA1}(SX_{0,Q}))Y_{1,P} - (k_{CSA1}Y_{0,P} + k_{CSA2}Y_{0,Q} + s)(SX_{1,P}) \quad (67)$$

$$\frac{d(SX_{2,P})}{dt} = (k_{CSA01}S_0 + k_{CSA1}(SX_{0,P}) + k_{CSA1}(SX_{0,Q}))Y_{2,P} - (k_{CSA1}Y_{0,P} + k_{CSA2}Y_{0,Q} + s)(SX_{2,P}) \quad (68)$$

$$\frac{d(SX_{0,Q})}{dt} = (k_{CSA02}S_0 + k_{CSA2}(SX_{0,P}) + k_{CSA2}(SX_{0,Q}))Y_{0,Q} - (k_{CSA1}Y_{0,P} + k_{CSA2}Y_{0,Q} + s)(SX_{0,Q}) \quad (69)$$

$$\frac{d(SX_{1,Q})}{dt} = (k_{CSA02}S_0 + k_{CSA2}(SX_{0,P}) + k_{CSA2}(SX_{0,Q}))Y_{1,Q} - (k_{CSA1}Y_{0,P} + k_{CSA2}Y_{0,Q} + s)(SX_{1,Q}) \quad (70)$$

$$\frac{d(SX_{2,Q})}{dt} = (k_{CSA02}S_0 + k_{CSA2}(SX_{0,P}) + k_{CSA2}(SX_{0,Q}))Y_{2,Q} - (k_{CSA1}Y_{0,P} + k_{CSA2}Y_{0,Q} + s)(SX_{2,Q}) \quad (71)$$

Solve Equations (66) to (71) at steady state:

$$(SX_{0,P}) = \frac{(k_{CSA01}S_0 + k_{CSA1}(SX_{0,Q}))Y_{0,P}}{(k_{CSA2}Y_{0,Q} + s)} \quad (72)$$

$$(SX_{1,P}) = \frac{(k_{CSA01}S_0 + k_{CSA1}(SX_{0,P}) + k_{CSA1}(SX_{0,Q}))Y_{1,P}}{(k_{CSA1}Y_{0,P} + k_{CSA2}Y_{0,Q} + s)} \quad (73)$$

$$(SX_{2,P}) = \frac{(k_{CSA01}S_0 + k_{CSA1}(SX_{0,P}) + k_{CSA1}(SX_{0,Q}))Y_{2,P}}{(k_{CSA1}Y_{0,P} + k_{CSA2}Y_{0,Q} + s)} \quad (74)$$

$$(SX_{0,Q}) = \frac{(k_{CSA02}S_0 + k_{CSA2}(SX_{0,P}))Y_{0,Q}}{(k_{CSA1}Y_{0,P} + s)} \quad (75)$$

$$(SX_{1,Q}) = \frac{(k_{CSA02}S_0 + k_{CSA2}(SX_{0,P}) + k_{CSA2}(SX_{0,Q}))Y_{1,Q}}{(k_{CSA1}Y_{0,P} + k_{CSA2}Y_{0,Q} + s)} \quad (76)$$

$$(SX_{2,Q}) = \frac{(k_{CSA02}S_0 + k_{CSA2}(SX_{0,P}) + k_{CSA2}(SX_{0,Q}))Y_{2,Q}}{(k_{CSA1}Y_{0,P} + k_{CSA2}Y_{0,Q} + s)} \quad (77)$$

Moment Equation for Dead Chains

The derivation of population balance and moments equations for dead polymer follows the same way used for living and dormant chains. The final expressions are shown below.

$$\frac{dX_{0,i}}{dt} = \left(k_{t\beta 1} + k_{tH1}H_2 + k_{d1}\right)Y_{0,P,i} + \left(k_{t\beta 2} + k_{tH2}H_2 + k_{d2}\right)Y_{0,Q,i} - sX_{0,i} \tag{78}$$

$$\frac{dX_{1,i}}{dt} = \left(k_{t\beta 1} + k_{tH1}H_2 + k_{d1}\right)Y_{1,P,i} + \left(k_{t\beta 2} + k_{tH2}H_2 + k_{d2}\right)Y_{1,Q,i} - sX_{1,i} \tag{79}$$

$$\frac{dX_{2,i}}{dt} = \left(k_{t\beta 1} + k_{tH1}H_2 + k_{d1}\right)Y_{2,P,i} + \left(k_{t\beta 2} + k_{tH2}H_2 + k_{d2}\right)Y_{2,Q,i} - sX_{2,i} \tag{80}$$

The moment equations for the overall dead polymer chain cane be given by:

$$\frac{dX_0}{dt} = \left(k_{t\beta 1} + k_{tH1}H_2 + k_{d1}\right)Y_{0,P} + \left(k_{t\beta 2} + k_{tH2}H_2 + k_{d2}\right)Y_{0,Q} - sX_0 \tag{81}$$

$$\frac{dX_1}{dt} = \left(k_{t\beta 1} + k_{tH1}H_2 + k_{d1}\right)Y_{1,P} + \left(k_{t\beta 2} + k_{tH2}H_2 + k_{d2}\right)Y_{1,Q} - sX_1 \tag{82}$$

$$\frac{dX_2}{dt} = \left(k_{t\beta 1} + k_{tH1}H_2 + k_{d1}\right)Y_{2,P} + \left(k_{t\beta 2} + k_{tH2}H_2 + k_{d2}\right)Y_{2,Q} - sX_2 \tag{83}$$

Solve Equations (78) to (83) at steady state:

$$X_{0,i} = \frac{\left(k_{t\beta 1} + k_{tH1}H_2 + k_{d1}\right)Y_{0,P,i} + \left(k_{t\beta 2} + k_{tH2}H_2 + k_{d2}\right)Y_{0,Q,i}}{s} \tag{84}$$

$$X_{1,i} = \frac{\left(k_{t\beta 1} + k_{tH1}H_2 + k_{d1}\right)Y_{1,P,i} + \left(k_{t\beta 2} + k_{tH2}H_2 + k_{d2}\right)Y_{1,Q,i}}{s} \tag{85}$$

$$X_{2,i} = \frac{\left(k_{t\beta 1} + k_{tH1}H_2 + k_{d1}\right)Y_{2,P,i} + \left(k_{t\beta 2} + k_{tH2}H_2 + k_{d2}\right)Y_{2,Q,i}}{s} \tag{86}$$

$$X_0 = \frac{\left(k_{t\beta 1} + k_{tH1}H_2 + k_{d1}\right)Y_{0,P} + \left(k_{t\beta 2} + k_{tH2}H_2 + k_{d2}\right)Y_{0,Q}}{s} \tag{87}$$

$$X_1 = \frac{\left(k_{t\beta 1} + k_{tH1}H_2 + k_{d1}\right)Y_{1,P} + \left(k_{t\beta 2} + k_{tH2}H_2 + k_{d2}\right)Y_{1,Q}}{s} \tag{88}$$

$$X_2 = \frac{\left(k_{t\beta 1} + k_{tH1}H_2 + k_{d1}\right)Y_{2,P} + \left(k_{t\beta 2} + k_{tH2}H_2 + k_{d2}\right)Y_{2,Q}}{s} \tag{89}$$

Reactants molar balance:

The molar balance for catalyst active site 1, C_1

$$\frac{dC_1}{dt} = -\left(k_{iA1}A + k_{iB1}B + s\right)C_1 + \left(k_{t\beta 1} + k_{tH1}H_2 + k_{d1} + k_{CSA01}S_0\right)Y_{0,P} + C_1^{in} \tag{90}$$

The molar balance for catalyst active site 2, C_2

$$\frac{dC_2}{dt} = -\left(k_{iA2}A + k_{iB2}B + s\right)C_2 + \left(k_{t\beta 2} + k_{tH2}H_2 + k_{d2} + k_{CSA02}S_0\right)Y_{0,Q} + C_2^{in} \tag{91}$$

The molar balance for chain shuttling agent, S_0

$$\frac{dS_0}{dt} = -\left(k_{CSA01}Y_{0,P} + k_{CSA02}Y_{0,Q} + s\right)S_0 + S_0^{in} \tag{92}$$

The molar balance for monomer A is given by

$$\frac{dA}{dt} = -\left(k_{iA1}C_1 + k_{iA2}C_2 + k_{pA1}Y_{0,P} + k_{pA2}Y_{0,Q} + s\right)A + A^{in} \tag{93}$$

The molar balance for monomer B is given by

$$\frac{dB}{dt} = -\left(k_{iB1}C_1 + k_{iB2}C_2 + k_{pB1}Y_{0,P} + k_{pB2}Y_{0,Q} + s\right)B + B^{in} \tag{94}$$

Solve Equations (90) to (92) at steady state:

$$C_1 = \frac{\left(k_{t\beta 1} + k_{tH1}H_2 + k_{d1} + k_{CSA01}S_0\right)Y_{0,P} + C_1^{in}}{\left(k_{iA1}A + k_{iB1}B + s\right)} \tag{95}$$

$$C_2 = \frac{\left(k_{t\beta 2} + k_{tH2}H_2 + k_{d2} + k_{CSA02}S_0\right)Y_{0,Q} + C_2^{in}}{\left(k_{iA2}A + k_{iB2}B + s\right)} \tag{96}$$

$$S_0 = \frac{S_0^{in}}{\left(k_{CSA01}Y_{0,P} + k_{CSA02}Y_{0,Q} + s\right)} \tag{97}$$